GAS DISTRIBUTION IN SHALLOW LARGE DIAMETER PACKED BEDS

A THESIS SUBMITTED FOR THE DEGREE

OF DOCTOR OF PHILOSOPHY

BY

QUASIM H. ALI

UNIVERSITY OF ASTON IN BIRMINGHAM,
GOSTA GREEN,
BIRMINGHAM
B4 7ET

DECEMBER 1984

In the Name of Allāh,
the Most Compassionate, the Merciful

And we want to bestow our favours on those who were oppressed on earth, and make them leaders of mankind and make them the inheritors. (*The Story*, 28:5)

TO AL-MAHDI (P.B.U.H.)

The work described in this thesis was carried out between 1981 and 1984 in the Department of Chemical Engineering, University of Aston in Birmingham. It has been carried out independently and has not been submitted for any other degree.

Quasim H. Ali

THE UNIVERSITY OF ASTON IN BIRMINGHAM

GAS DISTRIBUTION IN SHALLOW LARGE DIAMETER PACKED BEDS

by

QUASIM H. ALI

A thesis submitted for the degree of
Doctor of Philosophy, December 1984.

SUMMARY

It is important to maintain a uniform distribution of gas and liquid in large diameter packed columns to maintain mass transfer efficiency on scaling up.

This work presents measurements and methods of evaluating maldistributed gas flow in packed columns. Little or no previous work has been done in this field.

A gas maldistribution number, ϕ, was defined, based on point to point velocity variations in the gas emerging from the top of packed beds. ϕ has a minimum value for a uniformly distributed flow and much larger values for maldistributed flows.

A method of testing the quality of vapour distributors is proposed, based on the variation of ϕ with packed height. A good gas distributor requires a short packed depth to give a good gas distribution.

Measurements of gas maldistribution have shown that the principle of dynamic similarity is satisfied if two geometrically similar beds are operated at the same Reynold's number.

The validity of ϕ as a good measure of gas maldistribution, and the principle of dynamic similarity are tested statistically by Multi-Factor Analysis of the variance, and visually by the response surfaces technique.

Pressure distribution has been measured in a model of a large diameter packed bed, and shown to be associated with the velocity of the gas in a tangential feed pipe. Two simplified theoretical models are proposed to describe the flow of gases through packed beds and to support the principle of dynamic similarity. These models explain why the packed bed itself causes the flow of gas to become more uniformly distributed.

A 1.2m. diameter scaled-down model was constructed geometrically similar to a 7.3m. diameter vacuum crude distillation column. The previously known internal cylinder gas distributor was tested. Three new distributors suitable for use in a large diameter column were developed and tested, these are:

a) Internal Cylinder with Slots and Cross Baffles
b) Internal Cylinder with Guides in the Annulus
c) Internal Cylinder with Internal Cross Baffles

It has been shown that (c) is an excellent distributor.

PUMP AROUND. GAS DISTRIBUTORS. GAS MALDISTRIBUTION. FLUID MECHANICS. SCALE-UP.

ACKNOWLEDGEMENT

I would like to sincerely thank Professor K.E. Porter for his supervision, assistance, encouragement and enthusiasm throughout the course of this research.

Thanks are also to the Norton Company for kindly providing the packings used in this work, and for providing the 1983/1984 Grant.

My thanks are also due to my parents for providing all possible moral and financial support.

Finally, I would like to express my gratitude to my wife for her patience, understanding and encouragement throughout the course of this work.

CONTENTS

LIST OF TABLES

LIST OF FIGURES

LIST OF GRAPHS

LIST OF PHOTOGRAPHS

SECTION I

INTRODUCTION

The use of packed towers of large diameters for distillation and absorption services has seen a steady increase in recent years. This has been mainly due to the lower pressure drops obtained in packed towers, compared to trayed towers for similar duties when implementing energy saving schemes.

A serious problem arises in the use of large diameter packed beds, namely, the possibility of an uneven distribution of gas and liquid through the packing. A non-uniform distribution of gases and liquids has a much greater effect on the performance of large diameter columns than on small diameter columns. For maximum efficiency, both the gas and liquid should be uniformly distributed over the bed cross-section, and this uniformity should persist through the packing height.

Although a considerable amount of work has been done on liquid distribution in packed columns, little or nothing has been done on gas distribution. Gas distribution is rarely a problem for small diameter columns where the packed height is very much larger than the diameter of the column. Now that larger diameters are being used the problem of gas distribution has become more important. The problem is particularly important when the gas or vapour inlet pipe is small compared with the diameter of the column. This can occur in revamping situations, but it is also found in large new plants where there are economic advantages from limiting the size of the feed pipe. A particularly difficult example is the pump around section in a vacuum crude tower, where the bed is 7.3m in diameter packed to a depth of 1 to 2m, and with a pressure drop of 1 mm Hg. across the

packing, and a vapour inlet pipe of 1m in diameter. This type of application has revealed a great need for better understanding of the problems of achieving a uniform gas distribution in packed beds of large diameter, and often with a diameter to height ratio of greater than one.

Although real packed columns usually involve the contact of gas and liquid, an investigation into maldistribution based on gas flow alone is a good starting point. The experimental work which will be discussed fully here, involves a detailed study of gas maldistribution and the use of laboratory models to investigate the gas flow patterns of full scale columns. Work was performed on a small scale model and on a prototype which are exactly geometrically and dynamically similar. The condition of dynamical similarity between two cases with geometrically similar boundaries is found to be satisfied if the Reynolds number has the same value in each case. Although it is to be expected that for compressible gas flow, the Reynolds number is not enough to define dynamic similarity, it was found to be sufficient for air flow through packed beds where the pressure drops and velocities are small.

However, Porter[25] (1982) indicates that the use of the principle of dynamic similarity to study gas distribution in a packed bed needs a concept to deal with the lack of geometric similarity resulting from the randomness of the bed.

In this work a maldistribution factor, "ϕ", which is related to the standard deviation, σ^2, is defined in terms of the point to point velocity variations of the flow of gas emerging from the top of packed beds. The effectiveness of ϕ for describing gas maldistribution in packed beds, the principle of dynamic similarity, and scale-up rules, are studied statistically by Multi-Factor Analysis

of the Variance, which shows that ϕ is a satisfactory measure of flow uniformity, and that the gas flow patterns in two geometrically and dynamically similar packed beds of different size are similar. As a result of the randomness of the packed beds it is found that ϕ never reaches a zero value, however good the distribution. Rather, it approaches a minimum value, ϕ_{min}, which represents the best possible gas distribution it is possible to achieve. It is demonstrated that the packed bed itself acts as a distributor and that at a sufficiently large depth of packing, gas distribution becomes as good as possible and ϕ reduces to ϕ_{min}.

The fluid mechanics of maldistributed gas flow in packed beds is then studied, and experimental measurements are made on the pressure distribution in the bed. Following this, two simple theoretical models are proposed in this work to describe these flow patterns. The understanding of the fluid mechanics gained in this work permits the development of new improved low pressure drop gas distributors. These are:

(1) Internal Cylinder with Four Slots and Cross Baffles.

(2) Internal Cylinder with Guides in the Annulus.

(3) Internal Cylinder with Internal Cross Baffles.

The reliability of ϕ in describing gas maldistribution in packed beds permits the establishment of a method to test the quality of gas distributors based on the variation of ϕ with packed depth. A good gas distributor is that one in which only a small packed depth is required for ϕ to reach ϕ_{min}.

The establishment of the scale-up rules enables the construction of a laboratory size model of the full scale pump around section mentioned above, and this was used to test the new distributors. The Internal Cylinder with Internal Cross Baffles is found to be the best.

SECTION II

LITERATURE SURVEY

2.1 The Effect of Maldistribution on the Performance of Packed Beds

It is known that poor liquid and gas distribution has an adverse effect on the performance of packed columns. For maximum efficiency both the liquid and gas should be uniformly distributed over the bed cross-section, and this uniformity should persist throughout the packed height.

The effect of maldistribution can be shown diagrammatically on the McCabe Thiele diagram where different parts of the packed bed have different liquid/gas ratios and a "pinch" can occur in some sections of the packed bed, see Fig. 2.1.

Some workers have studied the wall effect on the maldistribution of gas in dry or wetted beds, and more workers have studied the maldistribution of liquid in packed beds where the liquid is the only stream flowing through the bed.

Indeed, a few workers[1, 2] have attempted to study liquid maldistribution in the presence of a counteracting gas stream, but none of them have included the effect of the gas maldistribution on the mass transfer performance of the packed bed. All the previous workers on the effect of liquid maldistribution on mass transfer have assumed a uniform gas flow through the bed and the problem was defined as a case of liquid maldistribution only.

The first model for the effect of maldistribution on mass transfer put by Mullin[1] (1957) is a very much simplified one. The column was assumed to be divided longitudinally into two equal sections by an impermeable membrane as shown in Fig. 2.2.

The two sections take an equal vapour flow but unequal

liquid rates. It was assumed that there is no mixing of gas or liquid across this theoretical membrane, and that within each section, the distribution of gas and liquid is uniform. A degree of maldistribution, M, was defined as the ratio of the liquid rate to gas rate, in each section. Maldistribution M = 1 means that the liquid rate is the same in each theoretical section; M = 2 means that one section takes twice as much liquid as the other.

G, G_1 and G_2 = The overall, Section 1, and Section 2 gas mass velocities respectively and

$$G = G_1 + G_2 \qquad \text{..... (2.1)}$$

L, L_1 and L_2 = The overall, Section 1, and Section 2 liquid mass velocities respectively, and

$$L = L_1 + ML_1 \qquad \text{..... (2.2)}$$

$$R_{overall} = \frac{G}{L} \text{ ; the overall gas:liquid ratio} \qquad \text{..... (2.3)}$$

R_{mean} = The arithmetical mean of the ratios existing in each of the two hypothetical sections.

$$\text{i.e. } R_{mean} = \frac{1}{2}\left(\frac{G_1}{L_1} + \frac{G_2}{L_2}\right) \qquad \text{..... (2.4)}$$

Then

$$R_{mean} = R_{overall} \cdot \frac{(M+1)^2}{4M} \qquad \text{..... (2.5)}$$

If m = The slope of the equilibrium line

L_m, G_m = The molar liquid and gas flow rates respectively

Then equation (2.5) will be as follows:

$$m\left(\frac{G_m}{L_m}\right)_{mean} = \frac{(M+1)^2}{4M} \cdot m\left(\frac{G_m}{L_m}\right)_{overall} \qquad \text{..... (2.6)}$$

Therefore, liquid maldistribution increases the value of the operating gas:liquid ratio G_m/L_m, i.e., it decreases the slope of the operating line L_m/G_m, resulting in a closer approach of this line to the equilibrium line (pinch), at one end of the tower. The effect of M on the number of transfer units N_{OG} is shown in Fig. 2.3.

Mullin's method is only useful in explaining the observed reduction in the performance below predicted theoretically. It does not explain the reduction in the efficiency with increasing the diameter of the bed.

Huber and Hiltbrunner[2] (1966) have introduced the idea of cross mixing of the vapour or liquid which acts to cancel out the effect of maldistribution of the liquid. Their theory suggests that the number of transfer units of packed columns depends on the degree of maldistribution and on the amount of cross mixing, τ_r, produced in the gas and liquid streams by the movement around the packing element, see Fig. 2.4.

Where $\tau_r = -D \frac{\partial y}{\partial r}$ ..... (2.7)

τ_r = The amount of cross mixing or the horizontal mass transfer.

D = The diffusion constant.

y = The mole fraction in gas phase.

r = Radius of the packed bed.

Huber and Hiltbrunner predicted that in a small diameter column, only a small amount of cross mixing is required to put right a large amount of maldistribution, but that in a large diameter column, (more than 0.5m), the cross mixing will be less effective. Thus, large diameter packed beds are more likely to suffer from maldistribution than small diameter beds. That is, the performance of large diameter packed beds depends greatly on designing effective liquid and gas distributors. If the liquid and gas are uniformly distributed, column scale-up is satisfactory; if not, large diameter columns will fail.

2.2 Design of Distributors

Most packed tower failures are associated with maldistribution

of the vapour or liquid. The failures of "standard" packed towers is mainly due to liquid maldistribution, because in such towers the ratios of packed height to column diameter and vapour feed inlet diameter to column diameter are large. This causes the gas distribution to be usually satisfactory. Thus,there is as yet no scientific basis for the design of gas distributors.

A large diameter vacuum crude fractionation tower is chosen as an example of an extreme need of liquid and gas distribution devices.

2.2.1 Description of the Vacuum Crude Fractionation Column

Vacuum crude fractionation towers work at a very low pressure to increase the relative volatility of the light components in the crude. In the past, when trays were used it was found that to maintain low partial pressure of the vapour, it was necessary to provide "Open" steam to compensate for the pressure drop through the trays.

Modern vacuum crude fractionators make the use of the low pressure drop of packed beds and in most cases use of open steam is no longer necessary.

The example used in this work is a pump around vacuum crude fractionation tower 7.3m in diameter, which consists of three pump around sections, see Fig. 2.5: a bottom stripping section; a heavy gas oil section; and a light gas oil section. Each pump around section contains a bed, which is usually packed to a depth of no more than 2m. The pump around packed bed acts as a condenser. That is, some of the rising vapour is condensed by the liquid which is recycled round the bed passing through an external heat exchanger. The use of the pump around condensing systems causes some of the heat of

condensation to be removed at a high temperature (higher than that of the conventional condensation at the top of the column). This permits more heat recovery to be achieved by exchange of heat to the crude oil feed which is used to cool the pump around heat exchangers.

The section of the vacuum crude fractionator under investigation in this work is the stripping pump around section which is immediately above the feed inlet. Most of the liquid in the feed, which is a mixture of vapour and liquid, is flashed in this section due to the reduced pressure, leaving the slop wax flowing down the column to be removed at the bottom.

The rising vapour passes through a draw-off tray, (troughs and slots type), such that the rising vapour passes through the slots to the packed bed above, and the falling liquid is collected by the troughs and drawn out of the column to a heat exchanger for heat recovery and cooling of the required product which is separated, and the rest of the liquid is recycled to the column above the bed. This liquid will contact the rising vapour in the bed and the condensation process takes place. The remaining vapour goes up for further separation.

There are many practical problems associated with these large diameter columns operated under a reduced pressure, some of which are listed below.

(1) Vapour phase maldistribution is very severe in the packed bed due to the highly maldistributed vapour feed which enters the bottom of the bed and the short depth of the bed compared to its diameter. These two factors reduce the efficiency of the bed due to poor contact between the gas and liquid.

(2) The size of the inlet nozzle is determined by the

flow rate and the degree of vaporization in the feed area. The conventional distillation columns with natural circulation reboilers necessarily have relatively large area inlets, because a large diameter pipe is required to minimize pressure difference between the top of the reboiler tubes and the top space in the column. The vacuum crude fractionator is fed by vapour (and liquid) from the bottom of the atmosphere pressure column which is passed through a pipe still to gain heat. Thus, a large diameter feed inlet is not required. Smaller pipe diameters (about 1m) are used to reduce the cost of the pipe and column.

(3) The pressure drop through these columns is very important in the process of fractionation. A lower pressure drop means a cheaper operating cost by avoiding steam distillation. This necessity limits the design of any gas distributor. Gas distributors (and all the column internals) should be designed to produce the lowest possible pressure drop.

(4) Due to the large diameter, the column internals, such as the draw-off tray, the support plàte, etc., need to be supported by a mechanically strong support beam, which increases the capital cost and the complexity of the tower.

2.2.2 Liquid Distributors

In vacuum crude fractionators, spray type liquid distributors are usually used due to low liquid rates involved in such towers.

Liquid distributors are very important for the successful operation of a packed bed. An ideal liquid distributor should have the following attributes:

1 - Uniform-liquid distribution.

2 - Resistance to plugging and fouling.

3 - High turndown ratio.

4 - High free area for gas-flow.

5 - Sectional construction for installation through manways.

Two basic types of distributor are commonly used: the orifice type and the weir type. Both are gravity flow devices.

Orifice type devices are available in two basic designs: pan or ladder type. The ladder type (Fig. 2.6), is made from perforated pipes. It has a large free area for gas flow. In small diameter towers it is often more convenient to use a pan type orifice distribution.

In weir type distributors, (see Fig. 2.7), a series of closed end troughs are placed across the tower. Notches are cut in the sides of the troughs. The incoming liquid is distributed to the troughs in the appropriate amounts by closed end troughs which rest upon them.

2.2.3 Gas Distributors

Gas distributors are most important in large diameter towers packed to short depths, as is the case of the pump around beds. A good gas distributor should have the following features:

1 - Uniform-gas distribution.

2 - Low pressure drop.

3 - Sectional construction.

Two types of gas distributor are commonly used according to the way of introducing the feed. For a tangential feed inlet, an internal cylinder type gas distributor is commonly used. The internal cylinder is built inside the column below the bed, such that it leaves an annular space for the swirling gas to flow. The tangential motion of the feed helps in separating the entrained

liquid from the vapour. It is believed that the annular gap, (see Fig. 2.8) causes the vapour to be uniformly distributed around the base of the internal cylinder.

In the radial feed inlet situations, the feed inlet is extended inside the column, (see Fig. 2.9). Holes are cut in the sides of the extension which is closed at its end. The vapour is caused to leave the extended feed inlet through these holes.

2.3 Theories of Distribution in Packed Beds

Very little work has been done on the distribution of gases through packed beds, but a considerable investigation of liquid distribution is found in the literature and many theories have been developed to explain the nature of liquid distribution in packed beds.

2.3.1 Theories of Liquid Distribution

The distribution of liquids through randomly packed beds has been studied by many workers[3-16].

There are different kinds of models proposed in the literature to describe the spread of liquid in the packing. In fact, these models can be specified into the following types: Random walk and diffusion models.

(a) Random Walk Models

At very early stages, Thormann[3] (1928) suggested that the spread of liquids in packing may be described as one of a random walk of particles of liquid over the surface of the packed bed. Scott[4] (1935) and Tour and Lerman[5,6] (1939 and 1943) proposed a statistical model based on the random walk probability theory in the absence of wall effects. This work showed an expected normal distribution of liquids below a point source. However, the

mathematical complexities of the random walk theory are such that it is limited to a single point or line source and it is not suitable to predict, for example, the flow below a distributor or the wall effect.

(b) Diffusion Models

Because of this disability in random walk models and because the mathematics of diffusion are in general more convenient than those of random walk, Cihla and Schmidt[7] (1957), Porter and Jones[8] (1963), Dutkai and Ruchenstein[9] (1968) and Onda and Takeuchi[10] (1973) used a diffusion type equation. A radial spread factor is applied in this equation by which the spreading of a liquid stream in a packed bed is characterised. Porter and Jones[8] developed a theoretical model to predict the liquid distribution in terms of two factors, a liquid spread factor and a wall factor. They carried a mass balance on an elemental volume dxdydz, shown in Fig. 2.10, which results in:

$$D \left[\frac{\partial^2 f(x,y,z)}{\partial x^2} + \frac{\partial^2 f(x,y,z)}{\partial y^2} \right] = \frac{\partial f(x,y,z)}{\partial z} \qquad \ldots\ldots (2.8)$$

where

D = liquid spread factor (dimensions:L).

f(x,y,z) = Vertical flow of liquid per unit area in unit time expressed as a function of x, y and z.

x,y,z = Spatial co-ordinates.

This theoretical model predicts flow profiles in a packed column but at small packed depths, the model overestimates the flow next to the wall.

(c) Other Models

There are many other models proposed in this field. Le Goff and Lespinasse[11] (1962) suggested according to their observations that the liquid flow pathways are stable with respect to time. Thus the liquid must follow "Preferred Paths" in the bed, and the liquid cannot be considered to take a random movement as it descends through the packing.

Porter[12] (1968) accepted the stability of the liquid flow pattern but proposed that if the stable flow paths change direction in a random manner then diffusion theory may still be used to predict the expected flow distribution. The agreement between experiment and the predicted flow per unit area will then depend on the number of flow paths, or "Rivulets", collected in the experiment. If a large number of rivulets are collected the agreement will be better than when a small number of rivulets are collected.

Porter, Barnett and Templeman[13] (1968) then used a statistical method based on χ^2 goodness of fit test to calculate the number of the rivulets collected in an experiment from the agreement (or lack of agreement) between experiment and theory.

A model proposed by Charpentier and Le Goff[14,15] (1968) consists of representation of the liquid flow in the form of "Films, Rivulets, and Drops", which describes the form of configuration and texture of the liquid distribution.

Bemer and Zuiderweg[16] (1978) concluded that the bulk of the liquid is flowing through "Stable Channels" through the bed even at good wetting conditions and that a large proportion of the axial mixing has to be attributed to the irregular flow distribution.

There are more recent models, such as the "Parallel Channels Model" and the "Triregional Model" and many others which are

related to the dynamic behaviour of liquid flow and channelling through packed beds.

2.3.2 Point to Point Variation in Liquid Flow

It is obvious from the experimental work performed by the above workers that the liquid leaves the bottom of the bed non-uniformly, and that there is a point to point variation in liquid flow through the packing. Porter[12] described this phenomenon in his theoretical model, "The Rivulet Model", and suggested that the liquid flows in the form of rivulets which sometimes coalesce to form larger rivulets, and sometimes break up into smaller ones.

Similar point to point variations in gas flow through packed beds are dealt with in this work.

2.3.3 Gas Distribution

Nothing has been done on maldistribution of gas flow in packed beds except the work performed by Zaytoun[17] (1981), which describes the gas flow above a randomly packed bed, and which forms the starting point for this work. A hot-point anemometer was used to measure air velocity at several points above a 38 cm packed bed over four equally spaced diameters. The bed was randomly packed with 1.6 cm metal Intalox packing to depths of 12.7 and 25.4 cm. A maldistribution factor ϕ was defined as follows:

$$\phi = \Sigma \left(1 - \frac{v}{\bar{v}}\right)^2 \qquad \ldots\ldots (2.9)$$

where $v, \bar{v}$ = Point velocity and average velocity respectively (measured in ft/min).

The lowest possible value of this maldistribution factor, ϕ_{min}, was obtained and further experiments were performed to investigate the effects of bed height and inlet diameter on the maldistribution factor, see Fig. 2.11. The work showed point to point velocity variations even in deep beds and that the gas distribution is improved with packed height, that is the packed bed itself is a gas distributor. Zaytoun's work[17] provides a starting point to this work.

All the other experimental work on gas distribution which has been done, has been concerned with the variation of gas flow near the column wall and the voidage variation across the diameter of packed beds.

Saunders and Ford[18] (1940) measured the velocities of a gas emerging from the top of a bed packed with uniform spheres. Their results showed a uniform gas velocity distribution in the pack, and about 50% higher velocities in the annular region around the wall, approximately one packing diameter wide.

Schwarts and Smith[19] (1953) have predicted that 30 to 100% higher velocity in the wall region than the average velocity in the centre of the packed bed. They indicated that an important velocity maldistributions exist across the packed bed unless the column to packing diameter ratio is greater than 30.

These workers and many others have performed their works on columns with a large packed height to bed diameter ratios, and all agree that higher gas velocities exist near the column wall than in the rest of the bed, like that obtained by Calderbank and Pogorski[20] (1957), shown in Fig. 2.12. Such a velocity distribution is due to the voidage distribution in packed beds.

Roblee et al., Baird and Tierney[21] (1958) found a decrease in the void fraction from a value of unity near the wall which oscillates in a damped fashion up to a distance of 5 particle diameters. Afterwards the porosity is effectively constant as shown in Fig. 2.13. Such nonuniformities cause channelling which causes a poor performance of packed beds.

2.4 Theoretical Analysis of Flow through Packed Beds

It was seen that a very little has been done on the investigation of gas maldistribution in packed beds. However, a few workers[22-25] have attempted to analyse, theoretically, the flow of fluids through packed beds. These theoretical studies involve the following categories: Dimensional analysis, Dynamic similarity and Gas maldistribution number.

2.4.1 Dimensional Analysis of Two-Phase Flow

Johnston and Thring[22] (1957) demonstrated the incompatibility of choosing values of dimensionless groups when considering the simultaneous effect of the liquid and gas streams on geometrically and dynamically similar packed beds of a different size. In gas-liquid packed towers the flow pattern of the gas phase is controlled by the viscosity of the gas and the pressure difference; the flow of liquid is controlled by liquid viscosity and the force of gravity. The criterion for liquid flow in a packed tower, according to Johnston and Thring, was derived from Nusselt's equation for the isothermal streamline flow of liquid down a vertical wall

$$\frac{W}{l} = \frac{\rho_l^2 g \delta^3}{3\mu_l} \qquad \ldots\ldots (2.10)$$

where, W = liquid rate, kg/sec.

l = length of wetted perimeter, m .

δ = thickness of streamline film, m .

ρ_1, μ_1 = density, viscosity of liquid at film temperature in kg.m.sec. units .

g = acceleration of gravity, m/sec^2 .

For a complete tower packing, this equation may be written

$$Ld = \frac{1}{C} \frac{\rho_1^2 g \delta^3}{\mu_1} \qquad \ldots\ldots (2.11)$$

where, L = Superficial mass velocity of the liquid, $kg/m^2.sec.$

d = Diameter or equivalent diameter of packing elements, m.

C = A constant .

which gives the dimensionless equation

$$\frac{\delta^3}{d^3} = C \frac{L\mu_1}{\rho_1^2 d^2 g} \qquad \ldots\ldots (2.12)$$

For kinematic similarity, δ/d is constant, whence

$$\frac{L\mu_1}{\rho_1^2 d^2 g} = \text{constant} \qquad \ldots\ldots (2.13)$$

This is the similarity criterion for the liquid phase.

For the gas phase, the similarity requirement is a constant Reynolds number:

$$\frac{Gd}{\mu_g} = \text{constant} \qquad \ldots\ldots (2.14)$$

where, G = Superficial mass velocity of the gas, $kg/m^2.sec.$

μ_g = Viscosity of the gas, kg/sec.m.

For chemical similarity, as defined by Johnston and Thring, there is a further requirement of constant liquid/gas rate;

$$\frac{L}{G} = \text{constant} \qquad \ldots\ldots (2.15)$$

In homologous systems, these three requirements reduce to

$$\frac{L}{d^2} = \text{constant} \qquad \ldots\ldots (2.13a)$$

$$Gd = \text{constant} \qquad \ldots\ldots (2.14a)$$

$$\frac{L}{G} = \text{constant} \qquad \ldots\ldots (2.15a)$$

which are incompatible when d is varied.

Therefore, packed towers with two phase flow cannot be scaled up due to the incompatibility problem.

But, it is of value to know the requirements for establishing the rules of scale-up of packed beds. Thus it is possible to investigate flow patterns using models with the gas phase only.

2.4.2 Dynamic and Geometric Similarity in Single-Flow Packed Beds

Moor[23] (1964), has suggested that two steady flows, at high speeds compared with the speed of sound, are dynamically similar if the Mach number, M, Reynolds number, Re, as well as many other properties of the fluid are similar. These include the equation of state (for relating changes of density to changes of pressure and temperature), specific-heat (for relating changes of temperature to changes of kinematic energy), and results on thermal conductivity and on the variation of viscosity and thermal conductivity with

temperature. The following is then a list of nondimensional parameters used in dynamic and geometric similarity:

$$M = \frac{V}{A} \qquad \text{..... (2.16a)}$$

$$Re = \frac{\rho V d}{\mu} \qquad \text{..... (2.16b)}$$

$$Pr = \frac{\mu C_p}{k} \qquad \text{..... (2.16c)}$$

$$\gamma = \frac{C_p}{C_v} \qquad \text{..... (2.16d)}$$

where

V = Velocity of the fluid, (m/sec.).

A = Velocity of the sound in the air, (m/sec).

ρ, μ = Density, (kg/m^3) and viscosity, (kg/m.sec.) respectively.

C_p, C_v = Specific heat at constant pressure and constant volume respectively, (kg-cal/kg.^oC).

k = Thermal conductivity, (kg-cal/m.sec.^oC).

Pr = Prandtl Number, (dimensionless).

γ = Ratio of specific heats, (dimensionless).

It is in general assumed that the Prandtl number depends on the nature of the fluid only. Also, it is often assumed that the ratio of the specific heats γ does not vary with temperature, pressure etc. Therefore, if the same fluid is used in the model and the prototype (as is the case in this work), then only M and Re should be kept constant, but they are incompatible, see eqns. 2.10a and 2.10b. That is, for a model which is exactly geometrically similar to a prototype with scale ratio, R, the gas velocity in the model should be R times that in the prototype to keep Re constant.

This will change the value of Mach number and hence be incompatible. This problem is generally solved, (in wind tunnels), by choosing a different gas in the model whose density is $\frac{1}{R}$ that in the prototype or using the same gas and a different pressure since the speed of sound is independent of the pressure.

But in this work, Mach number values are very small. The maximum air velocity through the model bed is 1 m/sec.

$\therefore$ $M = \frac{1}{340} = 2.9 \times 10^{-5}$

where sound velocity, A = 340 m/sec. at room temperature.

In this case, the bed/feed inlet diameter ratio = 6.

$\therefore$ The maximum air velocity in the feed inlet = 36 m/sec and

$M = \frac{36}{340} = 0.1$ in the feed inlet

which is still very small and may be expected to have a negligible effect on the flow pattern of air through packed beds.

Therefore, the principle of dynamic similarity stated by Kay and Nedderman[24] should be applicable to the systems used in this work. That is, (the flow pattern in the model should be the same as in the prototype provided that Reynolds number of each is the same). The validity of this assumption on packed beds is tested by the experiments described below.

Johnston and Thring[22] stated, that under a viscosity controlled dynamic regime, i.e. Re constant, a geometrically similar packed bed suffers no frictional wall effects. The difference in both interior and boundary surface/volume ratio is compensated by the increased velocity in the model. At equal Reynolds numbers, the gas flow patterns in the model and prototype are similar.

2.4.3 Gas Maldistribution Number

Porter[25] (1982) proposed the idea of a maldistribution number, ϕ, which has a finite but minimum value for the uniform flow

of gas (or liquid) through a packed bed, and that was because:

1. At the small scale (of the order of the dimensions of a packing piece) even the well distributed flow is maldistributed.

2. It is not practically possible to make an exactly geometrically similar small scale model of a large randomly packed bed such that each packing piece is in the same position and orientation in both systems. However, the maldistribution factor should take care of the bed randomness.

The idea of this maldistribution number ϕ, which is defined in equation 2.2, forms the basis of this work where the ability of ϕ to take care of the randomness of the bed is tested.

2.5 Conclusions

Mass transfer through packed beds shows that it is of great importance to provide very uniform gas and liquid distribution in large diameter packed columns. Although considerable work has been done on liquid distribution, nothing has been on gas distribution except the work of Zaytoun[17], which provided the starting point for this work.

There is need for a greater understanding of gas maldistribution in packed columns, and in particular for a method which will permit the design and evaluation of distributors for large diameter packed columns. One approach to this is described below.

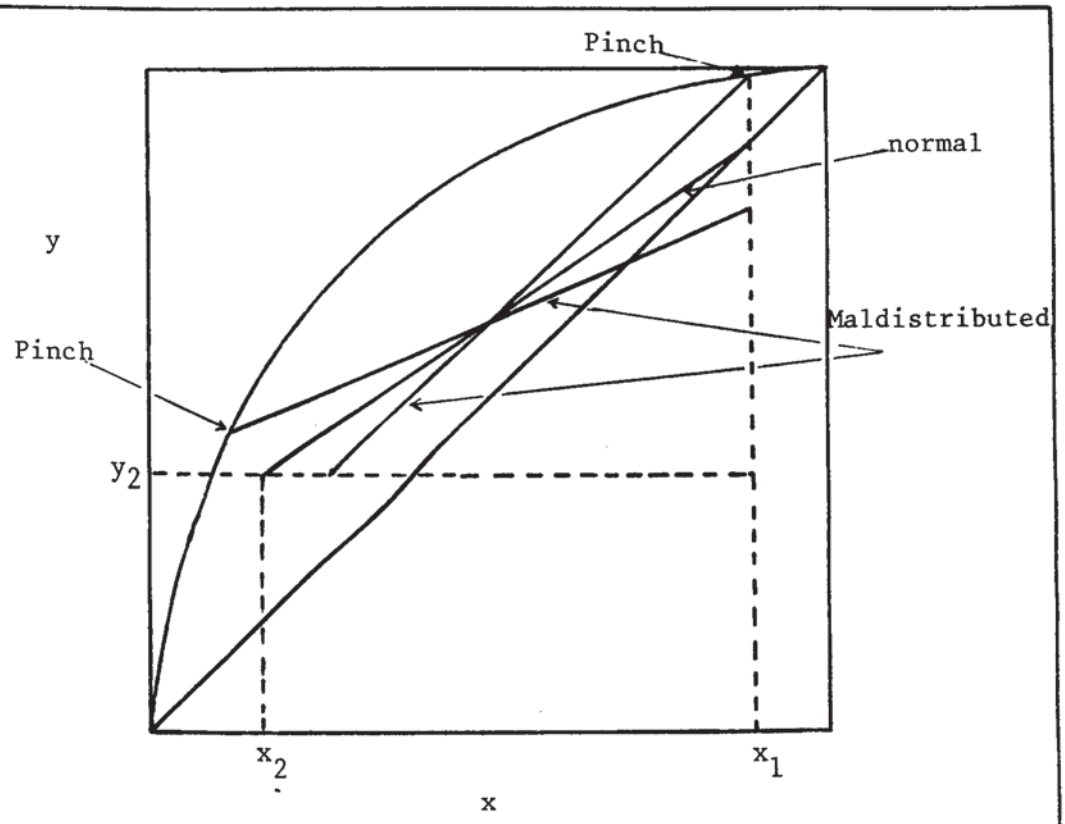

Fig. 2.1 McCabe Thiele diagram for a part of packed bed operating under conditions of maldistribution

Not Equal Liquid Rates

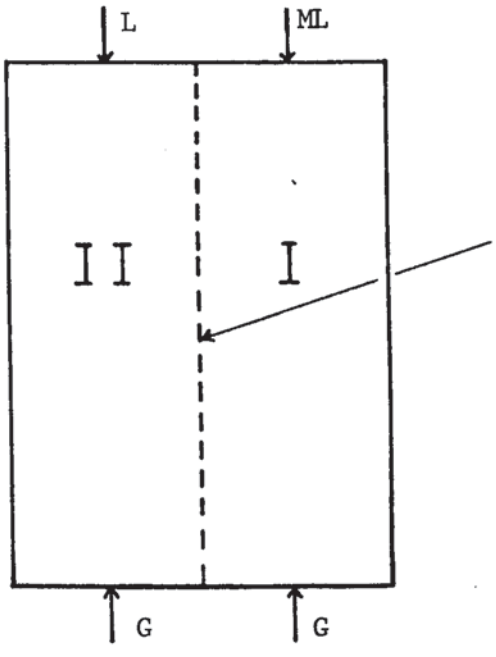

Equal Gas Rates

Fig. 2.2 Simple Channelling Model (after Mullin)

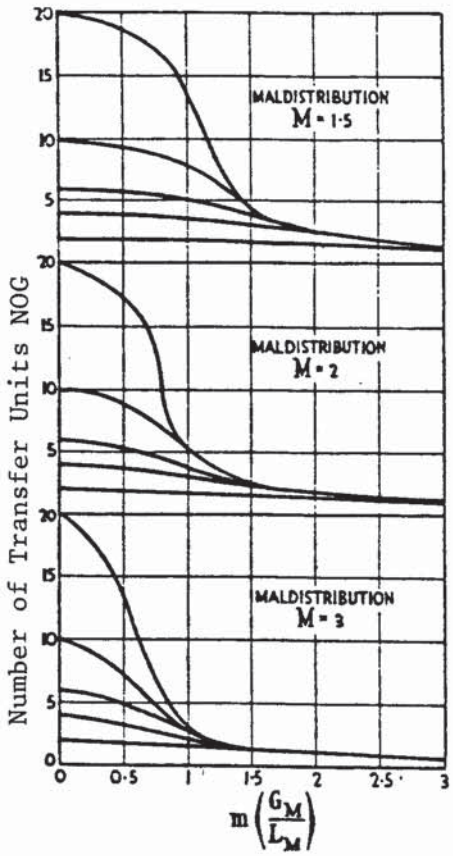

Fig. 2.3 The effect of various degrees of maldistribution on the number of transfer units. (After Mullin[1])

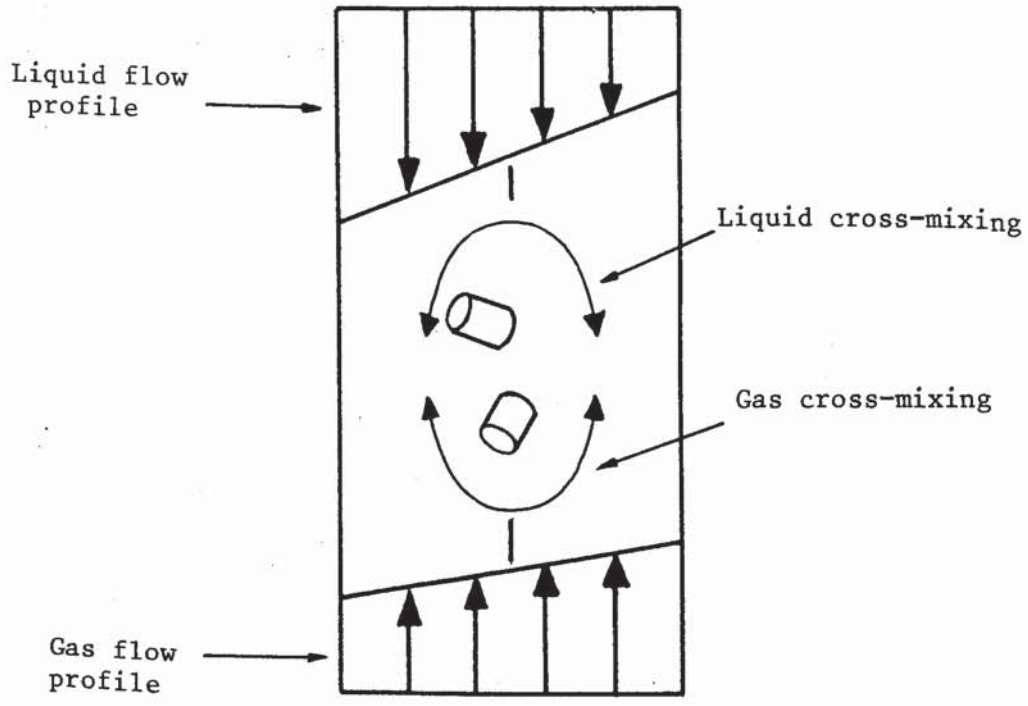

Fig. 2.4 The effect of cross-mixing on maldistribution (Huber[2])

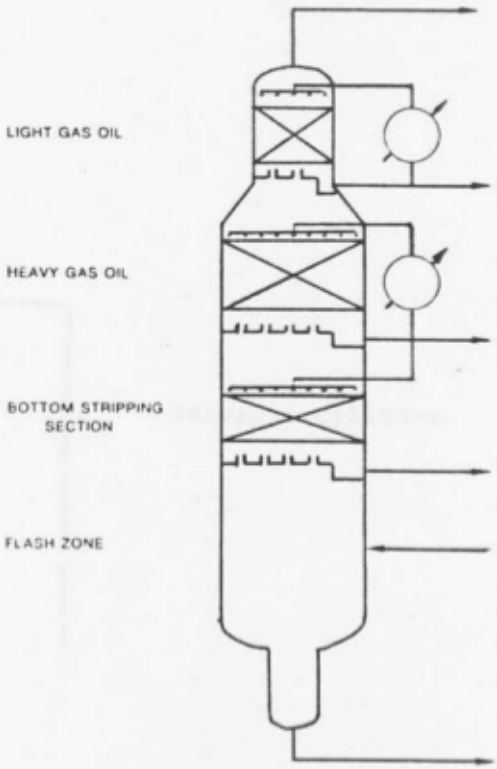

Fig. 2.5 A typical vacuum crude fractionation tower

Aston University

Illustration removed for copyright restrictions

Fig. 2.6 Ladder type liquid distributor

Aston University

Illustration removed for copyright restrictions

Fig. 2.7 Weir type liquid distributor

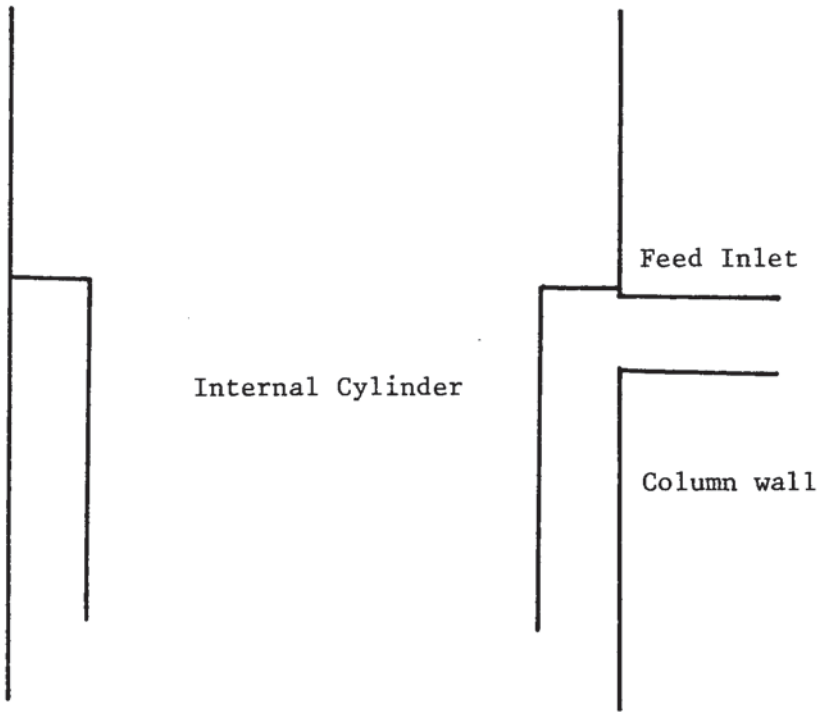

Fig. 2.8 Internal Cylinder gas distributor used with tangential feed inlets

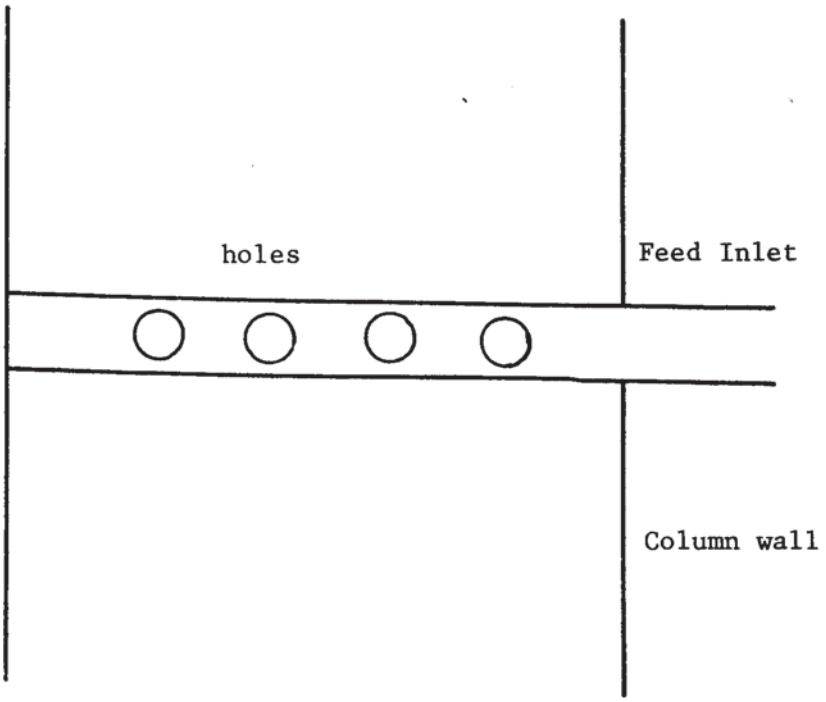

Fig. 2.9 Extended Feed Inlet gas distributor used with radial feed inlets

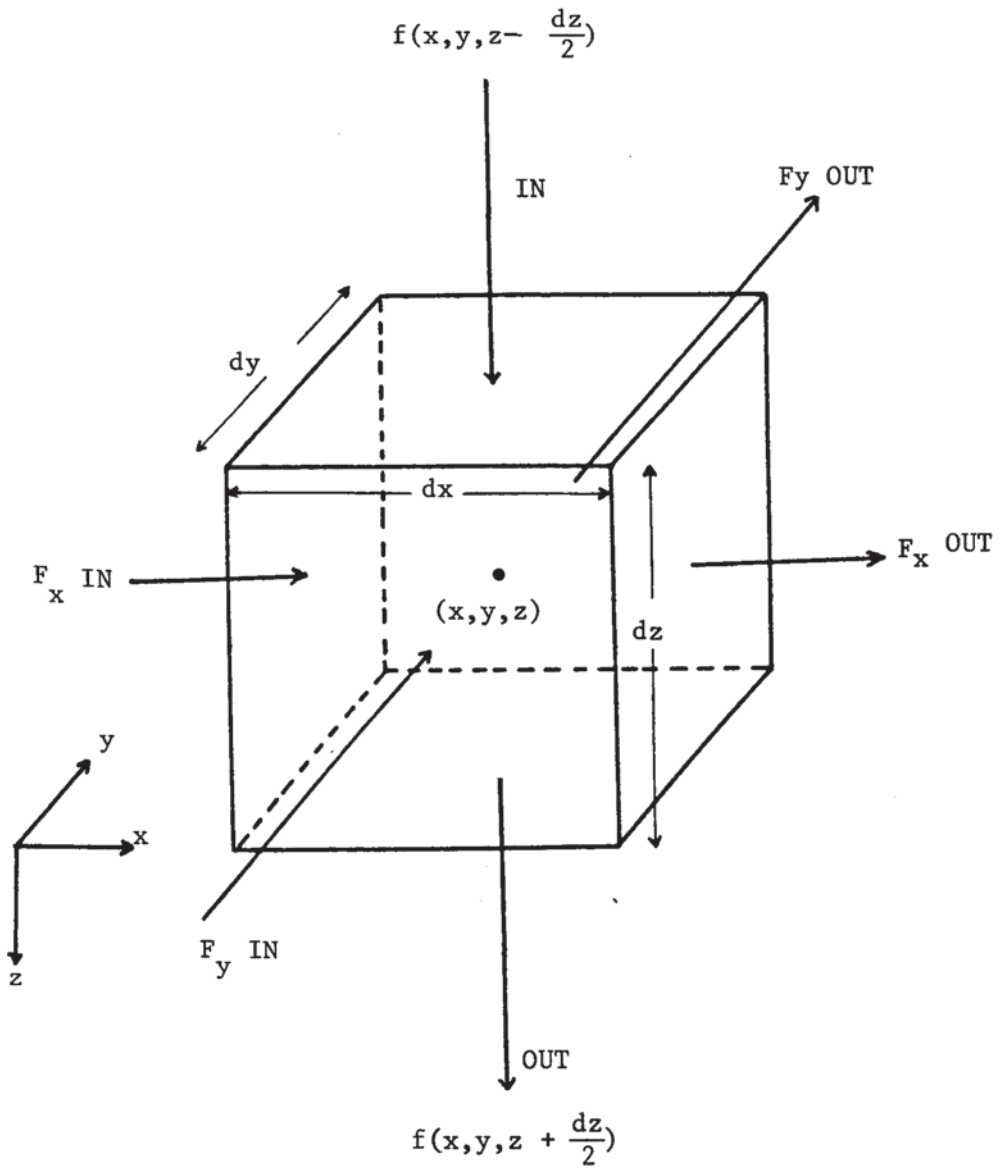

Fig. 2.10 Liquid flows into and from an elemental volume (Porter and Jones[8])

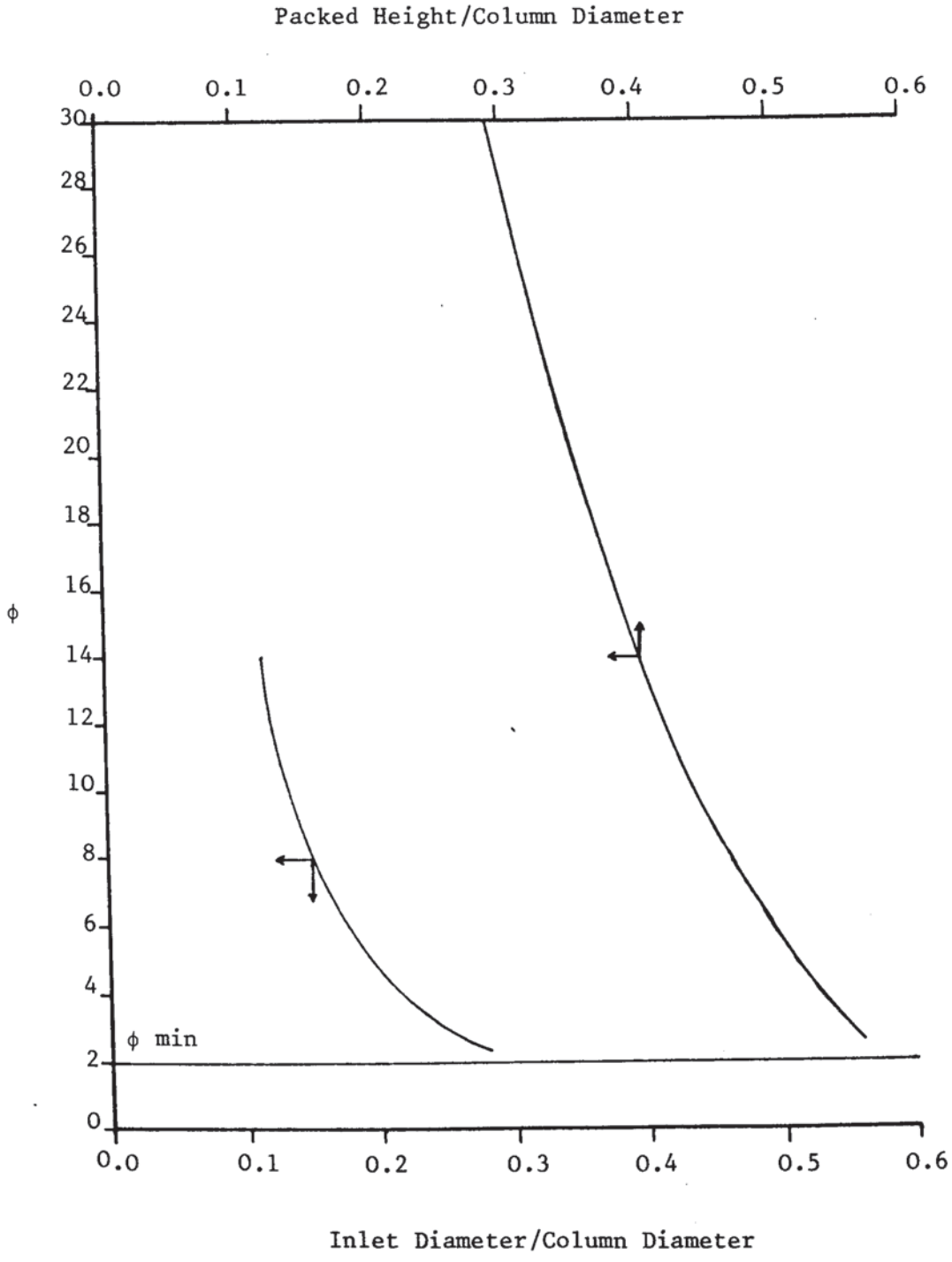

Fig. 2.11 Variation of ϕ with packed height and inlet diameter (Zaytoun[17]).

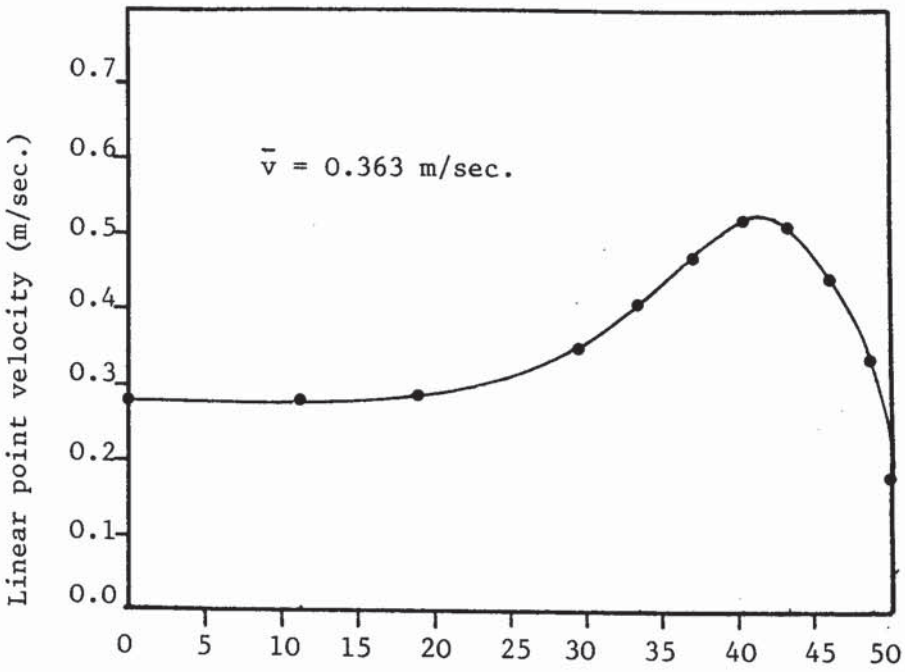
[20]

Fig. 2.12 Radial velocity profile in packed bed for 12.7 mm diameter spheres

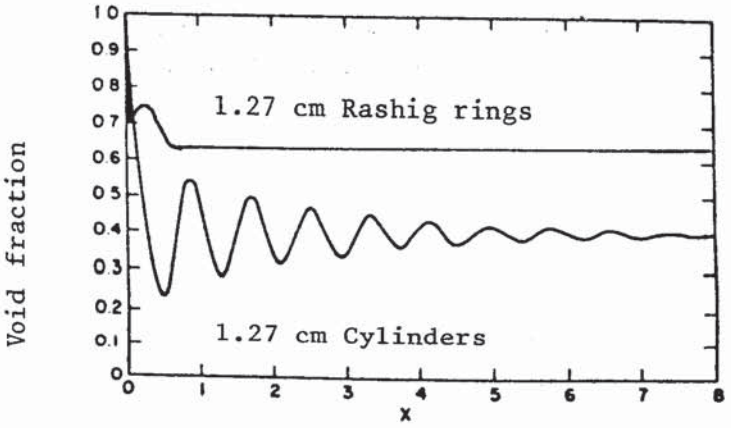

Fig. 2.13 Void fraction versus distance from the wall.
(Results obtained by Roblee et al.[21] in a 17 cm diameter column.)

SECTION III

APPROACH TO THE PROBLEM

It was noted above that the packed bed itself acts as a gas distributor which increases the uniformity of gas distribution.

In this work, the proposal which is investigated is that a gas distribution device may be evaluated in terms of the depth of packing required to reach the best possible uniform gas flow, i.e. a good distributor requires short packed depth; a poor distributor requires large packed depth.

Following Zaytoun[17], the problem of point to point variation in gas flow, is dealt with by defining a Maldistribution Factor which is to have a minimum value for the most uniform flow and a much larger value for a badly distributed flow. The Maldistribution Factor is based on gas velocities leaving the top of the packed bed because these are easily measured. Thus gas distribution devices may be compared in terms of a variation in the maldistribution factor with packed depth.

As the work is directed towards solving the real need for distribution evaluation in large diameter columns, it is necessary to investigate the validity of using dynamic similarity to design experiments on laboratory models of full-scale columns.

This is followed by an investigation into the fluid dynamics of maldistributed gas flow and the work concludes with the development of new low pressure drop distributors for large diameter packed beds.

The main objective of this work can be listed as follows:

(1) Experimental investigation of point to point flow variation in gas emerging from top of a deep packed bed with a uniform inlet distribution.

(2) Definition of the Maldistribution Factor ϕ, and determination of ϕ_{min}, the minimum value of maldistribution factor for a well-distributed gas flow.

(3) Experimental investigation of the variation of ϕ with packed depth as a method of evaluating the quality of feed gas distributors, and simultaneously to investigate whether at Reynolds number dynamic similarity in geometrically similar columns of different sizes, the value of ϕ is the same.

(4) Statistical interpretation of the results by multivariable analysis of the variance to investigate the validity of scale-up rules and provide more insight into the meaning of the maldistribution factor ϕ.

(5) An experimental investigation of the fluid mechanics of maldistributed gas flow.

(6) Simple theoretical models of maldistributed gas flow so as to:

(a) Support scale-up rules.

(b) Identify packed column designs at risk; i.e. subject to gas maldistribution.

(7) Evaluation of existing gas distribution devices in an "at risk" packed tower. The example chosen is the pump around section of 7.3m diameter vacuum crude distillation column.

(8) Development of new low pressure drop gas distributors for large towers.

SECTION IV

EQUIPMENT

Introduction

In all of the experiments, air was caused to flow through packed beds of various designs. This section describes the equipment used to provide the air supply and measure the rate of flow. It also describes the techniques used to measure point velocities and to reduce noise level.

4.1 Air Supply Equipment

Air was pumped under atmospheric pressure into the packed bed from a 10 horse power fan through a 152mm inside diameter QVF pipe. The flow could be controlled by means of two butterfly valves of 152 mm inside diameter, and measured by a "Dall Tube" flowmeter of the same pipe diameter, see Plate 4.1.

In order not to exert pressure on the fan, the excess air was released through a specially designed silencer to atmosphere. The piping system and the silencer were supported by a bench built of 38 x 38 mm steel handy angle bars. The QVF tubes are fitted to the bench by specially designed wooden attachments and secured by belts to the attachments, see Plate 4.1, and the whole system is on the same level as the fan exit. The fan exit is joined to the QVF pipe by a 600 mm long and 180 mm inside diameter flexible tube to absorb the vibration and the start-up shock of the fan. Air enters the test column through changeable nozzles of different sizes.

4.2 Measurement of Flow, Velocity, and Pressure

In the experiments described in this work, special techniques were used to measure total flow rates, point velocities and pressure.

These are described below.

4.2.1 Flow Measurement by a Dall Tube

The Dall Tube was chosen due to its short length, 152 mm, and low pressure loss. The Dall tube, see Fig. 4.1, consists of a short length of parallel lead-in-pipe followed by the converging upstream cone and the diverging downstream cone. A small gap between the two cones allows the fluid to fill the annular space between the liner and the case. The throat pressure is transmitted to the annular chamber and then via a pressure pipe to the measuring instrument.

The Dall Tube has the desirable features of high measured pressure drop (similar to an orifice)[26], and low permanent pressure loss (pressure difference between fully developed upstream flow and fully developed downstream flow), similar to, and sometimes better than, a venturi. These apparently inconsistent advantages have been checked experimentally but are not fully explained theoretically. The permanent pressure loss of a Dall tube is of the order of 50% or less of that of a venturi tube with the same pressure drop.

However, Kent[27] summarizes the important advantages of the Dall tube over other kinds of variable-pressure-drop flow meters; the flow nozzle and the venturi tube, and these advantages are as follows:

(a) Lowest head loss; the pressure loss of the Dall tube varies between $\frac{1}{2}$ and $\frac{1}{3}$ of that of the long-pattern venturi tube.

(b) Easier and cheaper installation than a venturi tube. The length and weight of the Dall tube are about $\frac{1}{2}$ those of a short-pattern venturi tube.

(c) Lower first cost than venturi tube owing to economies in materials and machining.

The Dall Tube flow was calibrated against the flow calculated from the velocity profile measured by a hot-wire anemometer, see Appendix 1A.

4.2.2 Velocity Measurement by a Hot-Wire Anemometer

Hot-wire anemometers are commonly made in two basic forms; the constant-current type and the constant-temperature type[26]. The difference between these types is primarily in the electric circuits.

The hot-wire anemometer consists essentially of an electrically heated, fine wire (generally platinum) exposed to the gas stream whose velocity is being measured. An increase in fluid velocity increases the rate of heat flow from the wire to the gas, thereby tending to cool the wire and alter its electrical resistance. In a constant-current anemometer, gas velocity is determined by measuring the resulting wire resistance; in the constant-temperature type, gas velocity is determined from the current required to maintain the wire temperature, and thus the resistance, constant.

For the measurement of average (steady) velocities, the constant-temperature mode of operation is often used (as in this work). Another factor may effect the rate of heat flow from the wire, namely the gas temperature which effects the convection film coefficient, therefore, to get more accurate work, a given hot-wire probe must be calibrated in the fluid in which it is to be used. For this purpose the anemometer must be set to zero by putting the probe in a hole in which the fluid velocity is zero, where both the

probe and the hole have the same temperature as the fluid stream.

The hot-wire anemometer can accurately measure velocities from about 0.15 m/sec. to supersonic velocities.

4.2.3 Modification of the Hot-wire Anemometer

A 3000-ETA hot-wire anemometer was used in this work, (see Fig. 4.2), to measure point velocities above the bed. Some modifications were made to the anemometer to suit the measurement procedure.

This type of hot-wire anemometer is compact, hand held and measures air velocities from 0.1 m/sec up to 15 m/sec with a semi-logarithmic scale. The probe is situated in the middle of a 10 mm diameter hole in an arm 15 mm diameter and 160 mm long which can be extended to give a maximum length of 850 mm. The arm is connected to the meter by 2m, telephone-type, probe wire. The arm should be positioned such that the hole is exactly in-line with the air stream. This design does not always suit the sampling procedure followed in this work, because, sometimes it is necessary to hang the arm from a position high above the column to read point velocities just above the packed bed inside the column with minimum or negligible obstruction to the air stream emerging from top of the bed. So, the ordinary extension to the arm was removed and the probe-cable was inserted inside a 6 mm diameter steel extension 1.5m long and fitted to the arm in a way such that the arm could be put either in-line with, or perpendicular to this new extension. The other end of the extension was clamped to a spirit level to ensure accurate positioning of the probe, and graduations were engraved on this new long, convenient arm, (see Plate 4.2). Also, the power was supplied through a stabilized transformer instead of a battery power supply

which decays after 20 hours work. The use of stabilized DC supply is very essential, because in an ordinary transformer, the output DC has a resonance which is detectable on the hot-wire anemometer and a distorted air velocity reading is obtained. The stabilized transformer solves this problem, where the output power is smooth.

4.2.4 Measurement of Pressure by a Micromanometer

A micromanometer was used to measure very small pressure variations throughout the packed bed. The MDC micromanometer, shown in Plate 4.3, was chosen because it is a sensitive pressure measuring device capable of measuring gas pressures down to 10 dynes/cm^2 for Full Scale Deflection, (F.S.D.). This is equal to 0.004" wg (0.1 mm). Its accuracy as a percent of F.S.D. of the instrument is 0.1%.

To measure the pressure difference, the micromanometer should be adjusted to read zero on the scale before any connection. The pressures to be measured are taken to the measuring head via two small hose entries on the front panel of the instrument, one hose entry for the low pressure side, the other for the high pressure side. The measuring head consists of two symmetrically arranged cavities separated by a metal diaphragm. The diaphragm, together with a fixed electrode on either side, forms two condensers. Movement of the diaphragm due to a pressure difference in the cavities causes a variation in the capacitance between it and the adjacent electrode, thus unbalancing the voltage across the circuits. These voltages are compared by a differential voltmeter, and the difference is amplified and is shown on a meter calibrated directly in pressure. The diaphragm in the measuring head will respond to sine wave pressure variation up to 200 pulses/sec. or more, but the long length of the PVC tubes (3m each) acted as attenuators.

To read static pressure at a point in the packed bed, the high pressure entry is connected by the 3m long PVC tube 2mm inside diameter, the other end of the tube is connected to the static pressure side of a pitot-static tube whose circumferential ring of small holes is at that point. The low pressure side of the manometer is left open to atmosphere.

To measure air velocity at a point in a swirling stream or straight stream below packed beds where the velocity varies significantly from point to point, the low pressure side is connected to the static pressure side of a pitot-static tube and the high pressure side is connected to a 0.5 mm inside diameter steel tube which measures the total pressure. The open end of the tube was put as near as possible to the circumferential ring of holes on the pitot-static tube, they should not be very close to each other to avoid interfering between them, (see Plate 4.4).

4.3 Noise Reduction by the Development of a Special Silencer

A major source of noise in process plant is from moving fluids, particularly gases. In this work, noise comes from the vent to discharge excess air, from the blower and from the motor.

The noise generated by flowing of air in the blower inlet was reduced by lining it with 2 cm thick sponge. The mechanical noise was reduced by sticking sponge all-over the blower. At the vent, noise caused by the high velocity discharge is created by the shearing action of turbulent air mixing with the essentially stationary outside air.

A simple silencer was designed to achieve two aims:

(1) To reduce the level of the noise by orienting the discharge vertically to direct the noise away from the work area, and

to keep the noise source as far away as possible.

(2) To act as an attenuator to absorb the fluctuation of the flowing air, where it has been noticed that without this silencer the air velocity, detected by the hot-wire anemometer, was fluctuating above the bed with frequency of around 0.5 cycle/sec.

Air enters the silencer through a 152 mm diameter butterfly control valve. The silencer itself, (Figure 4.3), consists of the following parts:

(a) Two QVF pieces 300 mm inside diameter flanged together to form a pipe 2m long standing vertically on a bench and closed at the bottom. This part acts as a reservoir to absorb the flow fluctuation.

(b) A perforated 12 mm thick PVC plate, with holes 5 mm in diameter and 50% free area; (the total free area equals the silencer outlet area and double the inlet area to reduce the likelihood of regenerated noise). Each hole will act as a pipe to generate some pressure for uniform upstream flow

(c) A QVF reducer flanged to the part described in (a) holding the perforated plate described in (b) between the flanges, and flanged from above to a 200 mm diameter QVF pipe, 1 m long, to the exit which was made as high as possible.

By this special design, the noise level is reduced to less than half of its level without the silencer, and the air emerging from the bed is flowing smoothly.

Fig. 4.1 Cross-section in a Dall Tube

Fig. 4.2 Ordinary Hot-wire Anemometer

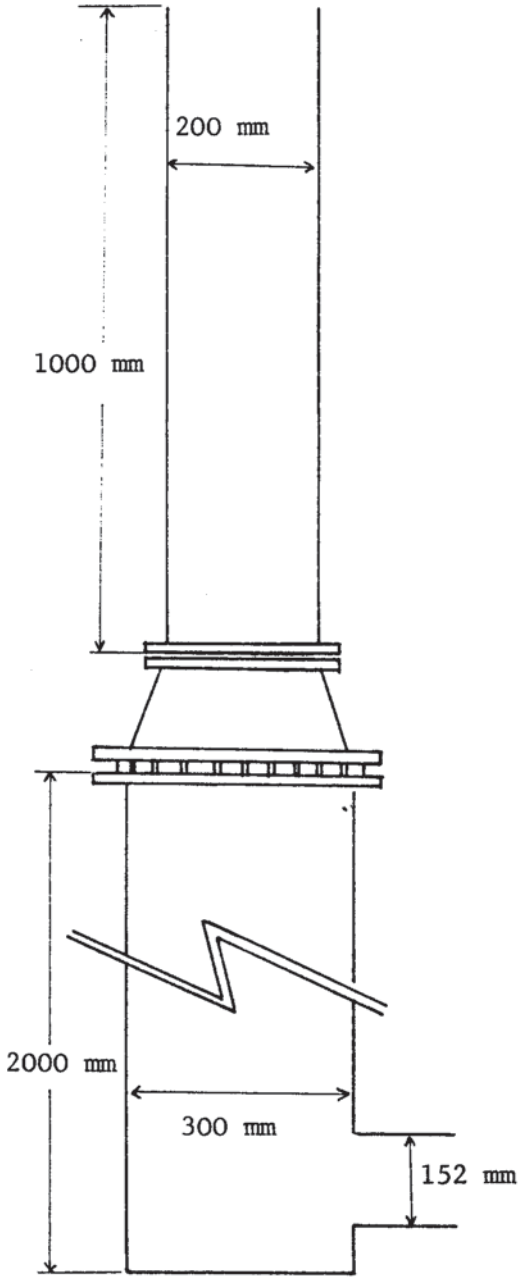

Fig. 4.3 Diagram of the Specially Designed Silencer

PLATE 4.1

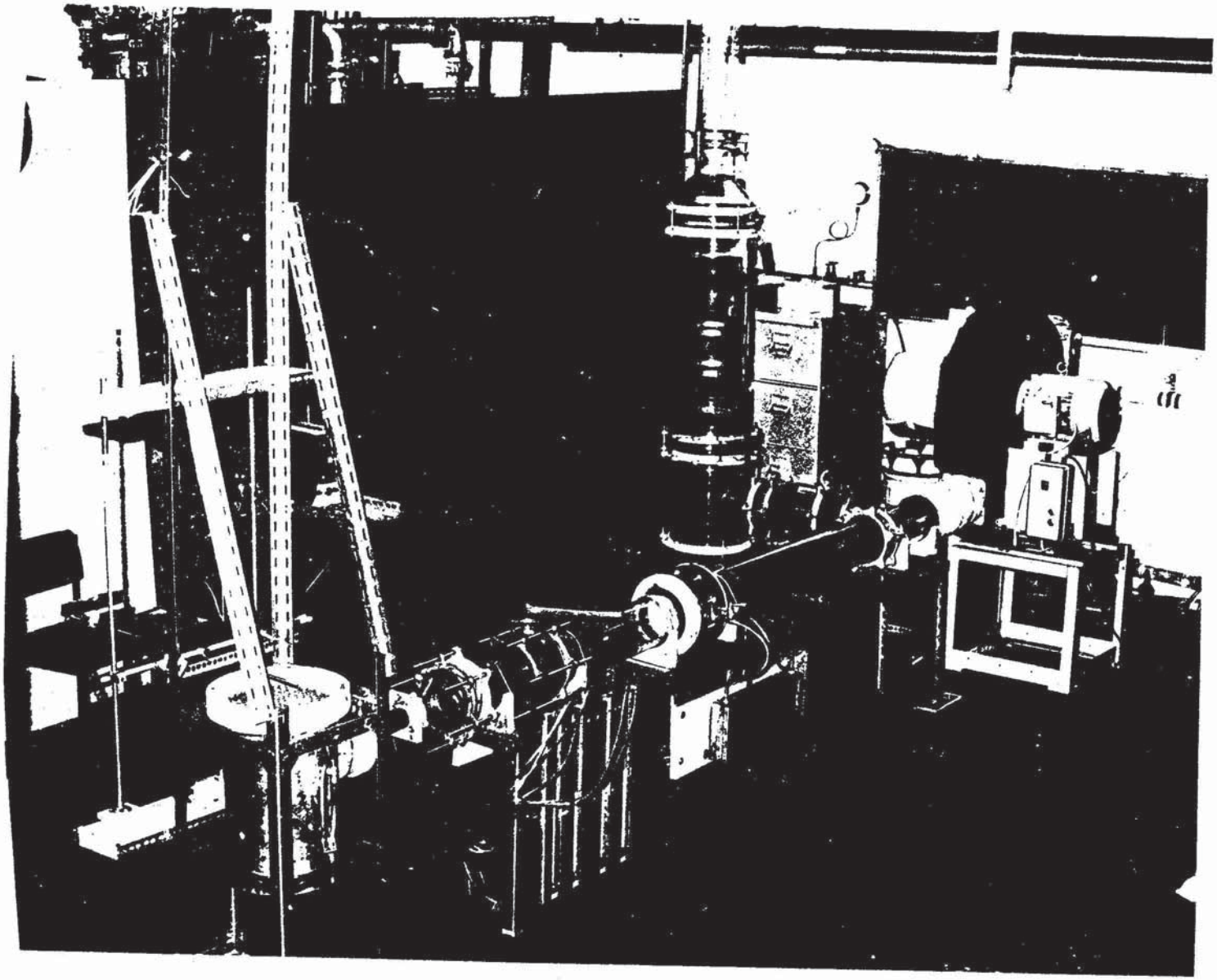

PLATE 4.2

E.T.H.

PLATE 4.3


Micromanometer
FURNESS CONTROLS LTD.
BEXHILL ENGLAND
M.D.C.
PRESET ZERO
CALIBRATE
SCALE LENGTH
MAINS
x100
x30
x10
x3
x1
FAST METER
OUTPUT

PLATE 4.4

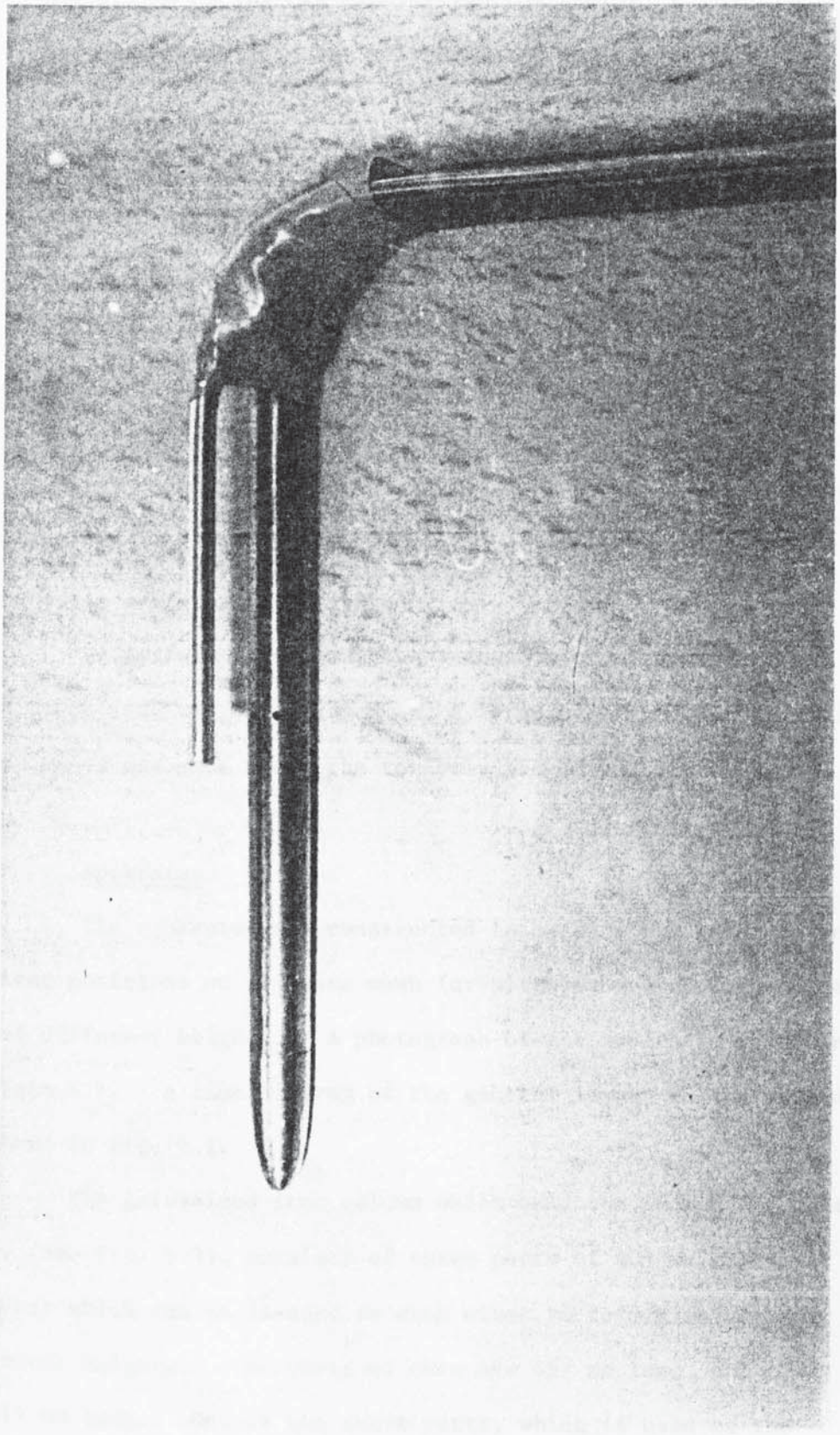

SECTION V

POINT TO POINT GAS VELOCITY VARIATION, DEFINITION OF THE GAS MALDISTRIBUTION FACTOR, ϕ AND DETERMINATION OF THE MINIMUM VALUE OF ϕ, ϕ_{min}.

Introduction

There are two objects in the work described in this section;

(1) An experimental investigation of point to point flow variations in gas emerging from the top of a deep packed bed with a uniformly distributed gas entering bottom of the bed.

(2) Definition of a gas maldistribution factor, ϕ, and determination of ϕ_{min}, the minimum value of the maldistribution factor for a uniformly distributed flow.

To perform this work, the technique of measuring gas point velocities was established and a large number of point velocity measurements was made above the randomly packed bed.

5.1 Apparatus

The apparatus was constructed to measure the point velocity at fixed positions on a square mesh (or pitch) above a randomly packed bed of different heights. A photograph of the apparatus is shown in Plate 4.1. A line diagram of the general layout of the apparatus is shown in Fig. 5.1.

The galvanized iron column which held the packed bed under test, (see Fig. 5.2), consists of three parts of 305 mm inside diameter which can be flanged to each other to form a column of different heights. Two parts of them are 457 mm long, the third is 914 mm long. One of the short parts, which is used as the

bottom part, was fitted with one flange, the other two parts were each fitted with two flanges. All the flanges are 308 mm inside diameter to fit the outside of the column, and 38 mm wide and 6 mm thick. Four wooden rings lined with galvanized iron were made, with an inside diameter of 305 mm, 38 mm wide and 25.4 mm thick. These rings enabled a series of short bed heights to be obtained. A 9.5 mm square mesh made from 1 mm diameter wire was used as a packing support. A similar mesh was put over the bed to prevent the packing from floating at high air velocities. A 1.5 mm thick galvanized iron ring of 10 mm width with six attachments to the column shell was designed to hold securely the support wire mesh. The air was fed radially to the column through a 152/51 mm diameter QVF reducer, the reduced end was extended by a 457 mm long PVC pipe 51 mm inside diameter, which is flanged to the column at the feed inlet.

An elaborate gas distributor was designed, (see Fig. 5.3), to give an even gas distribution below the bed. It consists of three parts;

(1) A galvanized iron cylinder of 254 mm inside diameter and 355 mm long, fitted with a flange 305 mm outside diameter at the top end. 8 slots, each 50 mm long and 30 mm deep, were made at equal distances at the bottom end of the cylinder. This was inserted inside the bottom part of the column which is blocked at the bottom end by a PVC plate such that the 8 legs between the slots are fitted securely to the blocking plate and the flange is positioned just above the feed inlet. A sealant was used to close any gap between the flange and the inside surface of the column. A small wooden screen was put in the annular space between the column

shell and the cylinder near the feed inlet to direct the feed in one direction, forcing the air to swirl in the annular space. The swirling air, after travelling a long distance from the feed inlet down to the slots at the base, which is about 6 times the feed pipe diameter, is distributed equally around the base of the cylinder. This equally distributed swirling air which enters the cylinder through the 8 slots of equal areas, will swirl uniformly inside the cylinder travelling upwards a distance of 203 mm to ensure a complete mixing before hitting four baffles measured 152 x 127 mm fitted to each other to form a cross baffle whose duty is to straighten the flow of the air before leaving the cylinder.

(2) Air leaving the cylinder enters the next part of the distributor which is a uniform bed of knitted mesh, 305 mm diameter and 100 mm high, held between two pieces of 300 mm diameter wire mesh, and fitted to the flange of the cylinder.

(3) Above the knitmesh, a perforated PVC plate, 380 mm diameter and 13 mm thick, is fitted. The 729 perforations are distributed on 1 cm square pitch, each 5 mm diameter. Each performation will act as a tube; (length more than diameter), to produce a high pressure drop for even gas distribution. This plate, with 20% free area, is flanged between the bottom part and the main part of the column which contains the packed bed. In a preliminary check, the velocity of the air emerging from each of the holes was measured and found to be constant.

The support ring and the support wire mesh were fitted to the main part of the column at a distance of 150 mm above the perforated plate, so as to ensure a complete mixing of the air jets before entering the bottom of a bed randomly packed with 25.4 mm plastic pall rings to different heights.

This design of apparatus ensured a uniformly distributed air flow entering the bottom of the bed. This is subsequently referred to as the "Ideal distributed case".

On the other hand in the "Maldistributed case"; (where the feed enters the bed as it is, without passing through any kind of distributor), the distributor is removed and the feed entered radially to the column through the feed pipe of a relatively small diameter; (51 mm).

A modified hot-wire anemometer, described in Section 4.3, was used to measure the point velocities above the bed.

5.2 Gas Velocity Distribution Measurement Technique

The point velocities above the bed were measured by a modified hot-wire anemometer, with the arm in-line with the extension, (see Plate 4.2). A scaled extension was clamped at right angles to a fixed scaled rail, such that the anemometer's arm can be moved to any required position across the bed by moving the scaled extension in the x and y directions along the fixed rail.

Two more important factors should be known to establish the complete proposed technique of measuring the gas velocity distribution above a packed bed;

(1) The first is how far the anemometer probe should be situated above the bed to measure point velocities of different magnitudes.

It was found experimentally for a large range of gas flow rates, that a measured velocity of air at a specific point in the surface of the bed depends on the distance above that point that the anemometer's probe is situated. As the probe departs from the bed, the measured velocity decreases until reaching a position at which

the velocity remains constant over a short range of distances, after this range of distances, the measured velocity either increases or decreases. The probe was situated within this range of constant velocity. Also, it was found experimentally that this range of distances does not depend on the gas velocity at that point, but it does depend on the size of the packings.

The results show that for a wide range of air flows and for plastic pall rings of size 16 mm, 25.4 mm and 50.8 mm, the probe should be at a distance of 35 mm, 55 mm and 110 mm above beds packed with these different sizes respectively.X

(2) The second important thing was to minimize the number of point velocity measurements to give a reliable estimation of the maldistribution of the gas emerging from the top of a packed bed. This depends on the configuration of the points at which the air velocity is measured and on the definition of a maldistribution factor which gives an estimation of gas maldistribution in the packed beds.

It is a fact that in the packed beds there exist a variation in the magnitude of gas velocities from point to point across the bed due to various pathways that the gas follows through the packing. These pathways change when the bed is repacked. This fact is observed very clearly during the course of this work. This means that a full scanning of the velocity variation is required to obtain the most reliable picture of the distribution of the gas.

The way to do this scan is to measure the gas velocity at close enough, equally spaced positions.

Thus, the point velocity measurements were taken on a square mesh at a suitable distance above the packed bed.

X See additional comment on P.54.

5.3 Definition of Maldistribution Factor ϕ and Determination of ϕ_{min}

In this part of the work, two aims were achieved, the definition of a Maldistribution Factor and the minimum number of point velocity measurements required to obtain a reliable estimation of this maldistribution factor.

An appropriate maldistribution factor must have two essential properties:

(1) It varies significantly according to the quality of gas distribution.

(2) It has a minimum value for a well distributed gas flow and a much larger value for a maldistributed gas flow.

An attempt has been made to define a factor which gives an idea about the uniformity of the distribution based on the variance, σ^2, where

$$\sigma^2 = \frac{1}{n-1} \sum_{i=1}^{n} (\bar{V}-V_i)^2 \qquad \ldots\ldots (5.1)$$

n : The number of positions at which point velocity is measured

$\bar{V}$: Value of the average point velocity, (m/sec.)

V_i : Value of point velocity at ith position (m/sec)

Equation 5.1 can be rewritten as:

$$\sigma^2 = \frac{\bar{V}^2}{n-1} \sum_{i=1}^{n} \left(1 - \frac{V_i}{\bar{V}}\right)^2 \qquad \ldots\ldots (5.2)$$

The summation term is taken as the "Maldistribution Factor", ϕ,

i.e.

$$\phi = \sum_{i=1}^{n} \left(1 - \frac{V_i}{\overline{V}}\right)^2 \qquad \ldots\ldots (5.3)$$

Equation 5.2 states the mathmetical formulation of ϕ which is the sum of deviations of point velocities from the average value of the point velocity. The properties of the maldistribution factor ϕ are estimated experimentally in this section of the work.

5.4 Experimental Work and Results

The experimental work was carried out on two extremely different beds packed with 25.4 mm plastic pall rings; a well-distributed bed and a maldistributed bed. The well-distributed bed, which represents an "Ideally distributed case", that is, the feed is uniformly distributed, is packed to a depth of 1220 mm, which is much greater than the bed diameter, (305 mm). The badly distributed bed was a shallow one with a packed depth, (51 mm), much less than the diameter, (305 mm), when air is fed through a relatively narrow pipe, (51 mm in diameter), without any distribution.

The first aim of these experiments is to evaluate ϕ for a well-distributed bed and at extremely maldistributed conditions so as to define the minimum value that ϕ can have and to find out the reliability of ϕ for describing gas maldistribution; the more the difference between ϕ_{min} and ϕ for a maldistributed bed, the more the reliability of this maldistribution factor.

The second aim is to minimize the number of point velocity measurements required.

Different numbers of point velocity measurements were taken at a distance of 5 mm above these two beds, the beds were then repacked several times, and each time the bed was rep acked, the

same numbers of point velocity measurements were made. This procedure was carried out at different Reynolds numbers for the ideally distributed case so as to estimate (if any) the effect of Reynolds number value on ϕ_{min}.

Examples of complete sets of observations are given in Tables 5.1 and 5.2. A computer program to evaluate ϕ is given in Appendix A2. The processed data is shown in Tables 5.3 and 5.4. In these tables a different value of ϕ was obtained each time the bed was repacked. These values of ϕ are averaged to obtain $\bar{\phi}$ which represents the average maldistribution of the gas emerging from the top of a packed bed. $\bar{\phi}$ is then divided by the corresponding number of point velocity measurements so as to evaluate the minimum number of measurements required. The smallest number of measurements which produces a $\bar{\phi}/n$ ratio nearest to that ratio obtained from the largest number of measurements, is considered as the minimum number required to obtain a reliable evaluation of ϕ.

5.5 Discussion of the Results

Table 5.3 summarizes the results obtained for a deep packed bed which is fed by uniformly distributed air. The results show that for 161 point measurements, $\bar{\phi}/n = 0.1025$ and for 100 point measurements, $\bar{\phi}/n = 0.097$, which are 2.3% and 7.6% below that obtained for 649 point measurements respectively. Therefore 161 point measurements could be considered as the minimum number that gives a reliable estimation of ϕ. This conclusion could also be reached for maldistributed case, where $(\bar{\phi}/n)$ for 161 point measurements is 2.6% less than that obtained for 649 point measurements.

The values of ϕ in both of these beds change as the beds were repeacked, these changes express the fact that the pathways followed by the gas through packed beds change when a repacking takes place.

Also, it could be noticed that for each bed, ϕ values are scattered around an average mean within a range of $\pm$ 30%.

But the most important thing to be noticed is that $\bar{\phi}$ for the maldistributed case is more than 11 times greater than that obtained for the ideally distributed case.

The average value of ϕ obtained for the ideally distributed case is subsequently referred to as ϕ_{min}, the minimum value of ϕ, which has a constant value at different Reynolds number values where Reynolds number, Re, is defined as:

$$Re = \frac{\rho \bar{V} D}{\mu} \qquad \ldots\ldots (5.3)$$

where

ρ = Air density (kg/m^3).

$\bar{V}$ = Average value of point velocity, (m/sec).

D = Bed diameter, (m).

μ = Air viscosity, (kg/m.sec.).

The non-zero value of ϕ_{min} is explained by the fact that point to point velocity variations do exist in packed beds, and an even gas distribution could not be reached due to the pathways followed by the gas through the bed which cause this unavoidable maldistribution estimated by ϕ_{min}.

Comparing the observed data for a well-distributed bed and a maldistributed bed given in Tables 5.1 and 5.2, it could be noticed clearly that for a well-distributed bed, point velocities either above or below the average value, are randomly distributed all over the bed.

But for the maldistributed bed, there exists a number of point velocities concentrated in one region which all have relatively very low velocities. At the same time, there exists a concentration of high point velocities in other regions. The region near to the feed inlet contains the lowest point velocities and that opposite to the feed inlet has the highest point velocities. From this it could be concluded that ϕ_{min} represents the summation of point to point velocity variations, and ϕ represents that variation plus the variations due to the regional variation of gas velocity.

It is important to note that the obstruction to the flow of the gas caused by the anemometer's probe is not effective since the relative velocity is measured. Also, because of low values of point velocities involved in the experimental investigation, and due to the dimensionless nature of ϕ, the values of point velocities were measured in ft/min. instead of m/sec. to avoid large reading errors.

5.6 Conclusions

The following conclusions could be abstracted:

(1) Point to point velocity variations do exist in a gas emerging from deep packed beds with a uniformly distributed gas entering the bottom of the bed. These variations are due to the existence of discrete pathways followed by the gas throughout the bed. These pathways change on repacking the bed.

(2) The defined maldistribution factor, ϕ, has a minimum value when the bed is deep and a well distributed gas enters the bottom of the bed.

(3) ϕ has a larger value for maldistributed beds.

(4) For a packed bed, ϕ has values scattered around an average value, $\bar{\phi}$, within a range of ± 30%.

(5) The minimum number of point velocity measurements required to give a reliable ϕ value is around 161 for the types of beds used in this work.

5.7 Summary

A technique was established to evaluate gas maldistribution above a packed bed and a maldistribution factor, ϕ, was defined. ϕ has a minimum value for an ideal bed; deep and fed by a uniformly distributed gas. Also, ϕ has a much larger value for a shallow bed with feed introduced through a relatively small pipe to the column and in which the gas was not evently distributed. In the next section, an investigation of the effect of packed height on gas distribution in the bed is going to be made.

Additional Comments

1. It was found that when the anemometer is positioned above the bed, at the distances specified on p. 48, the total air flow calculated from $\bar{v}$ differs by not more than 5% from the true air flow measured in an empty pipe. See Appendix A1.

2. There is no systematic increase or decrease of ϕ with repacking. The results are presented in order of increasing ϕ values in order to demonstrate the maximum variation in magnitude.

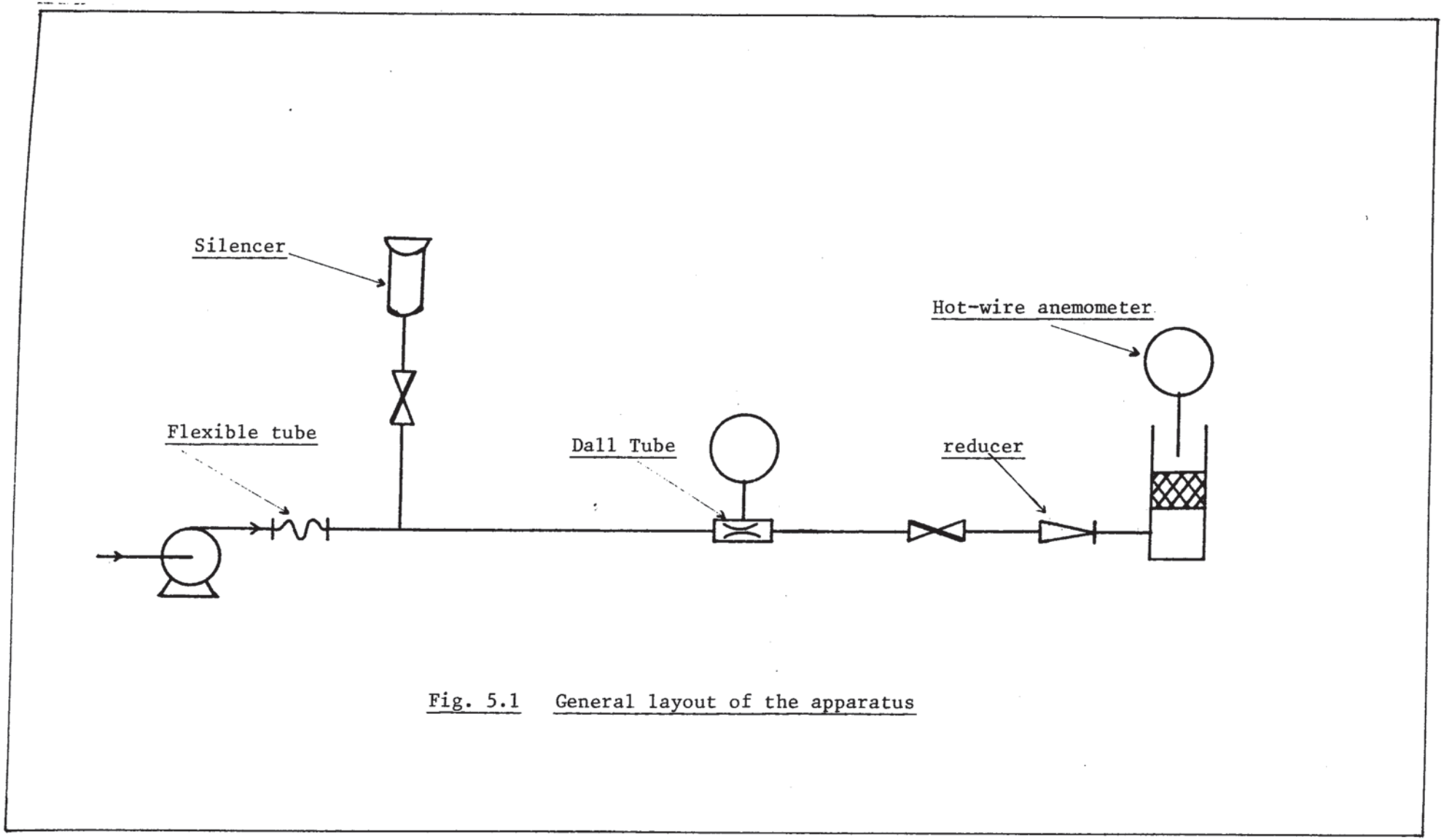

Fig. 5.1 General layout of the apparatus

Fig. 5.2 The 305 mm diameter packed column

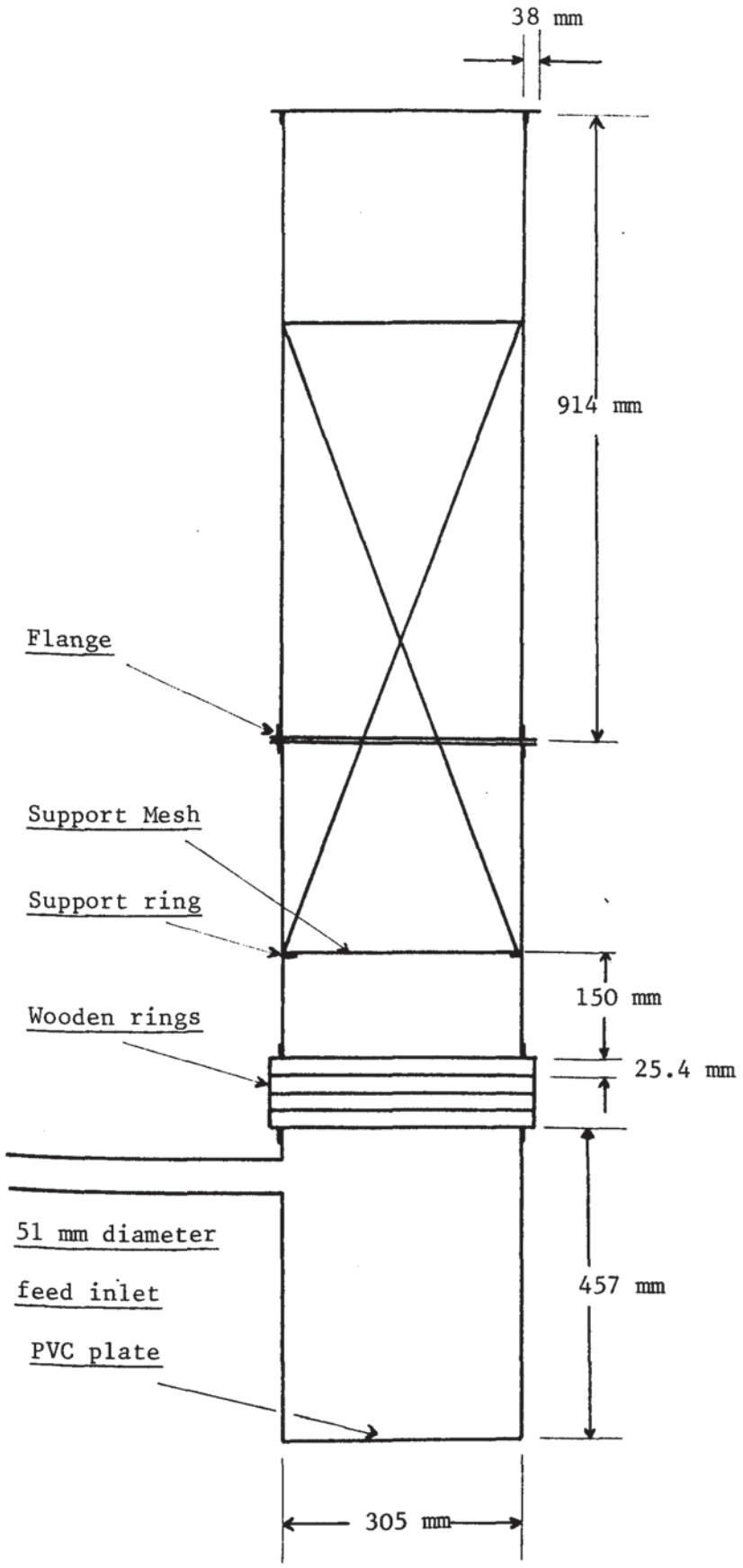

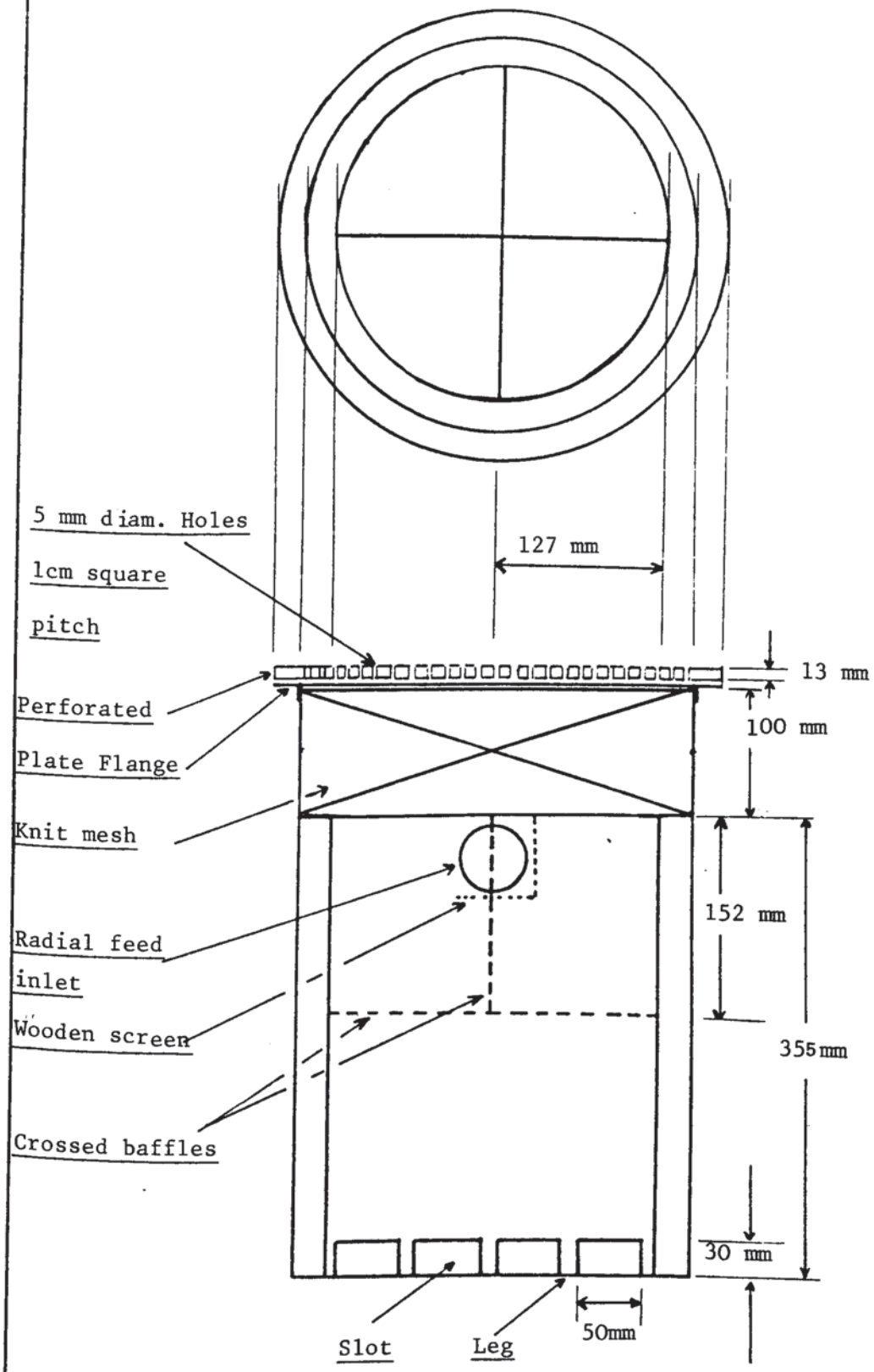

Fig. 5.3 Gas distributor

						300	240	165						
				420	315	300	305	440	330	280				
		325	280	275	65	85	360	450	485	295	345	299		
		365	300	240	135	300	335	500	420	375	315	250		
	200	170	315	220	215	305	260	415	460	340	275	245	295	
	369	295	290	180	180	280	295	135	150	240	245	220	340	
280	360	260	275	295	330	280	255	125	65	120	220	345	370	300
230	300	305	295	280	265	270	205	60	45	115	275	330	400	385
355	225	195	240	340	290	270	220	90	210	265	360	225	250	295
	75	360	210	300	175	320	300	200	210	280	290	300	270	
	135	220	315	160	95	125	225	215	240	155	310	350	395	
		220	235	140	140	95	185	225	45	85	195	240		
		235	360	350	340	260	65	55	380	360	400	280		
				160	380	200	200	250	385	315				
						350	250	165						

Table 5.1 Observed Point Velocities above a Deep Bed

						250	65	100						
				250	260	230	60	175	105	80				
		540	135	550	385	210	100	200	90	65	45	40		
		775	220	45	250	250	200	150	70	45	70	55		
	860	820	210	550	180	200	260	110	75	65	100	60	150	
	1600	1050	220	630	380	200	225	135	75	120	170	55	50	
770	1250	775	210	150	245	130	230	140	170	160	85	60	45	55
1100	1600	540	120	550	140	120	220	170	170	150	50	150	90	65
1050	880	800	950	820	650	250	250	450	180	130	55	170	70	125
	1730	480	675	240	670	250	260	400	240	75	100	90	75	
	570	220	430	110	410	130	290	200	150	45	260	45	70	
		230	290	210	565	115	180	220	45	90	160	60		
		50	140	250	570	340	175	160	45	140	100	65		
				290	135	550	350	70	50	190				
						490	250	60						

Table 5.2 Observed Point Velocities Above and Maldistributed Shallow Bed

Table 5.3 Maldistribution Factor, ϕ, for a 1200 mm Deep Well-distributed Packed Bed

NOTE: SEE COMMENT 2 ON P. 54 FOR ϕ VALUES

Re	n	repack	ϕ	$\bar{\phi}$	$\bar{\phi}/n$
29300	649	1	44.9	68.14	0.105
		2	58.1		
		3	60.7		
		4	70.5		
		5	72.1		
		6	74.0		
		7	76.2		
		8	88.6		
	161	1	12.4	16.5	0.1025
		2	12.6		
		3	13.2		
		4	16.8		
		5	18.3		
		6	18.7		
		7	19.82		
		8	21.2		
	100	1	13.29	9.7	0.097
		2	13.01		
		3	12.3		
		4	9.0		
		5	8.4		
		6	7.8		
		7	7.7		
		8	6.1		
39100	649	1	55.3	6.9	0.1063
		2	58.0		
		3	68.3		
		4	75.7		
		5	76.5		
		6	80.0		

Table 5.4 Maldistribution Factor ϕ for a 51 mm Deep Maldistributed Packed Bed at Re = 29300

NOTE: SEE COMMENT 2 ON P.54 FOR ϕ VALUES.

n	Repack	ϕ	$\overline{\phi}$	$\overline{\phi}/n$
649	1	650.5	768.5	1.184
	2	653.5		
	3	690.1		
	4	700.3		
	5	786.0		
	6	847.6		
	7	856.2		
	8	963.8		
161	1	132.1	185.7	1.153
	2	152.6		
	3	178.9		
	4	188.7		
	5	195.3		
	6	197.5		
	7	203.2		
	8	237.7		

SECTION VI

METHOD OF EVALUATING GAS DISTRIBUTORS AND SCALE-UP RULES

Introduction

The main purposes of the work described in this section are:

(1) To develop a method of testing the quality of feed gas distributors for large diamter packed columns, based on variation of the maldistribution factor ϕ with the packed depth.

(2) To determine experimentally the rules of scale-up for using laboratory models of a full-scale column to test different kinds of gas distributors.

These two aims are achieved simultaneously throughout the course of the work in this section.

Before progressing in describing this work and its result, it is necessary to make a note about the rules of scale-up.

6.1 Rules of scale-up of Packed Beds

The packed beds scale-up rules which are going to be determined experimentally in this work can be summarized as follows:

(1) At low Mach number, dynamical similarity is achieved by keeping Reynolds number constant in exactly geometrically similar packed beds.

(2) The lack of geometric similarity resulting from the randomness of the packed bed is taken care of by the use of the maldistribution factor ϕ.

(3) For geometrically and dynamically similar beds, whether the gas beneath the bed is well or badly distributed, the

value of the maldistribution factor ϕ is the same in both the model and the full-scale beds.

(4) The effectiveness of a gas distributor may be measured in terms of the height of packing required for the minimum value of the maldistribution factor to be achieved, i.e. good distributors require less packed height than bad distributors to attain ϕ_{min}.

That dynamic similarity is achieved by keeping Reynolds number, Re, constant needs to be confirmed experimentally because:

(a) The gas used in this work is air, which is compressible; that means the Mach effect does exist.

(b) The randomness of the packed bed, which means that a different arrangement of the packings results each time the bed is repacked.

In this work, Mach number values are very small. The maximum gas velocity through the model bed is about 1m/sec. That is Mach number $M = 3 \times 10^{-5}$ and the maximum Mach number value in the inlet feed is about 0.1 which is still small and may have a negligible effect on the flow patterns. But the Mach number will be different in the model and the full-scale bed.

Therefore, if Reynolds number is sufficient to produce dynamic similarity, then the flow pattern in the model should be the same as in the prototype provided that the Reynolds number of each is the same. The validity of this assumption is tested by the experiments described in this section of the work.

Reynolds number is defined in this work based on the diameter of the packed bed, D, as follows:

$$Re = \frac{\rho \bar{V} D}{\mu} \qquad \ldots\ldots (6.1)$$

The first set of experiments was performed to check that at the same Re, ϕmin is the same in the model and the prototype.

However, the maldistribution factor ϕ should take care of the bed randomness, but this is also tested in these experiments.

6.2 Apparatus

Two exactly geometrically similar columns of different size were constructed and used to check the rules of scale-up stated above. Both columns were made of 1.5 mm thick galvanised iron. The small column is considered as a model of the large one. Both the model and prototype were constructed to permit measurements of the point velocities at fixed positions on a square mesh above geometrically similar beds randomly packed with geometrically similar packings.

The model, see Fig. 6.1, consists of two equal parts, 381 mm inside diameter and 571 mm long. Air enters the bottom part radially through a 63.5 mm feed pipe whose centre-line is 381 mm above a flat closed end of this part. The top end of this part is fitted with a 482 mm outside diameter flange. An elaborate distributor, similar in principle to that described in Section 5.1, was designed. It consists of the following parts:

(1) A cylindrical part, 317 mm in diameter and 412 mm long, held to a distance of 30 mm above the flat closed bottom end by means of four legs, each 30 mm long, equally spaced around the bottom end of the cylinder and fitted to the flat bottom of the column. The annular gap is closed at the top of the cylinder at a position exactly above the feed inlet. A wooden screen is inserted in the annular space at a position near the feed inlet to cause the air to swirl in the annular space. a 190 mm deep cross

baffle is fitted inside the cylinder with its top end is positioned parallel to the top end of the cylinder.

(2) A distribution bed packed with 16 mm plastic pall rings to a depth of 95 mm. The duty of this bed is to distribute the air emerging from the top of the cylinder. A distance of 64 mm is left above this bed to enable a complete mixing of air jets emerging from the top of the distribution bed before reaching a perforated plate.

(3) A perforated PVC plate, 13 mm thick, is flanged between the bottom part and the main part of the columm. A total of 1140 holes each 5 mm in diameter were made to give 20% free area. The velocity of the air emerging from each of these holes was checked and found to be constant.

A 12.5 mm wide support ring is fitted to the main part at a distance of 95 mm above the perforated plate. Two 6.3 mm diameter steel support beams were put below the support ring to hold the 9.5 mm square support mesh, made of 1 mm diameter wire, and to prevent it from being bent due to the weight of the packings. The bed under test is packed to different depths with 16 mm plastic pall rings.

This design is referred to as the "Ideal distributed case".

On the other hand, the "Maldistributed case" is achieved when the distributor is removed and the bottom of the bed under test is situated at a position just above the feed inlet, see Fig. 6.2.

The prototype whose inside diameter is 610 mm is designed with every single dimension is exactly geometrically similar to, and 1.6 times, the corresponding dimension in the model. This is true for both the ideal distributed case and the maldistributed case, see Figures 6.3 and 6.4 for these two cases respectively.

The modified Hot-wire anemometer, described in Section 4.3 was used to measure point velocity at any fixed position above the bed. The probe is situated at a distance of 35 mm and 55 mm above the model bed and the prototype bed respectively. The technique of moving the probe across the bed is similar to that described in Section 5.2.

6.3 The Minimum Number and Configuration of Point Velocity Measurements

A preliminary experimental investigation was carried out to estimate the minimum number of point velocity measurements required to obtain a reliable value of ϕ, on the 610 mm diameter bed packed to a depth of 152 mm with 25.4 mm plastic pall rings. The maldistributed feed was radially introduced immediately below the bed through a 100 mm diameter feed pipe at a rate of 24.35 m/sec. A total of 749, 188 and 89 point velocity measurements were made distributed on 20 mm, 40 mm and 60 mm square pitch above the bed respectively.

The results show that 188 point velocity measurements give a reliable estimates of both the maldistribution factor, ϕ, and the total flow. For more confidence, a sample size of 200 measurements was used throughout the work described in this section, distributed on 40 mm square pitch in the prototype and 25 mm square pitch in the model. The configuration of the positions of these points is shown in Fig 6.5.

6.4 Experimental Procedure

The two geometrically similar columns, the model and the prototype, were packed with 16 mm and 25.4 mm geometrically similar plastic pall rings respectively to proportional heights so as to

form a series of couples of geometrically similar packed beds, each couple is operated at the same Reynolds number.

This procedure was carried out in both the ideally distributed case and the maldistributed case. Each bed was repacked three times, each time at total of 200 point velocity measurements is taken at fixed positions as shown in Fig. 6.5.

6.5 Results

The complete sets of these observations are given in Appendix A3.

The processed data is summarised in Table 6.1 where the maldistribution factor, ϕ, was obtained for the geometrically and dynamically similar beds: Each bed was repacked three times and hence three ϕ values were obtained for each bed.

$\bar{\phi}$, the average value of ϕ was then calculated, which describes gas maldistribution in that packed bed.

6.5.1 Variation of $\bar{\phi}$ with Reynolds Number and Packed Height for Ideally Distributed Beds of Geometric and Dynamic Similarity

Gas maldistribution, expressed by $\bar{\phi}$, for dynamically and geometrically similar, ideally distributed packed beds, are listed in Table 6.1. The model bed, (D = 381 mm), is packed to depths of 63.5 mm and 127 mm, operated at a range of gas Re values. The prototype bed, (D = 610 mm), is packed to heights of 1.6 times those of the model; i.e. 101 mm and 203 mm. One further 610 mm deep bed was examined.

Variations of $\bar{\phi}$ for these beds with packed height, P.H., and Re are shown in Graph 6.1, which shows that the value of $\bar{\phi}$ is

not changed either with P.H. nor with Re. Also, $\bar{\phi}$ is the same for both beds with a value of about 20.

This means that the minimum value of ϕ observed for a packed bed by using the technique proposed in this work, is around 20, i.e.

$$\phi_{min} \simeq 20$$

6.5.2 Variation of $\bar{\phi}$ with Re and P.H. for Maldistributed Beds of Geometric and Dynamic Similarity

$\bar{\phi}$ values were calculated for the two beds at different heights and gas Re when the feed was badly distributed below the bed.

The 381 mm diameter bed was packed to 63.5 mm, 127 mm and 381 mm heights and was operated at a range of gas Re values.

The 610 mm diameter bed was packed to heights of 101.6 mm, 203 mm and 610 mm and was run under the same range of Re values.

The variation of $\bar{\phi}$ with Re in both beds is shown in Graphs 6.2 and 6.3 respectively.

The variation of $\bar{\phi}$ with packed height is given in Graphs 6.4 and 6.5 for the model and the prototype respectively.

6.6 Discussion of the Results

For the ideally distributed bed; (evenly distributed feed entering the bottom of the bed), the obtained value of ϕ_{min} represents the best distribution that can be achieved in a packed bed, because this distribution could not be improved either by changing the geometry, (the packed depth), nor by changing the operating conditions, (Re values). For this reason, ϕ_{min} could

be considered as a standard value, such that the goodness of any other distribution in a packed bed can be compared to or measured by that standard.

In the shallow maldistributed packed beds, (maldistributed feed enters the bottom of the bed), the gas maldistribution is severe and thus the values of ϕ are very high, but as the packed depth increases, the values of ϕ decrease, until eventually the value of ϕ obtained for that maldistributed bed converges with ϕ_{min} which represents ideal conditions. This can be shown clearly from graphs 6.4 and 6.5.

A maldistributed bed with enough packed depth to bring the gas maldistribution to the minimum, will adopt the facility of unresponding to any change in Re value; i.e. it will behave like an ideally distributed bed, this is very clearly shown in Graphs **6.4** and **6.5** where at short packed depths, $\overline{\phi}$ values vary with Re and this variation is reduced as the bed becomes deeper.

From this, it could be concluded that the packing itself acts as a distributor which improves the distribution of the gas passing through it, but on the other hand there will be many pathways that the gas follows throughout the packing, and hence, the gas is not evenly distributed. This means that the process of improving gas distribution by the packing is limited by the presence of such pathways.

At this stage, a method of testing the quality of feed gas distributors can be developed:

The quality of any gas distributor in any packed column can be tested by using the technique described in this work to measure gas distribution above a very short packed depth, compared to the diameter of the bed, then increasing the packed depth by

intervals, at each interval, the maldistribution factor ϕ is to be measured, until reaching a packed height above which, ϕ, is constant; i.e. ϕ_{min}. Then the best gas feed distributor is that which produces gas maldistribution closest to the minimum maldistribution at shortest packed depth.

But this method seems very difficult or impossible in a real-life column due to the practical difficulties facing the implementation of this test.

The results also show that if two beds of different sizes designed such that every single dimension in the small size bed (model) is exactly geometrically similar to that in the large-size bed (prototype), are operated at the same value of gas Re, i.e. geometrically and dynamically similar packed beds, then the flow patterns of the gas through these two beds are similar.

This could be seen from Graph 6.6, where the curves show that for a given value of $P.H/_D$ for both beds, there is only one value of $\bar{\phi}$ at a given Re value, or in other words, the gas maldistribution, or flow pattern, is similar in two geometrically and dynamically similar packed beds.

From that it could be concluded that shallow large diameterpacked beds (or packed beds in general) can be investigated using small models of exact geometric and dynamic similarity to the full-scale packed beds, and the dynamic similarity is achieved by maintaining similar gas Reynolds number.

From these rules of scale-up, the developed method of testing feed gas distributors can be generated to cover the real life gas distributors, by building a model packed bed which is exactly geometrically and dynamically similar to the full-scale column, and then performing laboratory tests on the model.

Apart from these two achievements; (the scale-up rules and the method of testing feed gas distributors), the results show an interesting phenomenon, which is that the obtained values of ϕ are scattered around an average value within a range not more than $\pm$ 8%, which is much narrower than that experimentally measured for the 305 mm bed packed with 25.4 mm plastic pall rings which was about $\pm$ 30%. This means that as the bed diameter to pack size ratio increases, the values of ϕ become more reproducible.

6.7 Conclusions

From this work, the following conclusions can be made:

(1) The gas flow patterns are similar in geometrically and dynamically similar randomly packed beds.

(2) The quality of feed gas distributors can be tested by a method based on the variation of maldistribution factor, ϕ, with the packed height.

(3) As the packed height to bed diameter ratio increases the values of ϕ decreases until reaching a minimum value, ϕ_{min}, at a certain depth.

(4) The observed ϕ values become more reproducible as the bed diameter to pack size ratio increases.

6.8 Summary

The rules of scale-up of large diameter packed beds have been determined experimentally and a method of testing the quality of feed gas distributors based on the variation of gas maldistribution with packed height, and on the determined scale-up rules. The development of this test method and the determination of these rules are originally based on the defined maldistribution factor ϕ. The

meaning of ϕ and its reliability as a measure of the gas maldistribution is to be examined in the next section of the work.

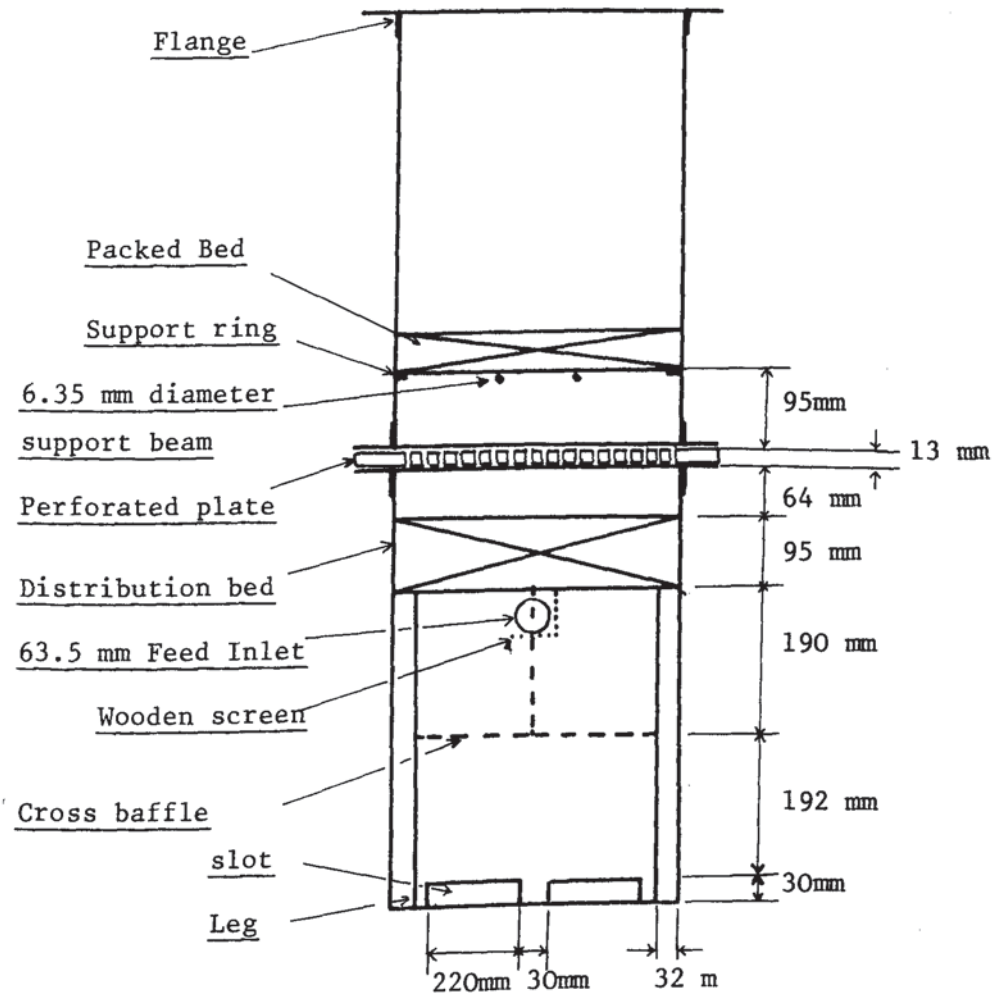

Fig. 6.1 Ideally distributed model packed column of 381 mm diameter

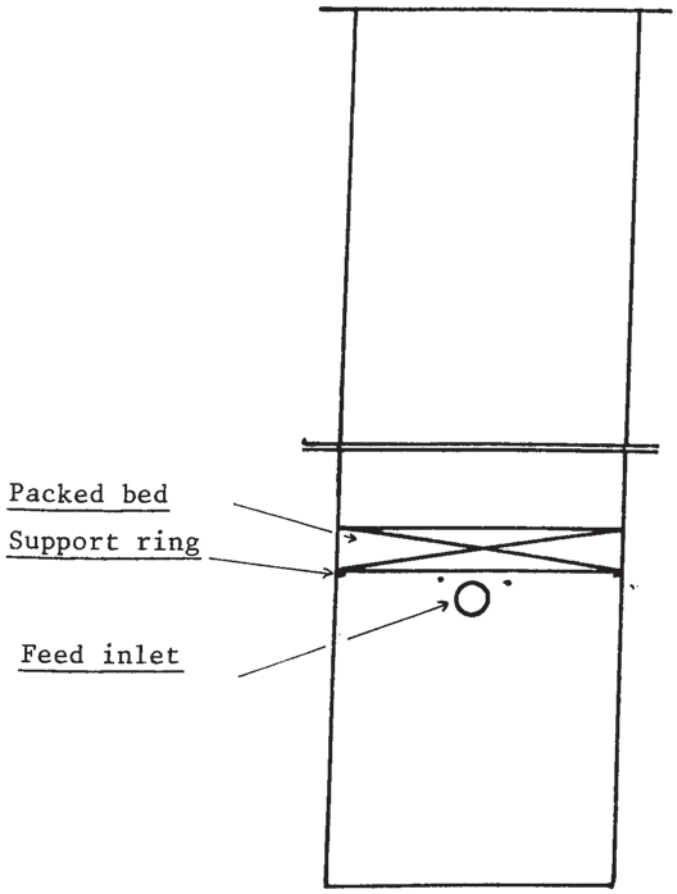

Fig. 6.2 Maldistributed model packed column of 381 mm diameter

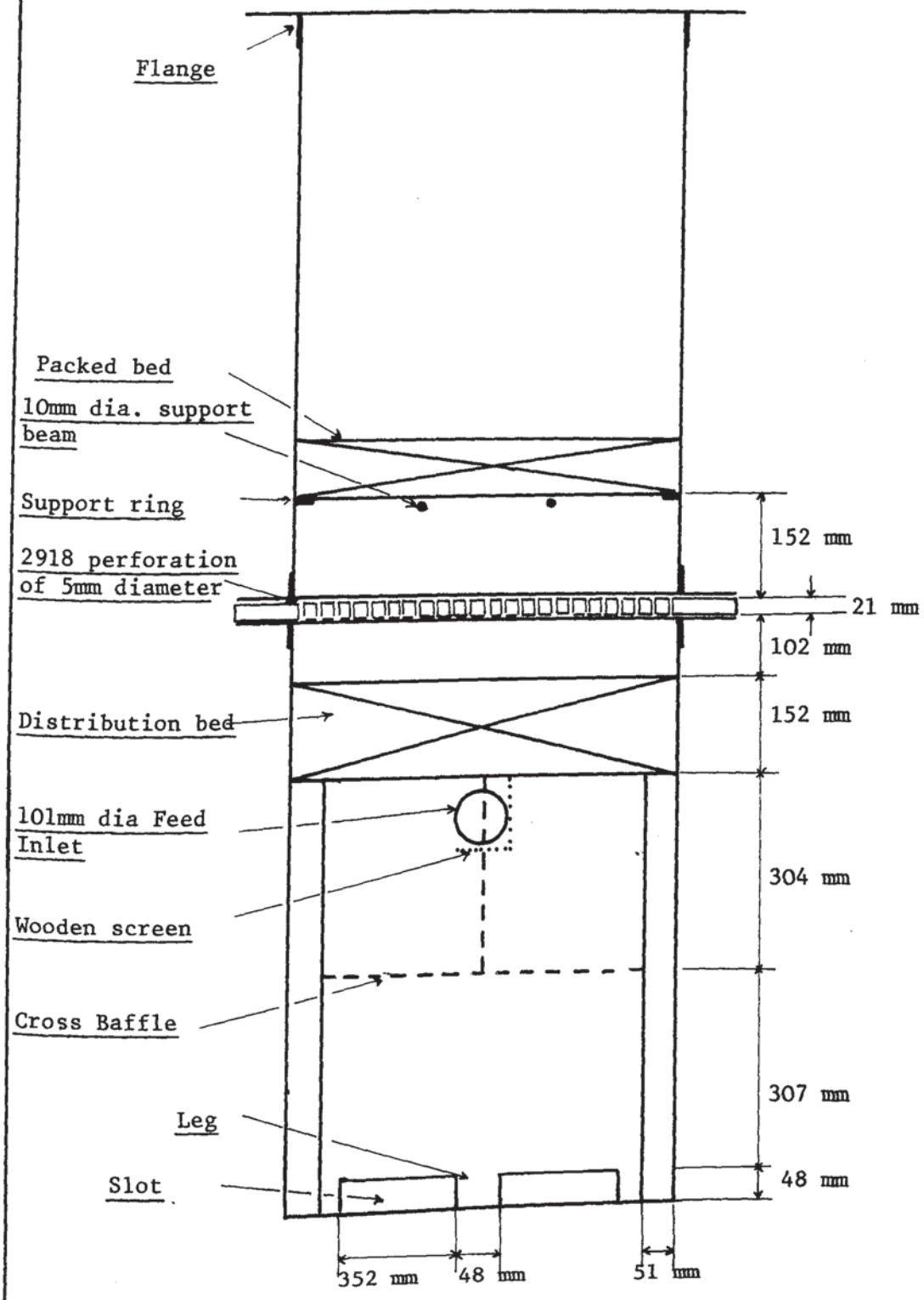

Fig. 6.3 Ideally distributed prototype packed column

column of 610 mm diameter

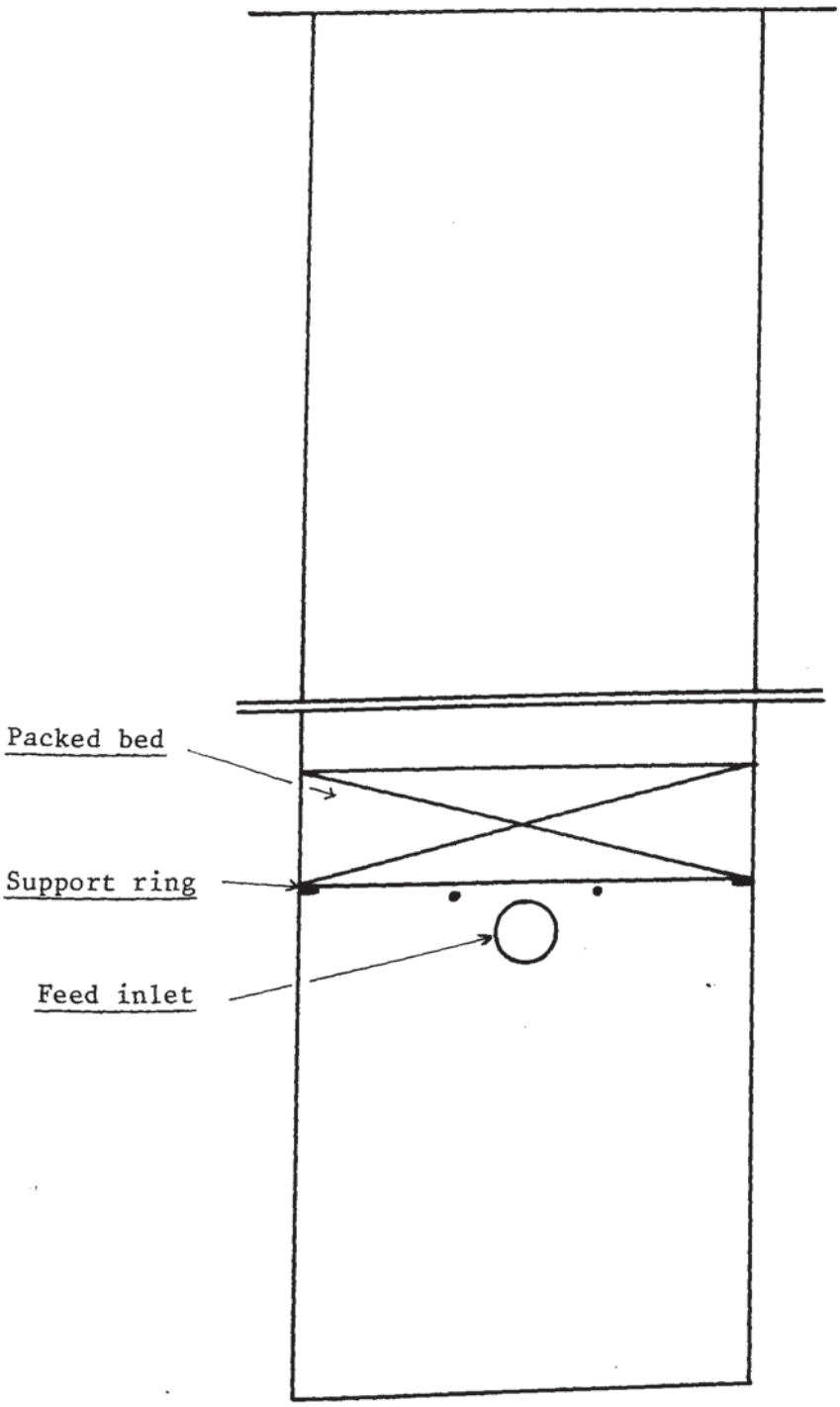

Fig. 6.4 Maldistributed prototype packed column of 610 mm diameter

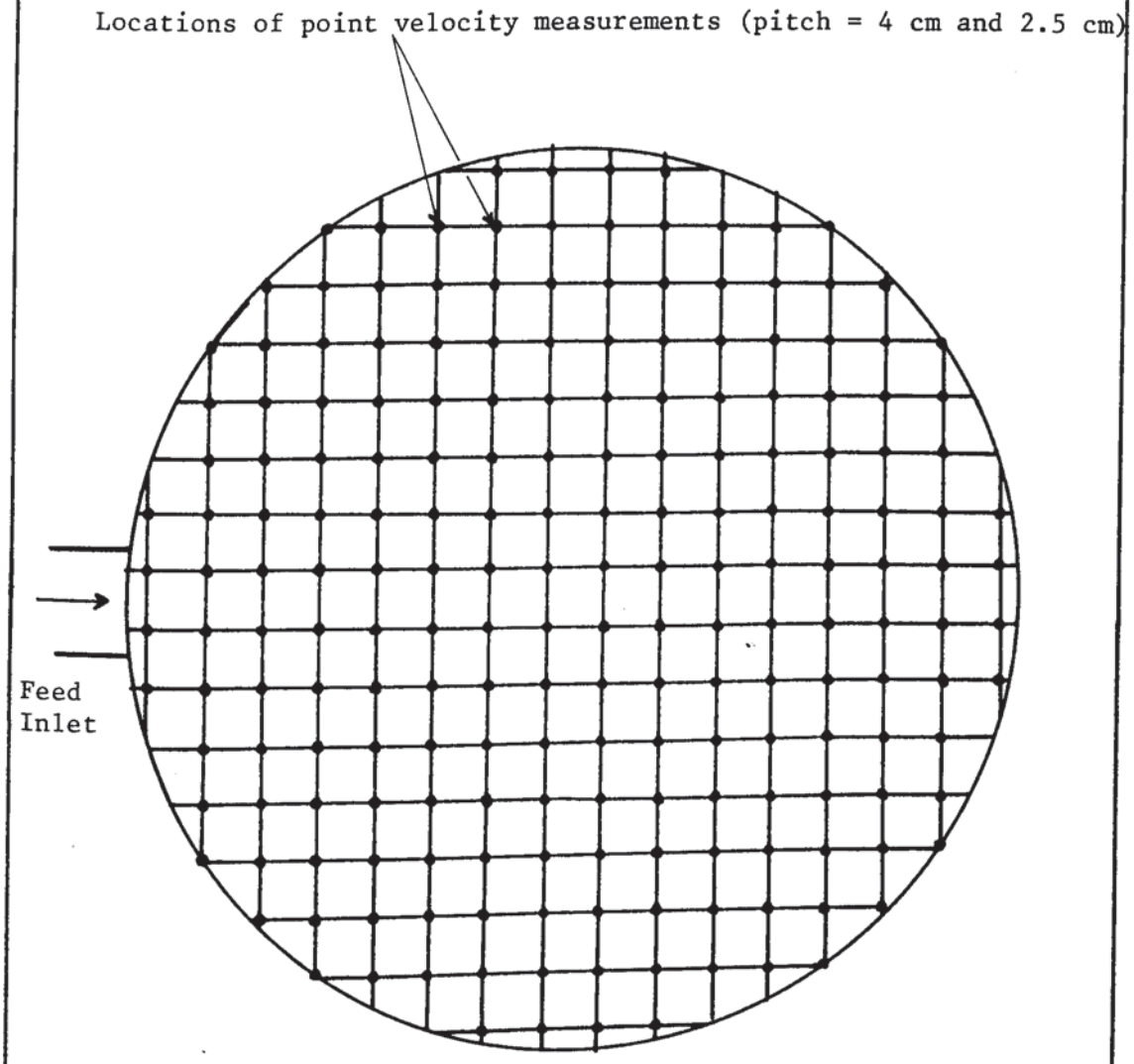

Fig. 6.5 Configuration of the 200 point velocity measurements

Table 6.1 Maldistribution Factor, ϕ, for Geometrically and Dynamically Similar Packed Beds

NOTE : SEE COMMENT 2 ON P.54 FOR ϕ VALUES.

Status	D (mm)	H (mm)	Re	Repack	ϕ	$\bar{\phi}$
Maldistributed	381	63.5	18000	1 2 3	70.6 76.8 78.1	75.17
			25000	1 2 3	70.0 70.9 79	73.3
			32000	1 2 3	81.6 85.4 88.4	85.1
		127	18000	1 2 3	28.0 29.76 31.8	29.82
			25000	1 2 3	26.92 27.61 30.17	28.2
			32000	1 2 3	27.75 29.2 30.14	29.03
		381	30000	1 2 3	19.1 20.22 21.15	20.15
	610	101.6	18000	1 2 3	73.2 73.8 74.9	74

/Continued .....

Table 6.1 continued

Status	D (mm)	H (mm)	Re	Repack	Ø	$\overline{Ø}$
Maldistributed	610	101.6	25000	1 2 3	72 72.16 81.65	75.27
			32000	1 2 3	81.46 81.74 92.15	85.11
		203	18000	1 2 3	27 27.5 30.6	28.4
			25000	1 2 3	26.7 29.3 31.4	29.13
			32000	1 2 3	27.01 29.79 31.08	29.3
Ideal Distribution	381	63.5	16150	1 2 3	19.45 20.4 21.64	20.4
			24500	1 2 3	19.5 19.56 22.48	20.5
			30700	1 2 3	18.42 20.6 22.43	20.48
		127	16150	1 2 3	19.65 19.9 21.84	20.46
			24500	1 2 3	19.13 20.2 21.96	20.43

/Continued .....

Table 6.1 continued

Status	D (mm)	H (mm)	Re	Repack	Ø	$\bar{Ø}$
Ideal Distribution	381	127	30650	1 2 3	19.65 20.55 22.45	20.88
	610	101.6	20000	1 2 3	19.63 20.28 20.93	20.28
			26000	1 2 3	19.72 19.95 20.64	20.1
			29000	1 2 3	19.73 20.13 22.3	20.72
		203	20000	1 2 3	19.7 19.95 22.14	20.6
			26000	1 2 3	20.1 20.13 20.67	20.3
			29000	1 2 3	19.3 20.5 21.3	20.37
		610	30000	1 2 3	20.0 20.18 20.47	20.2

Graph 6.1 $\bar{\phi}$ against Re for Two Geometrically similar Beds of Different Heights at Ideal Distribution Situation

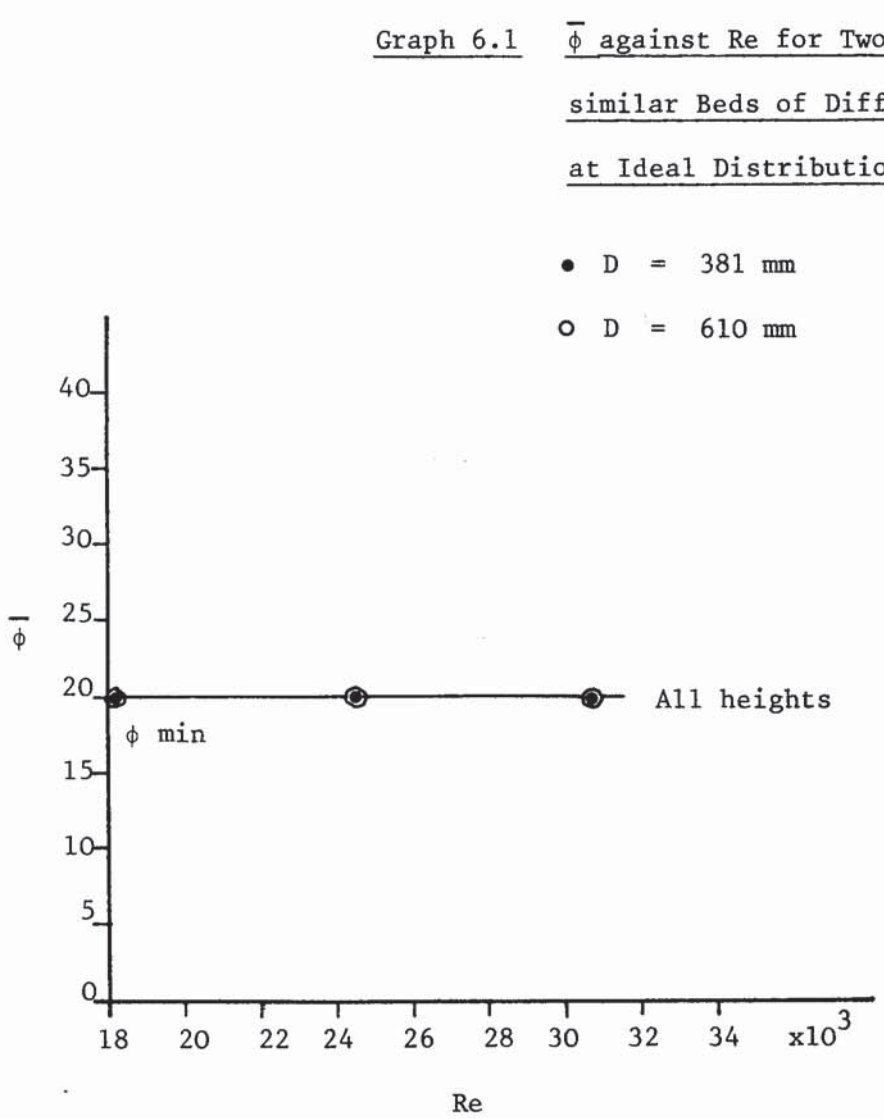

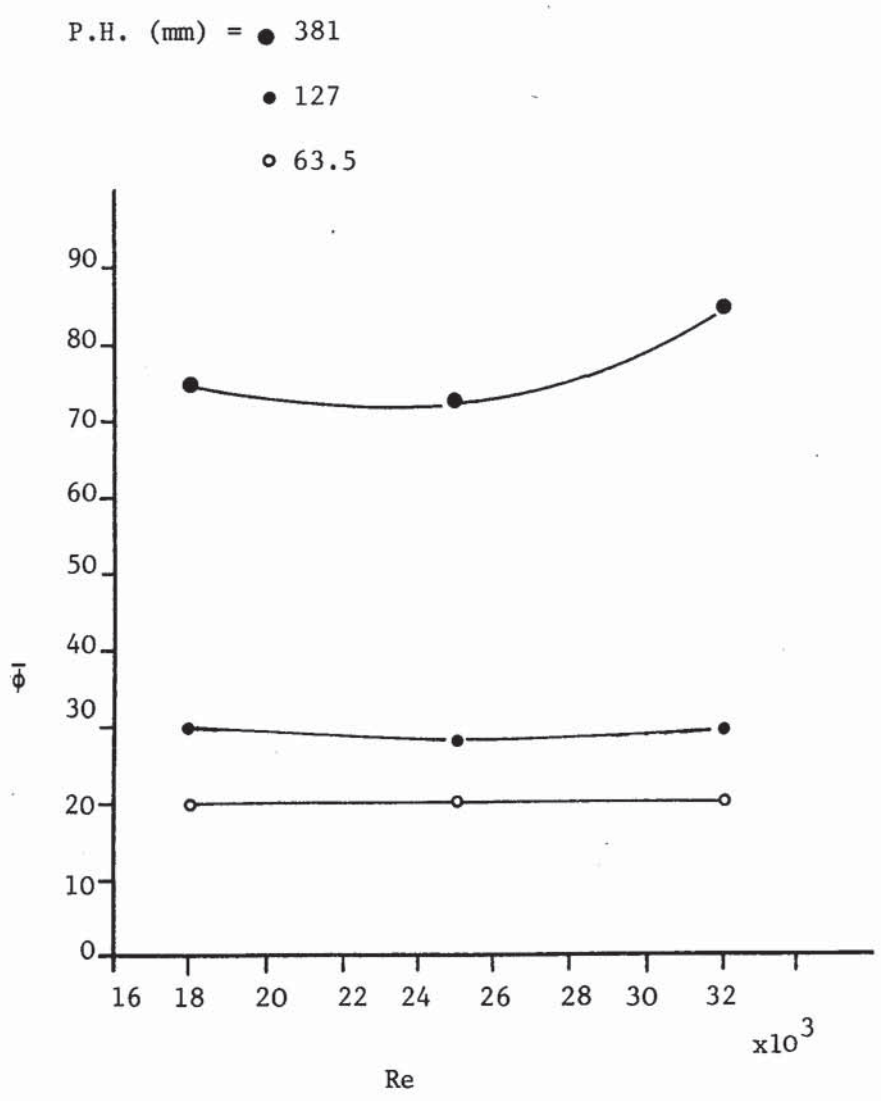

Graph 6.2 Variation of $\bar{\phi}$ with Re in a 381 mm diameter maldistributed bed

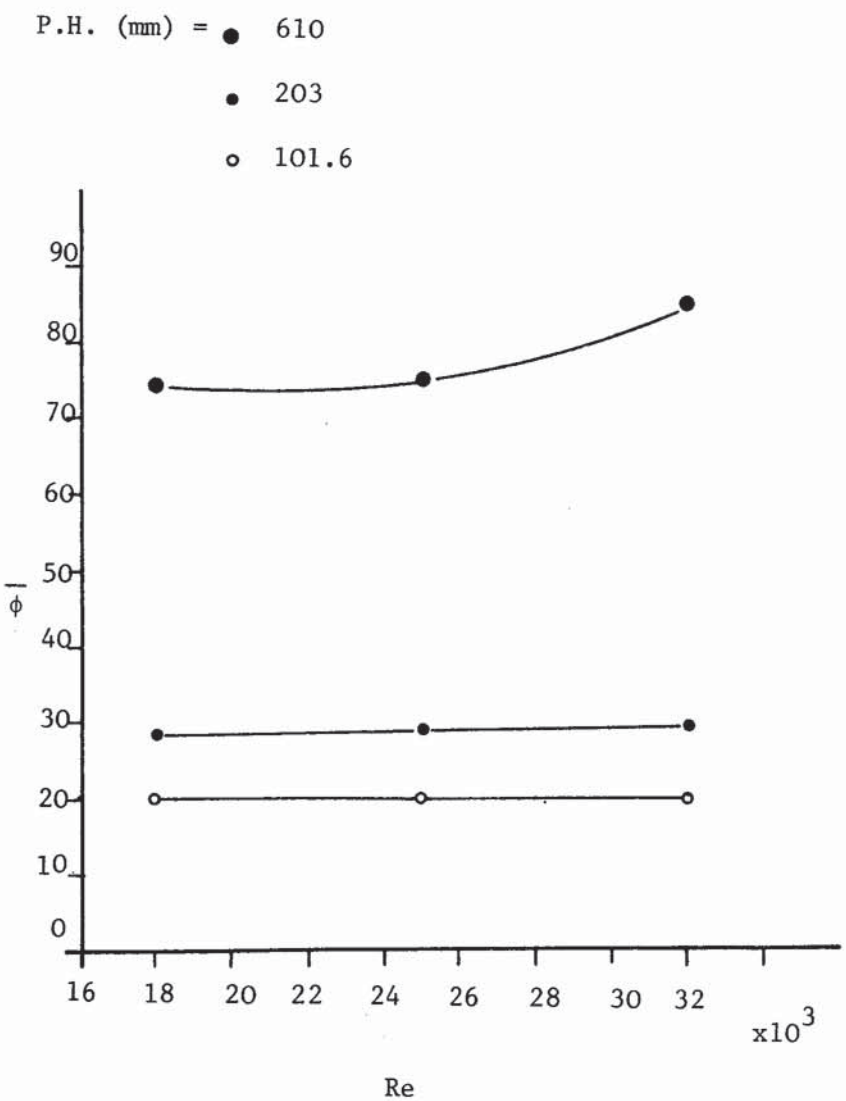

Graph 6.3 Variation of $\bar{\phi}$ with Re in a 610 mm diameter maldistributed bed

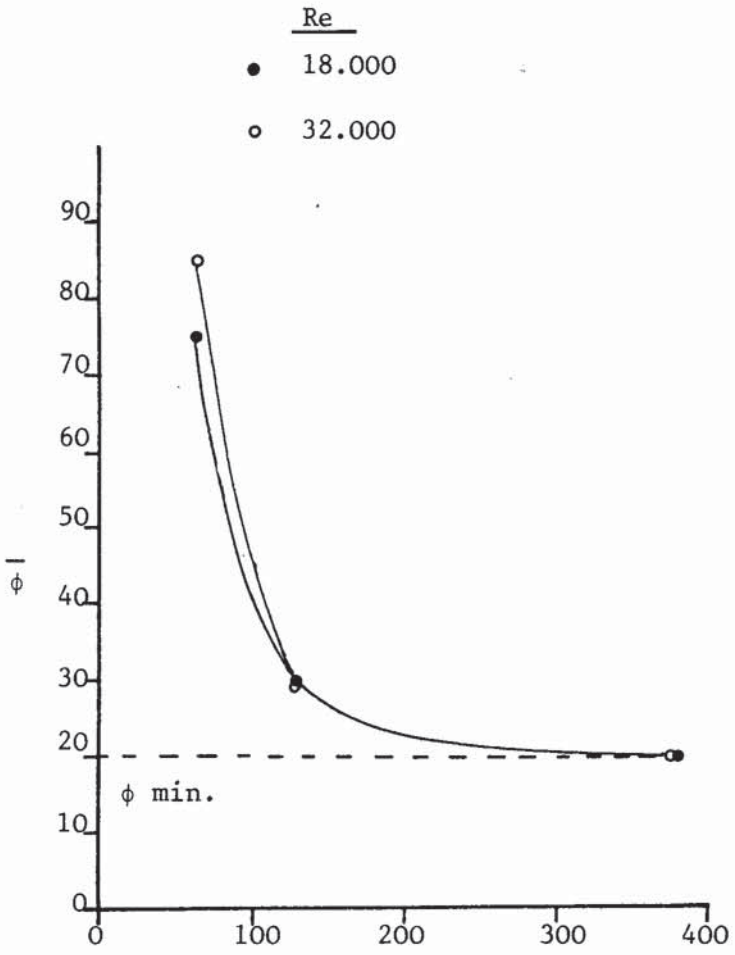

Graph 6.4 Variation of $\bar{\phi}$ with P.H. in the 381 mm diameter maldistributed bed

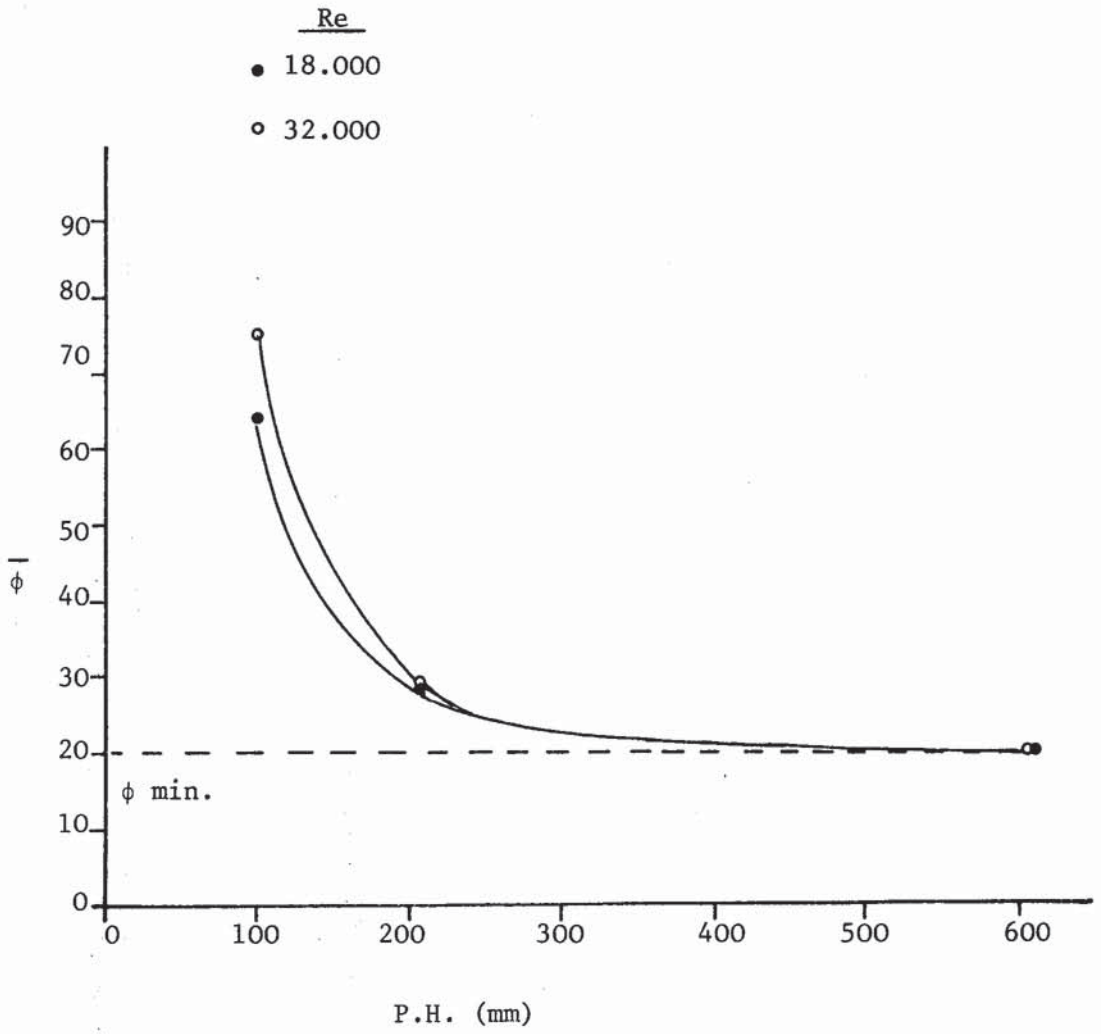

Graph 6.5 Variation of $\bar{\phi}$ with P.H. in the 610 mm diameter maldistributed bed

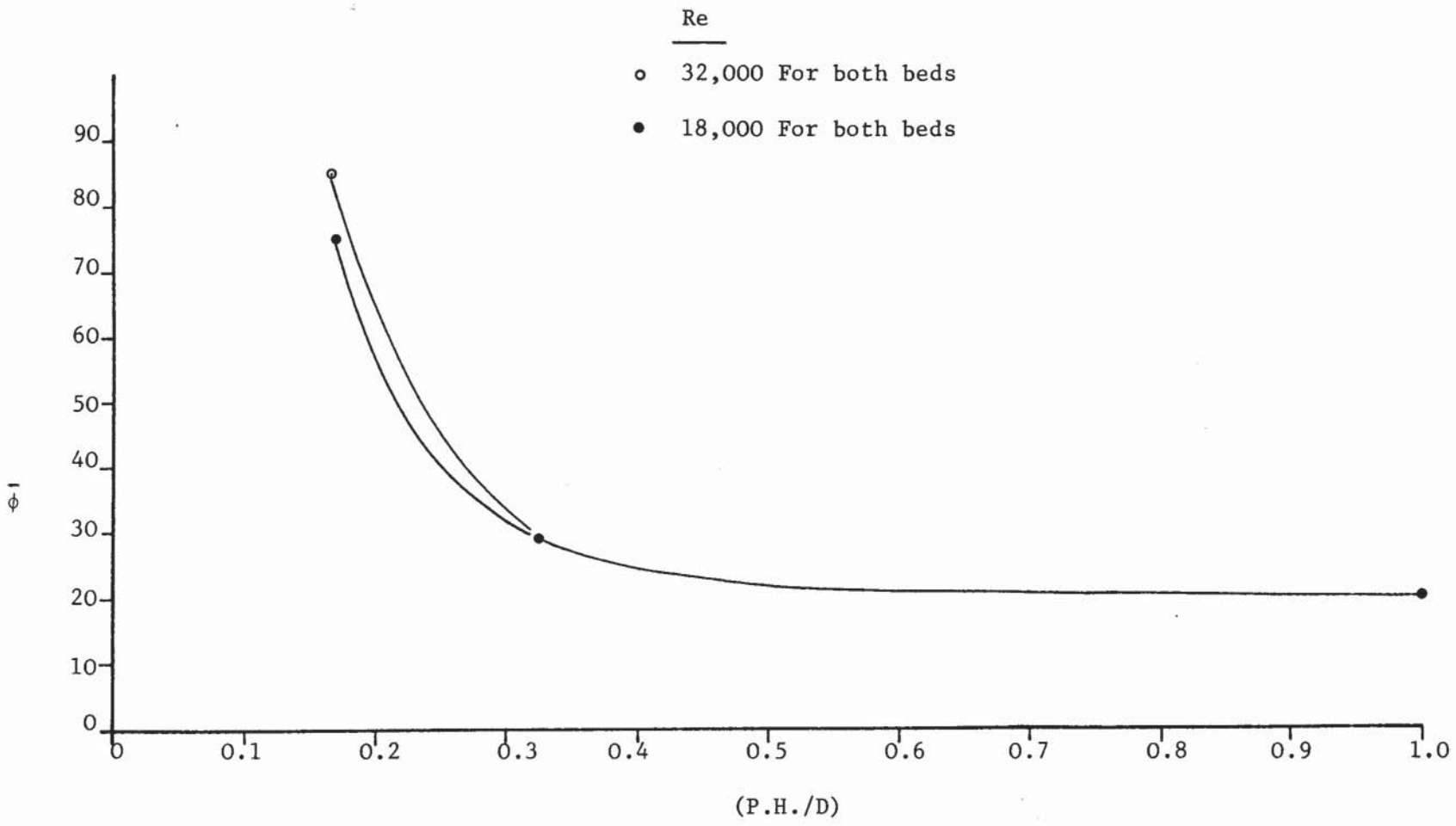

Graph 6.6 Variation of $\bar{\phi}$ with (P.H./D) for geometrically and dynamically similar maldistributed packed beds

SECTION VII

STATISTICAL AND GRAPHICAL INTERPRETATION OF THE EXPERIMENTAL RESULTS

Introduction

In this work, the experimental results are statistically interpreted by Multi-Factor Analysis of the Variance, and graphically illustrated by producing Response Surfaces to visualise the profile of the gas emerging from the top of a packed bed.

It was necessary to define the maldistribution factor ϕ, which is proportional to the variance, because of the random nature of packed beds. Noting that statistics is the study of random variations, in this section the nature of ϕ is studied and the validity of the scale-up rules is proved by showing that there is no statistically significant effect of column size upon the gas flow pattern for geometrically similar beds operated at the same Reynolds number.

7.1 Analysis of the Distribution of Gases Emerging from the Top of Packed Beds

In this part of the work an attempt has been made to investigate the effect of the spatial coordinates x and y on the gas distribution emerging from the top of packed beds by the use of Two-Factor analysis of the variance, whose mathematical formulation is given in Appendix A4, to show that:

(a) For a well-distributed gas, $\phi = \phi_{min}$, there is no spatial maldistribution, i.e. the effect of x and y is statistically insignificant.

(b) For a maldistributed gas, the effect of position, i.e. x and y spatial coordinates is significant and this is associated with $\phi > \phi_{min}$.

The two-factor analysis of the variance produces values, (computed f-values), to determine the effects of:

(1) x-spatial coordinate, (Factor-X).

(2) y-spatial coordinate, (Factor-Y).

(3) Interaction of Factor-X with Factor-Y.

(4) Repacking the bed.

on the distribution of air emerging from the top of a randomly packed bed.

These computed f-values are to be compared with their corresponding standard values found in the statistical textbooks, (tabulated F-values), at a predetermined level of confidence (α).

If the computed f-value for any factor is greater than or equal to its corresponding tabulated f-value, then that factor has a significant effect on the distribution and the gas is maldistributed due to that factor; if the computed f-value is less than the tabulated f-value, then that factor has no significant effect on the gas distribution.

The most important factors in this analysis are the x and y-factors whose computed f-values determine the gas maldistribution in the x and y directions.

If both, or one of them is significantly effective, then this means that the gas is severely maldistributed along both or one of the x and y-axes in the xy-plane above the bed. The x-axis represents the direction at which the gas feed is introduced to the column below the bed, (radial feed inlet). The y-axis is at right angles to the feed direction in xy-plane. The relationship

between ϕ and the computed f-values is discussed in detail at a later stage of this section.

7.1.1 Method

A sample of 200 point velocity measurements was used to evaluate the maldistribution factor ϕ. The locations of these points are equally distributed on a circular plane, see Fig. 6.5. But in order to fulfill the requirement of the two-factor analysis of the variance, (that is each position in x-direction should be used once in conjunction with each position in y-direction, or in other words, all the positions of point velocities should be specified by an x-coordinate and y-coordinate, see Appendix A4), and to use the largest possible sample size, (number of points), a sample size of 144 point velocity measurements, equally distributed in a square plane which represent the central part of the circular plane, was used in this analysis, see Fig. 7.1.

7.1.2 Results of the Gas Distribution Analysis and Discussion

The two-factor analysis of the variance has been performed on the observed point velocities above some of the packed beds described in Section 6 to study the effect of packed height on the gas distribution in both ideally and badly distributed feed situations.

Two sample solutions, one for a maldistributed bed and the other for an ideally distributed bed, are given in Appendix A4.

The results are summarized in Table 7.1.

The computed f-values obtained for any bed are to be compared with the standard tabulated f-values listed below

Table 7.1. For example, for the ideally distributed bed, 610 mm diameter and 203 mm height, the computed f-value for the effect of repacking the bed is 0.62. This value is to be compared with the standard f-value at 0.05 level of confidence (α) for the repacking effect, which is 3; the computed f-value is less than standard f-value, therefore, repacking the bed has no significant effect on the total picture of the distribution of the gas above that bed. Similarly, the computed f-value of x-effect = 1.46 < $f_{0.05}$ = 1.79, which means that the gas is not significantly maldistributed in the x-direction.

On the other hand, for the 610 mm diameter and 101.6 packed depth maldistributed bed, the computed f-value of x-effect = 47.06 > $f_{0.05}$ = 1.79, which means that the gas is severly maldistributed in the direction of the feed, (x-direction).

The results show that the computed f-values for the ideally distributed bed, 610 mm diameter and P.H. of 101.6 mm, are nearly equal to their corresponding values obtained for the same bed when its packed depth was doubled and, also, similar to those obtained for the ideally distributed 381 mm diameter bed of different Re value. This means that neither the packed height nor the Re values has any effect on gas flow patterns in ideally distributed packed beds. The computed f-values for the x-effect and y-effect show some maldistribution, however not significant, in both x and y direction; if the gas was evenly distributed then the computed f-values would have been equal to zero. This shows that there is a minimum maldistribution resulting from the point to point velocity variations.

For the geometrically and dynamically similar prototype and model beds packed to 101.6 mm and 63.5 mm respectively, the

computed f-values show severe gas maldistribution in the x-direction and slightly significant maldistribution in the y-direction. The similar magnitudes of the computed f-values show the similarity in maldistribution in both beds both in the x-direction and y-direction. As the P.H./D ratio increases in these similar beds, the computed f-values of the x-effect decreases to show that the maldistribution in the x-direction has been reduced to a new equal level in both beds, and becomes insignificant in the y-direction. At a deeper bed, the computed f-values show insignificant maldistribution in both x-direction and y-direction.

This shows that gas flow patterns are similar in maldistributed geometrically and dynamically similar beds, and that, gas maldistribution decreases as the packed height increases.

From the two-factor analysis of the variance, it could be concluded that gas flow patterns are similar in geometrically and dynamically similar packed beds, which is the same conclusion abstracted from using the simply defined maldistribution factor ϕ in the previous section of this work.

In the following part of this section, the similarity of flow patterns in geometric and dynamic similar beds is to be studied in more detail.

7.2 Analysis of the Gas Distribution in Geometric and Dynamic Similar Packed Beds

The distribution of the gas emerging from the top of geometric and dynamic similar beds of different size is investigated statistically by the use of Three-Factor Analysis of the Variance to show that at dynamic similarity, changing the scale of operation has an insignificant effect on the flow pattern. The mathematical

formulation of this analysis is given in Appendix A4.

Similar to the two-factor analysis of the variance, the three-factor analysis of the variance produces computed f-values to estimate the effect of the spatial coordinates x and y as well as the effect of the packed bed diameter on the flow patterns. These computed f-values are to be compared to the corresponding tabulated f-values at predetermined significance level, α.

7.2.1 Method

A sample size of 144 point velocity measurements, similar to that shown in Fig. 7.1, is used in this analysis. But instead of the gas velocity, the Reynolds numbers at these points are used, where Re is defined by the point velocity and the column diameter. These Re values are subsequently called as "point Reynolds numbers".

The point Res obtained for a bed repacked several times (3 times) are used in conjunction to other point Res obtained for another bed, of geometric and dynamic similarity to the first bed but of different size, repacked three times.

7.2.2 Results and Discussion

The distribution of the gas emerging from the top of two geometrically and dynamically similar beds is analysed in both situations of the ideally distributed feed and the badly distributed feed. The results are summarised in Table 7.2.

Comparison of the computed f-values with their corresponding tabulated f-values at a $\alpha = 0.05$, listed in Table 7.2, shows that the diameters of the two beds have no significant effect on the distribution of the gas in both ideally and badly distributed

feed situations. In the ideally distributed beds, $\phi = \phi_{min}$, gas maldistribution is insignificant in the x and y spatial direction, in maldistributed beds, associated with $\phi > \phi_{min}$, the gas is severly maldistributed in x-direction and slightly maldistributed in y-direction.

From this it could be concluded that gas flow patterns are similar in geometrically and dynamically similar packed beds and this supports the same result concluded by using ϕ to establish the rules of packed beds scale-up.

7.3 A Discussion of the Definition of ϕ_{min} in Terms of Multi-Factor Analysis of the Variance

In this part of the work an attempt is made to highlight the relationship between the estimates of the variance computed by the use of the multi-factor analysis of the variance technique and the value of ϕ obtained to describe the quality of the gas distribution above a packed bed. This relationship was shown clearly in the work performed above in this section, where for a well-distributed bed, ϕ , has the minimum value, ϕ_{min} and the multi-factor analysis of the variance shows that the maldistribution of the gas is insignificant; for a maldistributed packed bed, $\phi > \phi_{min}$ and the maldistribution is significant.

ϕ is defined by Eqn. 5.3 as:

$$\phi = \sum_{i=1}^{n} \left(1 - \frac{V_i}{\bar{V}}\right)^2$$

$\therefore$ From Eqn. 5.2

$$\sigma^2 = \frac{\bar{V}^2}{n-1}\,\phi \qquad \ldots\ldots (7.1)$$

The five estimates of the variance, σ^2, obtained by the two-variable analysis of the variance, see Appendix A4, are:

$$E\,(S_1^2) = E\,[\frac{SSx}{a-1}] = \sigma^2 + \frac{rb\sum_{i=1}^{a}\alpha_i^2}{a-1} \qquad \ldots\ldots (7.2a)$$

$$E\,(S_2^2) = E\,[\frac{SSy}{b-1}] = \sigma^2 + \frac{ra\sum_{j=1}^{b}\beta_j^2}{b-1} \qquad \ldots\ldots (7.2b)$$

$$E\,(S_3^2) = E\,[\frac{SS(xy)}{(a-1)(b-1)}] = \sigma^2 + \frac{r\sum_{i=1}^{a}\sum_{j=1}^{b}(\alpha\beta)_{ij}^2}{(a-1)(b-1)} \qquad \ldots\ldots (7.2c)$$

$$E\,(S_4^2) = E\,[\frac{SSR}{(r-1)}] = \sigma^2 + \frac{ab\sum_{k=1}^{r}\rho_k^2}{r=1} \qquad \ldots\ldots (7.2d)$$

$$E\,(S^2) = E\,[\frac{SSE}{(ab-1)(r-1)}] = \sigma^2 \qquad \ldots\ldots (7.2e)$$

where: S_1^2, S_2^2, S_3^2, S_4^2 and S^2 are the factor x, factor y, interaction, repacking and error mean squares respectively.

SSx, SSy, SSxy, SSR, SSE are the factor x, factor y, interation, repacking and error sum of squares respectively.

a: Is the number of point velocity measurements in x-direction, (a=12).

b: Is the number of point velocity measurements in y-direction, (b=12).

r: Is the number of times that the bed is repacked, (r=3).

α_i: Is the effect of (ith) point velocity in x-direction on the gas distribution.

β_j: Is the effect of (jth) point velocity in y-direction on the gas distribution.

$(\alpha\beta)_{ij}$: Is the interaction, or joint, effect of (ith) point velocity in x-direction and the (jth) point velocity in y-direction on the gas distribution

ρ_k: Is the effect of the (kth) replicate.

For an ideally distributed feed below a packed bed, the maldistribution of the gas above that bed is described by ϕ_{min} which means that:

$$\sigma^2 = \frac{\bar{V}^2}{n-1} \phi_{min} \qquad \ldots\ldots (7.3)$$

It is noticed in Table 7.1 that the interaction (xy) and the repacking effects are insignificant in both cases of ideally and badly distributed feeds. Thus in the ideally distributed feed case, (well distributed bed), it can be said that the total effect of the x-direction is the minimum.

$$\text{i.e.} \quad \sum_{i=1}^{a} \alpha_i^2 = \left(\sum_{i=1}^{a} \alpha_i^2\right)_{min} \qquad \ldots\ldots (7.4)$$

And that the total effect of the y-direction on the gas distribution is the minimum, i.e.

$$\sum_{j=1}^{b} \beta_j^2 = \left(\sum_{j=i}^{b} \beta_j^2\right)_{min} \qquad \ldots\ldots (7.5)$$

Substituting Eqns. 7.3, 7.4 and 7.5 in Eqns. 7.2a-7.2e will produce five estimates of ϕ_{min} as follows:

$$E\left[\frac{SSx}{a-1}\right] = \frac{\bar{V}^2}{n-1}\,\phi_{min} + \left[\frac{rb\sum_{i=1}^{a}\alpha_i^2}{a-1}\right]_{min} \qquad \ldots\ldots (7.6a)$$

$$E\left[\frac{SSy}{b-1}\right] = \frac{\bar{V}^2}{n-1}\,\phi_{min} + \left[\frac{rb\sum_{j=1}^{b}\beta_j^2}{b-1}\right]_{min} \qquad \ldots\ldots (7.6b)$$

$$E\left[\frac{SS(xy)}{(a-1)(b-1)}\right] = \frac{\bar{V}^2}{n-1}\,\phi_{min} + \frac{\sum_{i=1}^{a}\sum_{j=1}^{b}(\alpha\beta)_{ij}^2}{(a-1)(b-1)} \qquad \ldots\ldots (7.6c)$$

$$E\left[\frac{SSR}{(r-1)}\right] = \frac{\bar{V}^2}{n-1}\,\phi_{min} + \frac{ab\sum_{k=1}^{r}\rho_k^2}{r-1} \qquad \ldots\ldots (7.6d)$$

$$E\left[\frac{SSE}{(ab-1)(r-1)}\right] = \frac{\bar{V}^2}{n-1}\,\phi_{min} \qquad \ldots\ldots (7.6e)$$

That means that the sum of squares are functions of ϕ_{min} from which it would be immediately concluded that all five estimates of ϕ_{min} are unbiased when

$$\Sigma\alpha_i = \Sigma\rho_j = \Sigma(\alpha\beta)_{ij} = \Sigma\rho_k = 0 \qquad \ldots\ldots (7.7)$$

Eqn. 7.7 is satisfied only if the gas is evenly distributed, and this condition could not be found in the packed beds due to their random nature.

In a maldistributed packed bed $\phi > \phi_{min}$ and the gas is maldistributed in the x and y directions, i.e.

$$\sum_{i=1}^{a} \alpha_i^2 > \left(\sum_{i=1}^{a} \alpha_i^2 \right)_{min}$$

and

$$\sum_{j=1}^{b} \beta_j^2 > \left(\sum_{j=1}^{b} \beta_j^2 \right)_{min}$$

and the five estimates of ϕ will be:

$$E\left[\frac{SSx}{(a-1)}\right] = \frac{\bar{V}^2}{n-1}\phi + \frac{rb\sum_{i=1}^{a}\alpha_i^2}{(a-1)} \quad \ldots\ldots (7.8a)$$

$$E\left[\frac{SSy}{(b-1)}\right] = \frac{\bar{V}^2}{n-1}\phi + \frac{ra\sum_{j=1}^{b}\beta_j^2}{(b-1)} \quad \ldots\ldots (7.8b)$$

$$E\left[\frac{SS(xy)}{(a-1)(b-1)}\right] = \frac{\bar{V}^2}{n-1}\phi + \frac{r\sum_{i=1}^{a}\sum_{j=1}^{b}(\alpha\beta)_{ij}^2}{(a-1)(b-1)} \quad \ldots\ldots (7.8c)$$

$$E\left[\frac{SSR}{(r-1)}\right] = \frac{\bar{V}^2}{n-1}\phi + \frac{ab\sum_{k=1}^{r}\rho_k^2}{(r-1)} \quad \ldots\ldots (7.8d)$$

$$E\left[\frac{SSE}{(ab-1)(r-1)}\right] = \frac{\bar{V}^2}{n-1}\phi \quad \ldots\ldots (7.8e)$$

Where the right hand terms represent the effects of the point to point velocity variation and the regional velocity variation, and $\phi > \phi_{min}$.

Fig. 7.1 Configuration of the 144 Points, (bounded by dotted line). Used in Two-Factor Analysis of the Variance and Response Surfaces

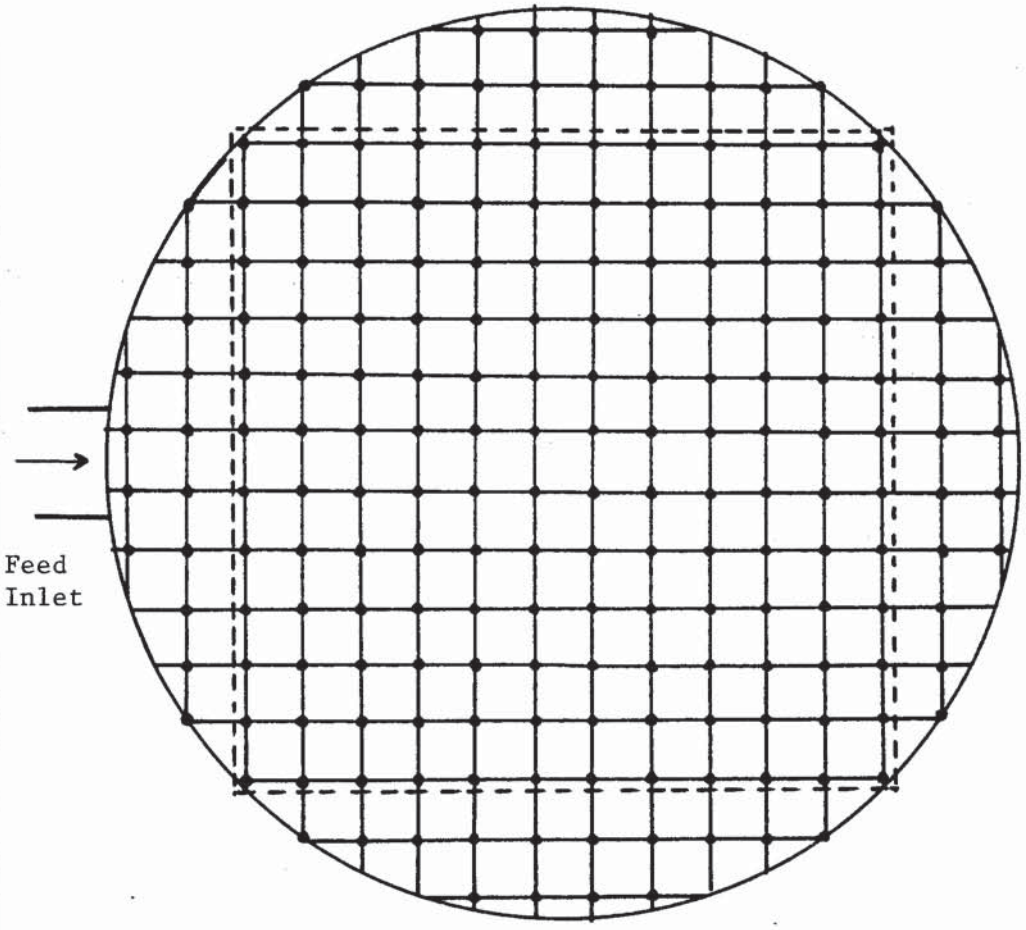

Table 7.1 Computed f-values Result from Two-Factor Analysis of the Variance

Status	D (mm)	$\frac{D}{H}$	Re	$\overline{\phi}$	Computed f-values			
					Rep.	x	y	xy
Ideal distribution	610	6	29000	20.72	0.65	1.46	1.18	1.06
	610	3	29000	20.37	0.62	1.405	1.0	1.12
	381	6	30700	20.48	0.611	1.446	0.979	1.02
Maldistributed	610	6	32000	85.11	0.614	47.06	1.823	0.736
	610	3	32000	29.3	0.57	11.8	1.012	1.04
	381	6	32000	85.1	0.587	46.78	2.03	0.853
	381	3	32000	29.03	0.236	11.57	1.13	0.577
	381	1	30000	20.15	0.53	1.43	1.05	1.17

Note: Standard tabulated f-values at 0.05 level of confidence obtained from Appendix A4, Table A4.4 are as follows:

(1) For x-effect and y-effect: $f_{0.05} = 1.79$

(2) For xy effect: $f_{0.05} = 1.22$

(3) For repacking effect: $f_{0.05} = 3$

Table 7.2 Computed f-values Result from Three Factor Analysis of the Variance for Geometrically Similar Beds Operated at Re = 30000 and D/P.H. = 3

Source of variation	Computed f-values for geometrically similar bed		$f_{0.05}$
	Ideal	Maldistributed	
x	1.613	11.753	1.71
y	1.315	2.216	1.71
D	0.543	0.568	3.84

7.4 Graphical Illustration of the Flow Pattern of the Gas Emerging from the Top of the Packed Beds

In two-factor analysis of the variance, a study was made to estimate the details of the distribution of the gas emerging from the top of packed beds.

In this section of the work the gas maldistribution is going to be studied graphically by producing graphical figures which represent the actual gas velocity distribution above the packed bed. These graphical figures (response surfaces), are formed by drawing lines through the observed point velocities by the use of the computer program listed in Appendix A5. Thus these response surfaces will provide more insight on the idea of the maldistribution of the gas in packed beds as a whole.

7.4.1 Method

The 144 point velocity measurements used previously in two-factor analysis of the variance and shown in Fig. 7.1 are again used here by feeding these observations, for any packed bed dealt with in this work, into the computer program listed in Appendix A5. Each point velocity of these 144 points is the average value of air velocity measured at a point each time the bed is repacked, (3 times). This means that each response surface represents the average gas maldistribution above that packed bed. Two views are produced for each response surface.

7.4.2 Results and Discussion

Response surfaces are produced to show the gas distribution above geometrically and dynamically similar ideally distributed and maldistributed packed beds and presented in Figures 7.2-7.9.

Figures 7.2 and 7.3 show the response surfaces of the gas distribution above two geometrically and dynamically similar ideally distributed packed beds of packed height to diameter ratio of 0.167. The interesting feature of these figures is that each response surface consists of points which go above and below an average value all over the surface. Similarly, Figures 7.4 and 7.5, which show the response surfaces for the same beds above but of packed depth to bed diameter ratio of 0.333, show the same phenomenon. All these response surfaces show a great deal of similarity amongst themselves which indicates a similar gas flow pattern in geometrically and dynamically similar beds of ideal feed distribution.

Figures 7.6 and 7.7 also show a great deal of similarity. They represent a gas distribution above maldistributed beds of P.H./D ratio of 0.167. Although they are not smooth, due to the point to point velocity variation but the most important feature of them is that the existence of areas near the feed inlet consist of point velocities lower than the average velocity, and that part of the surface as a whole is lower than the average value. At the same time, the other part of the surface is much higher than the average value. This means that the maldistribution of the gas is due to two sources. First, the point to point velocity variation which occurs all over the surface and second, the existence of regions of very high velocities and others of very low velocities, this phenomenon is subsequently referred to as regional velocity variation.

As the packed depth increases proportionally in the two beds mentioned above, the regional velocity variation decreases as shown in Figures 7.8 and 7.9 which are highly similar to each other.

From all these figures, the similarity of flow pattern in geometrically and dynamically similar packed beds can be visualized clearly through the similarity between their response surfaces.

7.4.3 Discussion of ϕ in Relation to Response Surfaces

Response surfaces produced for an ideally distributed bed show only point to point velocity variations, which are the same beds whose gas maldistributions are described by ϕ_{min} in Section 6.5.1. At that stage, it was claimed that ϕ_{min} cannot be equalled to zero due to the existence of point to point velocity variation. The response surfaces demonstrated the existence of such point to point velocity variation.

Also, the similarity between these response surfaces shows the similarity of the flow pattern of gas through these beds. This similarity exists between response surfaces of gas distribution through maldistributed beds of geometric and dynamic similarity which explains the similarity of the obtained ϕ values for such beds and gives some insight on the sources of the gas maldistribution; point to point velocity variations and regional velocity variations which are combined together to produce high ϕ value.

Therefore, the technique of producing response surfaces has provided further proof of the validity of ϕ as a reliable measure of the gas maldistribution through packed beds and also provides more evidence on the validity of the scale-up rules.

7.5 Conclusions

From these two techniques; Multi-factor analysis of the variance and response surface, it could be concluded that:

(1) The maldistribution factor, ϕ, is a reliable measure of the gas maldistribution in packed beds and specially in shallow large diameter packed beds due to its sensitivity to any change in feed distribution; where it has a minimum value for an ideally distributed feed and a much larger value for a maldistributed feed entering the bottom of the bed.

(2) The validity of the scale-up rules has been proved by two more techniques in addition to ϕ technique.

7.6 Summary

In this work, two techniques, Multi-factor analysis of the variance and the response surface, have been used to prove the validity of the scale-up rules and the efficiency of ϕ in measuring gas flow pattern in packed beds. In the next section of the work, an experimental investigation of the fluid mechanics of a maldistributed gas flow, is carried out to know the reasons behind such maldistributions and to provide a better understanding of this phenomenon.

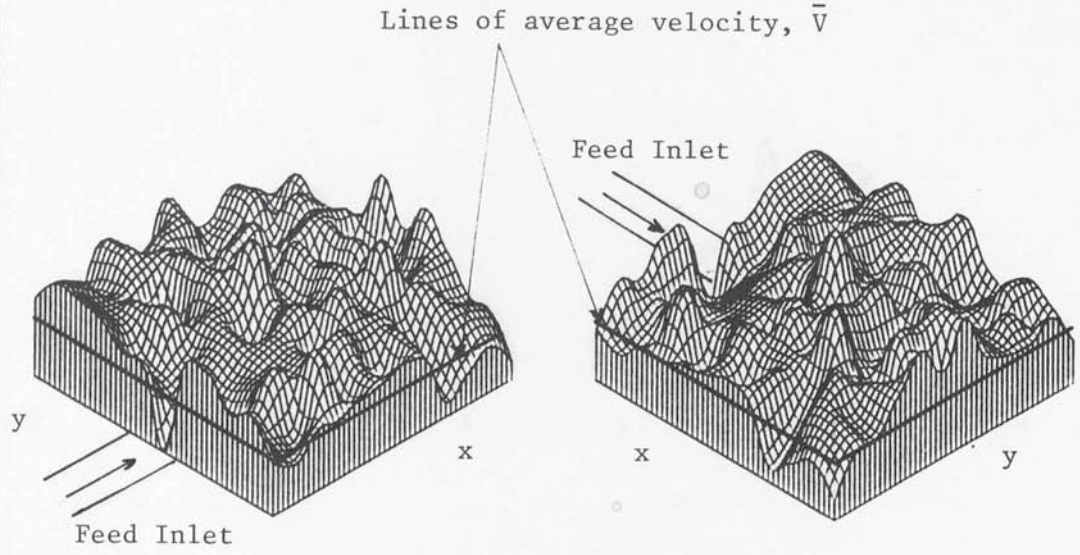

Fig. 7.2 Two views of Gas Distribution above an Ideally Distributed Bed of 381 mm diameter and 63.5 Packed Height

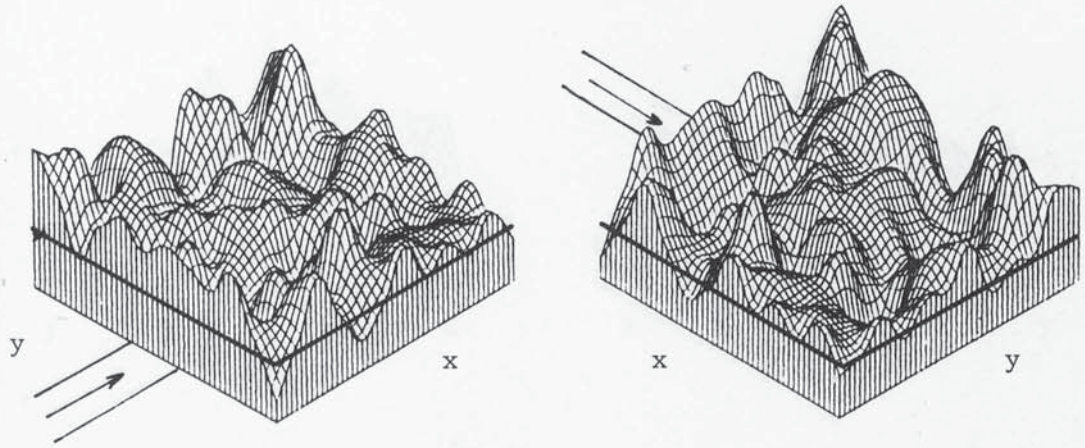

Fig. 7.3 Two Views of Gas Distribution above an Ideally Distributed Bed of 610 mm Diameter and 101.6 mm Packed Height

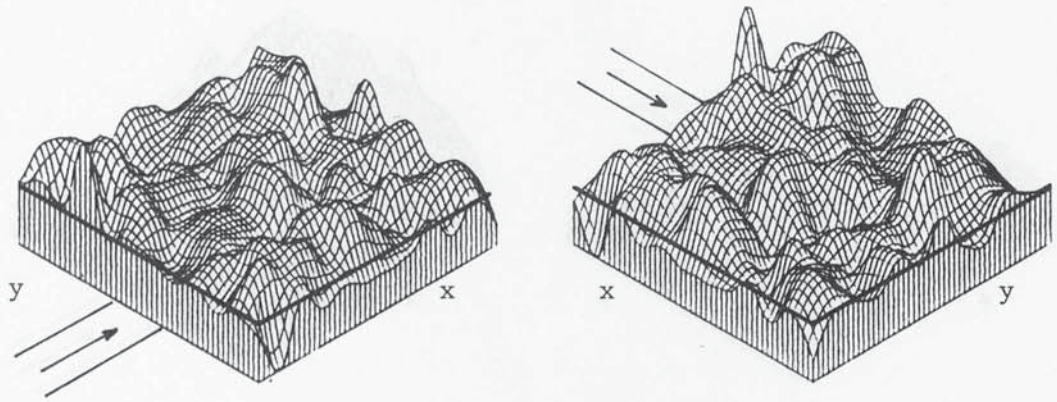

Fig. 7.4 Two views of Gas Distribution above an Ideally Distributed Bed of 381 mm Diameter and 127 mm Packed Height

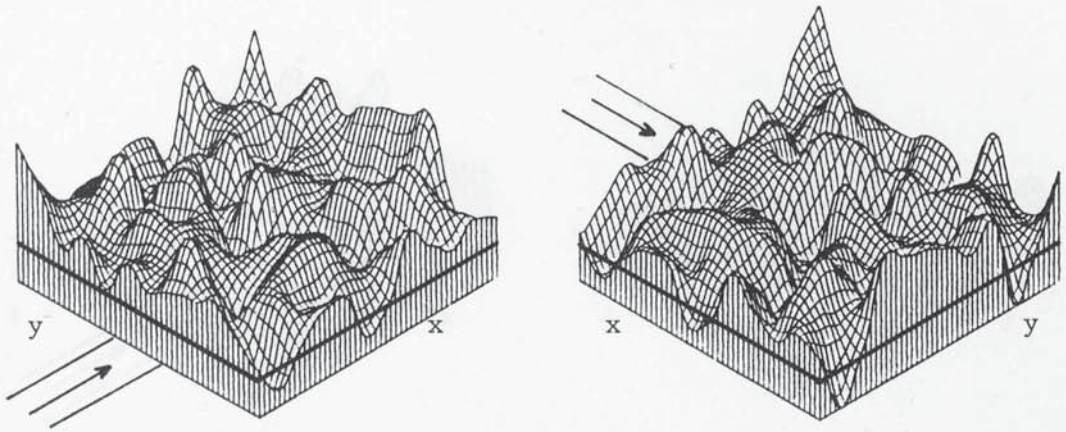

Fig. 7.5 Two views of Gas Distribution above an Ideally-Distributed Bed of 610 mm Diameter and 203 mm Packed Height

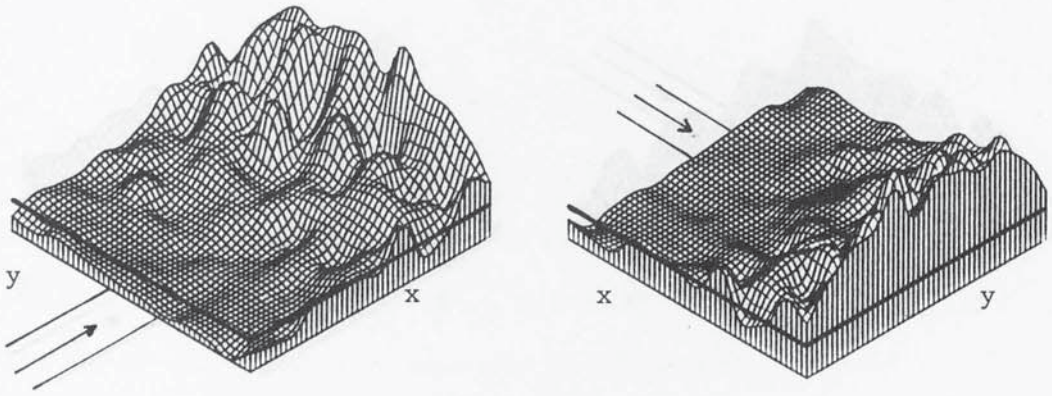

Fig. 7.6 Two views of Gas Distribution above a Maldistributed Bed of 381 mm Diameter and 63.5 mm Packed Height

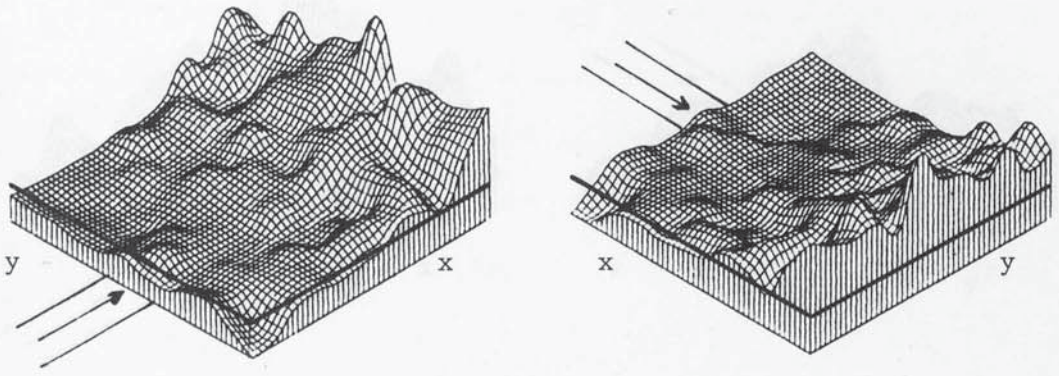

Fig. 7.7 Two Views of Gas Distribution above a Maldistributed Bed of 610 mm Diameter and 101.6 mm Packed Height

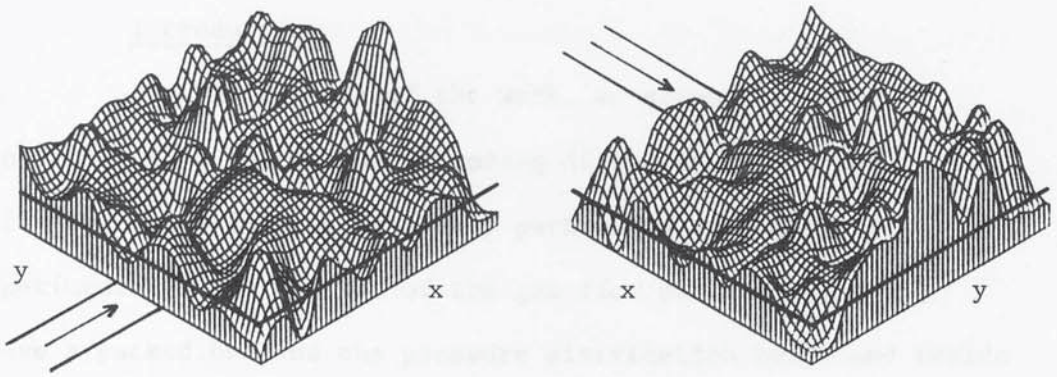

Fig. 7.8 Two views of Gas Distribution above a Maldistributed Bed of 381 mm Diameter and 127 mm Packed Height

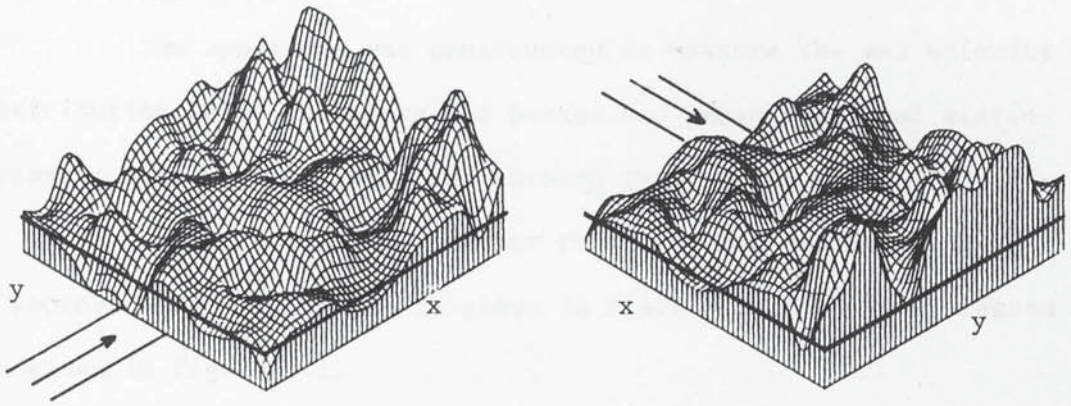

Fig. 7.9 Two Views of Gas Distribution above a Maldistributed Bed of 610 mm Diameter and 203 mm Packed Height

SECTION VIII

EXPERIMENTAL INVESTIGATION OF THE FLUID MECHANICS OF MALDISTRIBUTED GAS FLOWS

Introduction

In this section of the work, an attempt is made to contribute to a better understanding of the causes of gas maldistribution in packed beds by performing an elaborate experimental investigation of the gas flow pattern below and above a packed bed and the pressure distribution below and inside that packed bed. The clarification of the mechanism of the distribution of the gas in packed beds will provide the basis for solving the problem of gas maldistribution in packed beds and the principles of designing devices to overcome this problem will be established.

8.1 Apparatus

The apparatus was constructed to measure the gas velocity distribution below and above the packed bed under test, and static pressure distribution below and through that packed bed.

A 1220 mm inside diameter packed column was designed. A photograph of the column is shown in Plate 8.1 and a line diagram is given in Figure 8.1.

The shell is constructed from 3 mm thick mild steel sheets, it consists of two parts; a bottom part and a top part.

The bottom part, see Fig. 8.1, consists of an upside down truncated cone, 450 mm side length and 386 mm high. The small base, 756 mm inside diameter, is welded to a cylindrical part of 305 mm long whose other end is closed by a removable PVC plate. The big base of the cone is 1220 mm inside diameter welded to an 1320 outside

diameter flange. This part (bottom part) is held safely by a handy angle bar bench to a height of 600 mm above the ground to allow access for entering the column from beneath.

The top part, a 2000 mm long cylinder and 1220 mm inside diameter, is fitted with flanges from both ends and bolted to the bottom part.

The feed is introduced either tangentially or radially through a 152 mm inside diameter feed pipe whose central line is 400 mm above the bottom end of the cylindrical part.

A flat support plate of 1 cm x 1 cm square mesh made from 1 mm diameter wire is supported by a 1210 outside diameter support ring, 12.7 mm wide and 6.5 mm thick and fitted at 460 mm above the feed pipe central line to the inner side of the column. To keep the support plate flat when the bed is packed, a number of vertical 0.5mm diameter galvanized steel wires are used to support the weight of the bed by hanging the support plate to a steel beam above the column. These galvanized wires exert a negligible, (if any), obstruction to the gas flowing inside the bed.

The static pressure below and inside the bed is measured by a micromanometer, described in Section 4.2.4, using an ordinary pitot-tube. The gas velocity below the bed is measured by the same micromanometer mentioned above by using a combination of an ordinary pitot-tube and 0.5 mm inside diameter steel tube described in Section 4.2.4 and shown in Plate 4.4. The gas velocity above the bed is measured by a modified hot-wire anemometer, described in Section 4.2.3.

The bed itself is packed with size 16 mm plastic pall rings to 6 cm and 36 cm depths.

Air is fed tangentially or radially by the air supply

equipment described in Section 4.1 at different flow rates.

The work in this section is performed in two stages according to the way of introducing the feed to the column.

8.2 Shallow Large Diameter Packed Beds with Tangential Feed Inlets

The air is introduced tangentially to the column at rates of 0.814 m^3/sec., 0.706 m^3/sec., and 0.59 m^3/sec. below a bed packed to depths of 6 cm and 36 cm. The air velocity and the static pressure below, inside, and above the bed are measured along one diameter. It has been observed, below the bed, that the air is swirling tangentially and parallel to the bottom of the bed.

8.2.1 Results (Packed Depth = 6 cm)

The air was pumped at a rate of 0.814 m^3/sec., i.e. 44.5m/sec through the inlet pipe. It was observed that the feed temperature at the inlet of 20°C was raised to 25°C below and inside the bed. The static pressure below the bed, at the bottom of the bed and above the bed was measured and the air velocity below and above the bed was recorded along one diameter. These observations are listed in Table 8.1. The air velocity distribution is shown in Graph 8.1, the static pressure distribution is shown in Graph 8.2. The theoretical total number of heads of air just below the bed were compared with the actual heads measured, "static pressure", at the bottom of the bed in Graph 8.3.

The results show:

1) Below the bed, the air velocity is very high near the wall, especially the region opposite to the feed inlet, and

decreases towards the centre, see Graph 8.1.

2) The air, leaves the bed vertically, has a relatively high velocity near the wall and there is a negative flow in the middle part of the bed.

3) The static pressure below the bed is constant across the diameter and has a negative value of -0.025 mm W.G., see Graph 8.2.

4) The static pressure just inside the bottom of the bed has high values near the wall and negative values at the area of the negative air flows.

5) The total theoretical number of heads (the pressure measured by the pitot-tube), below the bed is very high near the wall and falls sharply towards the centre and has values greater than the measured static pressure at the bottom of the bed, especially in the area near the feed inlet.

6) The static pressure inside the bed near the top has the same trend as that at the bottom but with lower values, a smaller variation and a larger area of negative pressure.

8.2.2 Discussion of the Results (Packed Depth = 6 cm)

It is clear that the swirling air has a high velocity near the column wall which decreases towards the centre due to the nature of introducing the air. When this swirling gas, with such a velocity distribution, hits the packings at the bottom of the bed, its direction and its velocity are changed and some of its dynamic energy,(momentum), is transferred into a static pressure whose magnitude at a point depends on the velocity of the approaching swirling gas at that point. For that reason high

static pressure values are observed at the areas of high air velocities, i.e. near the wall. Theoretically, all the velocity heads just below the bed should be converted into a static pressure at the bottom of the bed, but, as shown in Graph 8.3, the measured static pressure is much less than the velocity heads. The difference between the theoretical and actual pressures is converted into a thermal energy due to the friction between the swirling air, on the one hand, and the support plate and the bottom layer of the packings, on the other hand. This explains the temperature rise from 20°C at the feed nozzel to 25°C inside the column.

Obviously, there should be a temperature variation in the bed, but this variation is unable to be detected due to the high rate of the gas mixing throughout and below the bed.

At the middle part of the bed where the swirling gas velocity is very low, a convergence between the values of the theoretical and actual pressures can be noticed, see Figure 8.3.

8.2.3 Negative Gas Flow in the Middle Area of the Packed Bed

The results show that the high static pressure is concentrated at the peripheral area of the bed, the width of this area is more or less equal to the diameter of the feed nozzel. This high pressure acts as a driving force which drives the air upwards, in that peripheral area, out of the bed at a quantity more than the feed inlet supplies. This results in a negative static pressure below the bed and negative air flows at the middle of the bed to maintain the mass balance.

8.2.4 Results (Packed Depth = 36 cm)

The bed depth was increased to 36 cm and air velocity and pressure measurements were made at 0.814 m^3/sec, 0.71 m^3/sec and 0.6 m^3/sec air volumetric flow rates. At air flow rate of 0.814 m^3/sec, the air velocity distribution below and above the bed is given in Graph 8.5. The static pressure distributions below the bed, at the bottom of the bed and at two levels inside the bed are shown in Graph 8.4 and listed in Table 8.2. The difference between the theoretical total number of the air heads and the measured static pressure is shown in Graph 8.6.

The static pressure is measured at the bottom of the bed and 15 cm above the bottom at air flow rates of 0.71 m^3/sec and 0.6 m^3/sec and listed in Tables 8.3 and 8.4 and plotted against the radial distance in Graphs 8.7 and 8.8 respectively.

The results show that:

1) The air below the bed has a high tangential velocity near the wall and decreases towards the centre, (see Fig. 8.5).

2) The air emerges from the top of the bed vertically and uniformly distributed except the point to point velocity variations, and there is no negative air flow.

3) The static pressure below the bed is constant and positive (+0.84 mm W.G.), see Fig. 8.4.

4) The static pressure distribution flattens as it moves up in the bed, and it is completely flat inside the bed near the top.

5) The theoretical number of heads of the air is higher than the measured static pressure near the wall; and lower than the static pressure at the middle area of the bed, (see Fig. 8.6).

6) The static pressure at a point in the bed increases

as the air velocity increases, (see Figs. 8.7 and 8.8).

8.3 Discussion

In a similar way to the experiments at a packed depth of 6 cm, the static pressure measured in the packing at the bottom of the bed is higher near the wall than that measured at the middle region due to higher air velocities near the wall. But neither the negative pressure nor the negative air flow is found in the middle region and the static pressure below the bed is positive and constant, (see Graph 8.4).

It is obvious that the pressure difference between two areas is the force which drives the air from the high pressure area to the low pressure area in the packed bed. This means that in addition to the upwards, "axial", flow of the air in the wall zone, (High Pressure Zone), some air is flowing "Radially" towards the middle area, (Low Pressure Zone).

In the 6 cm deep bed there was not enough packing depth to homogenize the pressure and the air flow. But the 36 cm depth has allowed for the homogenizing of the pressure, and consequently the air flows, to take place before emerging from the top of the bed. For this reason the pressure profile becomes flatter at higher levels in the 36 cm deep bed, until it becomes flat at a distance of 30 cm above the bottom of the bed. Above this level, the pressure profile has maintained its flatness causing the air to emerge uniformly from the top of the bed, (see Graph 8.5).

It is clear that the theoretical number of heads of the air below the bed is higher than the actual measured static pressure inside the packing near the bottom due to the friction energy losses.

This phenomenon is clearly observed in the 6 cm deep packed bed, but in the 36 cm deep bed, the situation is the same in the wall zone but it is apparently reversed in the middle area of the bed, (see Graph 8.6). In reality the actual static pressure in the middle area is also less than the theoretical pressure, but the measured static pressure shown in Graph 8.6 is the summation of the static pressure below the bed due to the bed resistance to air flow, and the velocity generated static pressure. Thus the summation of these two types of the static pressure is larger than the theoretical number of heads of the air at the middle area which is small due to the low tangential air velocity below this area.

8.4 Comments on the Velocity Generated Static Pressure Distribution

As shown above, the velocity generated static pressure at a point inside the packing near the bottom of the bed equals the measured static pressure at that point minus the static pressure below the bed, which has a constant value. This means that the velocity generated static pressure has a similar distribution to that of the measured static pressure. Thus, the following comments can be made:

1) The velocity generated static pressure at a point inside the packing near the bottom of the bed is proportional to the velocity of the swirling air below the bed approaching that point. That is proportional to the velocity of air in the feed pipe. This is shown in Graph 8.9, where the value of velocity generated static pressure at different points at the bottom of the bed is drawn against the air velocity (square) in the feed pipe. The straight lines indicate that:

$$P_g \propto V_p^2 \qquad \ldots\ldots (8.1)$$

where P_g is the velocity generated static pressure.

V_p is the air velocity in the feed pipe.

Eqn. 8.1 assumes a constant air density, ρ. Thus to generalize the equation:

$$P_g = k\rho(V_p)^2 \qquad \ldots\ldots (8.2)$$

Where k is the proportion of the theoretical total number of heads transformed into a static pressure at the bottom of the bed.

2) The velocity generated static pressure at the bottom of the packed bed is more or less the same in the small depth bed, (6 cm), and the large depth, (36 cm). This is shown in Graph 8.10 where the value of P_g for the two beds is drawn against the radial distance; [the values of P_g are obtained by subtracting the static pressure below each bed from the measured static pressure at the bottom of that bed respectively. These values are listed in Tables 8.1 and 8.2].

Therefore k can be assumed to be the same for both bed depths.

3) The width of the high pressure area in both beds, (the 6 cm and 36 cm deep beds), is constant and more or less equals the diameter of the feed pipe, (see Graph 8.10), where the width of high pressure zone equals the feed inlet diameter, (15.2 cm).

8.5 Pressure Distribution in Shallow Large Diameter Packed Beds with Radial Feed Inlets

The air is fed radially through 15.2 cm diameter pipe

below the 36 cm deep packed bed at a rate of 0.6 m^3/sec. The static pressure is measured, along one diameter in line with the feed direction, at the bottom of the bed and at 15 cm above the bottom. The results are listed in Table 8.5 and drawn against the radial distance in Graph 8.11.

The results show a very high static pressure in the area opposite to the feed inlet and a relatively high static pressure at the area near the feed inlet. The smallest static pressure was observed in the middle area. The static pressure profile flattens at higher levels in the bed.

8.6 Summary

The air velocity and static pressure distributions are observed in packed beds with a tangential feed inlet, in this section of the work. The low pressure and the high pressure zones were observed. A negative air flow was noticed at very short packed depths which disappears as the packed depth increases.

In the next stage of the work, simple models have been suggested to explain the flow patterns in packed beds based on the results observed in this section.

PLATE 8.1

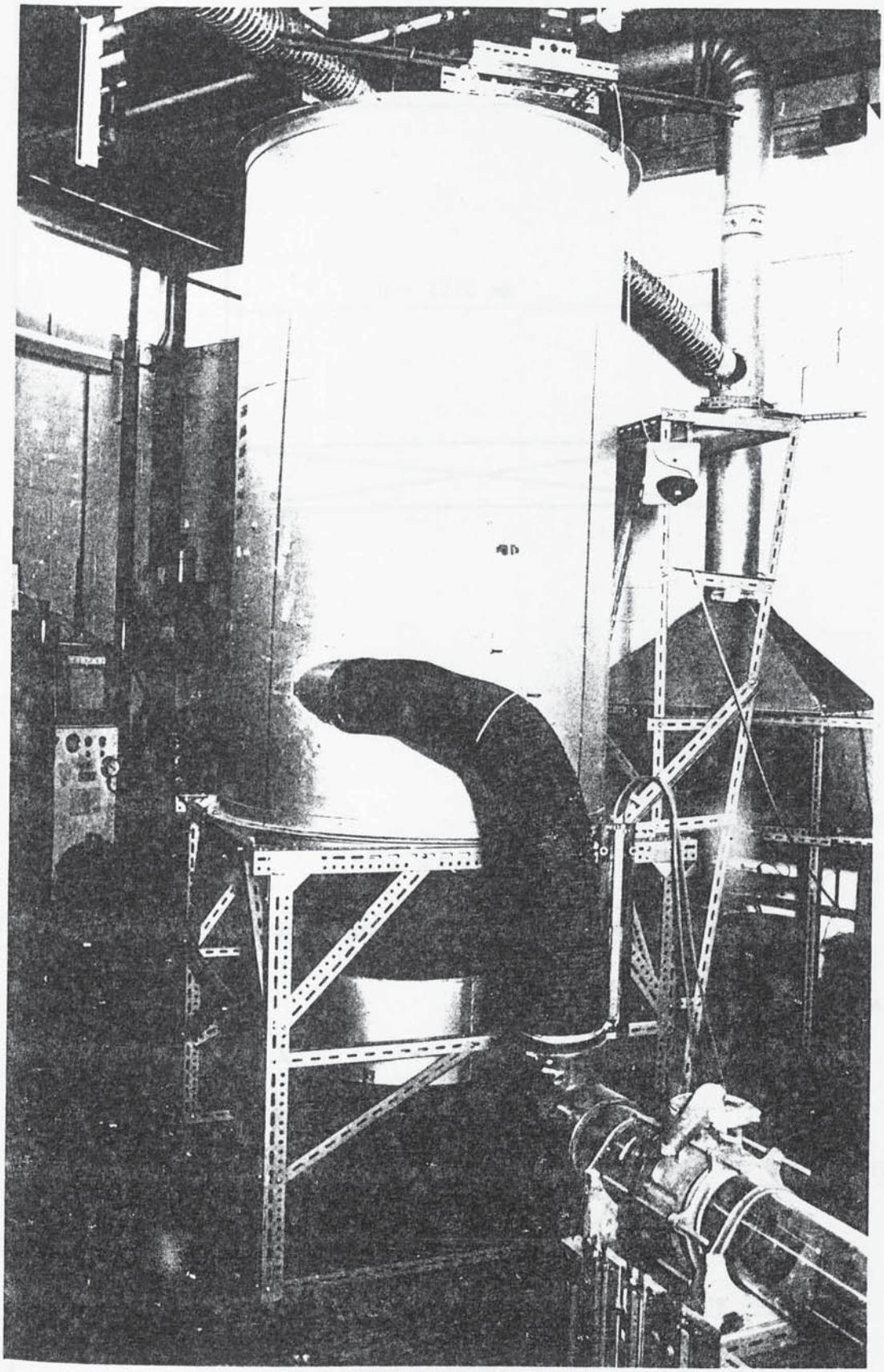

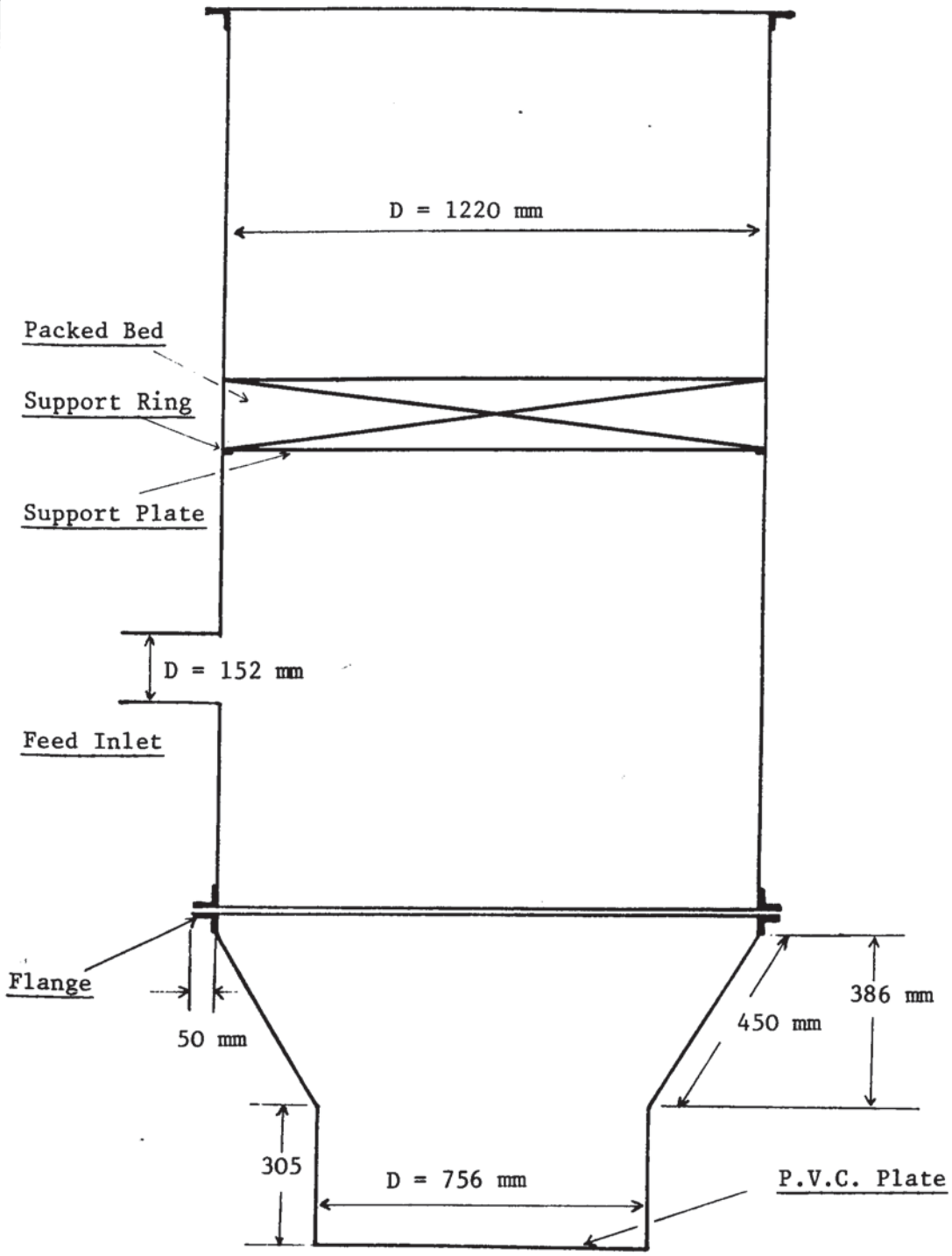

Fig. 8.1 Diagram of the Apparatus used in measuring Gas velocity and Pressure Distributions

Table 8.1 Pressure Distribution in a 6cm Deep Packed Bed

(Air flow rate = 0.814 m^3/sec)

r(cm)	Static Pressure (mm W.G.)			Below the Bed	
	Below the Bed	Distance above the Bottom (cm)		Pitot-tub Reading	Velocity m/sec.
		0	6		
60	-0.025	2.6	0.6	14.85	15.572
54	-0.025	2.3	0.5	14.25	15.254
48	-0.025	1.0	0.30	10.50	13.090
42	-0.025	0.30	0.10	5.90	5.815
36	-0.025	0.00	-0.15	2.00	5.715
30	-0.025	-0.06	-0.2	0.81	3.637
24	-0.025	-0.08	-0.38	0.60	3.130
18	-0.025	-0.09	-0.42	0.24	1.58
12	-0.025	-0.11	-0.42	0.09	1.202
6	-0.025	-0.14	-0.42	0.03	0.70
C	-0.025	-0.14	-0.42	0.02	0.571
6	-0.025	-0.14	-0.42	0.06	0.99
12	-0.025	-0.13	-0.40	0.3	2.213
18	-0.025	-0.12	-0.32	0.45	2.711
24	-0.025	0.075	-0.24	1.2	4.276
30	-0.025	0.10	0.0	5.4	9.39
36	-0.025	0.75	0.1	7.2	10.843
42	-0.025	1.1	0.2	12.0	14.0
48	-0.025	3.6	1.0	13.5	14.847
54	-0.025	4.0	2.0	14.1	15.173
60	-0.025	8.0	4.8	15.9	16.113

Table 8.2 Pressure Distribution in a 36 cm Deep Bed

(Air flow rate = 0.814 m^3/sec)

r(cm)	Static Pressure (mm W.G.)				Below the Bed	
	Below the Bed	Distance above the Bottom(cm)			Pitot-tube Reading	Velocity m/sec
		0	15	30		
60	0.84	5.20	1.90	0.35	15.0	15.65
54	0.84	4.10	1.80	0.30	14.4	15.334
48	0.84	2.45	1.30	0.30	10.8	13.28
42	0.84	1.70	1.20	0.25	5.4	9.4
36	0.84	1.30	0.99	0.25	2.2	6.0
30	0.84	0.96	0.69	0.20	0.8	3.614
24	0.84	0.90	0.69	0.19	0.45	2.711
18	0.84	0.81	0.69	0.18	0.12	1.4
12	0.84	0.84	0.66	0.18	0.08	1.143
6	0.84	0.80	0.64	0.18	0.03	0.7
C	0.84	0.77	0.63	0.18	0.02	0.571
6	0.84	0.80	0.60	0.18	0.20	1.807
12	0.84	0.84	0.65	0.18	3.6	7.667
18	0.84	0.90	0.60	0.19	2.1	5.856
24	0.84	1.00	0.65	0.20	3.4	7.451
30	0.84	1.50	0.90	0.25	6.9	10.615
36	0.84	2.75	1.35	0.25	9.6	12.52
42	0.84	4.30	2.0	0.28	12.6	14.343
48	0.84	6.50	2.5	0.35	13.8	15.01
54	0.84	7.70	2.75	0.50	14.1	15.173
60	0.84	8.50	2.85	0.60	15.3	15.80

Table 8.3 Pressure Distribution in 36 cm Deep Bed

(Air flow rate = 0.706 m^3/sec)

r(cm)	Static Pressure (mm W.G.)			Below the Bed	
	Below the Bed	Distance above the Bottom (cm)		Pitot-tube Reading	Velocity m/sec
		0	15		
60	0.53	4.1	1.5	11.2	13.52
54	0.53	3.22	1.43	10.7	13.2
48	0.53	2.15	1.07	8.1	11.9
42	0.53	1.35	0.95	4.35	8.43
36	0.53	0.98	0.79	1.7	5.27
30	0.53	0.7	0.56	0.7	3.38
24	0.53	0.63	0.5	0.36	2.42
18	0.53	0.58	0.5	0.12	1.4
12	0.53	0.55	0.49	0.08	1.14
6	0.53	0.54	0.47	0.035	0.75
C	0.53	0.54	0.47	0.025	0.64
6	0.53	0.57	0.45	0.2	1.8
12	0.53	0.61	0.49	0.9	3.83
18	0.53	0.67	0.51	1.9	5.57
24	0.53	0.77	0.55	3.2	7.23
30	0.53	1.23	0.74	5.95	9.85
36	0.53	2.25	1.08	8.1	11.5
42	0.53	3.5	1.57	10.0	12.78
48	0.53	5.1	2.0	16.85	13.31
54	0.53	6.1	2.3	11.45	13.67
60	0.53	6.7	2.37	12.5	14.28

Table 8.4 Pressure Distribution in 36 cm Deep Bed

(Air flow rate = 0.59 m^3/sec)

r(cm)	Static Pressure (mm W.G.)			Below the Bed	
	Below the Bed	Above the Bottom (cm)		Pitot-tube Reading	Velocity
		0	15		
60	0.21	2.8	1.02	7.4	11
54	0.21	2.2	0.58	7.0	10.69
48	0.21	1.2	0.8	5.4	9.39
42	0.21	0.93	0.65	3.3	7.34
36	0.21	0.6	0.55	1.2	4.42
30	0.21	0.38	0.40	0.6	3.13
24	0.21	0.32	0.35	0.27	2.1
18	0.21	0.30	0.29	0.12	1.4
12	0.21	0.29	0.28	0.08	1.143
6	0.21	0.28	0.28	0.04	0.81
C	0.21	0.28	0.28	0.03	0.7
6	0.21	0.3	0.28	0.20	1.81
12	0.21	0.35	0.3	1.0	4.04
18	0.21	0.4	0.35	1.7	5.27
24	0.21	0.5	0.43	3.0	7.0
30	0.21	0.9	0.55	5.0	9.03
36	0.21	1.65	0.75	6.6	10.38
42	0.21	2.58	1.05	7.4	11
48	0.21	3.4	1.4	7.1	10.77
54	0.21	4.2	1.75	8.0	11.43
60	0.21	4.6	1.8	8.6	11.85

Table 8.5 Pressure Distribution in a 36 cm Deep Bed with a Radial Feed Inlet (Air flow rate = 0.59 m^3/sec)

Distance from the feed side	Static Pressure (mm W.G.)		
	below the bed	Distance above the bed	
		0	15
0	0.21	1.9	0.85
12	0.21	1.6	0.85
24	0.21	1.4	0.75
36	0.21	1.35	0.80
48	0.21	1.20	0.70
60	0.21	1.15	0.70
72	0.21	1.0	0.70
84	0.21	1.2	0.80
96	0.21	1.7	1.0
108	0.21	3.0	1.3
120	0.21	5.6	1.6

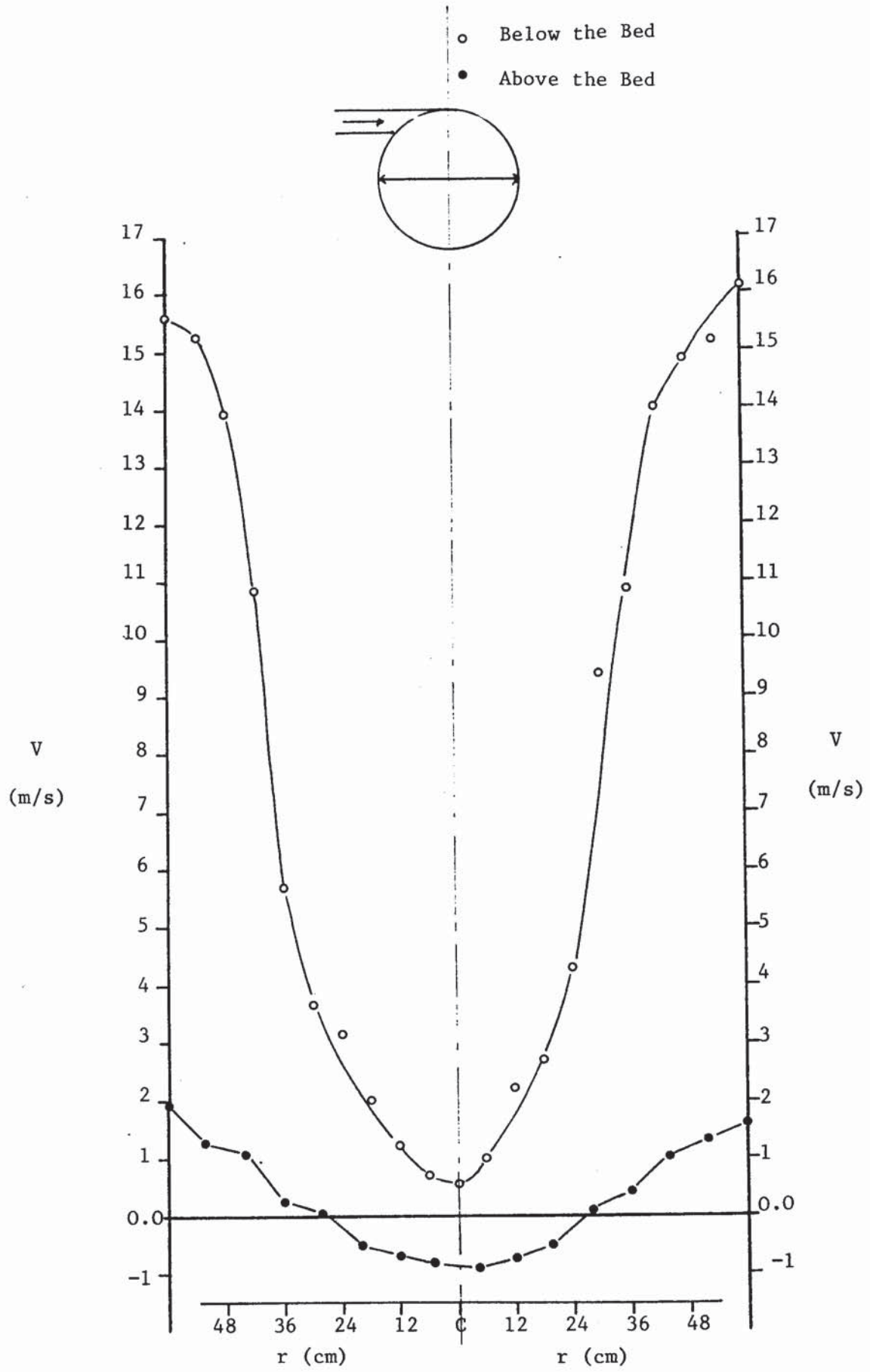

Graph 8.1 Velocity Distribution in a 6cm Deep Bed

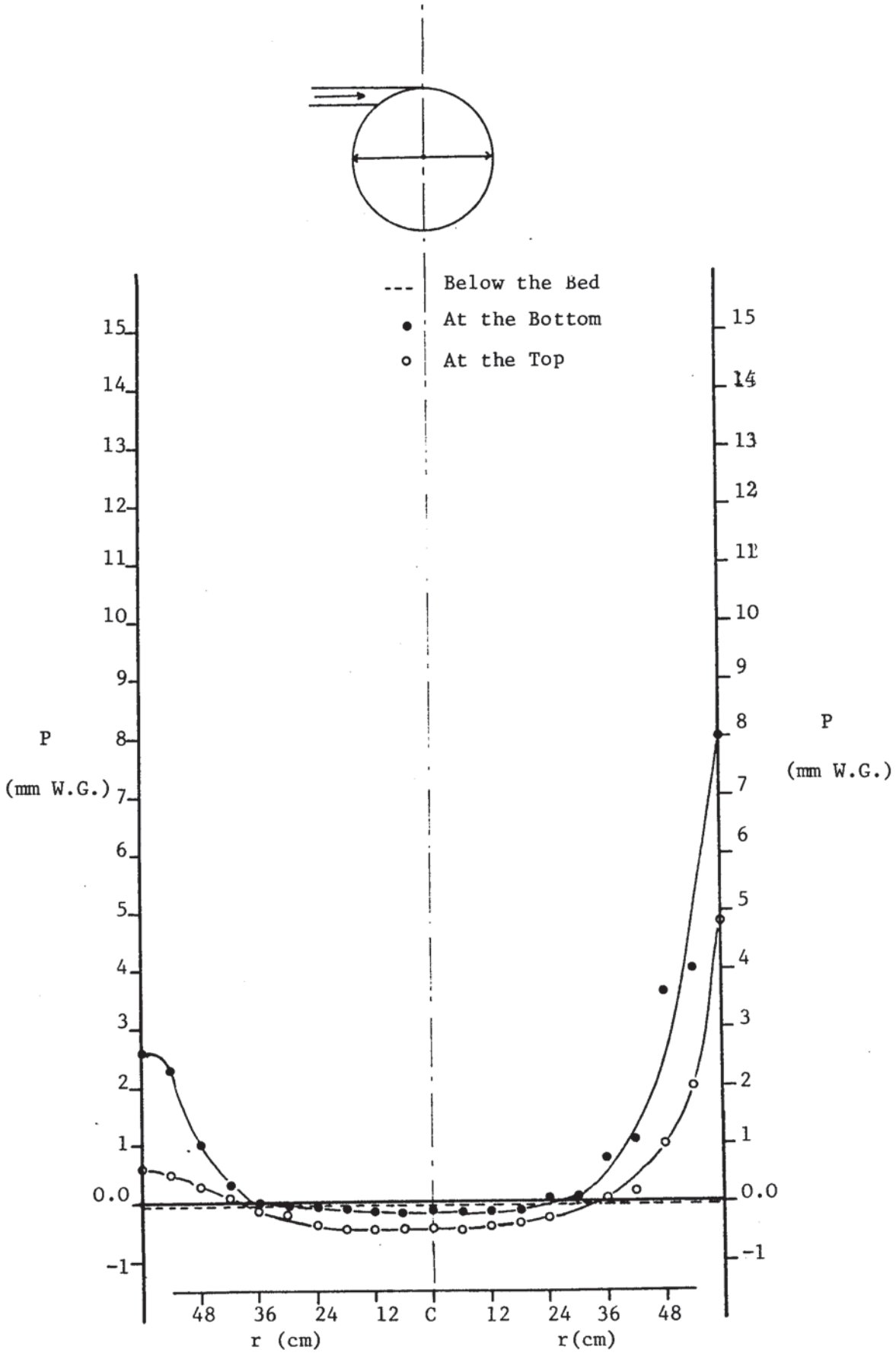

Graph 8.2 Pressure Distributionin a 6 cm Deep Bed

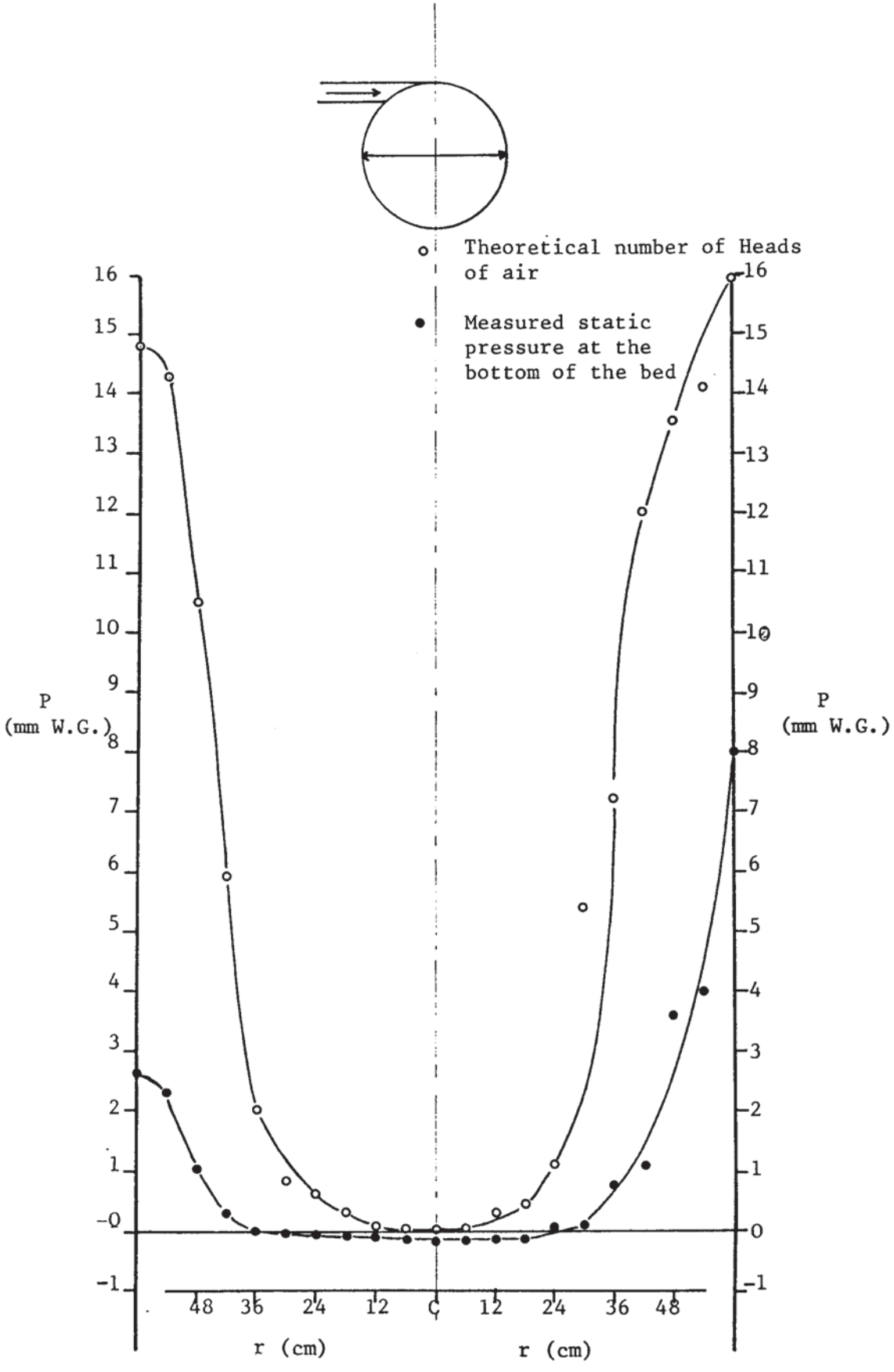

Graph 8.3 Theoretical and Measured Number of Heads in the 6cm Deep Bed

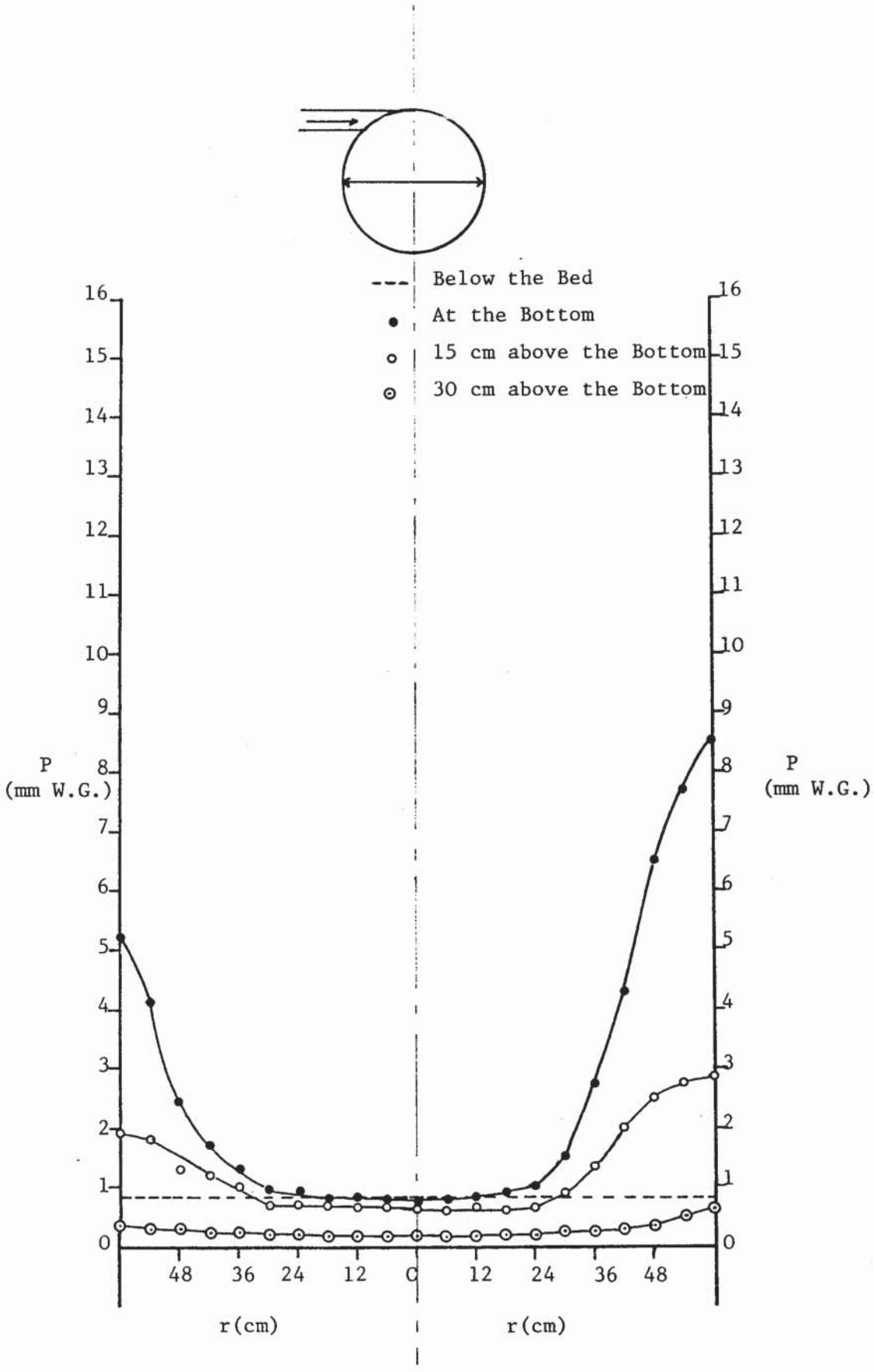

Graph 8.4 Pressure Distribution in a 36 cm Deep Bed

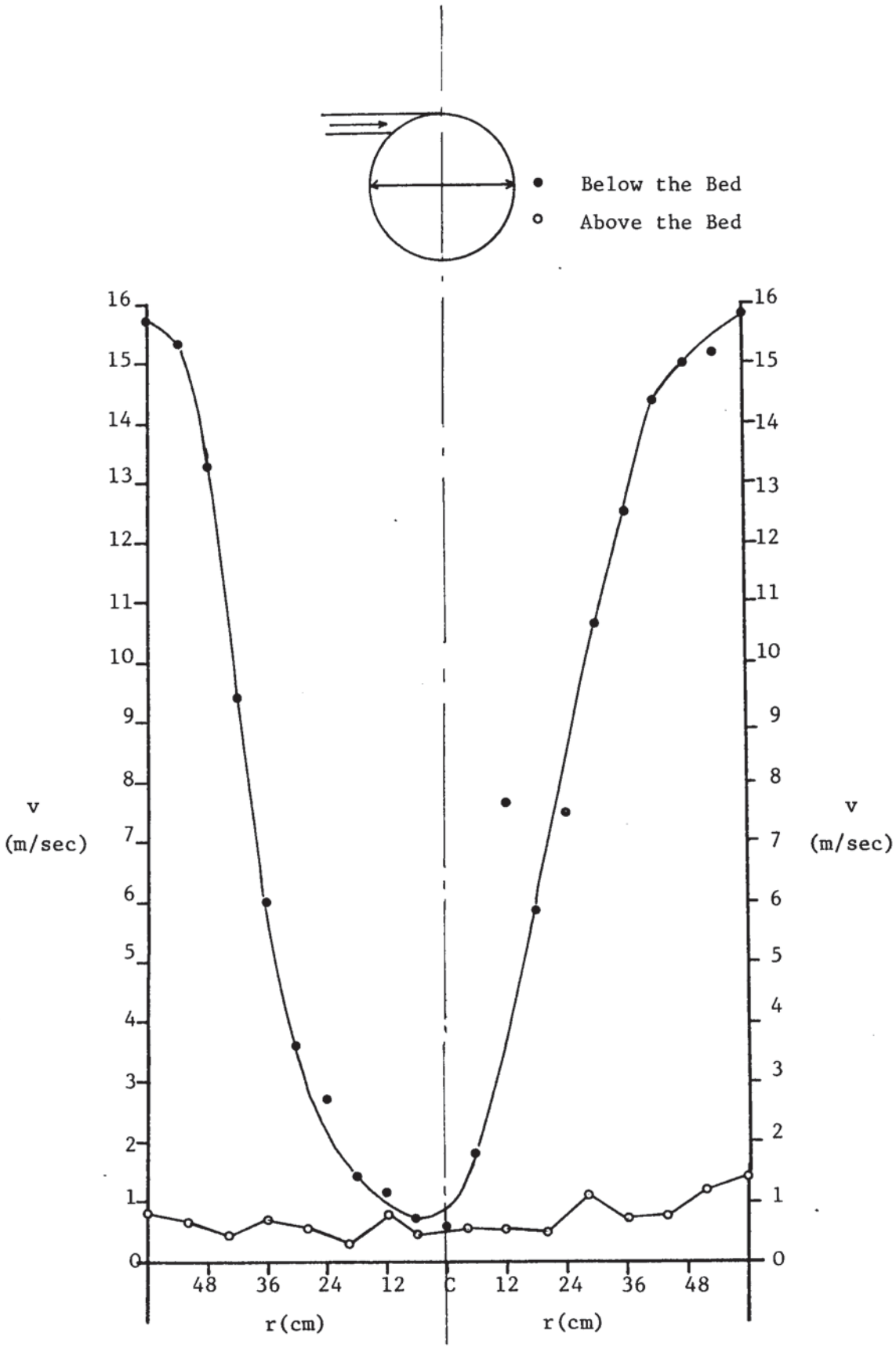

Graph 8.5 Air Velocity Distribution in the 36 cm Deep Bed

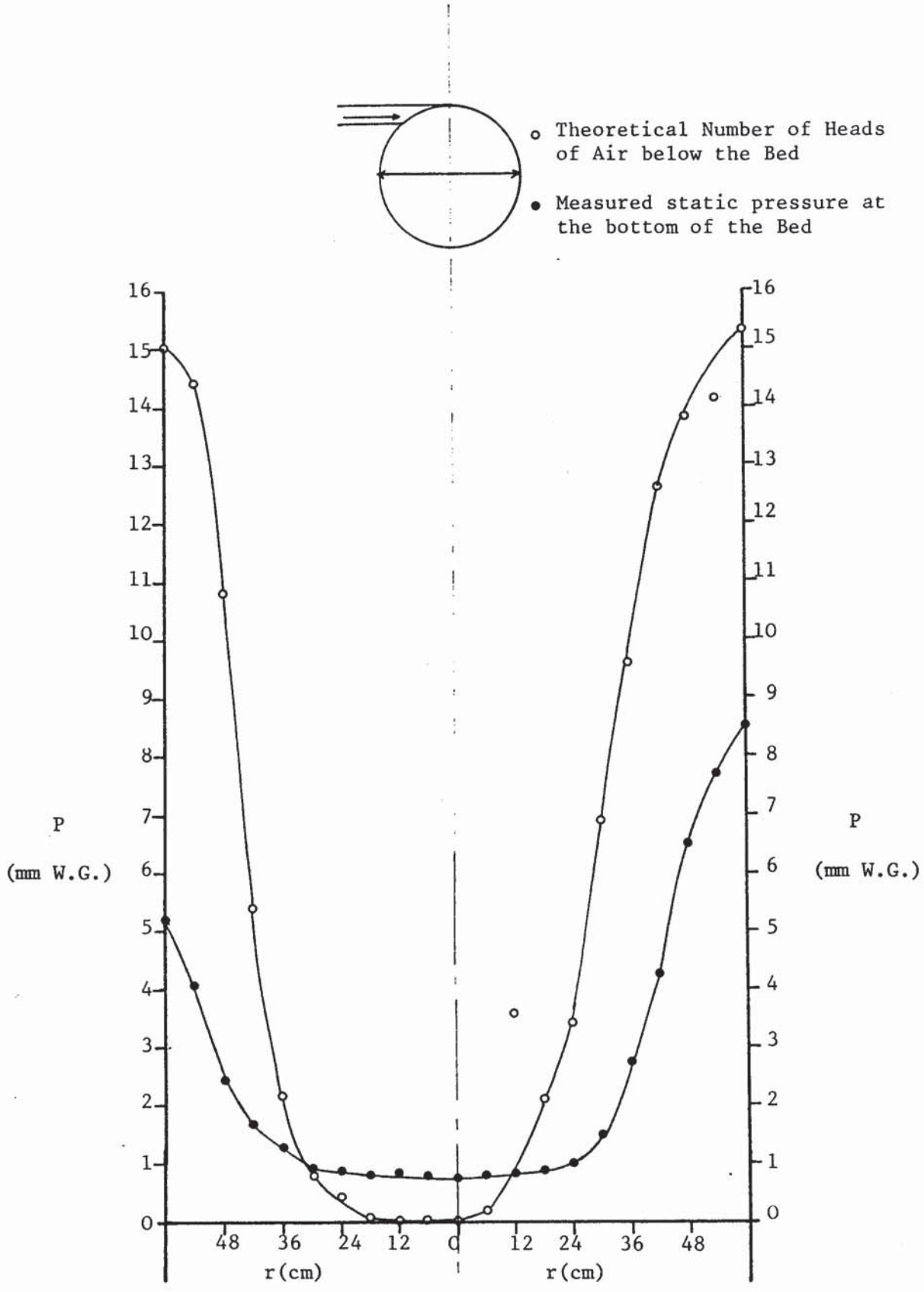

Graph 8.6 Theoretical and Measured Number of Heads in the 36 cm Deep Bed

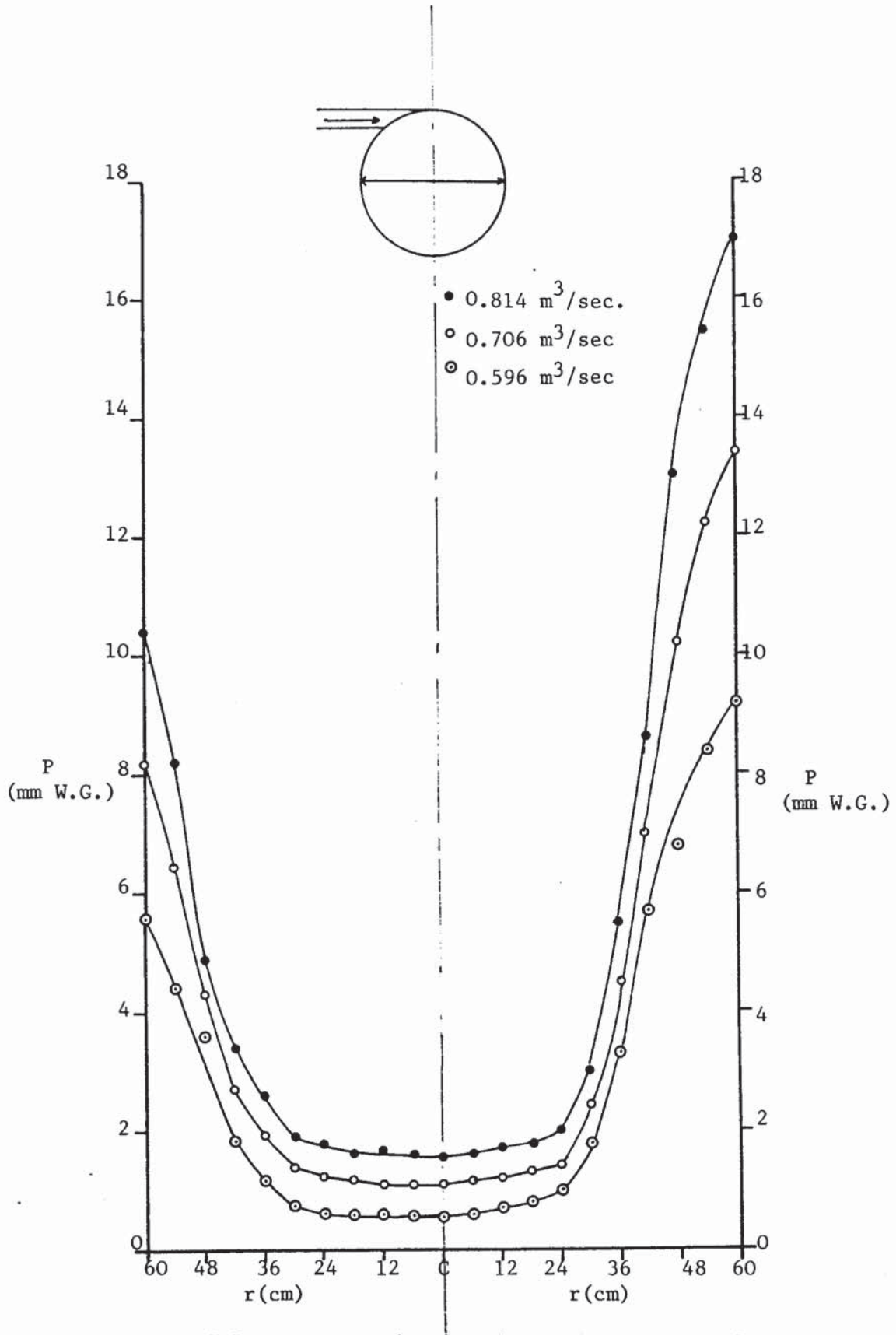

Graph 8.7 Pressure Distribution at the Bottom of 36 cm Deep Bed at Different Air Flows

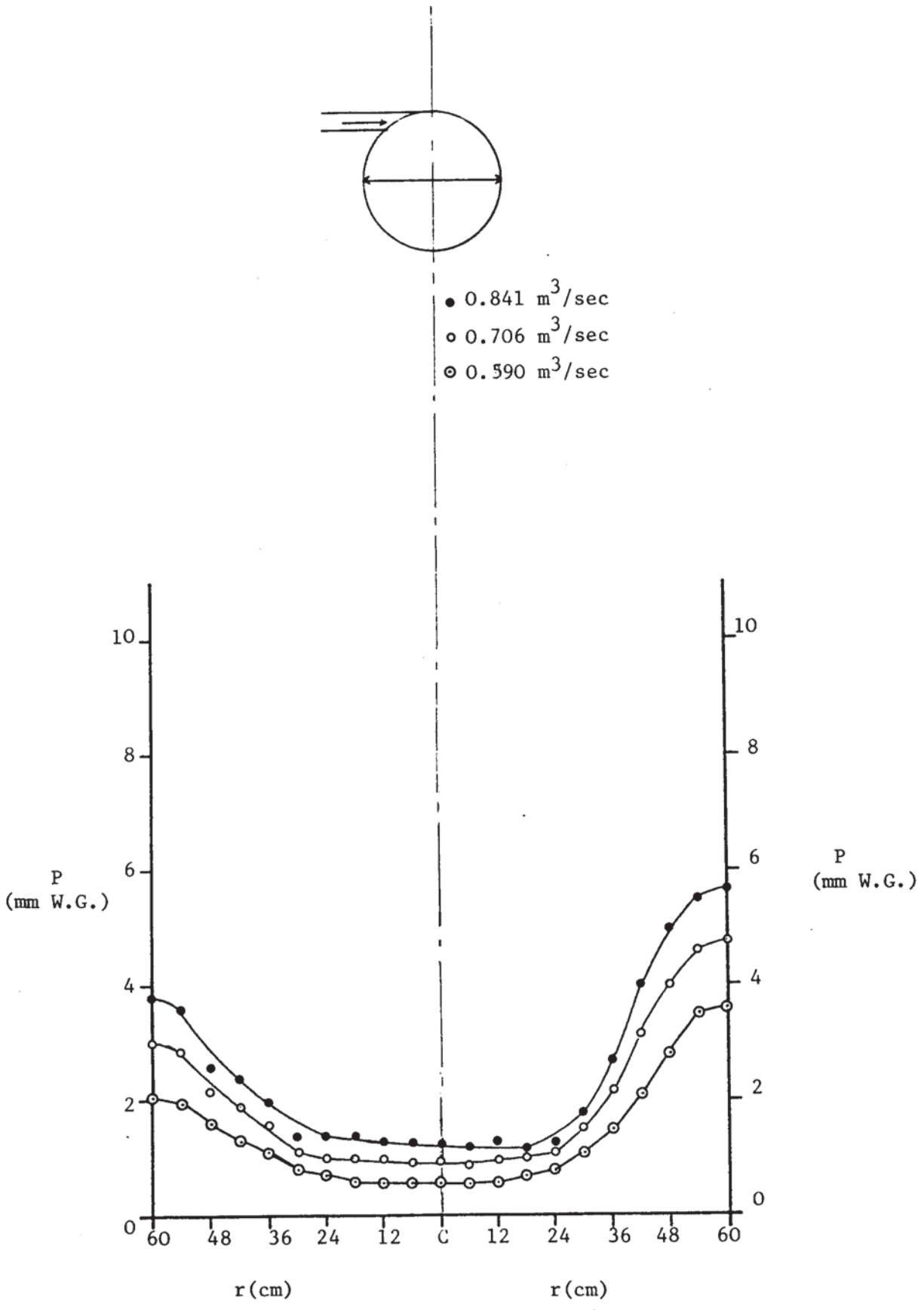

Graph 8.8 Pressure distribution at a Distance of 15 cm above the Bottom of 36 cm Deep Bed at Different Air Flows

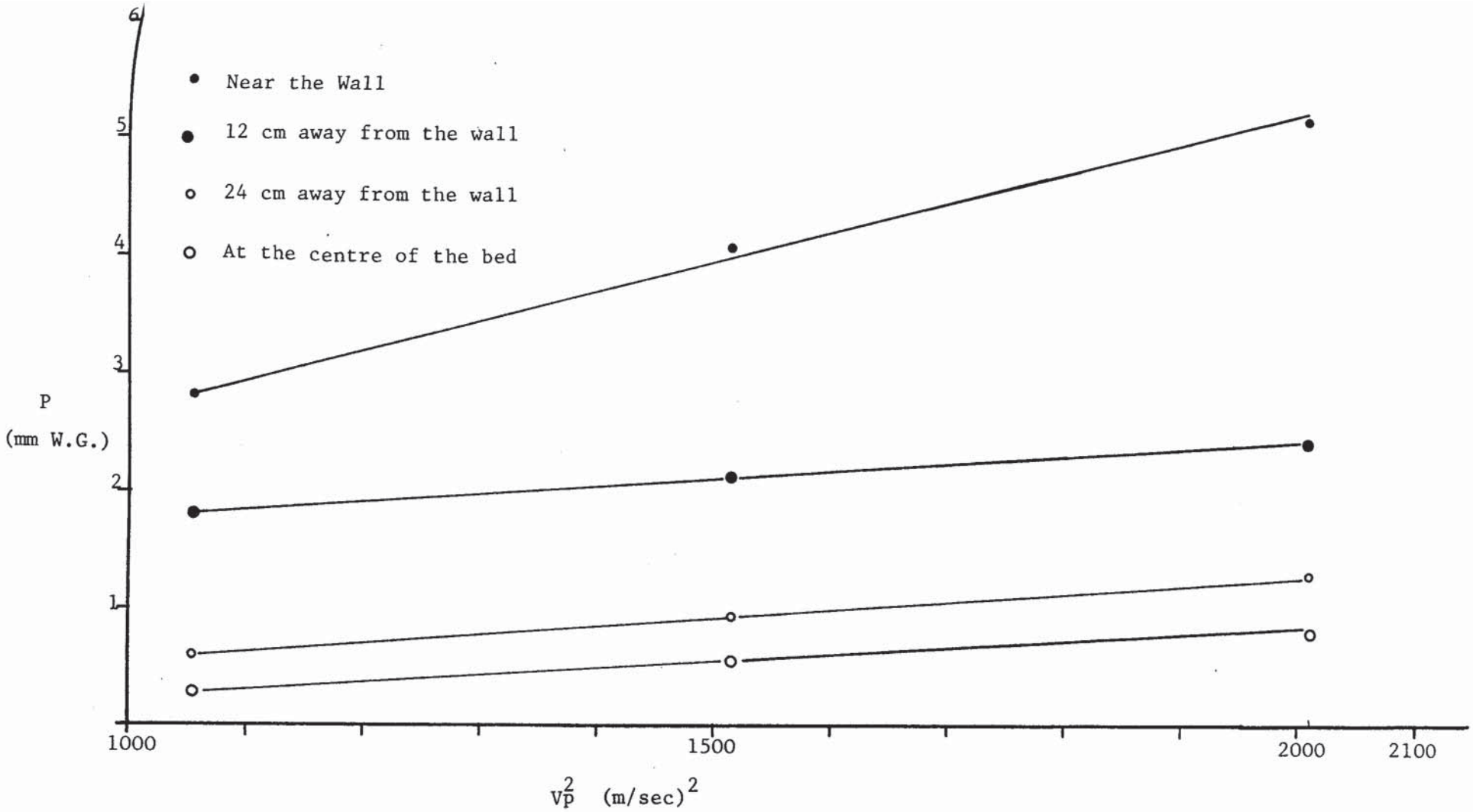

Graph 8.9 Variation of the static pressure generated at the bottom of 36 cm deep packed bed with air velocity in the feed inlet

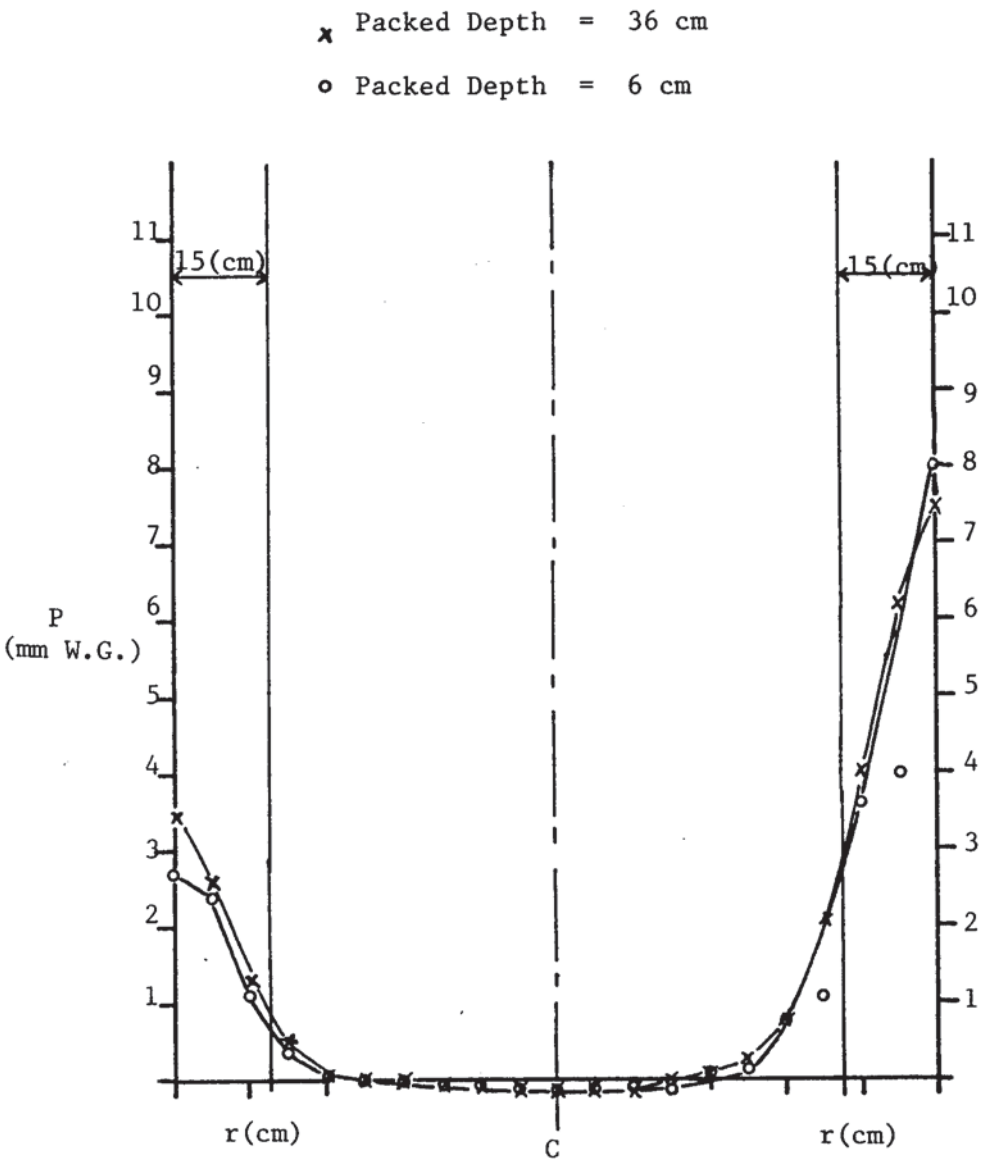

Graph 8.10 The Velocity Generated Static Pressure at the Bottom Of Packed Beds with a Tangential Feed Inlet, 15.2 cm in Diameter

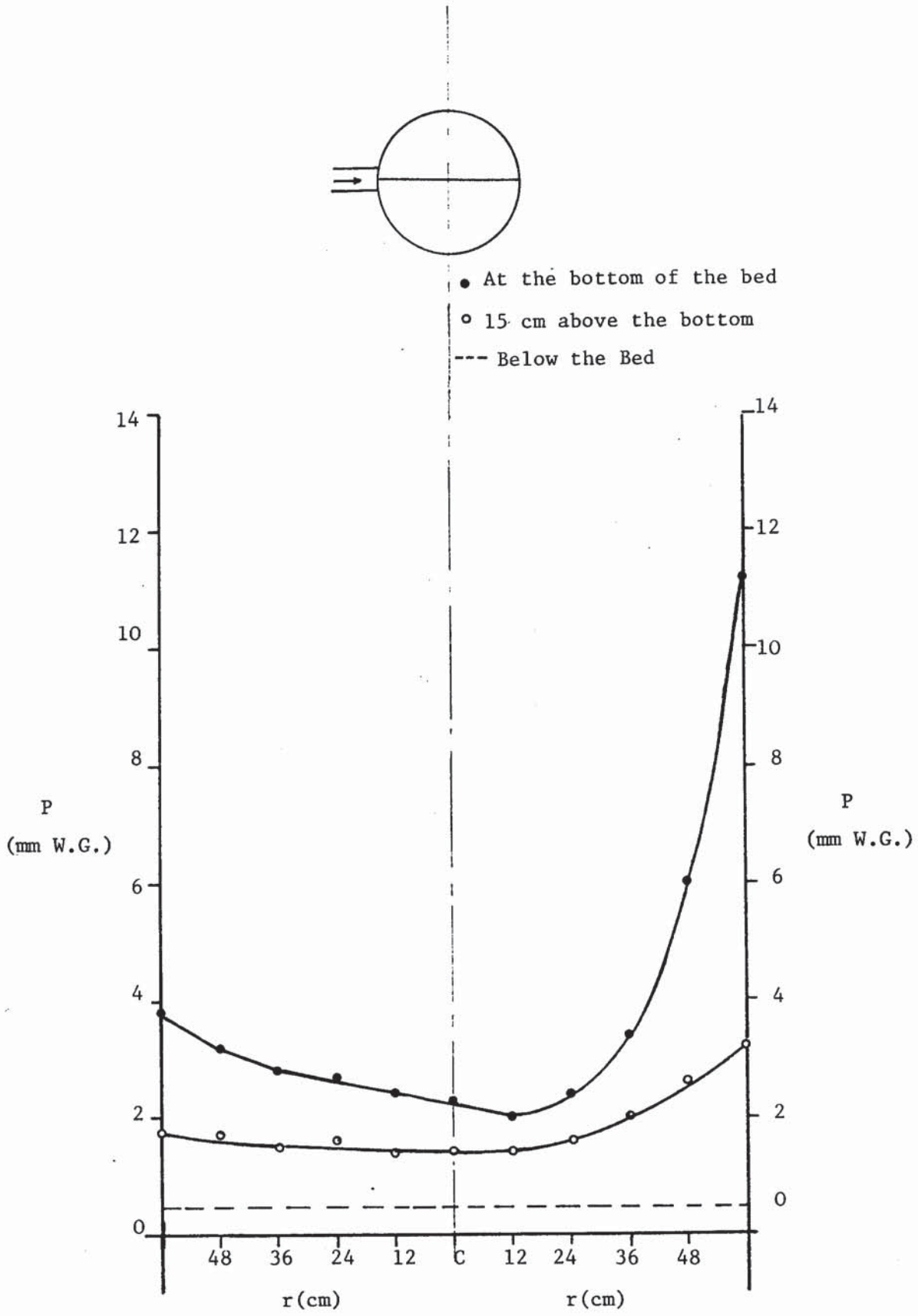

Graph 8.11 Pressure Distribution in a Radially Fed Bed Packed to a Depth of 36 (cm)

SECTION IX

THEORETICAL MODELS OF MALDISTRIBUTED GAS FLOW THROUGH PACKED BEDS

Introduction

The work has shown up to now that the gas is maldistributed through packed beds. This maldistribution ranges from a very mild situation of point to point velocity variation due to the channelling effect, to a very severe situation where the upwards flow near the wall of the column is accompanied by downwards flow at the middle of the bed.

In this section of the work, an attempt has been made to formulate models to describe this maldistribution of the gas in packed beds so as to support the scale-up rules obtained in Section 5, and to identify packed column designs subject to gas maldistribution. Three models have been described; a model based on three dimensional flow of gas through packed beds, which is more exact but too difficult for analytical solution, and two simplified models which are based on flow in one or two directions which permit the derivation of equations which aid interpretation of the observed flow patterns and which confirm the rules of scale-up proposed in earlier sections.

9.1 Three-dimensional Gas Flow Through Packed Beds

Consider an elemental volume dxdydz in the bed, where dx, dy and dz are the width, depth and height of the element shown in Fig. 9.1. For an incompressible fluid flowing in three dimensions through this element the x, y, and z components of the differential versions of the Ergun equation are written as:

$$-\frac{\partial P}{\partial x} = \frac{A\mu}{\rho} g_x + \frac{B}{\rho} g_x^2 \quad \ldots\ldots (9.1a)$$

$$-\frac{\partial P}{\partial y} = \frac{A\mu}{\rho} g_y + \frac{B}{\rho} g_y^2 \quad \ldots\ldots (9.1b)$$

$$-\frac{\partial P}{\partial z} = \frac{A\mu}{\rho} g_z + \frac{B}{\rho} g_z^2 \quad \ldots\ldots (9.1c)$$

where

$$A = \frac{150(1-\varepsilon)^2}{\varepsilon^3 \Phi\, dp}$$

and

$$B = \frac{1.75\ (1-\varepsilon)}{\varepsilon^3 \Phi\, dp}$$

P = Pressure

μ, ρ = Gas viscosity and density

g_x, g_y, g_z = Gas mass velocities in x, y and z directions

ε = Void fraction

Φ = Shape factor

dp = Particle size

Gas flow through this elemental volume may be laminar, turbulent or laminar in one part and turbulent in the other part of the element. These three situations are to be studied separately in detail.

9.1.1 Laminar flow

For laminar gas flow through the elemental volume dxdydz, equations 9.1a, 9.1b and 9.1c are reduced to

$$-\frac{\partial P}{\partial x} = \frac{A\mu}{\rho} g_x \quad \ldots\ldots (9.2a)$$

$$-\frac{\partial P}{\partial y} = \frac{A\mu}{\rho} g_y \qquad \ldots\ldots (9.2b)$$

$$-\frac{\partial P}{\partial z} = \frac{A\mu}{\rho} g_z \qquad \ldots\ldots (9.2c)$$

Obtaining g_x, g_y and g_z from these equations:

$$g_x = -a \frac{\partial P}{\partial x}$$

$$g_y = -a \frac{\partial P}{\partial y}$$

$$g_z = -a \frac{\partial P}{\partial z}$$

where

$$a = \frac{\rho}{A\mu}$$

Performing a mass balance over the elemental volume for no accumulation or depletion results in the following equation, (see Fig. 9.1),

$$\left[-a \frac{\partial P}{\partial x} dydz + a\left(\frac{\partial P}{\partial x} + \frac{\partial^2 P}{\partial x^2} dx\right)dydz\right] + \left[-a \frac{\partial P}{\partial y} dxdz + a\left(\frac{\partial P}{\partial y} + \frac{\partial^2 P}{\partial y^2} dy\right)dxdz\right]$$

$$+ \left[-a \frac{\partial P}{\partial z} dxdy + a\left(\frac{\partial P}{\partial z} + \frac{\partial^2 P}{\partial z^2} dz\right)dxdy\right] = 0$$

$$\therefore a \left[\frac{\partial^2 P}{\partial x^2} + \frac{\partial^2 P}{\partial y^2} + \frac{\partial^2 P}{\partial z^2} \right] dxdydz = 0$$

and finally

$$\frac{\partial^2 P}{\partial x^2} + \frac{\partial^2 P}{\partial y^2} + \frac{\partial^2 P}{\partial z^2} = 0 \qquad \ldots\ldots (9.3)$$

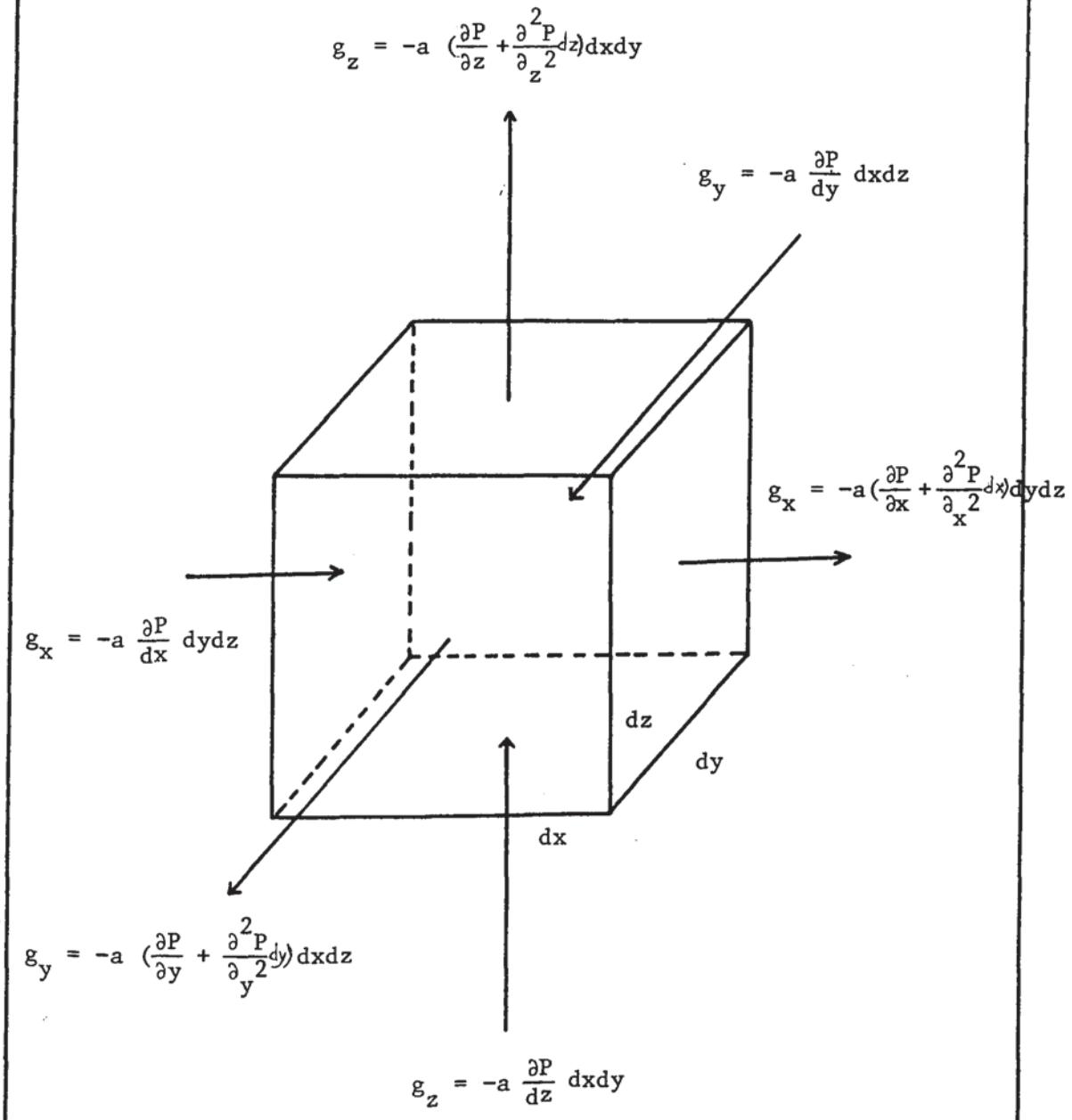

Figure 9.1. Mass Balance Over the (dxdydz) Elemental Volume in Laminar Gas Flow

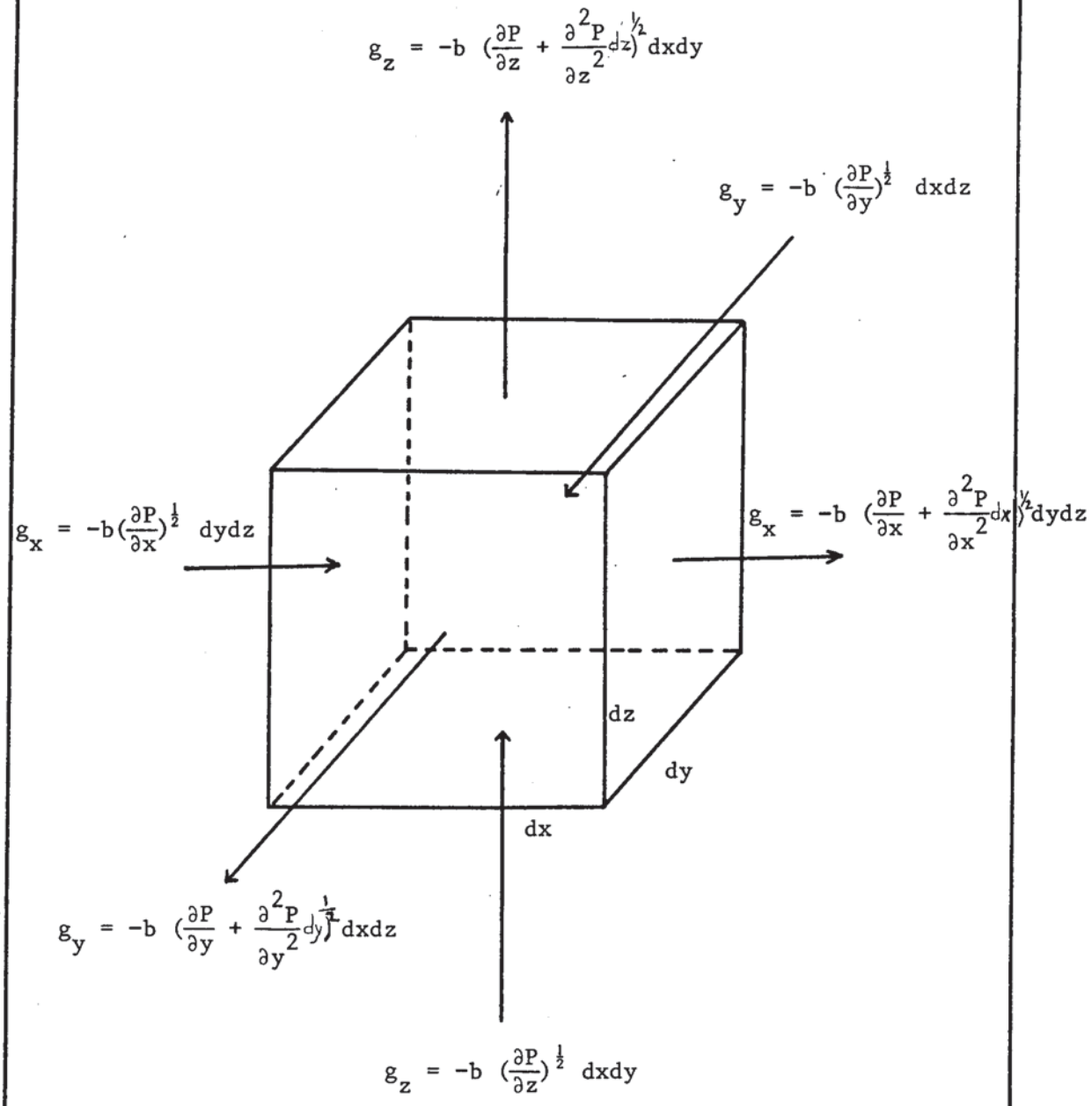

Figure 9.2 Mass Balance Over the (dxdydz) Elemental Volume in Turbulent Gas Flow

9.1.2 Turbulent Flow

For totally turbulent gas flow, equations 9.1a, 9.1b and 9.1c are reduced to:

$$-\frac{\partial P}{\partial x} = \frac{B}{\rho} g_x^2 \qquad \ldots\ldots (9.4a)$$

$$-\frac{\partial P}{\partial y} = \frac{B}{\rho} g_y^2 \qquad \ldots\ldots (9.4b)$$

$$-\frac{\partial P}{\partial z} = \frac{B}{\rho} g_z^2 \qquad \ldots\ldots (9.4c)$$

and

$$g_x = -b \left(\frac{\partial P}{\partial x}\right)^{\frac{1}{2}}$$

$$g_y = -b \left(\frac{\partial P}{\partial y}\right)^{\frac{1}{2}}$$

$$g_z = -b \left(\frac{\partial P}{\partial z}\right)^{\frac{1}{2}}$$

where $b = \frac{\rho}{B}$

Gas mass flow rate out of the elemental volume in x, y and z directions is given respectively below, (see Fig. 9.2).

$$g_x = -b \left(\frac{\partial P}{\partial x} + \frac{\partial^2 P}{\partial x^2} dx\right)^{\frac{1}{2}} dydz \qquad \ldots\ldots (9.5a)$$

$$g_y = -b \left(\frac{\partial P}{\partial y} + \frac{\partial^2 P}{\partial y^2} dy\right)^{\frac{1}{2}} dxdz \qquad \ldots\ldots (9.5b)$$

$$g_z = -b \left(\frac{\partial P}{\partial z} + \frac{\partial^2 P}{\partial z^2} dz\right)^{\frac{1}{2}} dxdy \qquad \ldots\ldots (9.5c)$$

To simplify these equations:

$$g_x = -b \left(\frac{\partial P}{\partial x} + \frac{\partial^2 P}{\partial_x 2}\, dx\right)^{\frac{1}{2}} dydz$$

$$= -b \left(\frac{\partial P}{\partial x}\right)^{\frac{1}{2}} \left(1 + \frac{\partial^2 P/\partial x^2}{\partial P/\partial x}\, dx\right)^{\frac{1}{2}} dydz$$

$$= -b \left(\frac{\partial P}{\partial x}\right)^{\frac{1}{2}} \left(1 + \frac{1}{2}\, \frac{\partial^2 P/\partial x^2}{\partial P/\partial x}\, dx\right) dydz$$

and finally

$$g_x = -b \left(\frac{\partial P}{\partial x}\right)^{\frac{1}{2}} dydz - \frac{b}{2}\, \frac{\partial^2 P/\partial x^2}{\sqrt{\partial P/\partial x}}\, dxdydz \qquad \ldots\ldots (9.6a)$$

Similarly

$$g_y = -b \left(\frac{\partial P}{\partial y}\right)^{\frac{1}{2}} dxdz - \frac{b}{2}\, \frac{\partial^2 P/\partial y^2}{\sqrt{\partial P/\partial y}}\, dxdydz \qquad \ldots\ldots (9.6b)$$

$$g_z = -b \left(\frac{\partial P}{\partial z}\right)^{\frac{1}{2}} dxdy - \frac{b}{2}\, \frac{\partial^2 P/\partial z^2}{\sqrt{\partial P/\partial z}}\, dxdydz \qquad \ldots\ldots (9.6c)$$

Performing a mass balance across the elemental volume for incompressible gas where there is no accumulation or depletion will result in:

$$\left[-b \left(\frac{\partial P}{\partial x}\right)^{\frac{1}{2}} dydz + b\left(\frac{\partial P}{\partial x}\right)^{\frac{1}{2}} dydz + \frac{b}{2}\, \frac{\partial^2 P/\partial x^2}{\sqrt{\partial P/\partial x}}\, dxdydz\right] +$$

$$\left[-b\left(\frac{\partial P}{\partial y}\right)^{\frac{1}{2}} dxdz + b\left(\frac{\partial P}{\partial y}\right)^{\frac{1}{2}} dxdz + \frac{b}{2}\, \frac{\partial^2 P/\partial y^2}{\sqrt{\partial P/\partial y}}\, dxdydz\right] +$$

$$\left[-b\left(\frac{\partial P}{\partial z}\right)^{\frac{1}{2}} dxdy + b\left(\frac{\partial P}{\partial z}\right)^{\frac{1}{2}} dxdy + \frac{b}{2}\, \frac{\partial 2_P/\partial z^2}{\sqrt{\partial P/\partial z}}\, dxdydz\right] = 0$$

Which is reduced to

$$\frac{b}{2}\left[\frac{\partial^2 P/\partial x^2}{\sqrt{\partial P/\partial x}} + \frac{\partial^2 P/\partial y^2}{\sqrt{\partial P/\partial y}} + \frac{\partial^2 P/\partial z^2}{\sqrt{\partial P/\partial z}}\right] dxdydz = 0$$

$$\therefore \quad \frac{\partial^2 P/\partial x^2}{\sqrt{\partial P/\partial x}} + \frac{\partial^2 P/\partial y^2}{\sqrt{\partial P/\partial y}} + \frac{\partial^2 P/\partial z^2}{\sqrt{\partial P/\partial z}} = 0 \qquad \ldots\ldots (9.7)$$

which is the mass balance equation for turbulent flow through the elemental volume.

9.1.3 Laminar and Turbulent Flows

For a laminar gas flow through some parts of the elemental volume and a turbulent gas flow through the other parts, the differential versions of the Ergun equation will contain both the laminar and the turbulent terms, and written as:

$$-\frac{\partial P}{\partial x} = \frac{A\mu}{\rho} g_x + \frac{B}{\rho} g_x^2$$

$$-\frac{\partial P}{\partial y} = \frac{A\mu}{\rho} g_y + \frac{B}{\rho} g_y^2$$

$$-\frac{\partial P}{\partial z} = \frac{A\mu}{\rho} g_z + \frac{B}{\rho} g_z^2$$

g_x, g_y and g_z are approximated as follows:

$$g_x = -\frac{\rho}{A\mu}\left(\frac{\partial P}{\partial x}\right) - \frac{\rho}{B}\left(\frac{\partial P}{\partial x}\right)^{\frac{1}{2}} \qquad \ldots\ldots (9.8a)$$

$$g_y = -\frac{\rho}{A\mu}\left(\frac{\partial P}{\partial y}\right) - \frac{\rho}{B}\left(\frac{\partial P}{\partial y}\right)^{\frac{1}{2}} \qquad \ldots\ldots (9.8b)$$

$$g_z = -\frac{\rho}{A\mu}\left(\frac{\partial P}{\partial z}\right) - \frac{\rho}{B}\left(\frac{\partial P}{\partial z}\right)^{\frac{1}{2}} \qquad \ldots\ldots (9.8c)$$

The continuity equation is given as:

$$\frac{\partial V_x}{\partial x} + \frac{\partial V_y}{\partial y} + \frac{\partial V_z}{\partial z} = 0 \qquad \ldots\ldots (9.9)$$

Where V_x, V_y, V_z are the velocities in the x, y and z directions respectively.

Since ρ is assumed to be constant, that is, incompressible fluid, then eqn. 9.9 can be rewritten as:

$$\frac{\partial g_x}{\partial x} + \frac{\partial g_y}{\partial y} + \frac{\partial g_z}{\partial z} = 0 \qquad \ldots\ldots (9.10)$$

From eqn. 9.8a

$$\frac{\partial g_x}{\partial x} = \frac{\partial}{\partial x}\left[-a\frac{\partial P}{\partial x} - b\left(\frac{\partial P}{\partial x}\right)^{\frac{1}{2}}\right]$$

$$= -a\frac{\partial^2 P}{\partial x^2} - \frac{b}{2}\left(\frac{\partial P}{\partial x}\right)^{-\frac{1}{2}}\left(\frac{\partial^2 P}{\partial x^2}\right)$$

Thus
$$\frac{\partial g_x}{\partial x} = -a\left(\frac{\partial^2 P}{\partial x^2}\right)\left[1 + \frac{b}{2a}\left(\frac{\partial P}{\partial x}\right)^{-\frac{1}{2}}\right] \qquad \ldots\ldots (9.11a)$$

Similarly

$$\frac{\partial g_y}{\partial y} = -a\left(\frac{\partial^2 P}{\partial y^2}\right)\left[1 + \frac{b}{2a}\left(\frac{\partial P}{\partial y}\right)^{-\frac{1}{2}}\right] \qquad \ldots\ldots (9.11b)$$

$$\frac{\partial g_z}{\partial z} = -a \left(\frac{\partial^2 P}{\partial z^2} \right) \left[1 + \frac{b}{2a} \left(\frac{\partial P}{\partial z} \right)^{-\frac{1}{2}} \right] \qquad \ldots\ldots (9.11c)$$

Substituting eqns. 9.11a, 9.11b and 9.11c in eqn. 9.10:

$$-a \left(\frac{\partial^2 P}{\partial x^2} \right) \left[1 + \frac{b}{2a} \left(\frac{\partial P}{\partial x} \right)^{-\frac{1}{2}} \right] + a \left(\frac{\partial^2 P}{\partial y^2} \right) \left[1 + \frac{b}{2a} \left(\frac{\partial P}{\partial y} \right)^{-\frac{1}{2}} \right]$$

$$+ a \left(\frac{\partial^2 P}{\partial z^2} \right) \left[1 + \frac{b}{2a} \left(\frac{\partial P}{\partial z} \right)^{-\frac{1}{2}} \right] = 0 \qquad \ldots\ldots (9.12)$$

If the flow is highly laminar, i.e. a >> b, then eqn. 9.12 will be reduced to the laminar gas flow eqn. 9.3; if the flow is highly turbulent, b >> a, then it will be reduced to the turbulent gas flow eqn. 9.7.

To solve eqns. 9.3, 9.7 and 9.12, the initial conditions are required as well as the boundary conditions, which will depend on a model for translating the velocity of the gas below the bed into pressure within the bed. Up until now this problem has not been solved, but some progress has been made by means of the much simpler models described below.

9.2 Simplified Models of Gas Maldistribution Through Packed Beds

It is clear that the solution of the differential equations given above is very complicated and it is very difficult to demonstrate similarity between flow patterns for geometrically and dynamically similar beds.

However, this demonstration can be done by assuming that the ratio of gas velocity in different parts of the packed bed is the

same in the model and the full-scale.

Two simple theoretical models have been proposed for this purpose for a tangential feed situation with no gas distributor.

9.2.1 Two Areas Model

Two geometrically and dynamically similar beds with scale ratio of R are shown in Fig. 9.3. The definitions of the symbols used in this model are given in Table 9.1.

As it was noticed in the last section that when the feed is introduced tangentially, there exist an annular part of the bed in which air always goes upwards at high velocities, whereas in the middle area the flow is downwards in short packed depths and upwards in deep beds.

Also, it was found that air below the bed has high velocities in the annular area and low velocities at the middle of the column. In the formulation of this model it is assumed that S_1 is equivalent to that part of the packed bed immediately above the high velocity gas flow where the high pressure is generated, (see Section 8). This part is separated by an impermeable membrane from the middle part.

In this model, the criteria for positive, zero, and negative flow in the other part of the bed is obtained, as well as that for similarity of flow patterns in geometrically and dynamically similar beds, (defined by identical velocity ratios).

Note that the experimental work in Section 8 showed that the width of the high pressure annulus is approximately the same as the inlet pipe diameter, and that k is assumed to be the same for both beds.

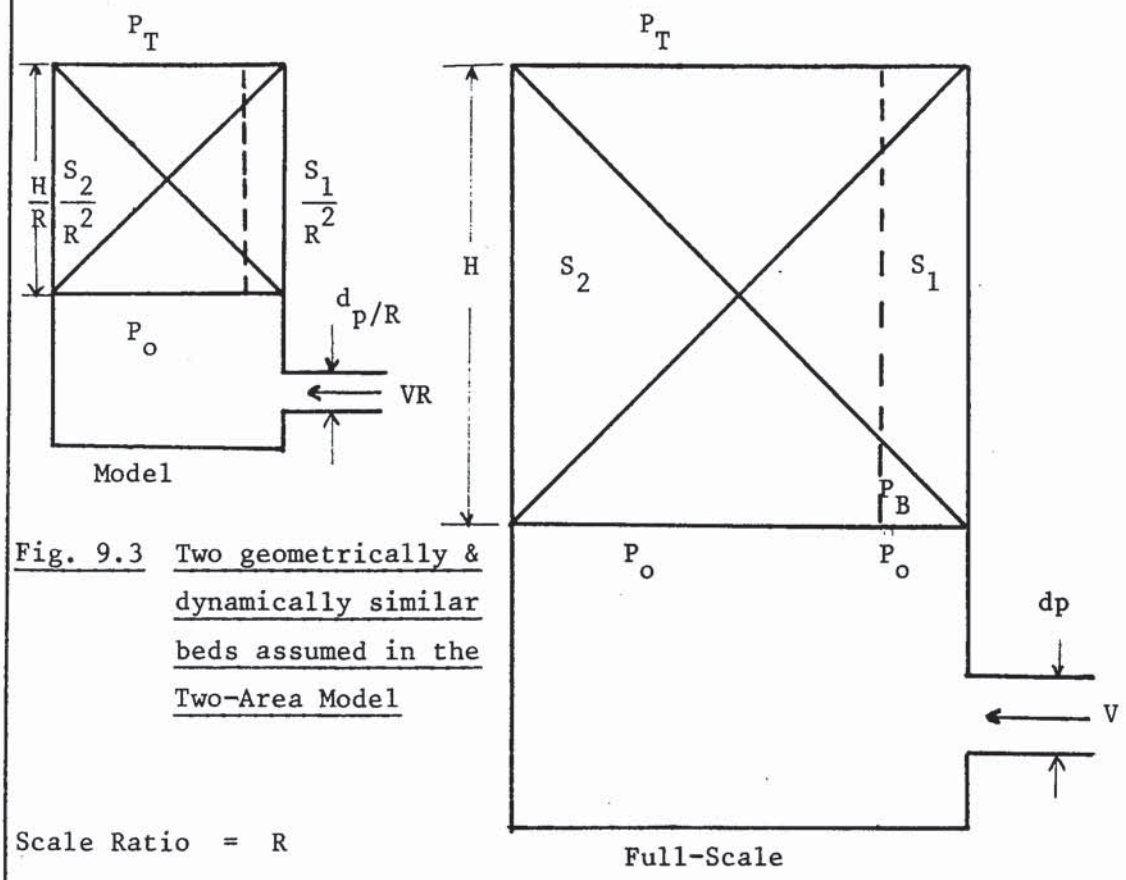

Fig. 9.3 Two geometrically & dynamically similar beds assumed in the Two-Area Model

Table 9.1 Definition of the symbols used in Section 9

Property	Symbol for:	
	full-scale	Model
Packed Height	H	H/R
Packing size	d	d/R
Packing area/unit volume	a	Ra
Bed Diameter	D	D/R
Inlet Pipe Diameter	dp .	dp/R
Inlet Pipe Velocity	V	RV
Up-flow Area	S_1	S_1/R^2
Up or Downflow Area	S_2	S_2/R^2
Up-Velocity in S_1	U_1	RU_1

Table 9.1 continued

Property	Symbol for:	
	Full-scale	Model
Velocity in S_2	U_2	RU_2
Drag Coefficient in Packed Bed	C	C
Pressure Generating Constant Below the Bed	k	k
Static Pressure at the Bottom of S_1	P_{Bf}	P_{Bm}
Pressure Drop across S_1	ΔP_{1f}	ΔP_{1m}
Pressure Drop across S_2	ΔP_{2f}	ΔP_{2m}
Gas Density	ρ	ρ
Pressure at the Top of the Bed	P_T	P_T
Static Pressure Below the Bed	P_{of}	P_{om}

For the full-scale bed, the pressure drop of the dry packing across S_1, (high pressure area), is given by

$$\Delta P_{1f} = C.(\rho U_1^2).H.a \qquad \ldots\ldots (9.13)$$

For $P_{of} = P_T$, the pressure generated is proportional to (ρV^2) inside the feed inlet, i.e.

$$P_{Bf} = k(\rho V^2) \qquad \ldots\ldots (9.14)$$

For the model bed, the pressure drop of the dry packing across S_1/R_1^2, (high pressure area), is given by:

$$\Delta P_{1m} = C\,[\rho(RU_1)^2]\,.\,\frac{H}{R}\,.\,Ra$$

$$= R^2.C.H.a\ (\rho U_1^2) \qquad \ldots\ldots (9.15)$$

In both the model and the full scale beds, the flow of gas is upwards in the area of high pressure. The direction of the gas flow in the area of low pressure (middle area) may be:

a) Zero-Flow in S_2: This case happens in the full-scale bed when $\Delta P_{1f} = P_{Bf}$.

$$\text{i.e.} \quad C.H.a\ (\rho U_1^2) = k(\rho V^2) \qquad \ldots\ldots (9.16)$$

And in the model when $\Delta P_{1m} = P_{Bm}$

$$\text{i.e.} \quad R^2.C.H.a\ (\rho U_1^2) = k\,R^2(\rho V^2)$$

$$\therefore \quad C.H.a\ (\rho U_1^2) = k\ (\rho V^2) \qquad \ldots\ldots (9.16a)$$

Which is the same condition for zero flow in the low pressure area in the full-scale bed.

$$\ldots\ldots (9.17)$$

$$\therefore \quad \boxed{C.H.a.U_1^2 = kV^2}$$

is the general equation for zero flow in the low pressure area in a packed bed.

An expression for zero flow in S_2 may be obtained in terms of the cross-sectional area of the inlet pipe and the upflow area S_1; that is:

$$S_1U_1 = Va_p \qquad \text{mass balance}$$

where a_p is the area of the feed pipe

$$\therefore \quad U_1 = V\ \frac{a_p}{S_1}$$

Substitute for U_1 in the general equation 9.17

$$C.H.a\ \left(\frac{a_p}{S_1}\right)^2 V^2 = kV^2$$

$$\therefore \quad \frac{C.H.a}{k(S_1/a_p)^2} = 1 \qquad \ldots\ldots (9.18)$$

eqn. 9.18 represents the critical condition.

b) Non-Zero Flow: In this case the gas is flowing either upwards or downwards in the low pressure area S_2.

In general

$$P_B = k(\rho V^2) + P_o \qquad \ldots\ldots (9.19a)$$

$$\Delta P_1 = (P_B - P_T) = C.H.a\ (\rho U_1^2) \qquad \ldots\ldots (9.19b)$$

$$\Delta P_2 = (P_o - P_T) \text{ or } (P_T - P_o) \qquad \ldots\ldots (9.19c)$$

Where P_o, P_B, ΔP_1 and ΔP_2 are the initial pressure below the bed, the static pressure at the bottom of the bed, pressure drop across S_1 and pressure drop across S_2 respectively.

Substituting for P_B from 9.19a into 9.19b

$$\therefore \quad \Delta P_1 = (P_o - P_T) + k(\rho V^2) = C.H.a(\rho U_1^2)$$

$$\therefore \quad \boxed{(P_o - P_T) = C.H.a(\rho U_1^2) - k(\rho V^2)} \qquad \ldots\ldots (9.20)$$

which is the general equation for upwards or downwards flow in S_2; that is:

if $C.H.a(\rho U_1^2) > k(\rho V^2)$

$\therefore$ $(P_o - P_T)$ is +ve and the flow is upwards in S_2,

and if $C.H.a(\rho U_1^2) < k(\rho V^2)$

$\therefore$ $(P_o - P_T)$ is -ve and the flow is downwards in S_2.

It is of interest to develop the model further to show the expected effect of inlet pipe diameter on the gas flow pattern.

It was found experimentally, (see Section 7), that the width of the high pressure area is almost equal to the feed pipe diameter

$$S_1 = \frac{\pi}{4}\left[D^2-(D - 2dp)^2\right]$$

$$= \frac{\pi}{4}\left[D^2 - (D^2 - 4\,Ddp + 4dp^2) \right]$$

$$= \frac{\pi}{4}\left(4Ddp - 4dp^2 \right)$$

$$\therefore \quad S_1 = \pi(Ddp-dp^2)$$

$$a_p = \pi \frac{dp^2}{4}$$

$$\text{then} \quad \frac{S_1}{a_p} = 4\left(\frac{D}{dp} - 1\right) \qquad \ldots\ldots (9.21)$$

In general, gas will flow either upwards or downwards in the lower pressure area of the bed, S_2. The similarity between the flow patterns in the full-scale and the model may be demonstrated by showing that the velocity ratio $\frac{U_1}{U_2}$ is the same in both the model and the full-scale.

The equations derived below all show the effect of the ratio of the inlet pipe diameter to column diameter on the $\frac{U_2}{U_1}$ ratio; that is on gas maldistribution. To perform this, each case is studied separately as follows:

b.1 Gas Flows Upwards in S_2

From eqn. 9.20

$(P_o - P_T) = C.H.a\ (\rho U_1^2) - k\ (\rho V^2)$ pressure drop across S_1

From eqn. 9.19c

$\Delta P_2 = P_o - P_T = C.H.a(\rho U_2^2)$ pressure drop across S_2

$\therefore \quad C.H.a\ (\rho U_1^2) + k(\rho V^2) = C.H.a\ (\rho U_2^2)$

$C.H.a\ (U_1^2 - U_2^2) = kV^2$

$\therefore\ (U_1^2 - U_2^2) = \dfrac{kV^2}{C.H.a}$

$$U_1^2 \left[1 - \left(\frac{U_2}{U_1}\right)^2\right] = \frac{kV^2}{C.H.a}$$

$$\therefore \boxed{\left(\frac{U_2}{U_1}\right)^2 = 1 - \frac{k}{C.H.a}\left(\frac{V}{U_1}\right)^2} \qquad \ldots\ldots (9.22)$$

$\dfrac{U_2}{U_1}$ defines the gas maldistribution and flow pattern in the packed bed.

To get eqn. 9.22 in terms of $\left(\dfrac{U_2}{U_1}\right)$ only:

$S_2 = \dfrac{\pi}{4} D^2 - S_1$

$S_1 = \pi\ (Ddp - dp^2)$

$\therefore\ S_2 = \dfrac{\pi}{4} D^2 - \pi(Ddp - dp^2)$

$$\therefore \frac{S_2}{S_1} = \frac{\left(\frac{D}{dp}\right)^2}{4\left(\frac{D}{dp} - 1\right)^2} \qquad \ldots\ldots (9.23)$$

Mass balance gives

$S_1U_1 + S_2U_2 = a_pV$

$$1 + \frac{S_2U_2}{S_1U_1} = \frac{a_p}{S_1}\left(\frac{V}{U_1}\right)$$

$$1 + \left(\frac{S_2}{S_1}\right)\left(\frac{U_2}{U_1}\right) = \frac{1}{S_1/a_p}\left(\frac{V}{U_1}\right)$$

Substitute for $\frac{S_2}{S_1}$ from eqn. 9.23 and S_1/a_p from 9.21 in the above equation:

$$\therefore \quad 1 + \left[\frac{(\frac{D}{dp})^2}{4\,(\frac{D}{dp} - 1)} - 1 \right] \left(\frac{U_2}{U_1} \right) = \frac{1}{4\,(\frac{D}{dp} - 1)} \left(\frac{V}{U_1} \right)$$

Let $A = \dfrac{(\frac{D}{dp})^2}{4\,(\frac{D}{dp} - 1)} - 1$, $\quad B = 4\,(\frac{D}{dp} - 1)$

$$\therefore \quad 1 + A \left(\frac{U_2}{U_1} \right) = \frac{1}{B} \left(\frac{V}{U_1} \right)$$

$$\therefore \quad \left(\frac{V}{U_1} \right) = B + AB \left(\frac{U_2}{U_1} \right)$$

and $$\left(\frac{V}{U_1} \right)^2 = \left[B + AB \frac{U_2}{U_1} \right]^2 \qquad \ldots\ldots (9.24)$$

Substitute for $\left(\frac{V}{U_1} \right)^2$ from 9.24 into 9.22:

$$\left(\frac{U_2}{U_1} \right)^2 = 1 - \frac{k}{C.H.a} \left[B + AB \frac{U_2}{U_1} \right]^2$$

$$AB = \left[\frac{(\frac{D}{dp})^2}{4(\frac{D}{dp} - 1)} - 1 \right] 4\,(\frac{D}{dp} - 1)$$

$$= \left(\frac{D}{dp} \right)^2 - 4\,(\frac{D}{dp} - 1)$$

$$= \left(\frac{D}{dp} \right)^2 - 4 \frac{D}{dp} + 4 = (\frac{D}{dp} - 2)^2$$

$$\therefore \left(\frac{U_2}{U_1} \right)^2 = 1 - \frac{k}{C.H.a} \left[4\,(\frac{D}{dp} - 1) + (\frac{D}{dp} - 2)^2 \left(\frac{U_2}{U_1} \right) \right]^2 \ldots (9.25)$$

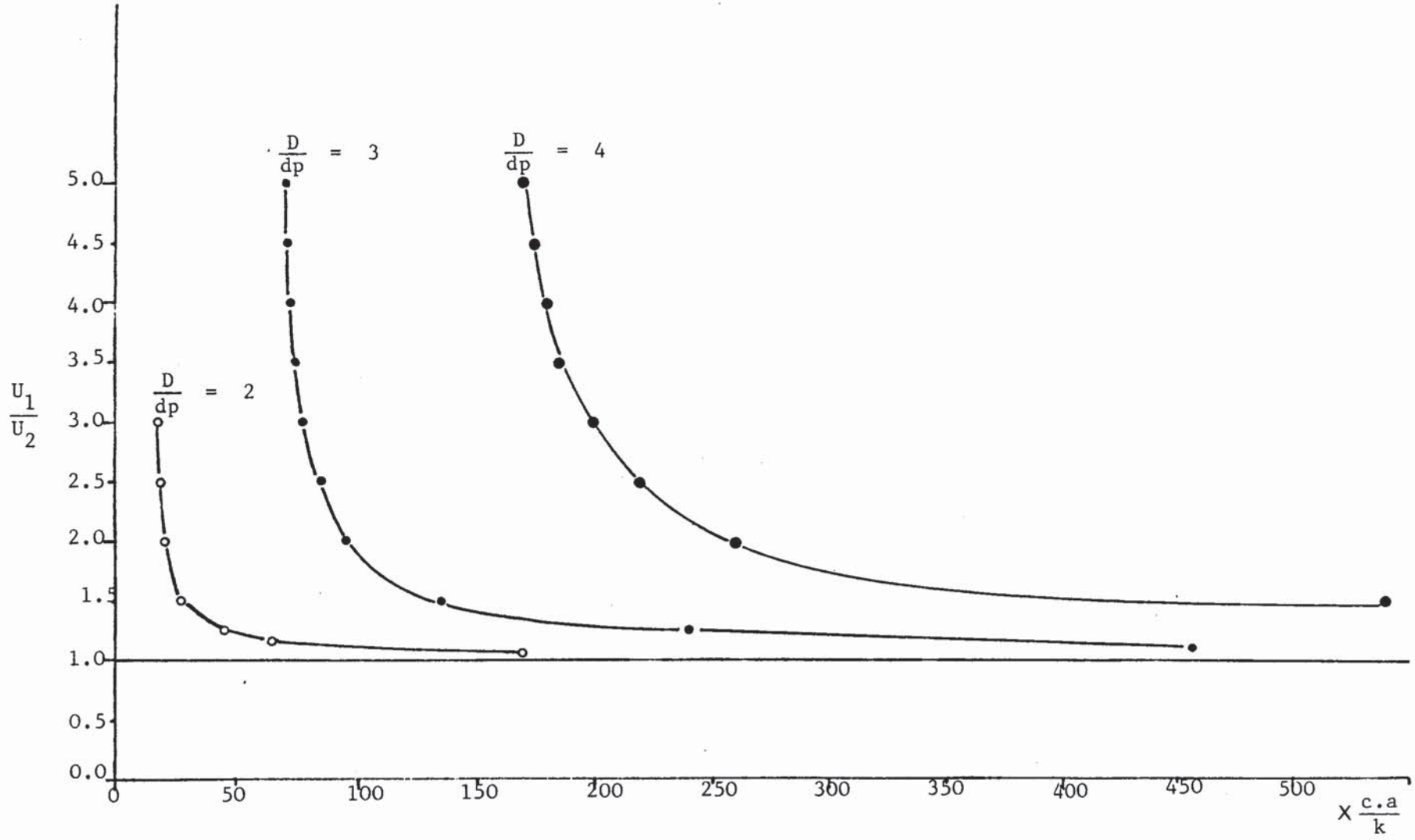

Graph 9.1 Variation of U_1/U_2 with P.H. at different D/dp ratios

This flow pattern function evaluates the packed height required for $\frac{U_2}{U_1} \rightarrow 1$ for different $\frac{D}{dp}$ ratios which describes the effect of inlet pipe diameter on gas maldistribution as shown in Graph 9.1.

Since $\left(\frac{k}{C.H.a} \right)$ is the same for geometrically similar beds at same Reynolds number

$$\therefore \quad \frac{U_2}{U_1} = f \left(\frac{D}{d_p}, \frac{k}{C.H.a} \right) \text{ only}$$

b.2 Gas Flow Downwards in S_2

In this case, the pressure drop across S_2 is given by

$$\Delta P_2 = P_T - P_o = C.H.a \ (\rho U_2^2)$$

And pressure drop across S_1 is given by

$$\Delta P_1 = P_o + k \ (\rho V^2) - P_T = C.H.a \ (\rho U_1^2)$$

$$P_o - P_T = C.H.a \ (\rho U_1^2) - k(\rho V^2)$$

$$\therefore \quad C.H.a \ (U_1^2 + U_2^2) = kV^2$$

and

$$\left(\frac{U_2}{U_1} \right)^2 = \frac{k}{C.H.a} \left(\frac{V}{U_1} \right)^2 - 1 \qquad \ldots\ldots (9.26)$$

Air flows upwards in S_1 at a rate greater than the feed, so air is flowing downwards in S_2 to maintain the mass balance. The mass balance equation is given by

$$S_1 U_1 - S_2 U_2 = a_p V$$

$$1 - \left(\frac{S_2}{S_1} \right) \left(\frac{U_2}{U_1} \right) = \frac{1}{S_1 / a_p} \left(\frac{V}{U_1} \right)$$

Substituting for $\frac{S_2}{S_1}$ from eqn. 9.23 and $\frac{S_1}{a_p}$ from 9.21 in the above equation

$$1 - \left[\frac{(\frac{D}{dp})^2}{4\,(\frac{D}{dp} - 1)} - 1 \right] \left(\frac{U_2}{U_1} \right) = \frac{1}{4\,(\frac{D}{dp} - 1)} \left(\frac{V}{U_1} \right)$$

$$1 - A \left(\frac{U_2}{U_1} \right) = \frac{1}{B} \left(\frac{V}{U_1} \right)$$

$$\therefore \left(\frac{V}{U_1} \right)^2 = \left[B - AB \left(\frac{U_2}{U_1} \right) \right]^2 \qquad \ldots\ldots (9.27)$$

eqn. 9.27 in eqn. 9.26

$$\therefore \left(\frac{U_2}{U_1} \right)^2 = \frac{k}{C.H.a} \left[4 \left(\frac{D}{dp} - 1 \right) - \left(\frac{D}{dp} - 2 \right)^2 \frac{U_2}{U_1} \right]^2 - 1 \qquad \ldots\ldots (9.28)$$

which again shows that $\frac{U_2}{U_1} = f_1 \left(\frac{D}{dp}, \frac{k}{C.H.a} \right)$ only

Both equations 9.25 and 9.28, if $\frac{U_2}{U_1} = 0$, i.e. $U_2 = 0$, will be reduced to

$$\frac{C.H.a}{k\left[4\left(\frac{D}{dp} - 1 \right)\right]^2} = 1 \qquad \ldots\ldots (9.29)$$

$\therefore$ For larger feed inlet diameter, dp, i.e. smaller $\frac{D}{dp}$ ratio, and larger packed height, H, the left hand side of equation 9.29 will become greater than 1. This means that the gas is flowing upwards in S_2, which explains the uniform flow in beds of small diameter and large packed height.

But in case of shallow large diameter packed beds, where pipe inlet diameter is small relative to bed diameter and packed depth is small, the left hand side of eqn. (9.29) will become less

than 1 and the downwards flow in the middle of the bed appears, giving rise to severe gas maldistribution.

Thus the designs of packed beds in which the left hand side of eqn. 9.29 less than one could be identified as "Designs at Risk" of gas maldistribution.

9.2.2 Cross-Flow Model

In this model it is assumed that the high pressure region, S_1, is connected at the bottom of the bed to the low pressure region, S_2, by a channel which permits the gas to flow across. This addition of cross-flow provides a more realistic description of the expected flow pattern. The gas can move radially through this channel. Fig. 9.4 shows cross sections in two geometrically and dynamically similar packed beds with a scale ratio R, where:

ΔP_c is the pressure drop due to the cross-flow

S_c is the cross sectional area of the channel.

In this model, the following assumptions were made

(1) The length of the channel, z, is proportional to $\frac{1}{R}$, but z is infinitely small, that is:

$$S_1 + S_2 = \frac{\pi}{4} D^2$$

(2) The width of the high pressure region S_1 is the same as the feed pipe diameter.

(3) k is the same for both the model and full-scale packed beds.

(4) The gas flow direction is:

(a) Always upwards in S_1.

(b) Zero-flow, upwards, or downwards in S_2

Similar to the two areas model, this model deals with the situations of zero-flow, upwards flow, and downwards flow in S_2 as

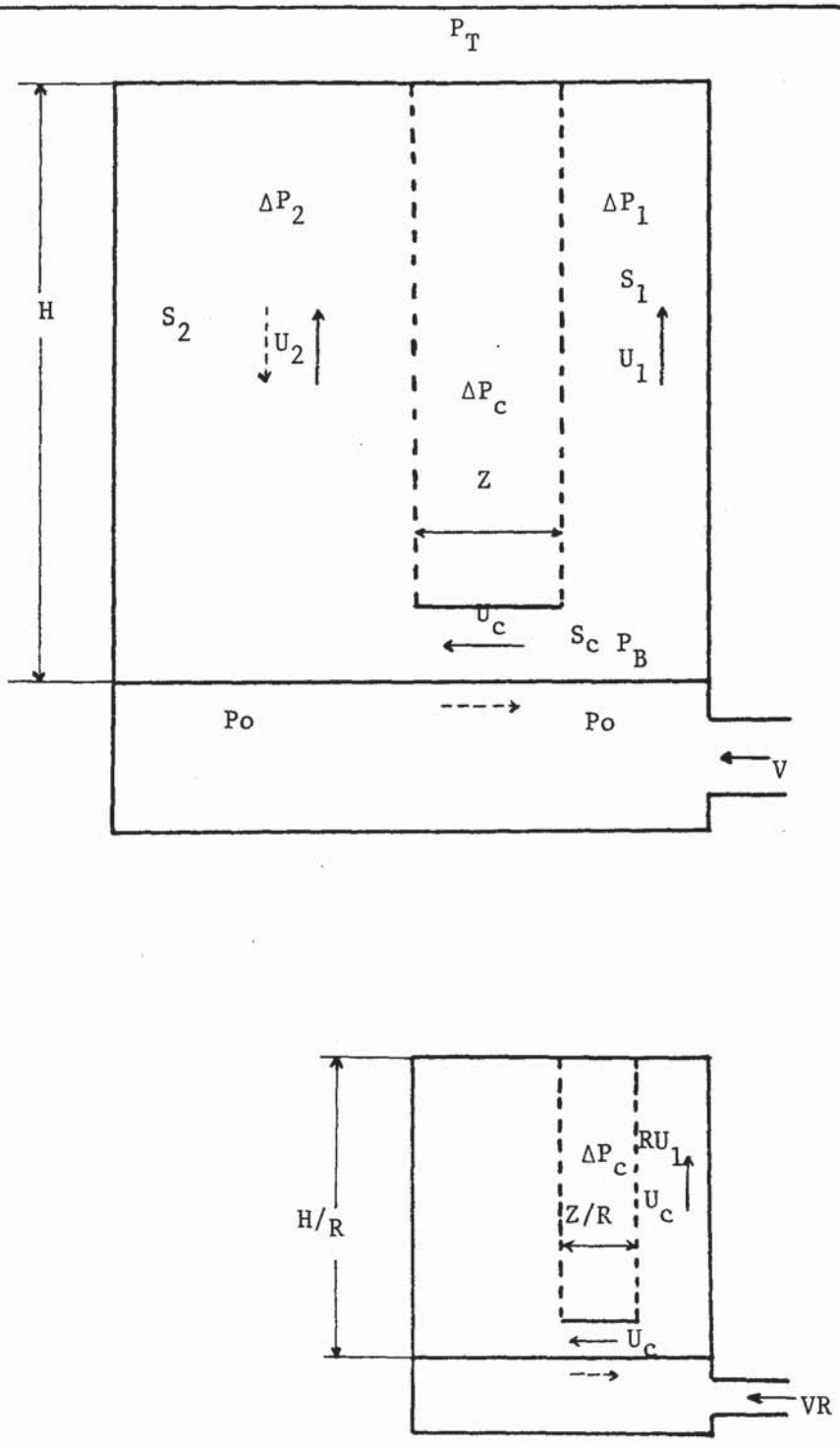

Fig. 9.4 Two Geometrically and Dynamically Similar Beds Assumed in the Cross-flow Model

follows:

(a) Zero-Flow in S_2

In this case there is no flow in S_2 which means that all the gas flowing across the channel from S_1 to S_2 is recycled to S_1 from beneath the bed, and that

$$P_o = P_T \qquad \ldots\ldots (9.30)$$

For the geometrically and dynamically similar beds shown in Fig. 9.4, the flow equation for zero-flow will be derived as follows:

(1) For the Full-scale bed:

$$\Delta P_{cf} = P_{Bf} - P_{of}$$

$$P_{Bf} = k(\rho V^2) + P_{of}$$

$$\therefore \quad P_{cf} = k(\rho V^2)$$

$$c.z.a\ (\rho U_c^2) = k(\rho V^2)$$

$$\therefore \quad U_c^2 = \frac{k}{c.z.a} V^2 \qquad \ldots\ldots (9.31)$$

(2) For the Model bed:

$$\Delta P_{cm} = P_{Bm} - P_{om}$$

$$P_{Bm} = k.R^2.(\rho V^2) + Pom$$

$$\therefore \quad P_{cm} = k.R^2.(\rho V^2)$$

$$c.\frac{z}{R}.a.R.R^2(\rho U_c^2) = k.R^2.(\rho V^2)$$

$$\therefore \quad U_c^2 = \frac{k}{c.z.a} V^2 \qquad \ldots\ldots (9.32)$$

which is identical to eqn. 9.31. This proves the validity of the principle of dynamic similarity.

(b) Non-zero Flow

In this case the gas flowing upwards or downwards in S_2.

In general:

$$\Delta P_1 = P_B - P_T \qquad \ldots\ldots (9.33a)$$

$$\Delta P_c = P_B - P_o \qquad \ldots\ldots (9.33b)$$

$$\Delta P_2 = (P_o - P_T) \text{ or } (P_T - P_o) \qquad \ldots\ldots (9.33c)$$

$$\therefore \quad \Delta P_2 = \Delta P_1 - \Delta P_c \qquad \ldots\ldots (9.34)$$

Eqn. 9.34 is the general equation of pressure drops in non-zero flow in S_2. If $\Delta P_1 > \Delta P_c$, then the flow is upwards in S_2; if $\Delta P_1 < \Delta P_c$, then the flow is downwards in S_2.

Substituting $P_B = k(\rho V^2) + P_o$ in eqn. 9.33b:

$$\Delta P_c = k(\rho V^2)$$

$$\text{c.z.a } (\rho U_c^2) = k(\rho V^2)$$

$$\therefore \quad \boxed{U_c^2 = \frac{k}{\text{c.z.a}} V^2} \qquad \ldots\ldots (9.35)$$

Eqn. 9.35 is identical to eqn. 9.31 in zero-flow situation. Thus it could be concluded that U_c is proportional to the velocity in the feed pipe, V, and that, at a constant V, the gas passing through the channel has a constant velocity, U_c from S_1 to S_2 whether or not there was a flow in S_2.

The upwards and downwards flows are going to be studied below:

b.1 Upward flow in S_2

From eqn. 9.34: $\Delta P_2 = \Delta P_1 - \Delta P_c$

$\therefore$ C.H.a (U_2^2) = C.H.a(U_1^2) - C.z.a (U_c^2)

Substituting for (U_c^2) from eqn. (9.35) gives:

$$C.H.a\ (U_2^2) = C.H.a\ (U_1^2) - k(V^2)$$

Dividing by C.H.a (U_1^2) gives:

$$\left(\frac{U_2}{U_1}\right)^2 = 1 - \frac{k}{C.H.a}\left(\frac{V}{U_1}\right)^2 \qquad \ldots\ldots (9.36)$$

Eqn. 9.36 is identical to eqn. 9.22 obtained for upwards flow in the "Two Areas" model. It implies that the cross-flow is simply recycled around the areas at the bottom of the bed with a high velocity generated pressure at those areas where the pressure is the static pressure under the bed.

The mass balance equation will be:

$$a_p V = S_1 U_1 + S_2 U_2 \qquad \ldots\ldots (9.37)$$

Therefore, eqn. 9.36 can be written in terms of $\left(\frac{U_2}{U_1}\right)$ and $\left(\frac{D}{dp}\right)$ by the same method followed in the "Two Areas" model as:

$$\left(\frac{U_2}{U_1}\right)^2 = 1 - \frac{k}{C.H.a}\left[4\left(\frac{D}{dp} - 1\right) + \left(\frac{D}{dp} - 2\right)^2\left(\frac{U_2}{U_1}\right)\right]^2 \qquad \ldots\ldots (9.38)$$

which is identical to eqn. 9.25.

This flow pattern equation evaluates the packed height required for $\frac{U_2}{U_1} \to 1$ for different $\frac{D}{dp}$ values in an identical way to that shown in Graph 9.1.

b.2 Downwards flow in S_2

In this case the gas is flowing downwards in S_2, which means that $P_T > P_o$, and equation 9.34 will be written as:

$$\Delta P_2 = \Delta P_c - \Delta P_1$$

By a similar method to that followed in the upwards flow, the flow pattern equation for downwards flow can be obtained as:

$$\left(\frac{U_2}{U_1}\right)^2 = \frac{k}{C.H.a}\left[4\left(\frac{D}{dp} - 1\right) - \left(\frac{D}{dp} - 2\right)^2 \left(\frac{U_2}{U_1}\right)\right]^2 - 1 \quad \ldots\ldots (9.39)$$

Taking into consideration that the mass balance equation is:

$$a_p V = S_1 U_1 - S_2 U_2 \quad \ldots\ldots (9.40)$$

Eqn. 9.39 is identical to eqn. 9.28 produced in the "Two Area" model for downwards flow in S_2.

Both eqns. 9.38 and 9.39 are functions of $\left(\frac{U_2}{U_1}\right)$ and $\left(\frac{k}{C.H.a}\right)$ only. And if $\frac{U_2}{U_1} = 0$, both equations will be reduced to:

$$\frac{C.H.a}{k\left[4\left(\frac{D}{dp} - 1\right)\right]^2} = 1 \quad \ldots\ldots (9.41)$$

Which is identical to eqn. 9.29 results in the previous model, and represents the critical conditions. The packed beds with designs "at risk" of gas maldistribution could be identified as those designs at which the left hand side of eqn. 9.41 is less than 1.

9.3 Discussion of the Simplified Theoretical Models

The two simplified theoretical models proposed above, the Two Areas model and the Cross-Flow model produce the same flow pattern function, given in eqns. 9.25 and 9.38, which evaluates the packed height required for uniform distribution at different $\frac{D}{dp}$

ratios. This function is solved and presented in Graph 9.1 which shows that the variation of $\frac{U_1}{U_2}$ with packed height is similar to the variation of ϕ with packed height observed in previous sections of this work. The graph shows the importance of the ratio of tower diameter to feed pipe diameter. A negligible packed depth is required to obtain a uniform distribution for $\frac{D}{dp} = 2$, but the depth required increases rapidly and it is quite large for $\frac{D}{dp} = 3$.

Also, the packed beds designs which are exposed to gas maldistribution, "Designs at Risk", could be identified from the general equation of the critical conditions which is produced by the two simple models as:

$$\frac{C.H.a}{k\ [4\ (\frac{D}{dp} - 1)]^2} \leq 1$$

From which it could be seen clearly that the large diameter packed beds with relatively small packed height and vapour inlet diameter are more likely to be maldistributed than the standard packed beds in which the packed height is much larger than the diameter of the bed, and the vapour inlet is relatively large.

One interesting result is that both simplified theoretical models one with cross-flow and one without gave the same equations. For the flow pattern ($\frac{U_1}{U_2}$), equations 9.25 and 9.38, and for the condition which determines a negative down flow in the bed, eqns. 9.28 and 9.40. A physical explanation of this is that the cross-flow gas simply recirculates at a constant rate between high pressure and low pressure regions in the bed. The rate of recirculation is proportional to the inlet pipe velocity, but is independent of the height of packing. It is evident that the

cross-flow model needs to be developed further to permit evaluation of the effect of cross flow at different distances above the bottom of the bed.

9.4 Conclusions

Three theoretical models of maldistributed gas flow in packed beds were proposed, these are; the three dimensional gas flow, the two areas model, and the cross-flow model. The last two models, which are simplified theoretical models could be solved and packed beds designs "at Risk" of maldistribution could be identified and the principle of dynamic similarity could be proved.

SECTION X

TESTING MODELS OF GAS DISTRIBUTORS USED IN EXISTING LARGE DIAMETER COLUMNS

Introduction

In this section of the work a pump around packed bed in the vacuum crude fractionation tower, described in Section 2, is chosen as an example of an "at risk" design. This pump around packed bed has all the "at risk" requirements of gas maldistribution; large diameter, (7.3m), short packed height, (1 to 2m), and relatively small vapour inlet, (usually less than 1m in diameter).

The experimental work in this section deals with the test of existing gas distribution devices of the type used in large diameter vacuum crude fractionation columns.

In Section 6 of this work, the rules of scale-up of packed beds were obtained experimentally. Those rules are going to be applied in the construction of the model used in this section.

It should be noted, (see Section 2.2), that at the present, the designers of the pump around sections regard the Internal Cylinder and the annular space as a gas distributor. As shown below, the internal cylinder does little to improve the distribution of the gas. In the full-scale column, which was the prototype for this work, most improvement of the gas distribution was obtained from the particular design of the draw-off tray which was used.

10.1 Construction of the Model

The laboratory study uses a scaled down model exactly geometrically and dynamically similar to the full-scale pump around section of a 7.3m diameter vacuum crude fractionation column but $\frac{1}{6}$ the size. A complete set of drawings of the full-scale column were obtained and used to provide the exactly scaled-down dimensions of the model.

10.1.1 The choice of the $\frac{1}{6}$ scale-down ratio

The $\frac{1}{6}$ scaling ratio was used because it is only possible to obtain commercially available Pall ring packings over a size range of ($\frac{5}{8}$ in to $3\frac{1}{2}$ ins), which means that the smallest packing is about $\frac{1}{6}$ the largest size. Thus a $\frac{1}{6}$ scale model packed with 16 mm, ($\frac{5}{8}$ in), packing is equivalent to a full scale column packed with ($3\frac{1}{2}$ in) packing.

The shell of the 122 cm inside diameter column, described in Section 8.1, and shown in Plate 8.1, is used in this work. The internals, (the draw-off tray, the support plate, the support beam and the internal cylinder), were designed and are described below.

10.1.2 The draw-off tray

The draw-off tray is used in the full-scale fractionator to separate the liquid to be drawn off from the rising vapour. In the model, a 121 cm diameter draw-off tray is designed geometrically similar to the full-scale draw-off tray and constructed from 1.5 mm thick galvanized iron. It consists of caps and troughs, slots and a sump, (see Plate 10.1).

The caps, (see Fig. 10.2), are closed at one end and slightly tilted to direct the trapped liquid to the sump. Each cap is fitted to the troughs by means of two slotted legs to allow

for the adjustment of the cap height above the troughs. The troughs, (see Fig. 10.1), are designed to leave slots between them to allow for the rising gas to pass through. The troughs are opened to the sump and connected to each other at the middle by channels. The sump, (see Fig. 10.4), is 10 cm deep.

The draw-off tray is held by a 1 cm wide and 0.5 cm thick support ring which is fitted to the column shell. The dimensions of the draw-off tray are shown in Fig. 10.3.

10.1.3 The Support Plate and the Lattice Support Beam

The packing support plate, (gas injection type), is constructed from an expanded metal plate and designed to combine the mechanical strength and convenience in installation. It is furnished in 2-piece construction, (see Plate 10.1). The dimensions of this 121 cm diameter plate are shown in Fig. 10.5.

The lattice support beam, (see Plate 10.1), is designed to support the weight of the packed bed and the column internals. It is constructed from 1 cm aluminium angle bar. The design specifications and dimensions are shown in Fig. 10.6.

10.1.4 The Internal Cylinder Distributor

This distributor consists of an ordinary cylinder 90 cm in diameter opened at both ends and welded at the top end to a 121 cm outside diameter flange which fits the inside diameter of the column. This design of the distributor causes the gas feed to swirl in the annular gap formed between the internal cylinder and the column wall which is closed at the top. Thus the swirling gas emerges from the annulus and flows upwards inside the internal cylinder.

The general layout of the assembled column is shown in Fig. 10.7.

10.2 Testing the Internal Cylinder Gas Distributor

The quality of the existing design of the internal cylinder was experimentally investigated. It is shown that this design does very little to improve the distribution of the gas, and that most of the gas distribution improvement was a result of the draw-off tray. The work proceeded to test the draw-off tray as a gas distributor.

10.2.1 Experimental Procedure

The quality of a gas feed distributor is evaluated according to the proposed method given in Section 6, that is, the maldistribution factor ϕ is plotted against the packed depth. The best distributor is that one which causes a uniform gas distribution, ($\phi = \phi_{min}$), at the shortest packed depth.

The minimum number of point velocity measurements required is evaluated by a method similar to that described in Section 6 and found to be 200 measurements equally distributed in a plane 3.5 cm above a bed randomly packed with 16 mm plastic pall rings. The configuration of the points, at which the air velocity is measured, is shown in Figures 10.8 and 10.9 for radial and tangential feed inlets respectively.

The modified hot-wire anemometer, described in Section 4 is used to measure the point velocities. The air is pumped to the column through a 15.2 cm in diameter feed nozzle.

The maldistribution factor ϕ is obtained for a series of deep packed depths, (20 cm to 80 cm) and the minimum value of the maldistribution factor is found ($\phi_{min} \simeq 19$).

10.2.2 Experimental Results

The point velocities were measured above a series of shallow packed depths, (6-36 cm), which are equivalent to (0.36-2.15m) in the real life pump around packed bed.

A complete set of experimental observations is given in Appendix A5.

The analysed results are summarized in Table 10.1 and presented below for the following situations:

1) Radial Feed with No Distributor

ϕ is drawn against packed depth in Graph 10.1 and the gas distribution response surfaces are shown in Figs. 10.10a to 10.10d.

The results show a sharp decrease in ϕ values with the packed depth increase at very short depths, this variation eases at higher packed depths. At a packed depth of 36 cm, ϕ converges with ϕ_{min}; that is more than 2m packed depth in the real pump-around packed bed.

2) Radial Feed with the Draw-off Tray Fixed

The air is pumped radially immediately below the draw off tray whose slots were perpendicular to the feed jet direction as shown in Fig. 10.7.

The results are shown in Graph 10.2 and Figs. 10.11a to 10.11d, which show that ϕ approaches ϕ_{min} at a packed depth of about 20 cm, that is about 1.2m depth in the full-scale pump-around packed bed.

3) Tangential Feed with No Distribution

The results, presented in Graph 10.3 and Figs. 10.12a and 10.12b, show a negative flow of the air at the middle area of the packed bed and high air velocities near the wall. This negative flow was observed in a bed packed to a depth of 12 cm which is equivalent to more than 0.7m in the full-scale packed bed. At a depth of 18 cm, this negative flow has disappeared but still very small air point velocities were obtained at the middle area. A depth of 30 cm, (equivalent to 1.8m in the full-scale bed) was not enough to bring the maldistribution factor to its minimum value. This implies the need for the gas distributor.

4) Tangential Feed with the Draw-off Tray Fixed

The processed results are shown in Graph 10.4 and Figs. 10.13a and 10.13b. No negative air flows were detected and ϕ converges with ϕ_{min} at a depth of 24 cm, which is equivalent to about 1.5 m in the full-scale bed.

5) Tangential Feed with Internal Cylinder Gas Distributor

The results, presented in Graph 10.4 and Fig. 10.14, show the existence of negative air flows in the middle area in beds packed up to 12 cm, that is equivalent to 0.7m in the full-scale packed bed.

10.3 Discussion of the Results

The most important result of this part of the work is the observation of a negative, (downwards), gas flow for a tangential feed inlet and a shallow bed at the middle area. This phenomenon was observed when no distributor is used which reveals the importance of the use of gas distributors. The internal cylinder is used as a device to improve the distribution of the gas. As the

work shows that the internal cylinder causes very little improvement where the negative flow phenomenon exists both with and without the internal cylinder, a packed depth of 30 cm, (that is equivalent to 1.8m in the full-scale bed), was not enough to obtain the minimum gas maldistribution, (see Graph 10.5).

Another interesting result was obtained from this work, that is in both cases of radial and tangential feed inlets, a relatively short packed depth is required to bring down the value of ϕ to its minimum when the draw-off tray is used. For a radial feed, ϕ is brought down to about 1.6 ϕ_{min} within a packed depth as short as 6 cm only which is equivalent to 36 cm in the full-scale bed; in the case when the feed is introduced tangentially, ϕ is brought down to about 1.45 ϕ_{min} within a depth of 12 cm only, that is about 0.7m in the full-scale bed.

This implies that this special design of the draw-off tray acts as a good distributor. Probably this is because:

1) The free area provided by this design of draw-off tray is usually25-30% of the total area. Thus it is obvious that the high pressure drop across the draw-off tray causes some improvement of the distribution of the gas.

2) In the tangential feed situation, the gas has high velocities at the peripheral area whose width is about the same as the feed inlet diameter (15.2 cm), (see Section 8).

This particular design of draw-off tray is completely blocked on two sides to a width of 23 cm by flat plates, used to collect the liquid, and also blocked by the 15 cm wide sump from the third side, (see Plate 10.1). Thus it can be said that about 70% of the area of the high swirling air velocity is blocked. This blockage improves the distribution of the gas

below the bed.

10.4 Conclusions

From this section of the work it could be concluded that the internal cylinder is doing a little to improve the distribution of the gas and that most of the improvement is caused by the particular design of draw-off tray used in this work.

10.5 Comments on the Test of Existing Distributors

The results summarized on Graph 10.5 not only reveal interesting differences between different methods of gas distribution, but they provide an illustration of the use of the proposed method of testing gas distributors. That is; when compared on a ϕ basis, the best distributor is the one which requires the least packed depth for ϕ to reduce to its minimum value. Thus the distributors represented by lines at the bottom of Graph 10.5 are better than those represented by lines at the top.

It is also significant that when no distributor is used with a tangential feed, a packed depth of 36 cm is not enough to reach ϕ_{min} and a well distributed gas flow. This is equivalent to a packed depth 2.16m on a full-scale plant, which is greater than that used in many pump around beds.

There is thus a need to develop improved distributors for this duty, and since, as noted above, the pump around column modelled here works at a pressure of 20 mmHg, the distributors used in practice are required to have a negligible pressure drop.

The development of new designs of gas distributors is described in the next section.

PLATE 10.1

Fig. 10.1 Diagram of slots and Troughs in the Draw-off Tray

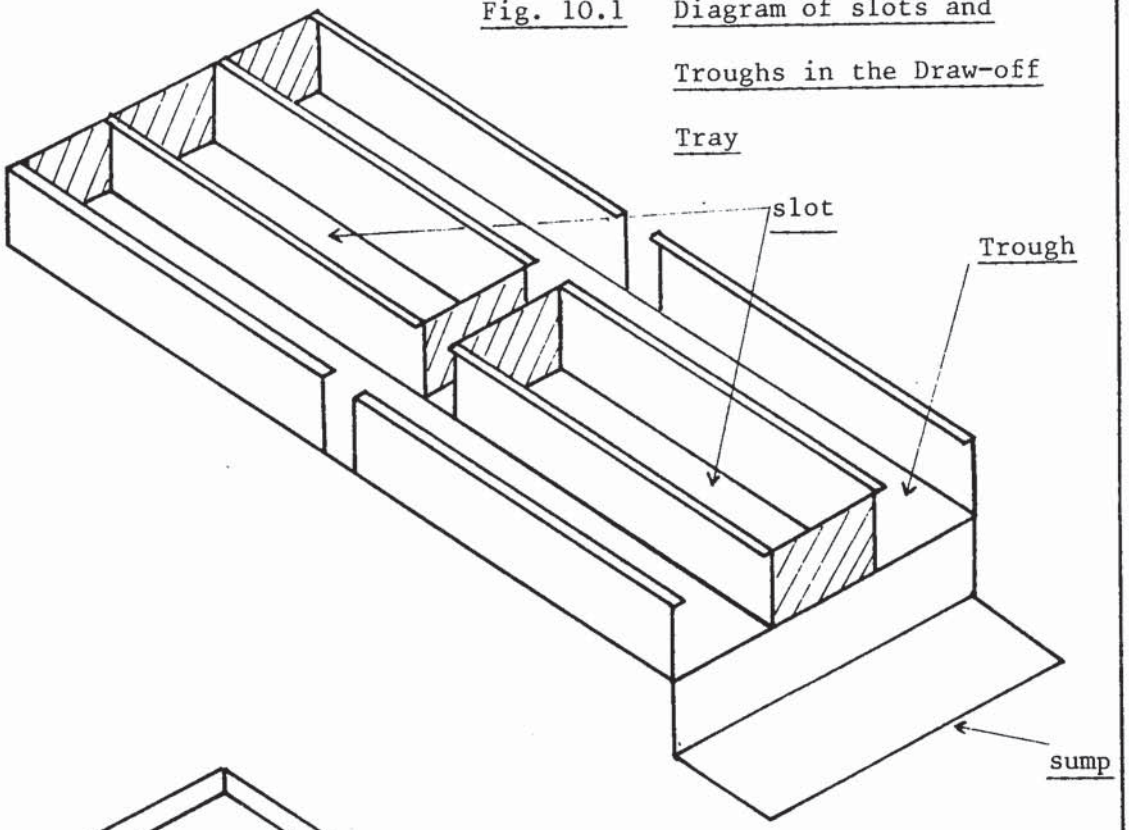

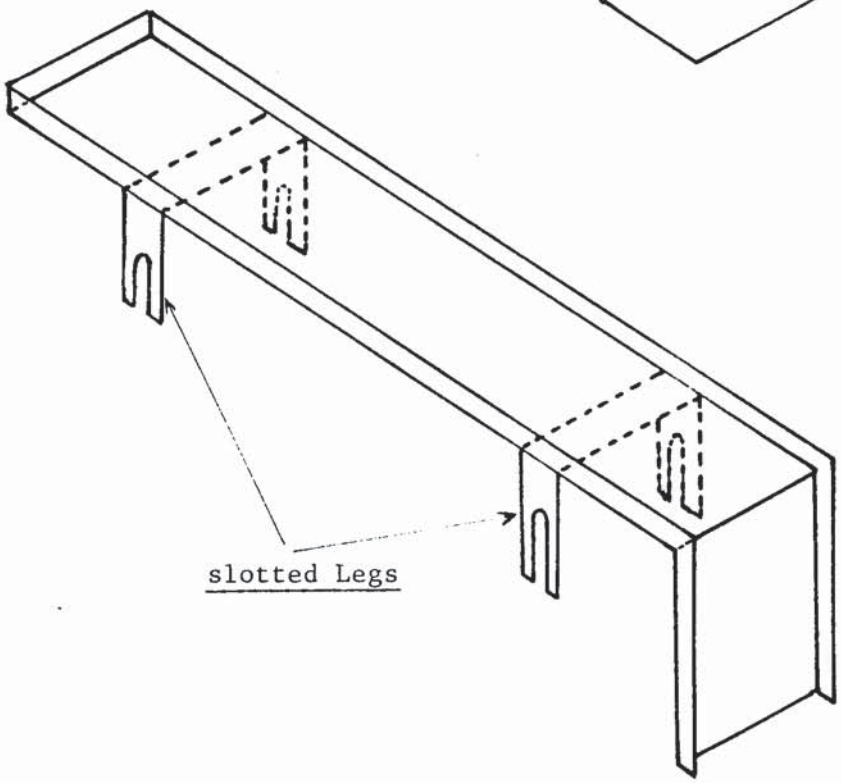

Fig. 10.2 Diagram of the Cap

Fig. 10.3 Cross Section in the Draw-Off Tray

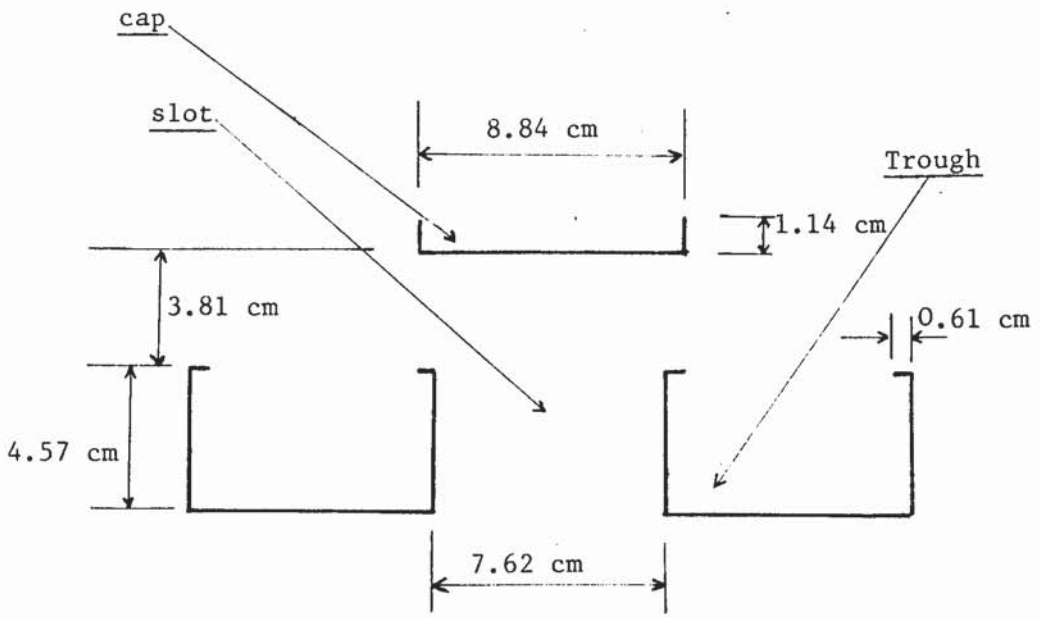

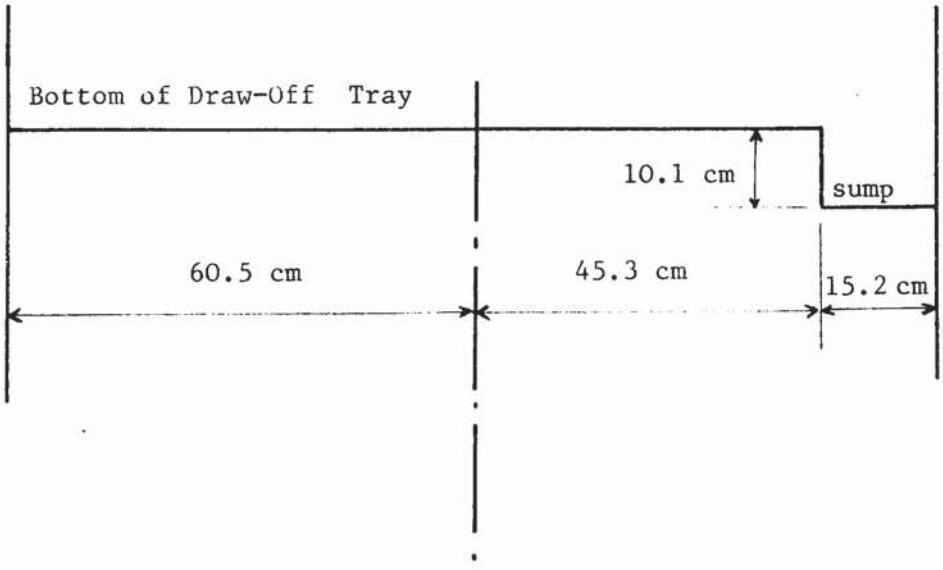

Fig. 10.4 Longitudinal Cross Section in the Draw-off Tray

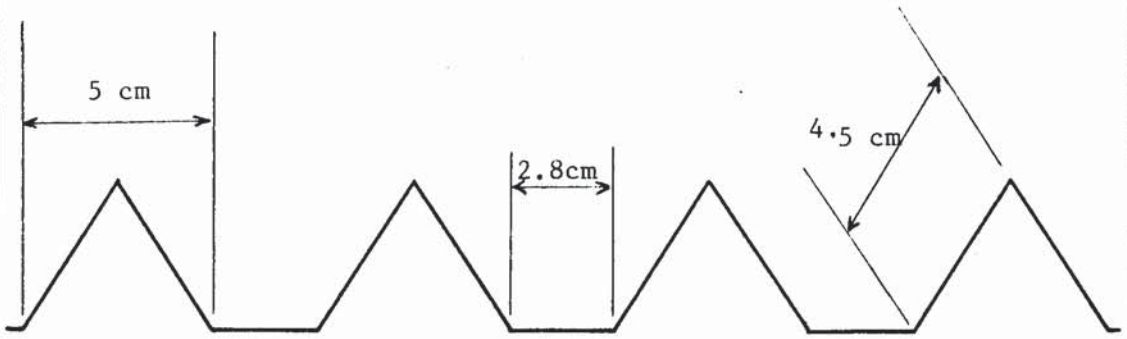

Fig. 10.5 Cross-section in the Support Plate

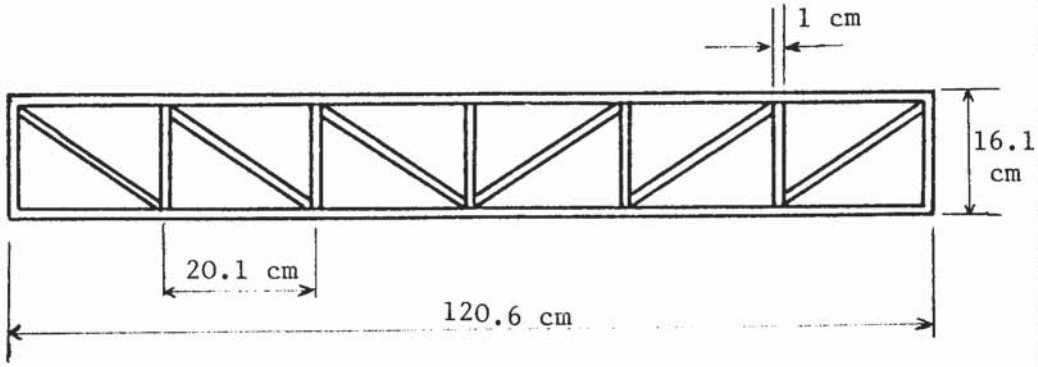

Fig. 10.6 Diagram of the Lattice Support Beam

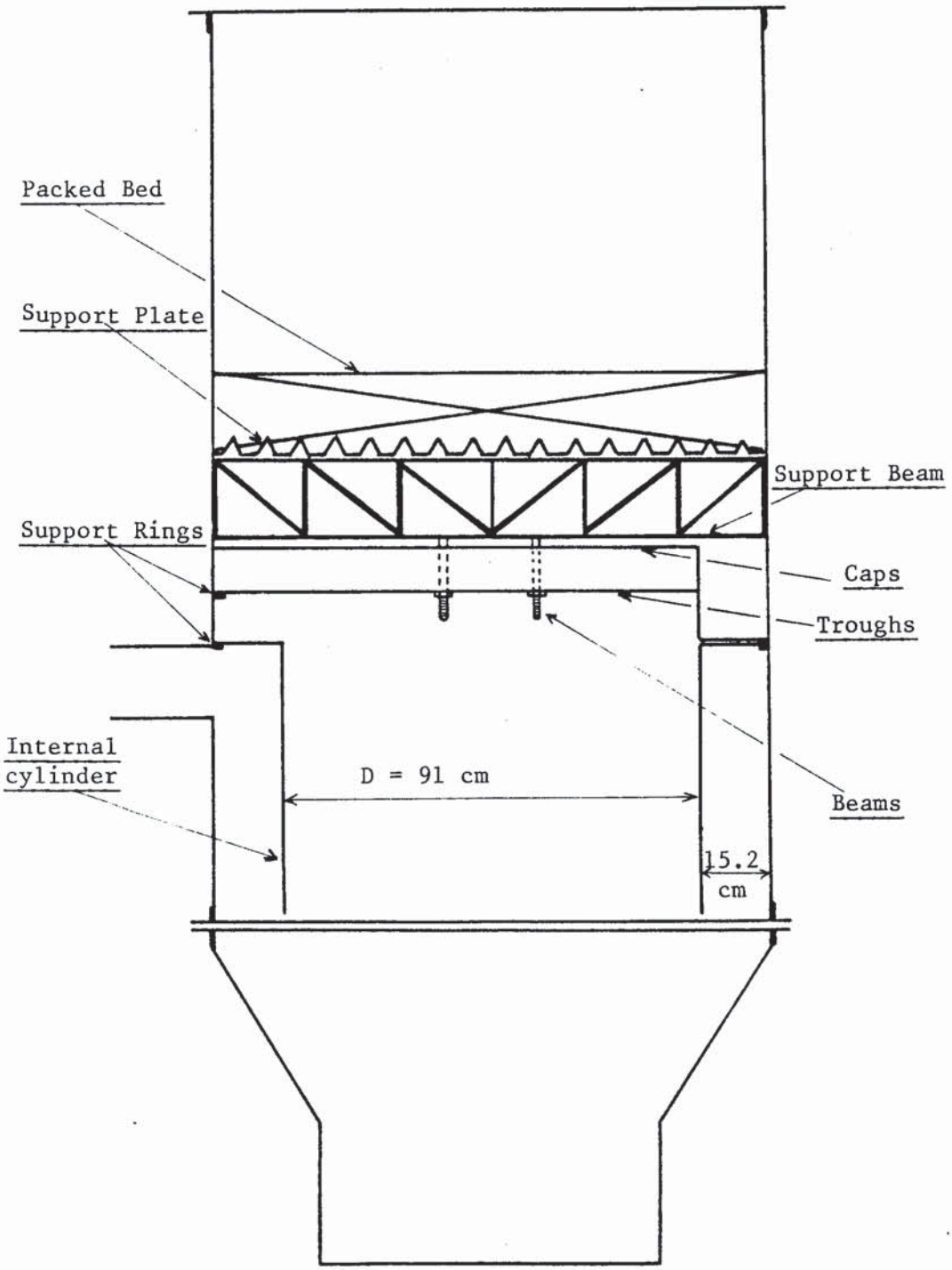

Fig. 10.7 Diagram of The Assembled Model

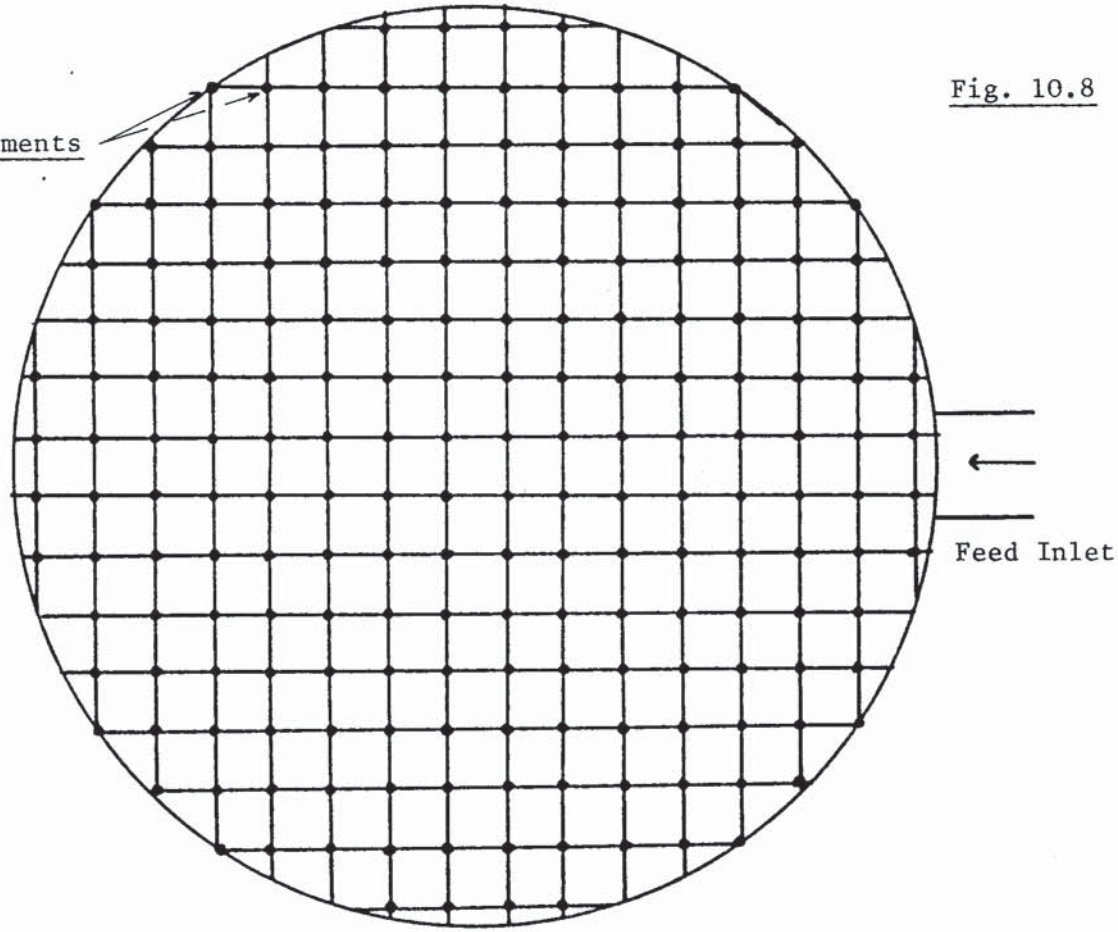

Fig. 10.8 Configuration of 200 Point Velocity Measurements taken above the 122 cm Diameter Bed with Radial Feed Inlet

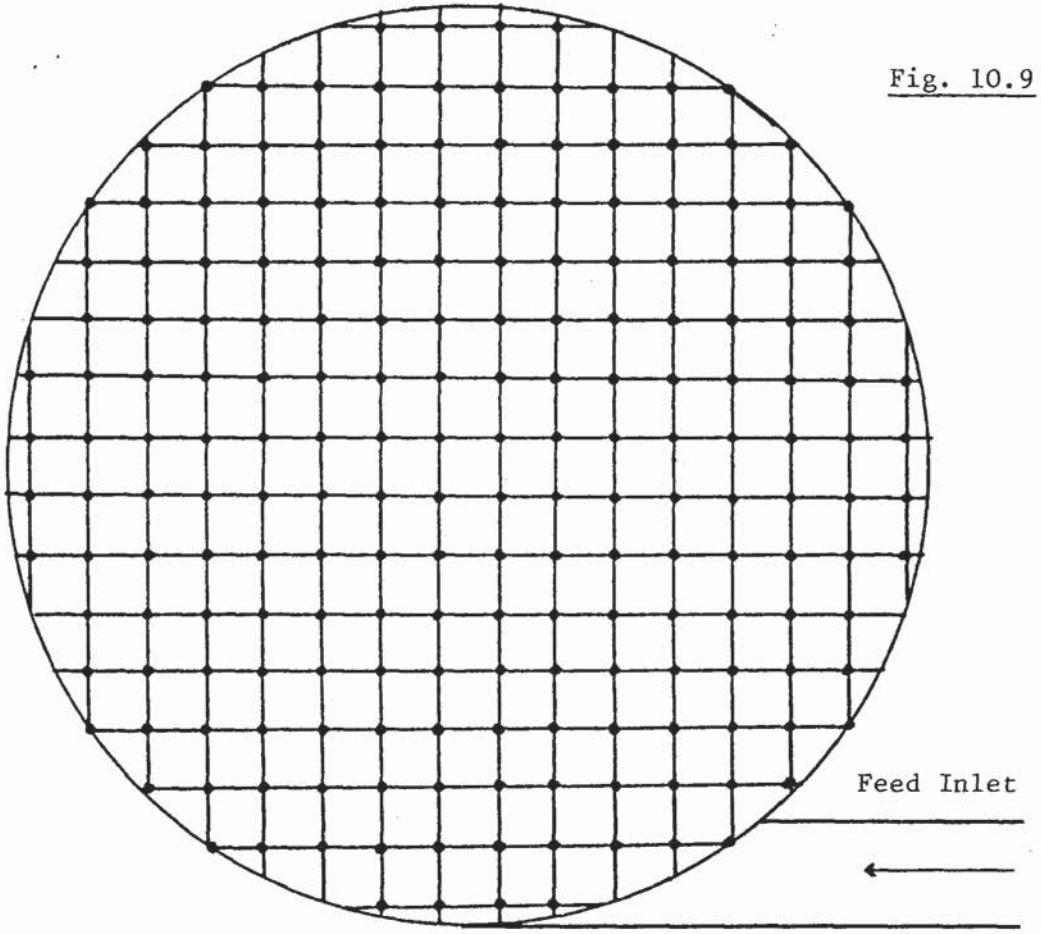

Fig. 10.9 Configuration of 200 point Velocity Measurements taken above the 122 cm Diameter Bed with Tangential Feed Inlet

Table 10.1 Maldistribution Factor, Ø, for Existing Designs of Gas Distributors at Different Packed Depths

Feed Inlet	Gas distributor	P.H. (cm)	Re	Ø
Radial	None	0	46,000	836
		6	"	210
		12	"	69
		30	"	21.4
Radial	Draw-off tray	0	46,000	98
		6	"	27
		12	"	22.6
		30	"	19
		36	"	19
		30	80,000	19
Tangential	None	12	46,000	148.5
		18	"	58
		30	"	26
Tangential	Draw-off tray	6	46,000	60
		12	"	38
		24	"	21
Tangential	Internal Cylinder	6	46,000	337.6
		12	46.000	110
		30	46.000	25

Graph 10.1 Ø against P.H. for a bed with Radial Feed with No Distributor

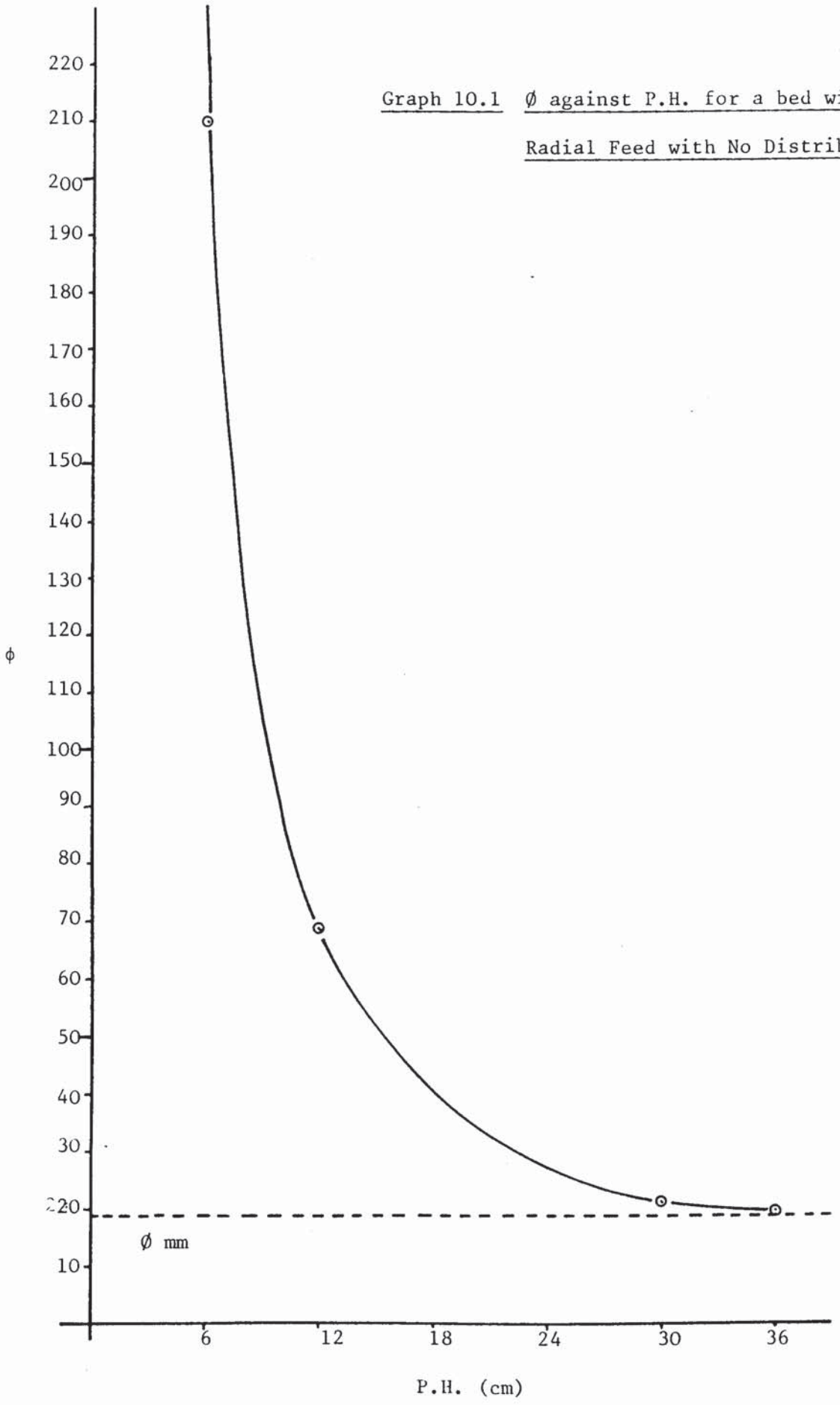

Fig. 10.10 Response surfaces for packed beds with radial feed and no distributor

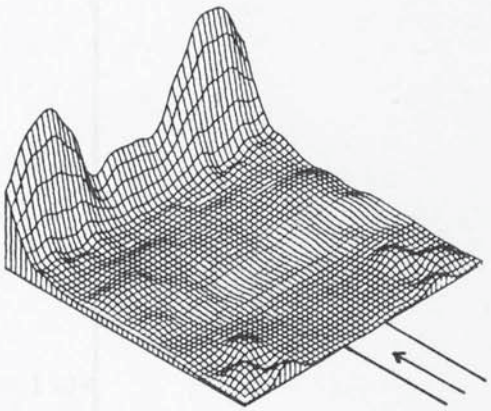

Fig. 10.10a P.H. = 0

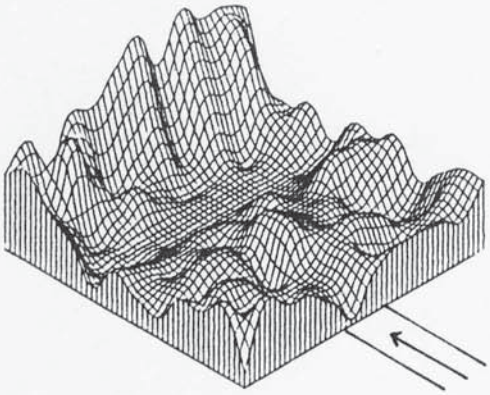

Fig. 10.10b P.H. = 6 cm

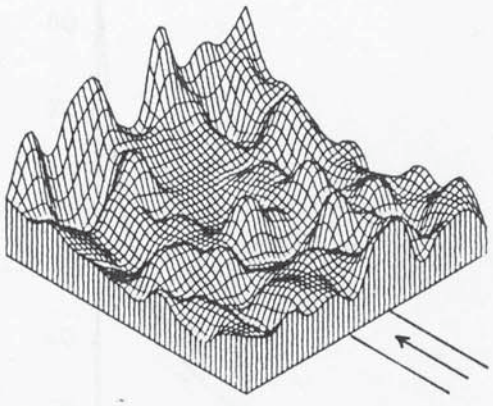

Fig. 10.10c P.H. = 12cm

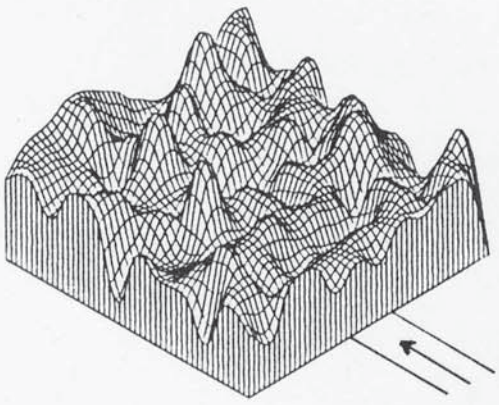

Fig. 10.10d P.H. = 30 cm

Fig. 10.2 Ø against P.H. for a Bed with Radial Feed and Draw-off Tray

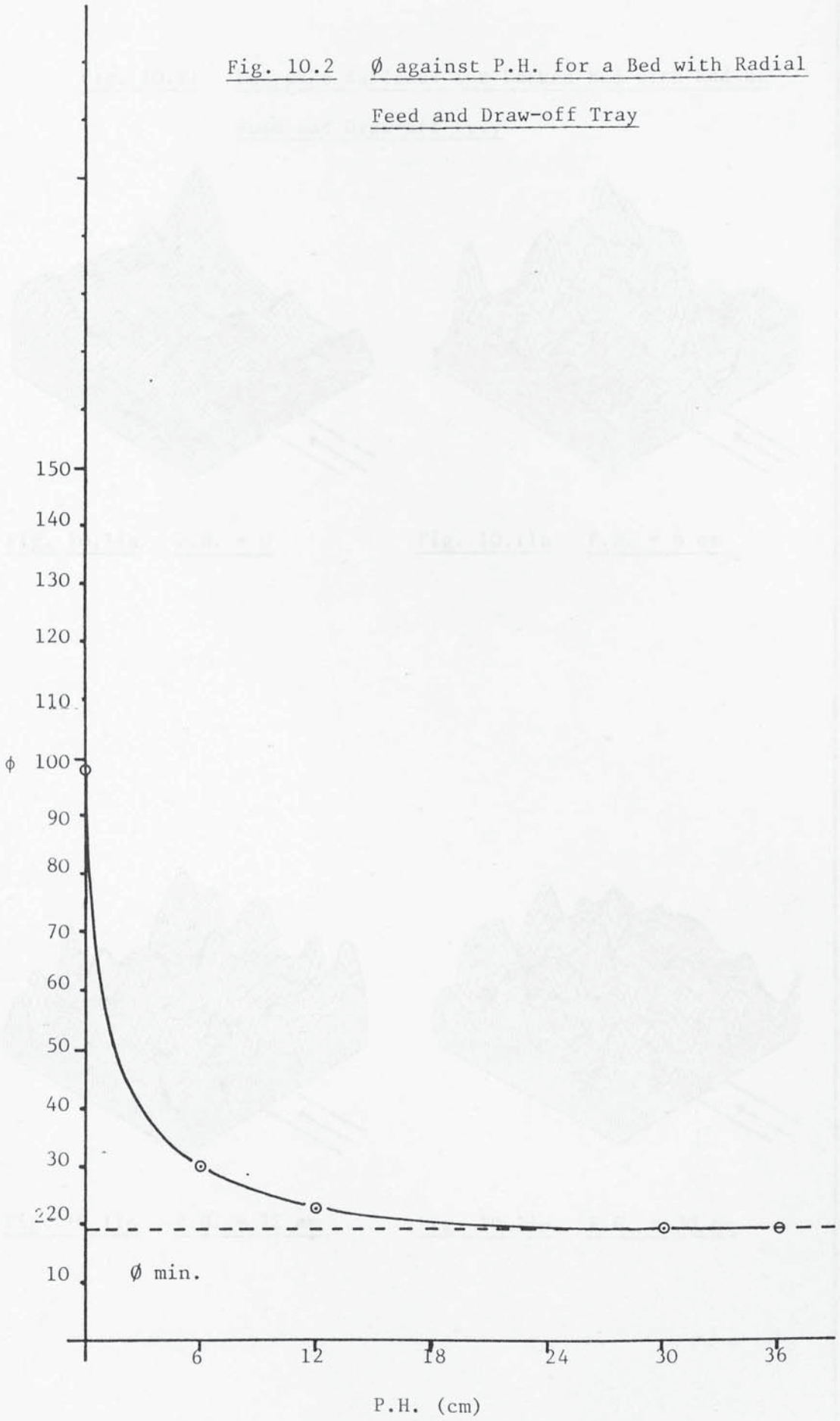

Fig. 10.11 Response Surfaces for Packed Bed with Radial Feed and Draw-off Tray

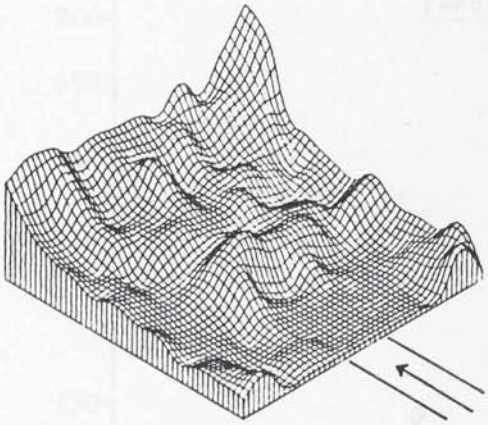

Fig. 10.11a P.H. = 0

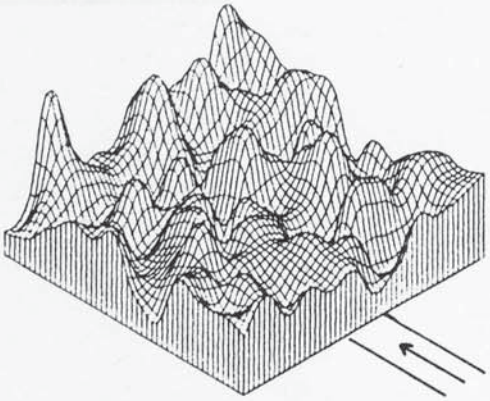

Fig. 10.11b P.H. = 6 cm

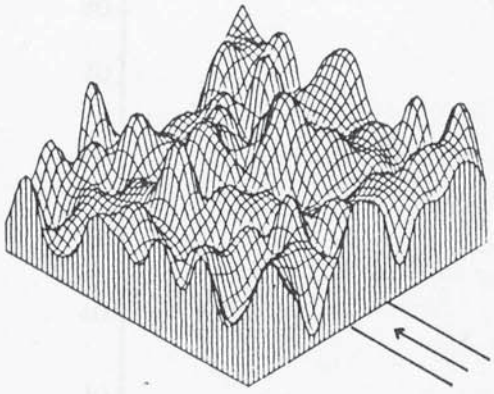

Fig. 10.11c P.H. = 12 cm

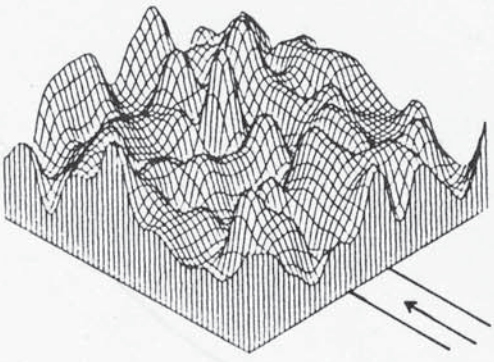

Fig. 10.11d P.H. = 30 cm

Graph 10.3 Ø against P.H. for a Bed with Tangential Feed and No Distributor

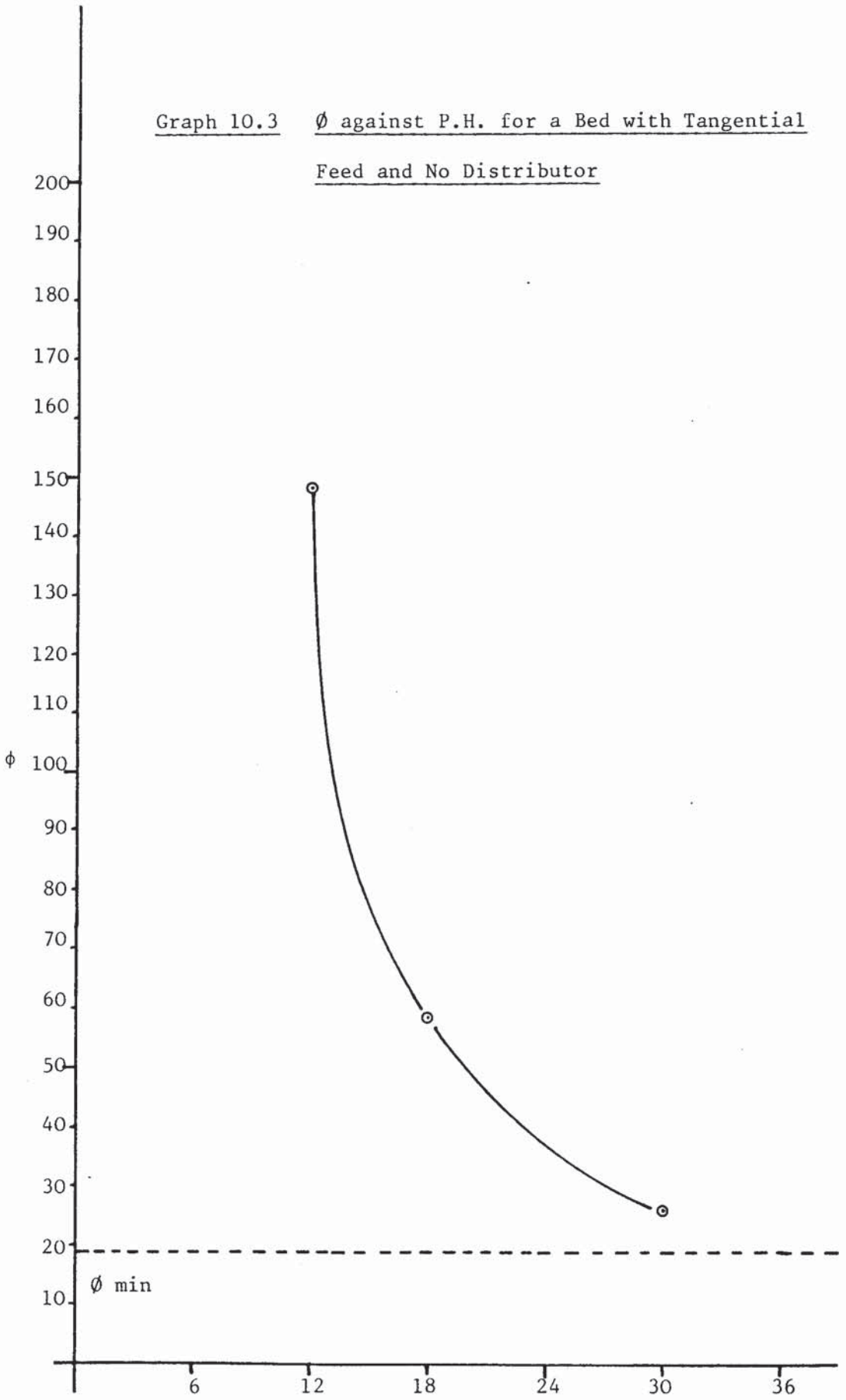

Fig. 10.12 Response Surfaces for Packed Beds with Tangential Feed and No Distributor

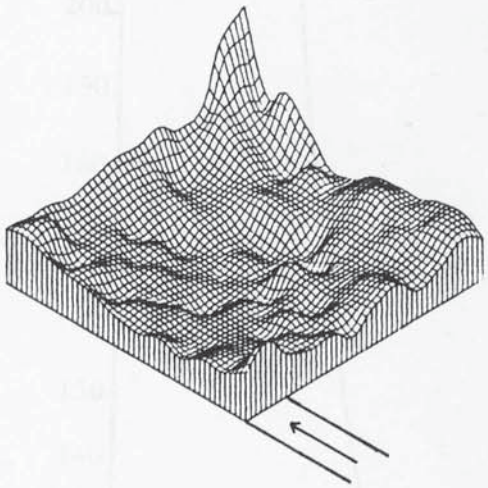

Fig. 10.12a P.H. = 6 cm

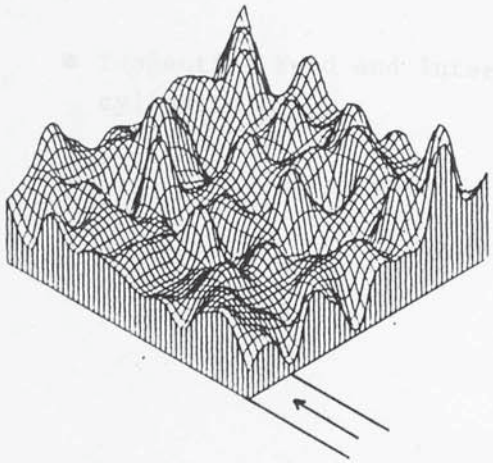

Fig. 10.12b P.H. = 30 cm

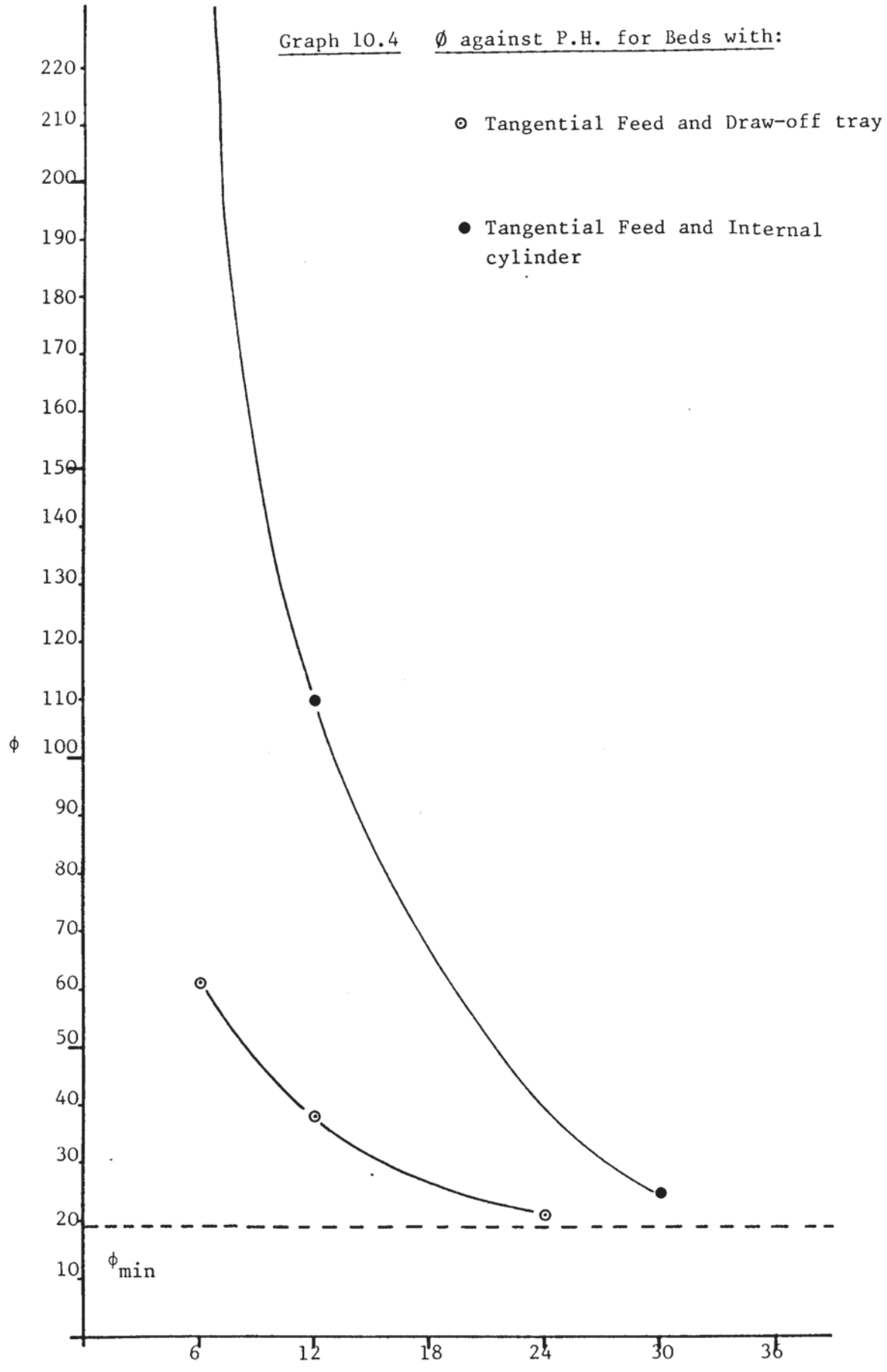
Graph 10.4 Ø against P.H. for Beds with:
⊙ Tangential Feed and Draw-off tray
● Tangential Feed and Internal cylinder
220
210
200
190
180
170
160
150
140
130
120
110
100
90
80
70
60
50
40
30
20
10
ϕ
ϕmin
6
12
18
24
30
36
P.H. (cm)

Fig. 10.13 Response Surfaces of Packed Beds with Tangential Feed Inlet and Draw-off Tray

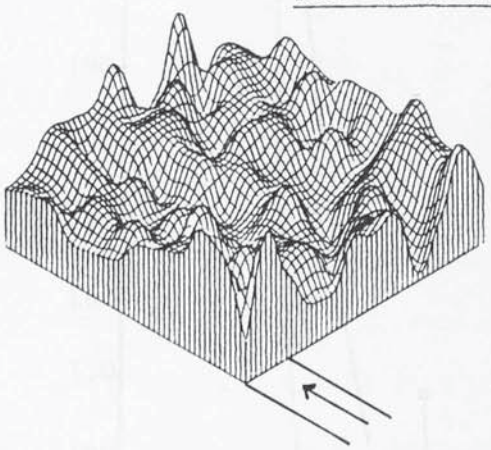

Fig. 10.13a P.H. = 6 cm

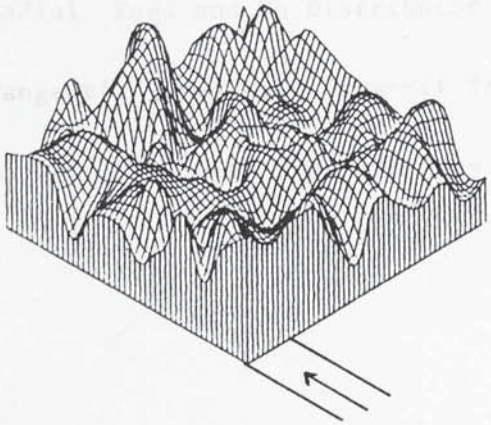

Fig. 10.13b P.H. = 12 cm

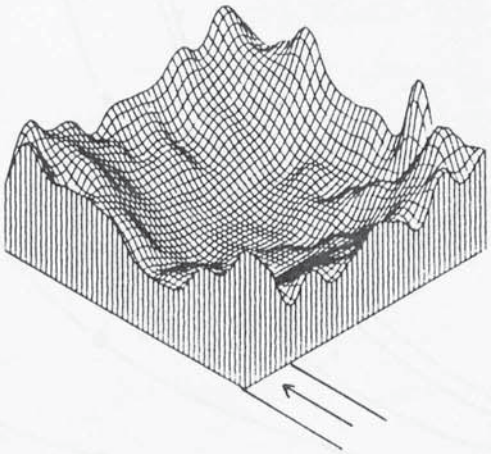

Fig. 10.14 Response Surface for a 6 cm deep Packed Bed with Tangential Feed Inlet and Internal Cylinder

Graph 10.5 Ø against P.H. for:

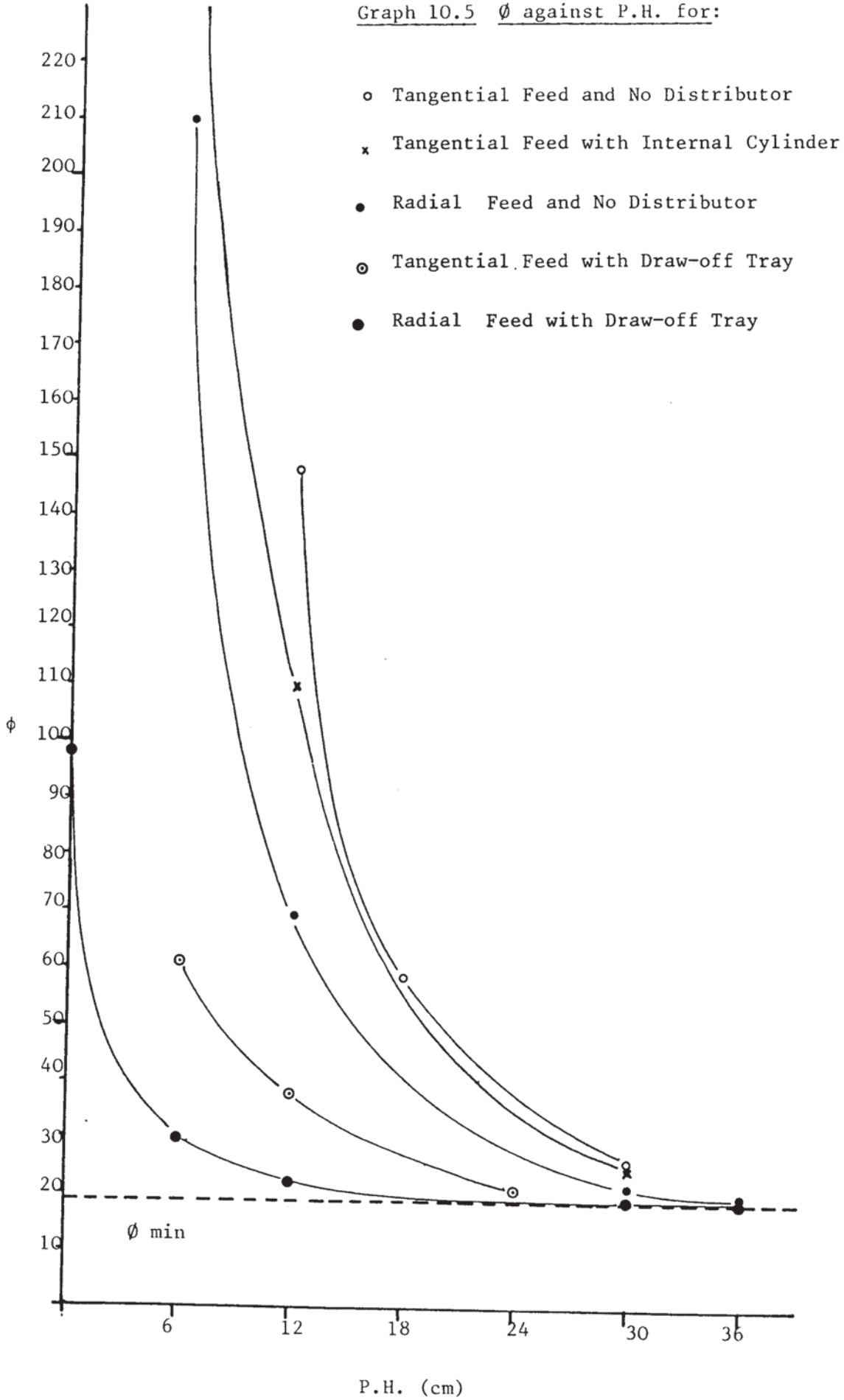

SECTION XI

DEVELOPING AND TESTING NEW DESIGNS OF GAS DISTRIBUTORS

Introduction

It was found, in the last section, that the particular design of the draw-off tray which Norton had supplied, is an effective means of improving gas distribution. But there will be situations where it is desired to achieve better gas distribution without fitting a liquid draw-off tray.

This stage of the work is concerned with developing and testing new low pressure drop gas distributors suitable for use in large diameter packed towers.

All the new designs of distributors below are modifications to the known use of tangential feed, combined with internal cylinder within the column, described in Section 9.1.3.

11.1 Modifications to the Internal Cylinder Gas Distributor

The gas emerging from the annulus is well distributed around the bottom of the internal cylinder, but is still swirling. It was observed, that at short packed depths associated with a swirling gas below the bed, a downward flow of air results in the middle of the bed.

All modifications are designed to remove this swirl.

11.1.1 Modification (A): Internal Cylinder with Four Slots and Cross Baffles near the Bottom of the Cylinder

This is shown separately in Fig. 11.1a and together with the column in Fig. 11.1b. Four cuts of 15 cm deep and 45 cm long

were made equally spaced around the lower end of the circumference of the internal cylinder, and the metal between the cuts was bent towards the middle of the cylinder. The four baffles formed were attached to each other at the centre to form a cross baffle. It is intended by this design to cause the swirling air at the bottom of the internal cylinder to change direction and go upwards vertically.

11.1.2 Modification (B): Internal Cylinder with Vertical Baffles in the Annulus

This distributor is shown in Fig. 11.2. Six vertical radial plates of depth of 20.3 cm and width of 15.25 cm were attached at the lower part of the annular space between the internal cylinder and the column wall. The number then increased, as shown in Fig. 11.3 and Plate 11.1, to 24 equally spaced plates to form air passages of length nearly twice that of the width. These plates are intended to straighten the swirling air at the bottom of the annulus and cause it to go down vertically, i.e. to produce a uniform distribution of gas around the bottom of the internal cylinder, but at the same time remove any swirl of the gas before it reaches the bottom of the internal cylinder.

11.1.3 Modification (C): Internal Cylinder with Internal Baffles

This is shown in Plate 11.2 and Fig. 11.4. The feed is again distributed equally around the bottom edge of the internal cylinder, and enters the cylinder with a swirling movement which is removed by two crossed baffle plates 90 cm in length and 45 cm in depth, put towards the top of the cylinder.

11.2 Tests on Distributor Modifications A, B and C

Typical unprocessed results are shown in Appendix A5 for Modification A, B with six baffles, B with 24 baffles, C, and Modification C combined with the draw-off tray described in Section 9.1.1. Response surfaces of gas distribution are given in Figs. 10.5-10.9 for the modifications respectively. The maldistribution factor, ϕ, values were obtained and listed in Table 11.1. The modified distributors are compared with the original simple internal cylinder and with each other in Graph 11.1, which shows plots of ϕ values against packed depth. That is; the new modifications are tested by the method proposed in this work, (see Section 6).

11.3 Discussion of the Results

All modifications; A, B and C, provide a significant improvement in the quality of gas distribution. The best modified distributor would be that one which produces a distribution of gas, expressed by ϕ, nearest to that described by ϕ_{min} at the shortest packed depth. That is, the comparison takes place at a packed depth of 6 cm which is equivalent to 36 cm in a real life packed bed.

Therefore, the unmodified internal cylinder is producing maldistribution factor, ϕ, as big as 18-fold the value of ϕ_{min} at packed depth of 6 cm. Modifications A, B (with 6 baffles), B (with 24 baffles) and C, are producing gas distribution which can be described in terms of ϕ_{min} as; 2.25 ϕ_{min}, 1.76 ϕ_{min}, 1.58 ϕ_{min} and 1.22 ϕ_{min} respectively, (see Table 10.1 and Graph 10.1). That means that Modification C; Internal Cylinder with Internal Baffles, is the best modified gas distributor.

In real life large towers, the performance, capital cost and pressure drop, are the most important guidances in the choice of gas distributor. All modifications mentioned above can be considered as low pressure drop distributors. Then the choice between these modified distributors would be solely related to their performances and capital costs, the best gas distributor would be that of best performance with least capital cost.

Modification A: Internal Cylinder with Four Slots and Cross Baffles, would be the cheapest of all, since the baffles used originate from the body of the internal cylinder itself.

However, Modification B: Internal Cylinder with Six Annular Baffles, is of better performance as well as providing an extra mechanical strength to the internal cylinder by attaching it at the bottom to the column wall.

Modification C: Internal Cylinder with Internal Baffles is providing best gas distribution; $1.22\ \phi_{min}$ within 36 cm in the real life packed bed. But it would be very expensive to build large internal baffles; two crossed baffles of dimensions of 540 cm x 270 cm in the real life distributor. But those baffles might replace the expensively constructed lattice support beam whose small model is shown in Fig. 10.6 in supporting the tower internals.

11.4 Conclusions

From above it could be concluded that Modification C: Internal Cylinder with Internal Baffles is the best low pressure gas distributor and it is believed that it would be suitable for large diameter towers with or without a liquid draw-off tray.

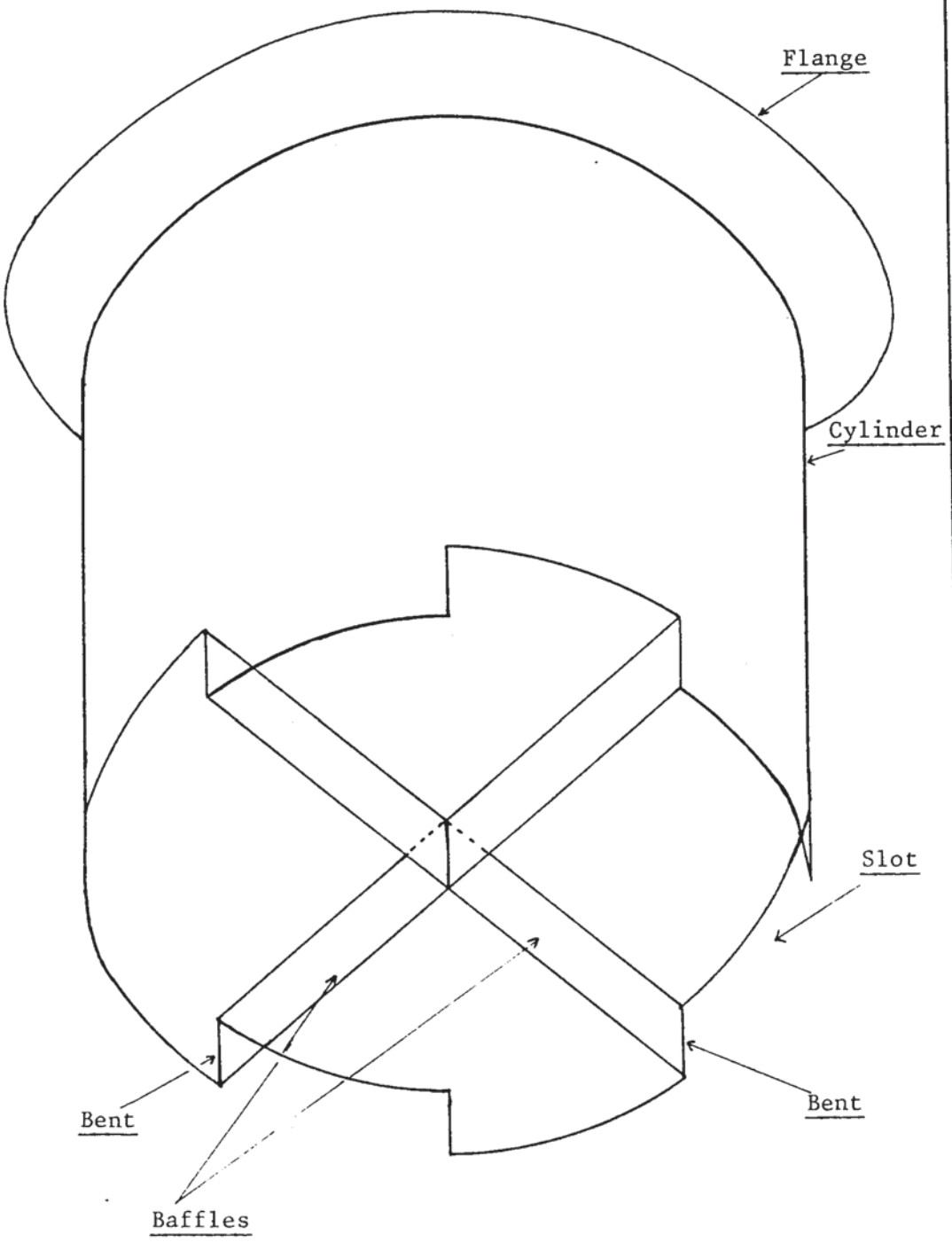

Fig. 11.1a Isometric Sketch of Modification (A)

Gas Distributor

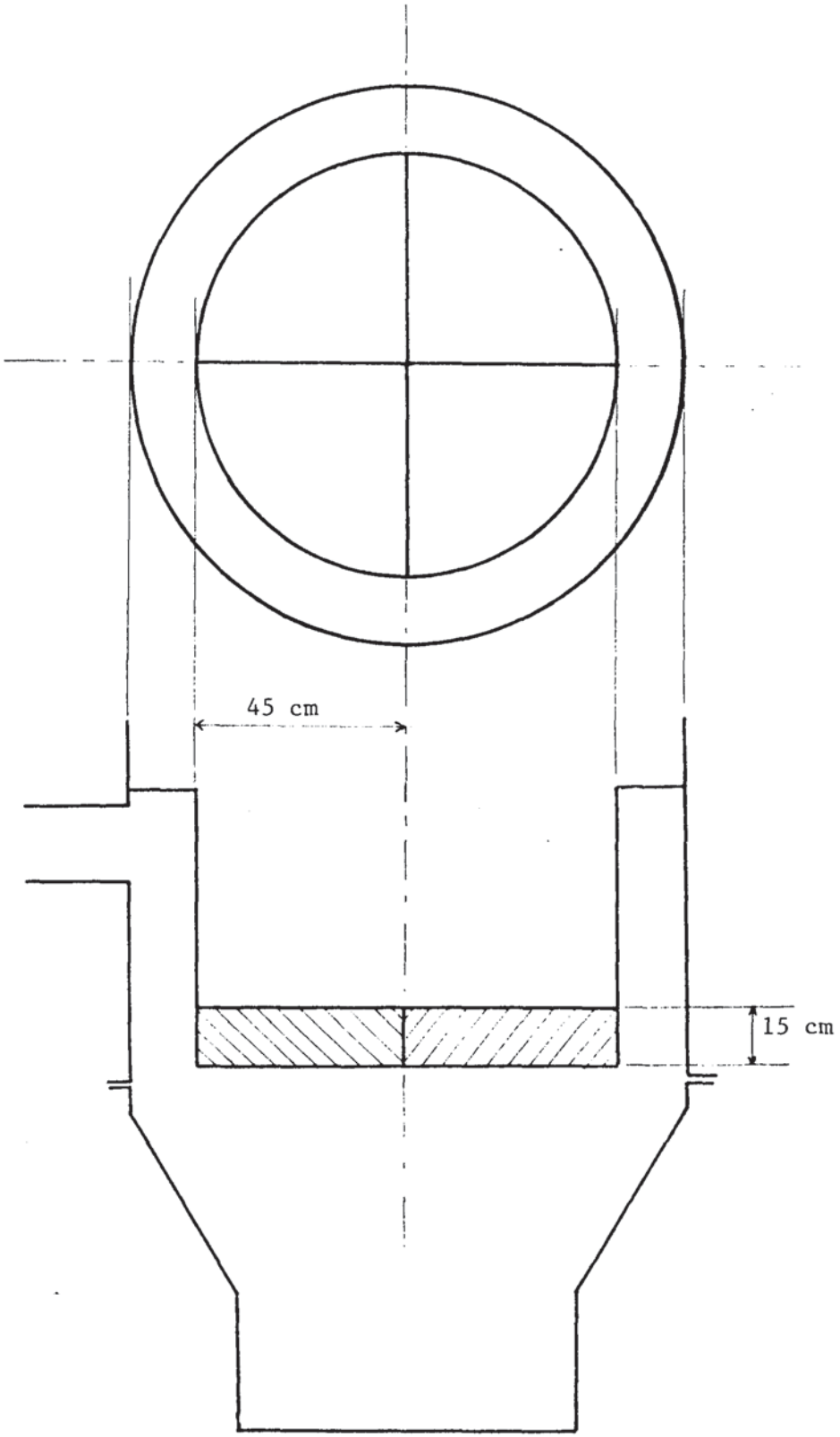

Fig. 11.1b Modification (A) within the Column

PLATE 11.1

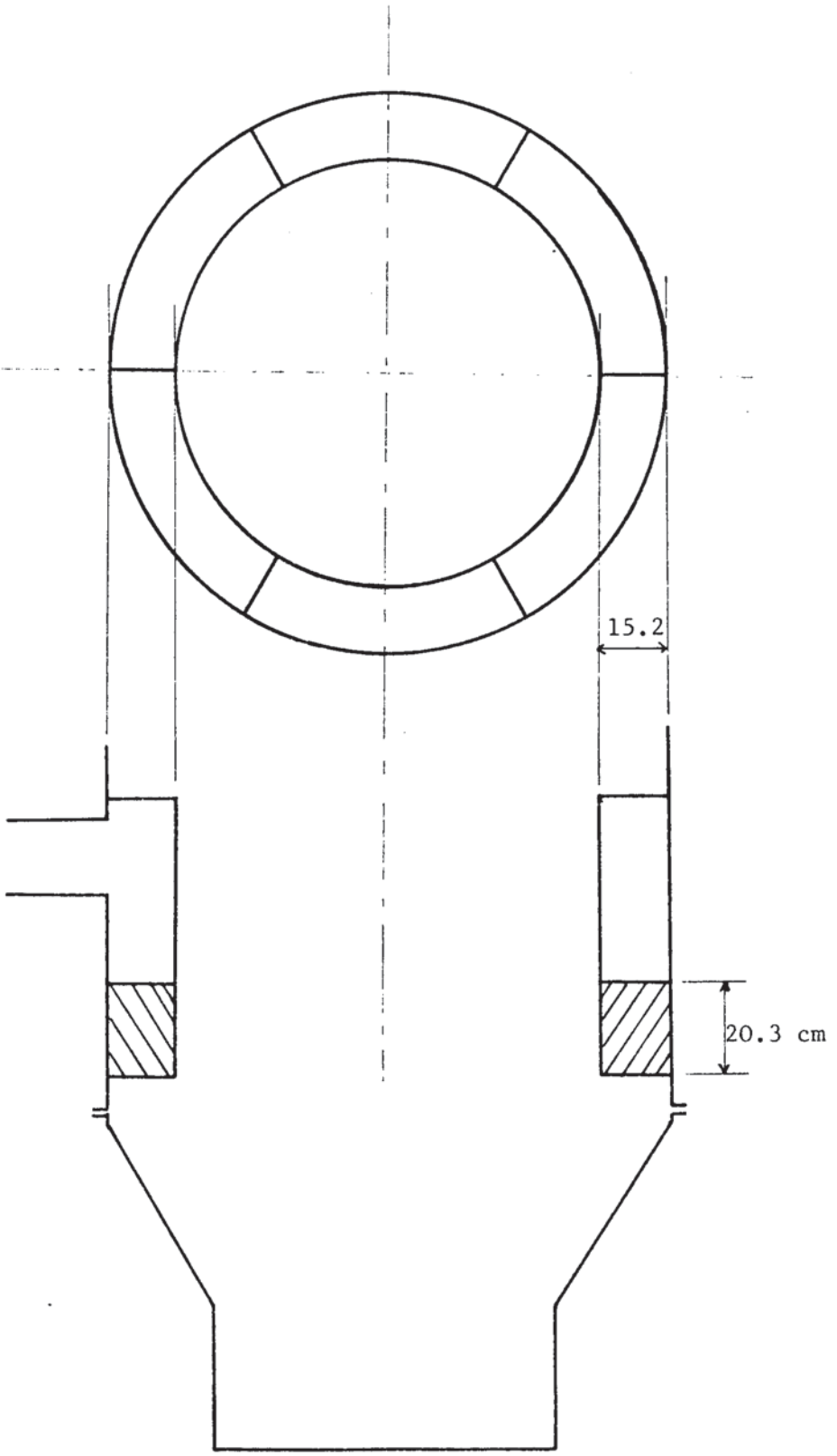

Fig. 11.2 Modification (B) with six annular Baffles

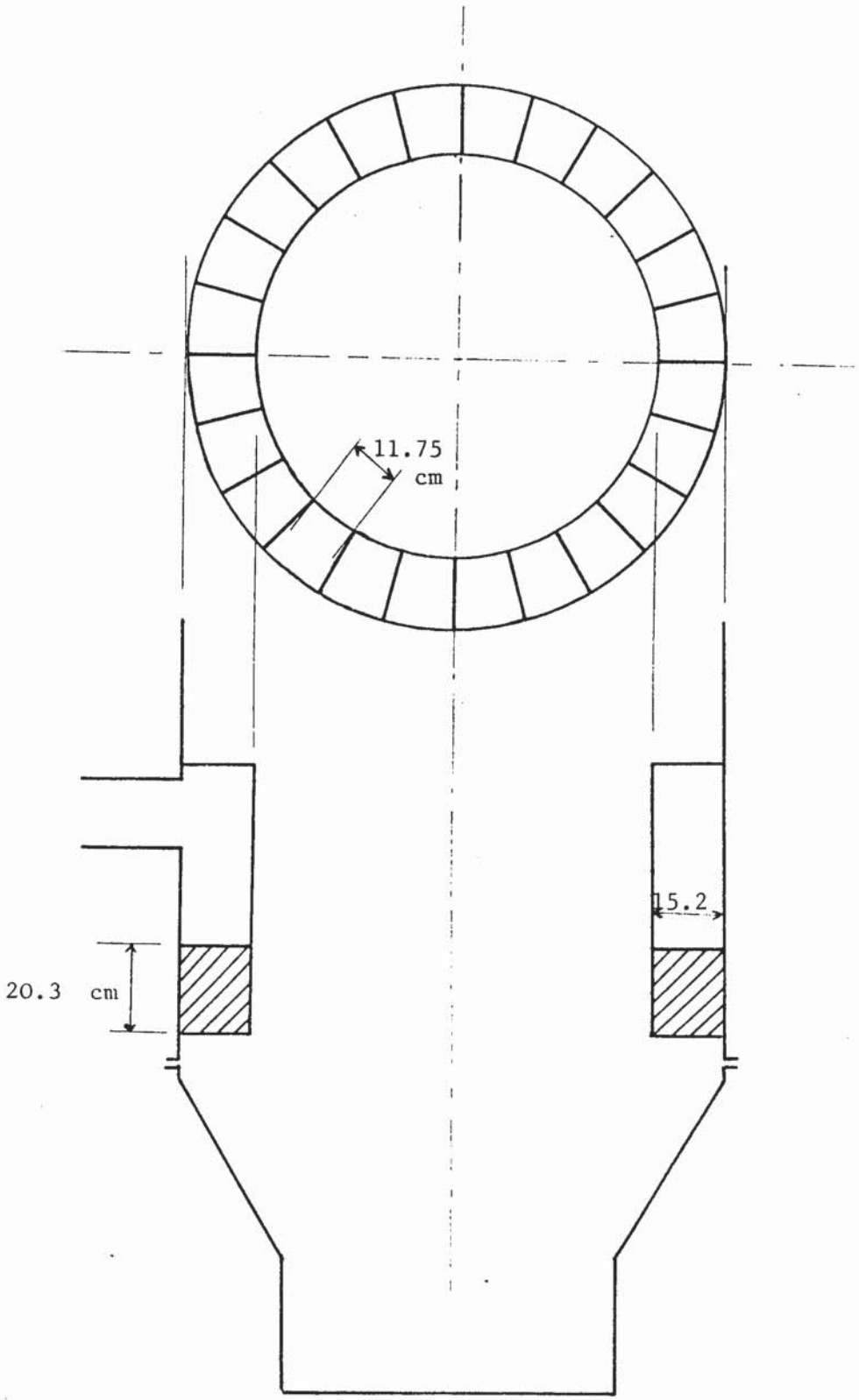

Fig. 11.3 Modification B with 24 Annular Baffles

PLATE 11.2

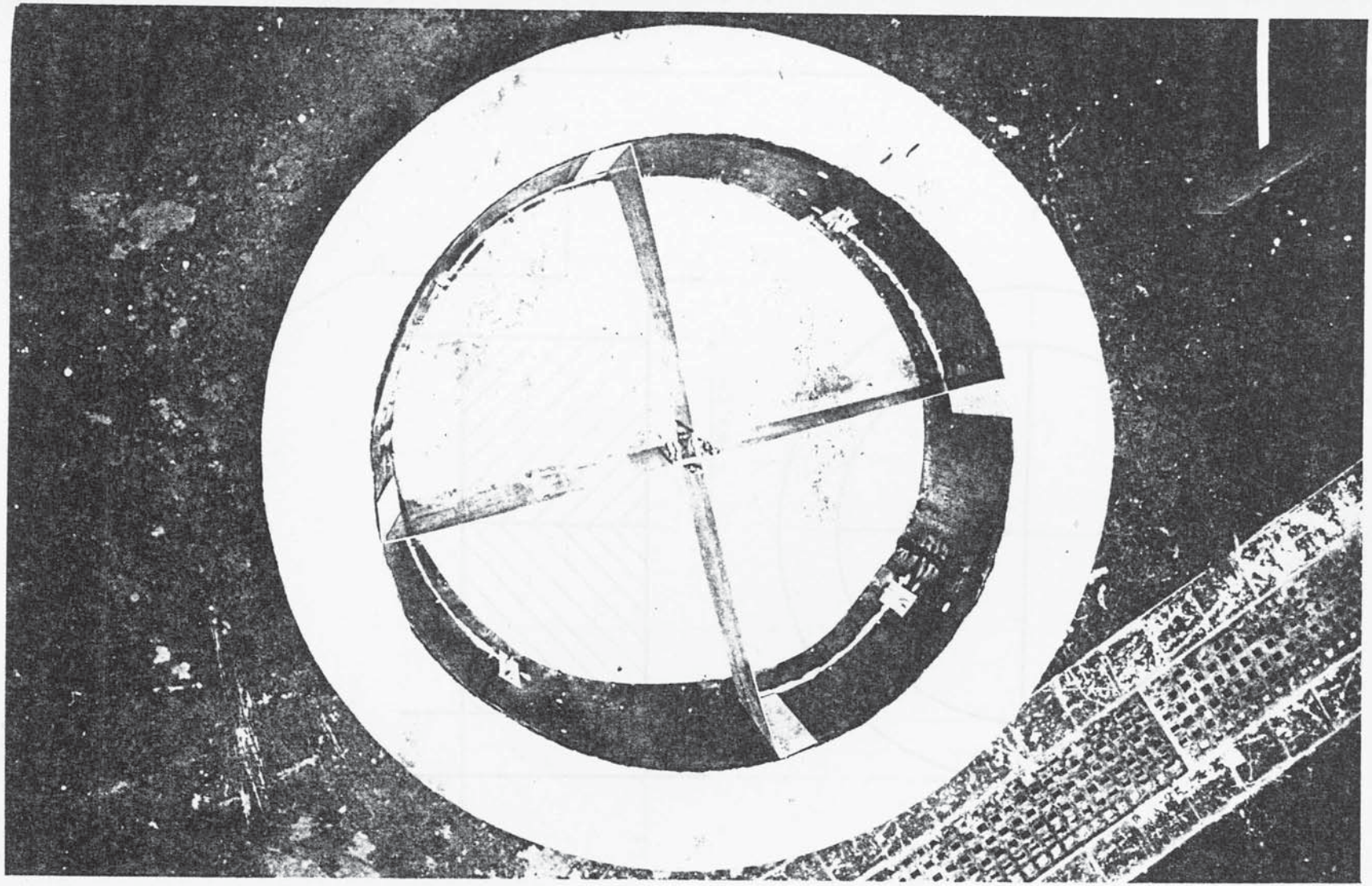

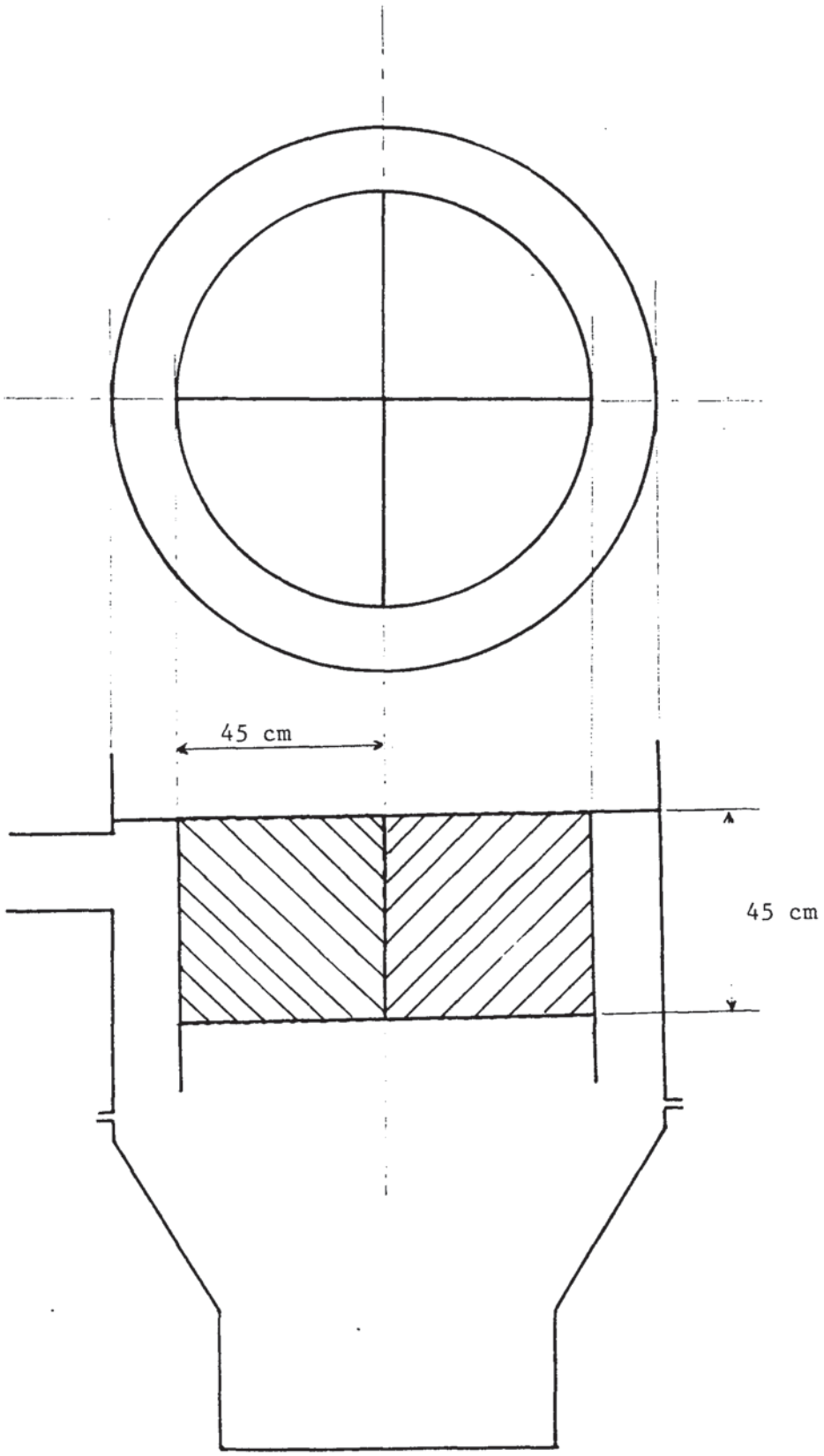

Fig. 11.4 Modification C

Table 11.1 Maldistribution Factor, Ø, for the Modified Gas Distributors at Different Packed Depths

Distribution	P.H.(cm)	Ø
Modification A	6	42.7
	12	31.3
	30	19
Modification B: with six plates	6	33.5
	12	26
	30	19
with 24 plates	6	30
	12	24.8
	30	19
Modification C: Alone	6	23.3
	12	21.1
	30	19
plus draw-off tray	6	22.8
	12	21
	30	19

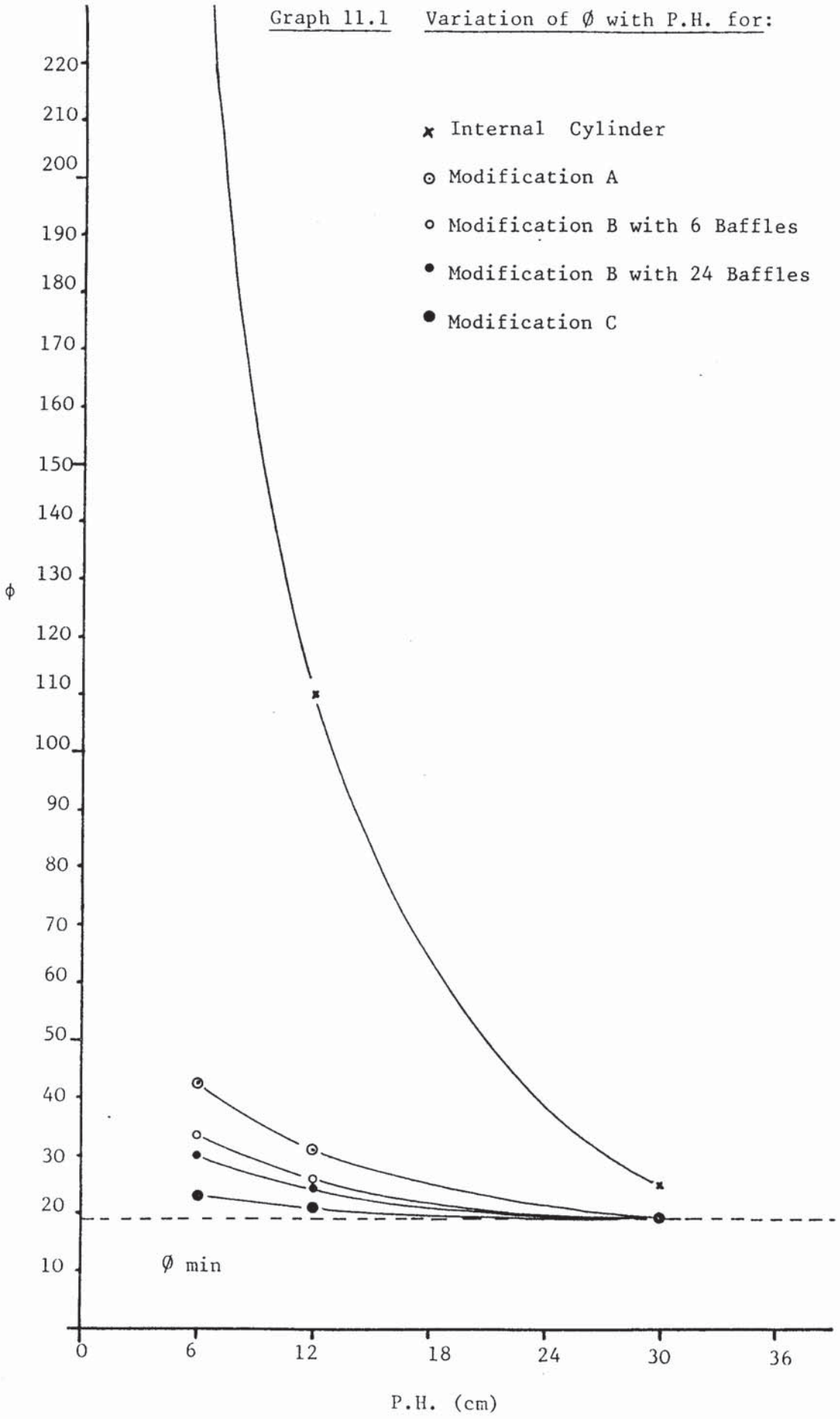
Graph 11.1 Variation of Ø with P.H. for:
Internal Cylinder
Modification A
Modification B with 6 Baffles
Modification B with 24 Baffles
Modification C
220
210
200
190
180
170
160
150
140
130
120
110
100
90
80
70
60
50
40
30
20
10
ϕ
Ø min
0
6
12
18
24
30
36
P.H. (cm)

Fig. 11.5 Modification A

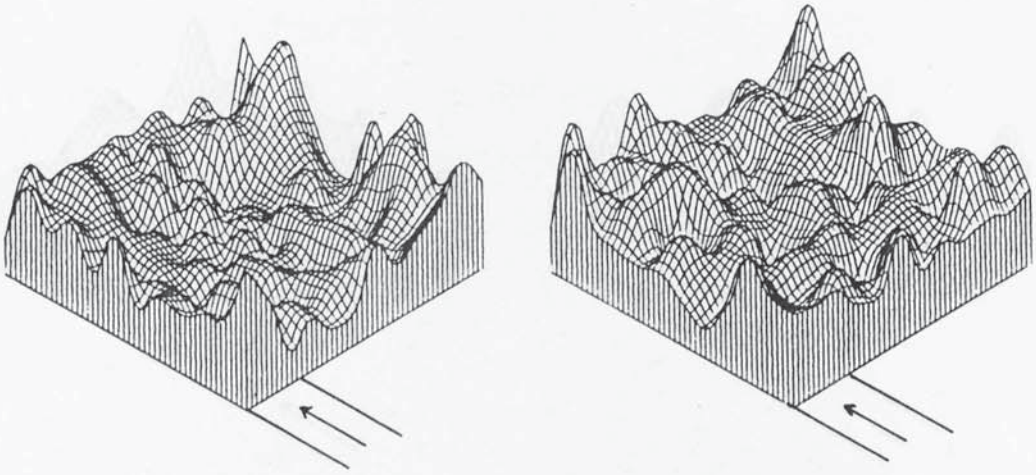

P.H. = 6 cm

P.H. = 12 cm

Fig. 11.6 Modification B with six baffles

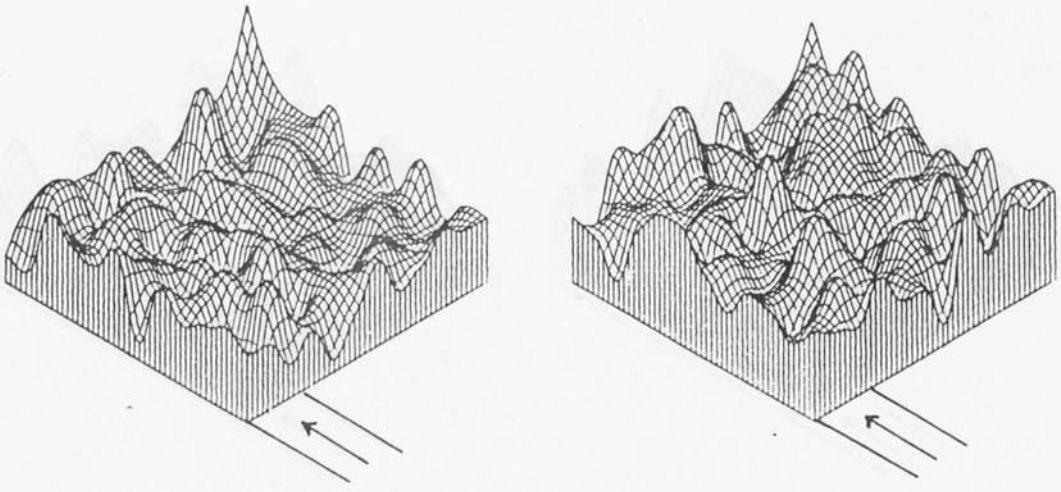

P.H. = 6 cm

P.H. = 12 cm

Fig. 11.7 Modification B with 24 Baffles

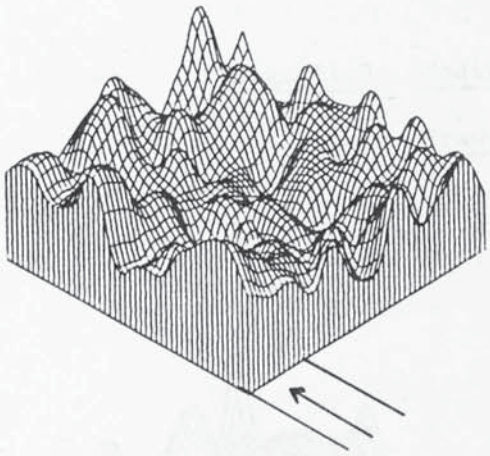

P.H. = 6 cm

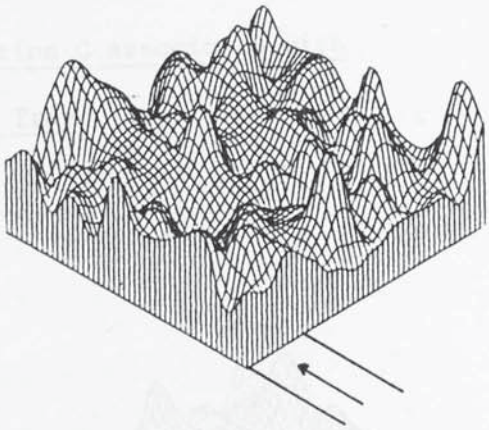

P.H. = 12 cm

Fig. 11.8 Modification C

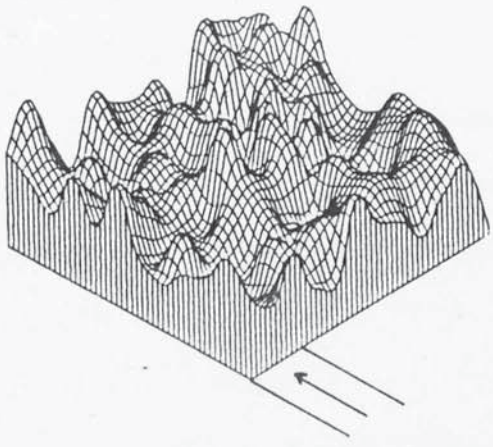

P.H. = 6 cm

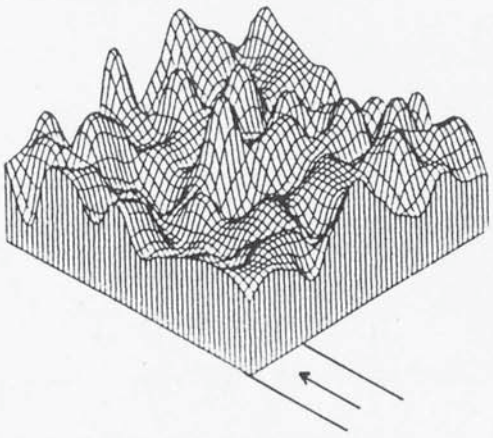

P.H. = 12 cm

Fig. 11.9 Modification C Associated with Draw-off Tray

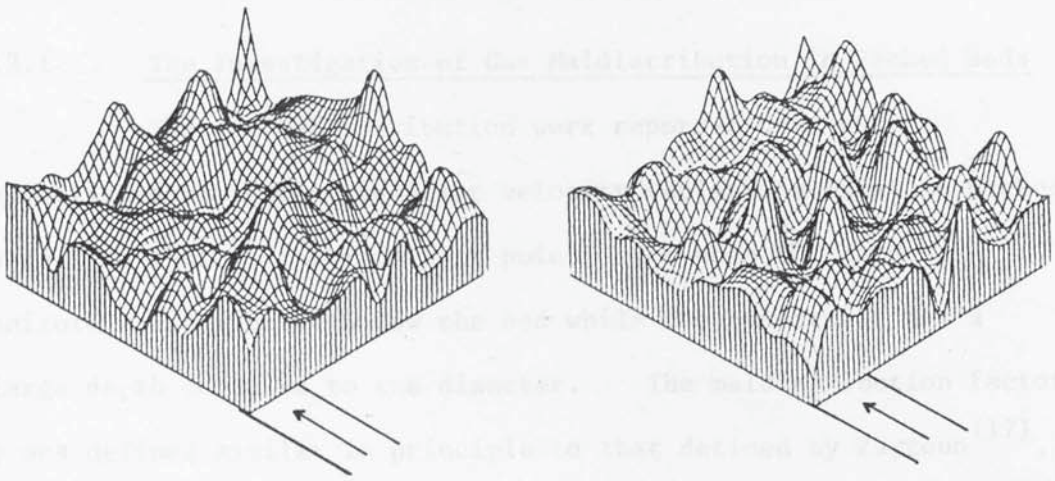

P.H. = 6 cm

P.H. = 12 cm

SECTION XII

DISCUSSION

It is known that the maldistribution of either gas or liquid may be expected to reduce the mass transfer performance of large diameter packed columns. All previous workers have studied the liquid maldistribution, and this work is believed to be the first extensive study of maldistributed gas flow in packed columns.

12.1 The Investigation of Gas Maldistribution in Packed Beds

The gas maldistribution work reported here has established that point to point velocity variations exist in packed beds, and that is the important point, even when the feed was uniformly distributed below the bed while the bed itself has a large depth compared to the diameter. The maldistribution factor ϕ was defined similar in principle to that defined by Zaytoun[17], but more representative because the point velocity measurement technique used here has covered all the cross-sectional area of the packed bed, as shown in Section V. The most important feature of ϕ is that it has a minimum value, ϕ_{min}, of about 20 for a deep bed when a uniformly distributed feed enters the bottom of the bed, and has much larger values for maldistributed beds. ϕ_{min} represents the best possible gas distribution. When this is achieved it is reasonable to expect that large diameter towers will work as well as small diameter towers (assuming of course that the liquid distribution also is uniform). The value of ϕ for a packed bed is changed each time the bed is rep acked, and this means that ϕ is not reproducible. For this reason, each bed was repacked several times, and each time ϕ was evaluated and then an average value, $\bar{\phi}$,

was obtained which is reproducible and considered as the most adequate measure of gas maldistribution in packed beds.

12.2 The Method of Evaluating Quality of Gas Distributors and the Scale-up Rules

A method of measuring the quality of gas distributors has been established in Section VI based on the variation of ϕ values with packed height, such that a good distributor is that one which produces gas maldistribution nearest to the minimum at the shortest packed height. It is practically impossible to apply this method to test the quality of a gas distributor in a large scale packed tower. Thus a laboratory size model of the full-scale column is needed to evaluate the gas distribution quality in such a large scale column. It is obvious that there should be rules to be followed in the construction of any model. Such rules of scaling up or scaling down a packed column were not available. A large part of the work was devoted to establish these rules which state that gas flow patterns are similar in two exactly geometrically similar packed beds of different sizes if the Reynolds number value is kept constant in both beds providing, and this is the important point, that the Mach number value is low enough to consider any change in it as ineffective. In this work, the maximum value of Mach number did not exceed 0.1. Therefore, these scale-up rules are applicable in systems whose Mach number, M, equals 0.1 or less. Vacuum crude columns work at high Mach number in the feed pipe, thus they require more investigations. But nevertheless it is expected that the proposed gas distributors will be better than those used up to now.

The basis of obtaining the scale-up rules is to get similar ϕ values for geometrically similar beds of different size operated at the same Re value. Thus the validity of ϕ as a reliable measure needs to be confirmed, and that confirmation will be discussed next.

12.3 The Statistical Study of Gas Maldistribution in Packed Beds

The multi-factor analysis of the variance was used to provide more insight on the meaning of ϕ and to prove the validity of scale-up rules. The choice of this statistical method was not only because it studies the maldistribution of the gas in more detail by producing numerical values to estimate the maldistribution in the spacial co-ordinates x and y, but because it studies the effect of increasing the size of the packed bed on the distribution of the gas while keeping Reynolds number constant. This study has concluded that the scale-up rules are valid, and that there are two constituents of ϕ. The first constituent, which is constant in all situations of packed height, Reynolds number, uniformity or nonuniformity of the feed, etc., is due to the point to point velocity variation. The second constitutent is due to the non-uniformity of the gas entering the bottom of the bed, and is referred to as the regional maldistribution, which varies significantly with the packed depth and the quality of the feed distribution.

Another technique was used in this thesis to visualize the velocity distribution of a gas emerging from the top of packed beds by producing response surfaces, which provides more evidence on the similarity of flow patternsin geometrically and dynamically similar beds and on the existence of the two sources of gas maldistribution; the point to point velocity variation and regional velocity variations.

12.4 Fluid Mechanics of Gas Maldistribution in Packed Beds

Having observed and evaluated the gas maldistribution above packed beds, the need to know what happens inside a packed bed with a maldistributed feed arises at this stage.

Commonly, the feed is introduced to the column either tangentially or radially. The case of a tangential feed inlet was used to study the mechanics of maldistributed gas flow. The choice of this case was because of the simplicity of performing the experimental investigation due to the symmetry of gas flow below the bed. Such a symmetry permits the measurements to take place along one diameter only. The gas velocity distribution and pressure distribution below and inside the bed were measured in Section VIII. As far as is known, these measurements of pressure distribution in the presence of maldistributed flow are the first ever to be presented. It was shown that the swirling air below the bed generates high pressure in the peripheral area whose width is more or less the same as the diameter of feed pipe, and a low pressure in the middle area. The air is driven by the pressure difference laterally from the high pressure area to the low pressure area and axially to atmosphere. If there was enough packed height, then the pressure will homogenize across the packed bed, and consequently the gas flow; if the packed height is short, then a quantity of gas is driven out of the bed by the high pressure more than the feed inlet supplies. Thus a downwards flow of air and a negative pressure was observed in the low pressure area. The case of the radial feed inlet needs more investigation to know the exact mechanism of gas maldistribution.

12.5 The Maldistributed Gas Flow Theoretical Models

Three models have been suggested to describe the

maldistributed gas flow in packed beds with tangential feed inlets. In the first model, the three-dimension model, a mass balance was performed on an elemental volume dxdydz in the bed in the cases of a completely laminar flow, a completely turbulent flow, and a laminar and turbulent flow. In each of these cases a differential equation was produced. The solution of these equations will depend on a mathematical model which translates the velocity below the bed into pressure within the bed, which is not available yet. This is an obvious area for future work. Two simple models are presented; the two area model and the cross-flow model. These two models can only be an approximation of the actual flow process, since almost certainly lateral flow takes place at different levels inside the packed bed up to the level where the pressure profile is flat, and the width of the high pressure area and low pressure area is not constant throughout the packed height. In these two models the column designs subject to gas maldistribution could be identified, that is, the height of a packed bed below which the flow is severely maldistributed due to the appearance of downwards gas flows in the low pressure area. These two models have produced a flow pattern function of maldistributed flow through the packing which has the property of an asymptotic approach to uniform distribution with increasing packed height and this is the common characteristic of the experimental observations, which show that the maldistribution factor ϕ decreases as the packed height increases to approach the best possible gas distribution represented by ϕ_{min}.

12.6 Existing and New Designs of Gas Distributors

The method of evaluating the quality of gas distribution devices proposed in Section VI was used in Section X to test some models of large-scale gas distributors. The construction of these models was governed by the scale-up rules obtained in this work. For this purpose, a real life pump around section in a 7.3m diameter vacuum crude factionation column described in Section II was used as an example to construct a laboratory size model, 1.22m in diameter i.e. a scale-down ratio of 1/6 is used. A widely used internal cylinder gas distributor is tested in this work, and it is shown in Section X, that this distributor does little to improve the gas distribution, and that most of the improvement is due to the particular design of liquid draw-off tray used below the packed bed. It should be noted that the improvement in gas distribution with this particular design is to a large extent fortuitous and a result of the use of blank areas near the wall through which no gas can flow.

The thesis concludes by designing three new gas distribution devices, which are modifications of the Internal Cylinder. The test performed on them in Section XI shows that the internal cylinder with internal cross baffle is the best low pressure gas distributor that would be suitable for large diameter packed beds.

It should be pointed out that the new distributors were designed with the objective of removing the high velocity swirl which the pressure distribution work had shown to be the cause of the maldistribution. Of great practical interest is that the simple geometries used are such that the pressure drop through these new gas distributors is expected to be exceedingly small.

Also, it is believed that there will be no serious practical difficulties in building and installing them on an industrial scale.

12.7 Future Work

The work described above might be usefully followed by several subsequent investigations. The value of development of a three dimensional theory has been mentioned above, but even the simple theoretical models suggest the need for experiments to determine the effect of inlet pipe to tower diameter ratio, and to investigate the way the variation of ϕ with packed height depends on packing size. Also it should be noted that more work is needed on radial inlets, both experimental and theoretical. Although the new distributors have shown to be effective there is much to be done on optimizing their dimensions.

SECTION XIII

CONCLUSIONS

The main conclusions from this experimental work can be summarised as follows:

(1) A method is proposed for evaluating the quality of gas distributors used in large diameter packed columns. A good distributor is that one which gives a good gas distribution in very short depths of a large diameter packed bed.

(2) A maldistribution factor, ϕ, was defined, which is related to the standard deviation by the number of measurements made. It has a minimum value for well distributed gas flow and much higher values for maldistributed gas flow. The average value of maldistribution factor, $\bar{\phi}$, is reproducible.

(3) It has been found that for two geometrically and dynamically similar systems of different sizes, $\bar{\phi}$ has the same value. The principle of dynamic similarity is satisfied when both systems are operated at the same Reynolds number. That is true in both uniformly and maldistributed gas flows.

(4) A laboratory study was carried out on a scaleddown model, exactly geometrically similar to a vacuum crude fractionation tower 7.3m in diameter with a packed depth of less than 2m, but 1/6 the size. Four types of gas distributors have been tested. These are:- The previously known Internal Cylinder associated with tangential flow distributor, and three modifications:

A) Internal Cylinder with Slots and Cross Baffles.

B) Internal Cylinder with Guides in the Annulus.

C) Internal Cylinder with Internal Cross Baffles.

The internal cylinder with internal cross baffles has been shown to be an excellent method of achieving a uniform gas distribution with a negligible pressure drop.

Also, it has been noticed that the particular design of draw-off tray used in the large scale tower helps in distributing the gas significantly.

5) The gas maldistribution in packed beds is associated with significant radial pressure gradients. These have been measured and shown to be associated with the velocity of the gas in the feed pipe.

6) Two simple theoretical models of gas maldistribution in packed beds have been proposed to describe the flow of gas through packed beds, and to support the use of geometrically and dynamically similar models to investigate gas distribution and distributors in full-scale plants. These two models identify the packed bed designs "at risk" of gas maldistribution.

7) The effect of the ratio of inlet pipe/tower diameter is expected to be a significant variable in determining gas distribution.

APPENDIX A1

Calibration Chart for the 152 mm Diameter Dall-Tube

Graph A1.1: Low air flow rates.

Graph A1.2: High air flow rates.

Graph A1.1 Calibration Chart for Low Air Flows

- Apparent air flow based on measurements above a randomly packed bed (based on $\overline{V}$)

- True air flow measured in an empty pipe

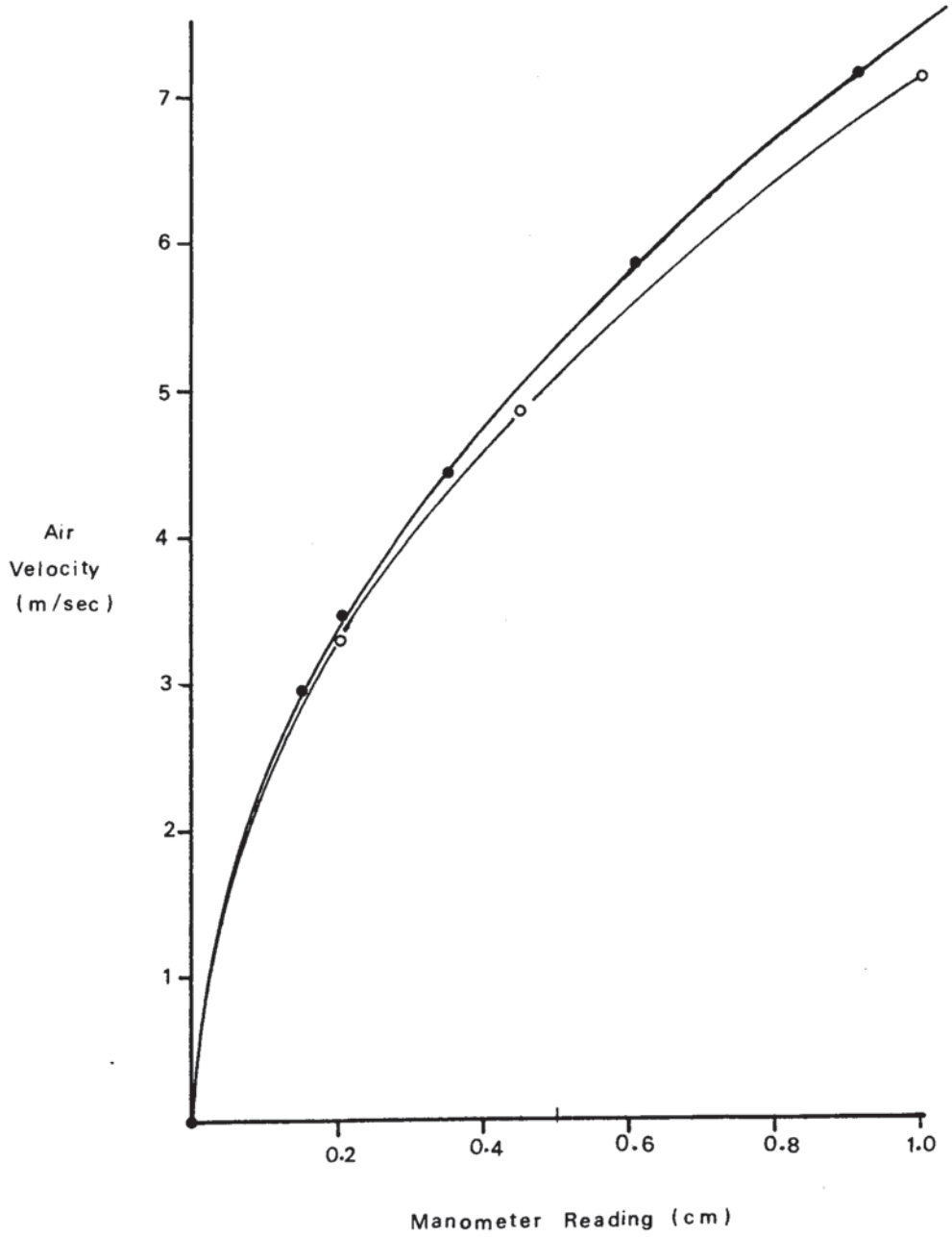

Graph A1.2 Calibration Chart for High Air Flows

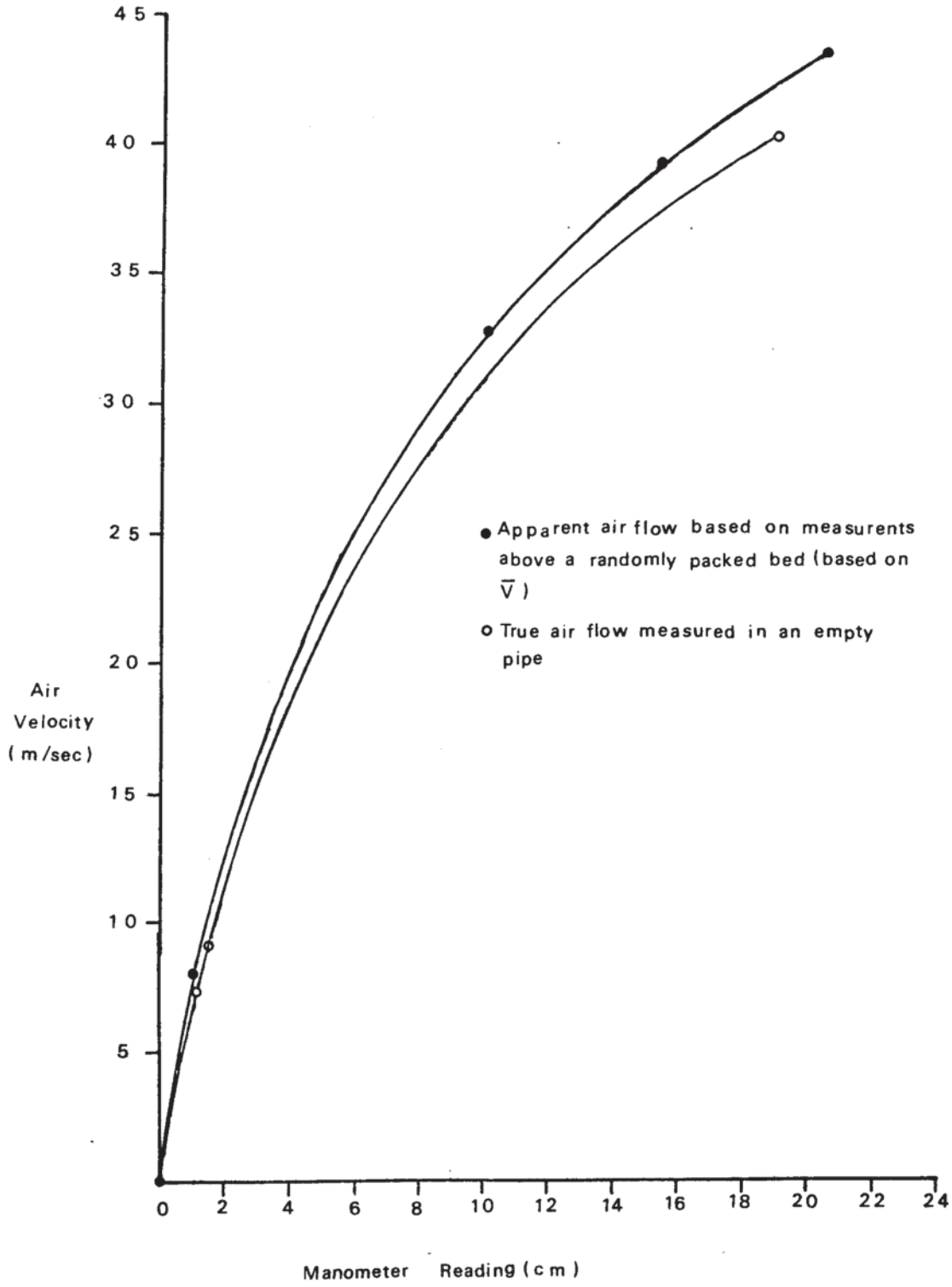

APPENDIX A2

A COMPUTER PROGRAM TO CALCULATE $\bar{V}$ and ϕ,(F), FOR n POINT VELOCITIES

```
      REAL V(n), VAV, SUM1, F
      INTEGER k
      READ*, (V(I),  I = 1,n)
      SUM1 = 0.0                          Evaluating V̄ (VAV) where
      DO 10  I = 1,k                      V̄ = ΣV_i / n
      SUM1 = SUM1 + V(I)
10    CONTINUE
      VAV = SUM1/k
      PRINT*, 'VAV =', VAV
      F = 0.0
      DO 20 I = 1,k                       Evaluating , (F), where
      F = F + (1-(V(I)/VAV)**2            φ = Σ (1 - V/V̄)
20    CONTINUE
      PRINT*, 'F =', F
```

APPENDIX A3

POINT VELOCITY MEASUREMENTS ABOVE GEOMETRICALLY AND DYNAMICALLY SIMILAR BEDS

Tables A3.1 to A3.7:	D = 381 mm
	P.H. = several values
	Re = several values
	Maldistributed feed
Tables A3.8 to A3.13:	D = 610 mm
	P.H. = several values
	Re = several values
	Maldistributed feed
Tables A3.14 to A3.20:	D = 381 mm
	P.H. = several values
	Re = several values
	Ideally distributed feed
Tables A3.21 to A3.26:	D = 610 mm
	P.H. = several values
	Re = several values
	Ideally distributed feed

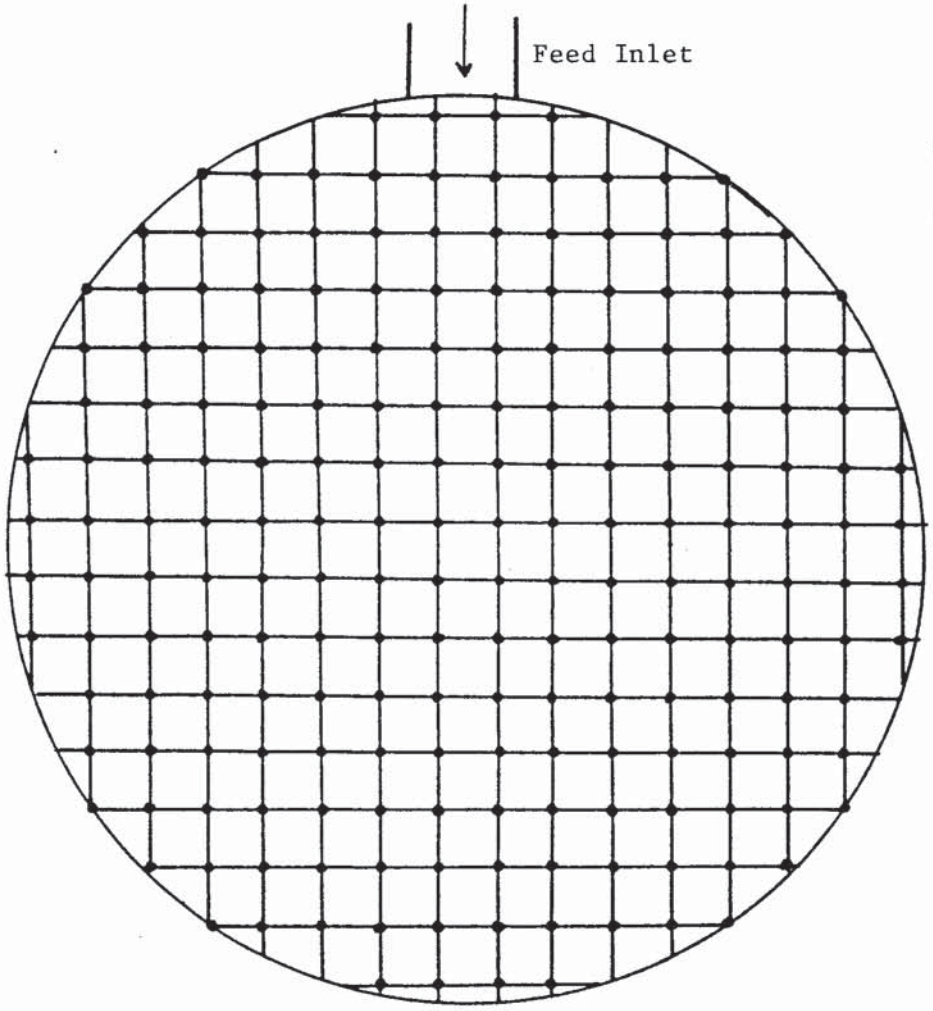

Key Figure A3.1

Positions of the 200 Point Velocity Measurement in Tables (A3.1) to (A3.26)

					10	120	60	90						
		10	25	40	80	105	125	145	95	215	230			
	15	75	40	50	90	110	120	130	145	160	180	135		
15	20	30	30	30	40	90	85	130	165	140	210	140	240	
15	10	10	15	45	65	105	70	165	225	145	260	275	180	
25	10	10	15	50	55	90	95	140	180	250	180	120	245	
20	35	15	30	15	50	50	65	125	90	240	115	145	125	320	240
145	245	15	10	10	15	40	85	140	190	185	135	18	265	25	30
20	25	20	10	15	15	40	100	90	160	250	190	245	345	260	225
10	30	50	25	20	35	80	70	100	105	175	175	380	340	300	165
	50	45	70	35	50	105	170	115	130	115	190	180	270	220	
	25	50	55	90	130	130	135	70	320	260	265	275	220	200	
	30	115	70	130	145	175	200	240	230	110	200	300	280	260	
		50	170	165	170	175	130	260	220	240	110	260	200		
			30	70	110	140	140	255	280	260	250	330			
						170	140	420	250						

Table A3.1 Point Velocity Measurements; Maldistributed, D = 381 mm, P.H. = 63.5 mm, P.S. = 16 mm

$\bar{V}$ = 0.66 m/sec. Re = 18000

$\emptyset$ = 101.4

					35	200	115	160						
			30	100	90	100	135	165	220	125	280	340		
		65	120	145	90	140	170	160	170	210	180	220	180	
	35	100	100	75	80	95	165	135	165	230	205	270	330	330
	45	100	95	80	85	140	160	90	250	280	190	370	330	180
	65	70	100	125	105	120	140	155	185	240	330	180	160	170
10	35	35	30	85	50	115	115	160	125	320	140	170	150	350	275
10	40	30	40	30	90	95	145	190	250	265	200	230	310	220	170
20	40	50	35	25	60	105	140	135	150	280	350	300	340	380	250
180	400	350	430	20	230	125	120	85	90	15	60	75	35	50	40
	280	350	280	250	120	145	135	180	175	75	75	65	65	90	
	255	340	350	155	145	65	65	15	100	140	95	400	350	345	
	345	275	180	350	230	50	130	115	155	190	330	310	426	350	
		95	240	200	270	220	320	400	280	285	150	370	320		
			550	550	450	160	120	60	280	230	450	510			
						270	40	750	560						

Table A3.2 Point Velocity Measurements; Maldistributed D = 381 mm, P.H. = 63.5 mm, P.S. = 16 mm

$\bar{V}$ = 0.94 m/sec. Re = 25,000

$\emptyset$ = 91.5

					55	250	130	180						
		50	140	120	120	370	220	270	420	150	160			
	75	200	250	185	140	160	225	220	255	220	285	215		
420	50	120	220	225	140	160	200	185	250	255	145	420	220	
270	450	420	190	100	200	130	70	150	120	110	300	240	450	
240	390	310	115	90	120	160	150	200	170	180	250	240	225	
330	225	180	25	40	80	100	160	150	200	160	410	180	410	170	350
325	300	20	250	55	315	50	170	330	50	80	125	100	260	170	450
20	70	70	120	160	280	650	550	550	200	295	155	105	55	75	50
55	40	35	170	180	340	450	325	370	500	365	210	100	75	60	25
	80	75	100	170	205	330	480	395	300	185	240	220	80	100	
	25	140	200	115	525	470	370	365	440	470	220	175	95	100	
	50	170	300	260	600	480	550	470	425	240	340	400	130	180	
		95	260	225	400	380	380	530	230	550	210	240	285		
			40	140	320	575	810	650	520	530	320	90			
						100	360	500	350						

Table A3.3 Point Velocity Measurements; Maldistributed, D= 381 mm, P.H. = 63.5 mm, P.S. = 16 mm

$\bar{V}$ = 1.186 m/sec, R = 32000

Ø = 85.4

					115	150	125	150						
		45	85	155	140	95	150	140	200	180	115			
	10	110	95	135	155	105	130	105	160	55	225	215		
35	10	45	115	105	115	100	120	145	135	125	210	145	175	
175	140	130	125	180	210	130	115	165	175	120	125	120	30	
110	100	125	180	140	115	105	140	200	140	195	30	180	110	
55	100	170	115	100	105	115	125	140	120	185	165	175	200	180	75
40	90	100	70	80	135	95	130	90	160	165	155	150	125	100	20
70	50	75	115	115	85	125	100	155	150	145	220	95	105	70	35
40	100	135	110	110	100	120	65	70	95	205	160	150	160	160	75
	90	100	100	120	120	120	110	160	140	160	260	175	150	135	
	170	65	180	70	175	145	160	135	125	120	160	150	205	135	
	40	55	170	130	170	120	180	190	160	155	145	265	125	140	
		150	130	90	105	290	195	160	205	185	290	180	185		
			50	35	85	160	225	200	60	245	180	85			
						130	140	155	155						

Table A3.4 Point Velocity Measurements; Maldistributed, D = 381 mm, P.H. = 127 mm, P.S. = 16 mm

$\bar{V}$ = 0.665 m/sec, Re = 18000

$\emptyset$ = 29.7

					150	235	190	210						
		45	170	270	250	130	205	210	285	245	145			
	30	140	140	225	260	130	155	150	220	75	250	265		
90	65	80	200	165	200	150	180	200	210	145	255	165	205	
35	220	230	195	165	185	160	160	220	220	165	225	280	220	
50	165	160	205	320	200	155	140	180	250	190	250	240	115	
55	145	215	200	155	155	190	170	190	145	260	220	225	245	240	105
95	120	165	115	130	205	155	200	140	205	210	200	200	120	115	40
105	80	50	110	180	150	140	170	110	210	215	175	240	140	110	90
160	70	180	160	155	145	195	90	100	95	275	175	200	210	200	130
	130	160	170	175	160	180	150	210	190	235	340	220	200	170	
	250	105	270	130	250	220	240	175	175	155	225	215	250	170	
	100	50	260	175	245	305	185	265	290	220	205	180	140	175	
		235	225	140	150	400	265	280	280	400	280	305	235		
			30	130	240	360	280	370	255	90	115	30			
						160	215	205	215						

Table A3.5 Point Velocity Measurements; Maldistributed, D = 381 mm, P.H. = 127 mm, P.S. = 16 mm

$\bar{V}$ = 0.93 m/sec Re = 25000

$\emptyset$ = 27.6

					175	135	125	210						
		85	165	175	250	375	245	140	200	190	225			
	330	105	145	190	150	280	280	175	210	260	240	360		
200	80	380	210	170	250	335	160	260	260	255	230	320	200	
95	240	260	170	160	225	160	165	220	295	385	290	250	85	
200	305	100	175	250	175	280	235	155	245	280	260	300	180	
125	235	70	145	330	245	250	305	280	360	265	130	225	100	235	290
230	205	160	105	180	225	280	305	290	165	165	200	265	310	260	180
225	260	260	225	210	265	245	140	340	285	465	320	220	345	345	120
300	280	175	175	85	205	165	245	200	315	210	380	150	250	300	235
	260	285	295	280	375	265	220	260	320	195	330	320	360	300	
	270	220	260	100	210	210	330	240	340	325	290	350	90	320	
	45	140	255	260	275	260	175	305	280	450	415	420	110	95	
		125	115	300	360	355	550	490	260	390	190	70	155		
			135	60	100	145	360	215	270	240	105	125			
						230	55	80	370						

Table A3.6 Point Velocity Measurements; Maldistributed, D = 381 mm, P.H. = 127 mm, P.S. = 16 mm

$\bar{V}$ = 1.19 m/sec Re = 32000

$\emptyset$ = 29.2

					15	20	85	70						
		50	65	80	60	70	55	45	70	75	45			
	10	30	80	80	75	70	65	50	50	60	55	75		
45	30	25	60	75	60	95	70	75	35	40	45	50	60	
45	65	100	60	50	60	90	75	60	60	45	65	50	30	
30	80	85	45	45	45	65	70	75	65	65	70	65	40	
40	65	65	75	70	60	80	90	90	85	105	55	50	75	85	60
70	80	80	95	75	95	130	65	65	120	55	50	85	65	85	100
55	75	65	130	100	90	95	90	120	85	75	85	65	70	80	120
130	90	105	70	95	105	80	80	110	105	90	125	115	80	80	80
	75	105	120	190	175	170	120	75	110	150	115	130	125	60	
	90	125	115	150	160	110	100	170	120	145	120	145	65	100	
	110	155	130	135	130	170	150	160	140	130	145	25	110	115	
		140	170	200	245	245	340	280	110	75	260	135	220		
			160	160	290	205	170	245	340	130	220	190			
						25	25	260	370						

Table A3.8 Point Velocity Measurements; Maldistributed, D = 610 mm, P.H. = 101.6 mm, P.S. = 25.4 mm

$\bar{V}$ = 0.5 m/sec., Re = 18000

$\emptyset$ = 73.2

					20	30	110	100						
		75	85	70	90	85	75	45	130	90	50			
	10	35	80	90	85	70	75	65	55	85	65	100		
45	25	35	70	85	85	105	80	90	45	45	50	70	80	
50	75	110	75	50	75	105	90	70	70	50	65	50	50	
35	85	100	75	50	55	50	65	85	70	75	90	70	55	
70	70	80	80	75	65	100	105	110	105	120	80	50	85	105	75
95	115	100	125	100	110	155	75	75	140	65	55	115	70	105	100
75	75	80	160	95	115	115	100	135	85	95	110	80	75	105	120
130	100	110	85	110	125	90	85	135	115	100	145	140	75	70	105
	95	100	140	220	210	230	125	85	120	175	130	130	140	90	
	80	140	140	180	190	120	100	195	140	180	125	180	70	135	
	125	200	165	170	165	215	175	200	150	165	170	30	140	130	
		180	220	250	315	310	445	350	110	80	300	150	235		
			250	190	380	260	190	300	430	150	270	240			
						45	25	300	460						

Table A3.9 Point Velocity Measurements; Maldistributed, D = 610 mm, P.H. = 101.6 mm, P.S. = 25.4 mm

$\bar{V}$ = 0.60 m/sec., Re = 25000

$\emptyset$ = 81.65

					105	80	40	100						
		100	180	170	115	100	110	140	105	100	105			
	45	110	120	95	65	80	100	80	100	125	135	85		
65	50	35	85	65	80	140	95	65	100	100	80	90	70	
25	55	105	130	110	80	120	105	60	40	75	105	85	55	
110	95	120	125	100	100	100	70	80	60	115	105	84	40	
120	130	115	160	180	130	65	80	90	120	75	110	70	65	70	45
40	25	75	160	85	105	120	130	135	125	110	105	110	85	80	75
25	40	90	145	100	115	170	105	130	140	105	130	140	110	90	220
75	180	150	200	120	85	190	120	70	200	130	130	120	80	115	190
	105	200	190	120	100	180	160	200	210	160	100	110	200	90	
	135	110	95	165	160	300	160	180	280	115	80	130	200	55	
	140	300	350	360	480	300	325	190	325	190	250	300	280	175	
		145	225	125	320	230	245	380	280	260	245	145	40		
			260	490	400	200	265	350	330	320	140	110			
						90	640	190	250						

Table A3.10 Point Velocity Measurements; Maldistributed, D = 610 mm, P.H. = 101.6 mm., P.S. = 25.4 mm

$\bar{V}$ = 0.72 m/sec., Re = 32000

$\emptyset$ = 81.5

				70	100	50	95						
		60	95	65	80	90	85	95	90	40	30		
	100	65	75	80	90	90	35	55	50	85	90	85	
65	75	105	110	100	85	95	95	85	95	85	125	105	75
90	110	100	90	60	120	100	85	65	70	100	100	120	45
75	105	90	55	105	110	90	65	85	120	115	95	120	60
25	30	75	90	100	110	115	90	85	90	90	75	85	70	95	175
45	80	90	115	125	90	70	115	95	55	80	40	75	125	100	35
70	110	85	100	95	90	100	105	130	100	100	75	70	80	90	80
5	45	70	65	95	60	90	70	100	125	80	80	85	105	85	100
	80	115	105	90	90	165	130	85	60	80	115	125	95	115	
	90	120	130	115	110	110	120	100	125	100	85	80	80	100	
	110	85	175	125	115	70	125	145	105	135	130	70	65	30	
		105	210	200	155	75	105	100	190	175	155	95	175		
			80	75	115	120	185	140	185	175	145	135			
						260	220	95	160						

Table A3.11 Point Velocity Measurements ; Maldistributed, D = 610 mm, P.H. = 203 mm, P.S. = 25.4 mm

$\bar{V}$ = 0.49 m/sec., Re = 18000

$\emptyset$ = 27.0

					100	130	80	140						
		65	115	80	100	100	105	120	120	65	45			
	130	90	95	100	115	105	45	65	45	90	110	85		
70	95	120	135	130	105	115	115	100	110	95	125	135	90	
115	125	115	95	80	125	120	100	80	75	115	115	135	55	
85	120	110	60	130	130	100	75	100	140	135	105	140	75	
35	30	90	95	125	125	130	105	95	100	100	95	95	85	110	205
65	90	110	135	165	110	85	135	105	65	90	60	90	145	120	60
85	135	105	120	120	115	130	125	150	120	115	90	80	95	100	110
15	55	80	80	110	75	110	125	75	125	155	85	95	105	130	100
	95	140	135	110	105	210	160	105	70	95	140	160	110	145	
	115	145	165	145	135	135	150	105	155	110	115	95	110	130	
	135	95	230	160	150	80	155	185	130	165	155	95	75	40	
		140	275	275	190	95	125	125	240	220	190	115	225		
			110	110	130	150	240	170	240	220	165	175			
						360	300	115	215					

Table A3.12 Point Velocity Measurements; Maldistributed, D = 610 mm, P.H. = 203 mm., P.S. = 25.4 mm

$\bar{V}$ = 0.6 m/sec., Re = 25000

$\emptyset$ = 31.4

					125	160	90	180						
		85	125	100	125	130	125	155	140	90	60			
	155	110	110	130	125	125	50	75	60	110	115	125		
100	115	160	160	150	130	150	140	120	135	115	135	165	105	
120	155	140	120	95	160	150	125	100	95	130	145	155	60	
105	140	130	70	150	160	125	85	115	165	165	135	155	85	
75	45	110	110	150	150	150	130	110	125	115	105	105	105	140	245
75	115	135	165	195	135	105	165	130	80	110	60	110	185	150	90
115	165	135	150	150	130	140	155	190	145	140	115	105	120	120	135
15	60	80	85	120	80	115	80	120	190	105	110	125	160	120	145
	115	160	155	130	125	240	180	125	75	115	160	190	135	170	
	130	165	190	170	160	160	170	130	180	110	135	110	120	145	
	170	130	280	170	165	190	90	215	140	195	180	110	85	60	
		160	320	325	230	85	135	145	285	265	235	140	265	
			150	130	160	160	295	210	275	260	205	200		
						440	350	125	280					

Table A3.13 Point Velocity Measurements; Maldistributed, D = 610 mm., P.H. = 203 mm, P.S. = 254 mm

$\bar{V}$ = 0.723 m/sec., Re = 32000

$\emptyset$ = 31.08

					65	130	125	130						
		45	50	200	115	140	170	140	90	120	145			
	65	40	110	125	95	55	55	145	165	115	160	130		
195	165	105	100	115	145	105	120	150	160	130	120	75	140	
75	90	125	135	115	130	125	150	115	135	100	155	105	180	
70	130	130	105	65	130	105	90	70	115	115	40	80	155	
100	140	85	145	120	120	155	100	70	135	100	160	85	110	225	105
105	155	100	160	90	140	85	140	140	140	125	135	135	120	130	90
85	160	100	130	185	135	140	150	160	160	45	135	155	140	115	105
80	145	130	70	95	75	200	120	75	175	135	90	55	120	200	145
	160	80	105	140	100	220	105	120	80	70	80	55	50	60	
	100	110	90	100	120	105	140	135	110	90	135	135	75	65	
	30	45	110	130	125	140	115	50	95	110	145	160	90	120	
		150	160	120	130	110	120	135	80	115	135	135	115		
			110	115	130	115	95	210	190	120	165	140			
						30	105	180	115						

Table A3.14 Point Velocity Measurements; Ideally distributed, D = 381 mm, P.H. = 63.5 mm, P.S. = 16 mm

$\bar{V}$ = 0.6 m/sec, Re = 16150

$\emptyset$ = 19.45

					110	195	190	160						
		60	65	330	175	220	270	215	120	185	230			
	75	75	175	200	145	95	80	225	255	170	250	180		
290	250	160	180	195	235	160	200	235	240	200	180	105	255	
145	130	215	200	200	170	160	215	175	210	150	235	160	205	
85	180	195	165	100	195	130	135	105	155	180	65	100	240	
175	200	115	205	175	185	225	135	145	205	150	250	105	180	280	140
190	260	145	260	150	225	145	220	200	205	175	205	195	185	200	110
115	245	150	200	280	205	220	225	280	265	65	235	250	215	175	120
115	200	165	105	145	95	300	205	115	275	220	145	70	160	305	220
	230	120	155	220	140	345	125	165	130	120	70	100	95	80	
	125	150	80	145	180	135	225	180	175	140	200	240	100	120	
	60	60	165	175	175	200	180	115	125	160	240	260	145	140	
		250	240	175	180	175	180	215	120	165	205	210	185		
			230	200	220	160	115	325	290	160	240	220			
						45	170	310	145						

Table A3.15 Point Velocity Measurements; Ideally distributed D = 381 mm, P.H. = 63.5 mm, P.S. =16 mm

$\bar{V}$ = 0.906 m/sec, Re = 24500

Ø = 2 2.48

					220	195	230	185						
		70	180	205	200	210	205	245	205	255	225			
	175	260	235	305	300	50	230	235	285	300	305	240		
175	145	165	200	135	145	140	155	175	240	255	280	220	135	
75	195	150	280	210	185	210	185	280	260	240	225	185	100	
375	190	330	225	220	230	245	255	200	75	265	300	285	200	
160	225	210	160	250	235	245	180	265	305	310	290	255	220	390	230
130	300	220	225	280	180	280	255	385	260	215	250	285	185	70	95
90	125	240	155	245	320	265	225	235	215	280	180	285	300	125	175
160	240	220	245	250	255	325	300	320	215	305	205	140	205	380	220
	165	85	125	205	385	225	195	170	275	185	190	190	185	230	
	190	125	220	275	240	155	290	280	295	225	160	255	240	260	
	245	160	220	205	260	215	175	100	275	215	250	160	205	200	
		95	185	190	265	340	260	360	235	210	205	240	155		
			180	75	185	105	190	315	200	210	230	240			
						80	110	130	115						

Table A.3.16 Point Velocity Measurements; Ideally distributed, D = 381 mm, P.H. = 63.5 mm, P.S. = 16 mm

$\bar{V}$ = 1.10 m/sec, Re = 30700

$\emptyset$ = 18.42

					105	80	100	100						
		100	40	115	120	120	140	130	130	240	185			
	40	80	105	155	110	135	145	115	120	120	125	125		
40	95	125	115	155	130	120	125	110	50	125	105	175	140	
135	10	90	180	165	145	100	100	165	145	95	140	110	100	
105	100	120	125	105	45	120	115	150	135	140	120	85	125	
45	140	145	95	85	25	120	145	130	140	135	115	70	100	115	85
80	25	40	155	120	125	165	140	140	70	120	110	90	155	135	80
40	160	105	105	95	40	140	140	120	120	125	80	110	115	125	75
100	125	100	185	100	115	100	85	140	140	80	125	100	105	110	145
	150	160	80	145	90	75	90	110	115	80	115	115	125	110	
	65	110	70	125	120	120	120	130	110	145	115	180	115	115	
	110	120	140	165	90	95	100	145	135	125	70	145	135	165	
		50	125	115	100	135	110	165	110	135	135	105	30		
			65	80	135	85	125	140	160	130	135	105			
						85	120	195	150						

Table A3.17 Point Velocity Measurements; Ideally distributed, D = 381 mm, P.H. = 127 mm, P.S. = 16 mm

$\bar{V}$ = 0.6 m/sec, Re = 16150

$\emptyset$ = 21.84

					140	195	145	180						
		150	80	165	180	170	240	215	200	390	320			
	100	100	175	230	190	205	230	130	185	215	215	180		
50	130	170	185	240	175	180	195	190	75	225	150	260	210	
15	115	215	280	260	210	120	145	260	220	115	210	150	130	
135	165	165	200	155	100	150	175	225	210	220	175	105	160	
135	210	215	145	145	45	170	260	185	200	230	195	90	155	170	115
40	135	55	245	200	180	260	215	230	120	170	140	130	210	185	90
75	245	145	165	145	65	210	210	205	195	190	145	185	190	165	120
145	220	140	145	150	165	140	120	195	220	100	200	180	165	165	230
	225	245	130	225	145	110	115	175	180	155	180	200	180	170	
	80	150	110	180	175	175	210	190	160	240	195	280	210	200	
	130	200	240	260	145	140	160	220	200	180	130	230	215	250	
		55	180	170	130	185	160	240	165	200	240	160	105		
			130	115	195	150	180	215	285	225	200	140			
						130	160	320	255						

Table A3.18 Point Velocity Measurements; Ideally distributed, D = 381 mm, P.H. = 127 mm, P.S. = 16 mm

$\bar{V}$ = 0.905 m/sec., Re = 24500

$\emptyset$ = 20.2

					165	170	245	195					
		165	100	200	215	200	295	255	240	500	420		
	120	135	220	285	250	240	280	185	215	230	255	220	
75	155	205	230	290	240	240	215	240	90	305	180	340	250
120	135	260	230	300	260	175	180	320	260	270	280	185	175
120	205	210	225	180	125	185	205	280	250	265	205	105	195
175	260	245	160	170	50	200	305	240	235	230	205	95	170	205	140
45	145	65	310	225	220	320	260	280	125	190	160	140	245	240	100
85	295	155	205	180	80	255	250	240	255	220	160	225	205	230	140
200	260	155	160	180	195	160	175	245	250	140	230	220	190	225	270
	250	285	145	265	175	155	130	215	255	220	225	250	230	200	
	110	180	110	200	215	200	265	240	180	300	250	320	240	225	
	160	190	280	305	175	175	180	220	245	205	160	275	265	305	
		75	240	206	160	225	210	285	200	250	290	220	125		
			150	120	210	150	205	245	350	270	240	180			
						160	205	420	300						

Table A3.19 Point Velocity Measurements (Ft/min) Ideally distributed, D = 381 mm, P.H. = 127 mm, P.S. = 16 mm

$\bar{V}$ = 1.1 m/sec, Re = 30650

$\emptyset$ = 22.45

					85	100	70	75						
		50	70	120	100	30	45	80	55	110	115			
	15	50	120	135	130	130	120	100	75	85	125	145		
45	70	95	100	65	105	90	80	95	55	90	130	110	105	
95	120	100	125	90	95	70	80	90	90	120	120	100	70	
120	100	125	85	110	80	55	50	130	125	115	105	110	100	
100	80	90	100	65	110	80	100	95	95	85	120	100	65	95	105
100	40	45	60	105	70	85	120	85	70	100	20	60	70	100	140
40	90	90	85	55	60	85	145	100	70	100	65	90	90	75	135
20	80	100	110	110	90	115	105	105	70	90	65	95	70	100	85
	60	120	70	115	90	95	105	70	15	90	90	120	60	140	
	125	75	120	110	115	105	60	90	65	50	120	120	110	115	
	115	120	80	85	110	100	120	120	95	80	155	115	110	90	
		95	40	60	70	85	80	130	85	155	115	155	85		
			55	35	95	135	110	65	35	75	180	160			
						130	45	75	30						

Table A3.20 Point Velocity Measurements (ft/min); Ideally distributed; D = 610 mm, P.H. = 101.6 mm, P.S. = 25.4 mm

$\bar{V}$ = 0.466 m/sec, Re = 20000

$\emptyset$ = 20.28

					90	130	105	105						
		70	85	145	125	40	55	120	90	155	160			
	25	75	150	175	170	170	150	130	100	110	200	150		
40	100	125	130	90	135	120	140	115	95	120	175	160	170	
100	135	125	165	110	110	90	100	120	115	160	150	125	145	
160	140	165	115	150	115	75	70	165	170	135	130	135	140	
125	140	125	135	100	140	110	125	125	130	90	140	135	100	80	150
125	60	60	85	140	100	110	160	110	110	140	35	85	80	115	220
90	105	130	75	65	80	120	170	130	90	130	70	95	110	55	180
40	120	150	140	140	105	150	145	140	85	100	85	110	100	120	65
	95	160	110	135	90	120	130	70	35	120	110	155	100	150	
	175	125	170	165	140	135	50	125	70	60	160	135	105	135	
	145	180	120	120	145	140	165	160	135	95	210	140	120	120	
		140	90	100	90	75	90	155	105	180	125	180	130		
			75	70	120	150	90	45	85	210	125	150			
						135	25	80	30						

Table A3.21 Point Velocity Measurements (ft/min); Ideally distributed, D = 610 mm, P.H. = 101.6 mm, P.S. = 25.4 mm

$\bar{V}$ = 0.604 m/sec, Re = 26000

$\emptyset$ = 19.72

					105	135	100	115						
		85	160	160	135	50	70	130	90	160	180			
	35	165	195	190	205	160	150	115	120	200	225	75		
75	140	140	85	145	125	150	130	95	135	200	175	180	115	
115	155	140	180	125	130	100	115	130	115	170	160	140	150	
175	150	175	120	150	105	75	70	180	180	145	145	150	145	
150	130	120	135	105	145	105	140	130	140	100	120	150	110	80	170
140	65	70	80	140	110	120	175	125	110	140	135	110	90	115	235
90	110	140	100	70	80	120	180	135	100	140	80	100	110	70	185
45	125	165	155	155	125	160	155	155	95	120	80	130	105	130	85
	80	175	120	155	85	130	150	75	25	110	120	155	85	165	
	190	120	180	170	155	140	40	120	60	70	150	140	130	215	
	185	180	145	125	160	140	170	180	140	105	100	230	140	150	
		145	65	105	95	120	105	170	135	220	155	210	180		
			95	70	160	210	140	130	40	100	270	210			
						190	40	90	30						

Table A3.22 Point Velocity Measurements (ft/min); Ideally distributed, D = 610 mm, P.H. = 101.6 mm, P.S. = 25.4 mm

$\bar{V}$ = 0.66 m/sec Re = 29000

$\emptyset$ = 22.13

					90	75	70	95						
		95	110	25	70	75	80	95	110	125	220			
	85	75	115	120	100	100	95	65	115	135	160	175		
75	80	95	70	95	120	90	70	65	45	75	50	120	70	
100	95	50	75	60	80	65	130	100	100	120	85	140	95	
75	65	70	75	90	100	90	100	70	80	125	95	150	105	
45	115	75	80	105	90	115	50	65	140	135	115	65	75	95	110
140	125	100	75	95	90	100	55	70	100	140	75	130	75	100	140
40	105	85	115	95	100	75	85	140	80	115	75	65	110	135	135
90	115	125	95	65	70	55	80	85	30	120	85	55	75	55	50
	70	85	80	50	140	95	70	80	70	100	110	135	140	105	
	110	90	80	95	90	95	90	120	130	80	120	115	95	50	
	100	115	90	90	115	65	100	70	90	110	30	60	110	85	
		35	55	100	145	150	165	110	90	115	15	30	100		
			65	45	120	115	80	115	65	105	170	100			
						30	70	25	55						

Table A.23 Point Velocity Measurements (ft/min); ideally distributed, D = 610 mm, P.H. = 203 mm, P.S. = 25.9 mm

$\bar{V}$ = 0.466 mm/sec, Re = 20000

$\emptyset$ = 19.95

					115	90	85	110					
		120	130	55	100	100	115	120	160	160	280		
	115	100	165	155	125	125	115	85	160	175	210	240	
110	105	110	95	115	155	115	70	95	70	90	60	145	100
125	120	60	85	60	100	90	165	120	130	145	100	160	115
95	80	90	85	115	125	100	120	85	95	150	120	180	110
50	140	100	100	135	105	130	50	70	180	175	145	90	100	120	150
185	150	115	90	115	110	125	70	85	125	170	100	160	70	125	185
55	140	100	144	120	120	95	100	170	105	145	85	70	130	155	170
120	140	155	115	90	85	70	100	95	35	155	115	70	100	55	65
	90	110	95	55	170	125	80	95	100	120	125	160	180	125	
	140	100	100	120	120	105	105	140	150	95	155	135	125	180	
	115	140	110	110	135	80	110	85	115	145	70	75	140	115	
		60	70	135	180	195	200	135	120	140	35	40	130		
			100	55	140	150	110	155	70	135	200	180			
						30	95	35	75						

Table A3.24: Point Velocity Measurements (ft/min); Ideally distributed, D = 610 mm, P.H. = 203 mm, P.S. = 25.4 mm

$\bar{V}$ = 0.6 m/sec, Re = 26,000, ϕ = 20.13

					130	105	100	135						
		140	145	60	110	110	125	135	190	160	340			
	125	105	180	170	140	145	130	80	180	195	240	290		
120	115	120	105	120	170	130	85	100	75	100	85	170	110	
160	140	75	110	70	110	95	190	135	145	170	120	185	120	
115	90	100	100	130	140	120	140	105	110	180	140	215	150	
65	165	115	115	145	120	160	45	90	200	200	180	100	115	140	160
205	165	140	100	130	130	140	80	95	140	205	110	200	75	160	220
80	160	115	165	140	145	115	115	195	130	165	105	75	155	180	175
140	180	175	130	105	95	85	115	110	45	180	120	75	115	75	80
	100	125	105	60	205	145	85	110	100	145	145	185	235	150	
	160	125	115	140	135	125	130	160	180	110	170	160	140	100	
	130	150	120	150	160	105	120	110	140	170	100	90	170	145	
		80	70	160	230	235	240	160	135	165	45	55	150		
			115	60	175	165	135	180	95	160	240	240			
						45	110	30	95						

Table A3.25. Point Velocity Measurements (ft/min); Ideally distributed, D = 610 mm, P.H. = 203 mm, P.S. = 25.4 mm
$\bar{V}$ = 0.66 m/sec, Re = 29,000, ϕ = 21.3.

APPENDIX A4

MULTI-FACTOR ANALYSIS OF THE VARIANCE

(Adopted from "Probability and Statistics for Engineers", by IRWIN MILLER and JOHN E. FREUND)

A4.1 Two-Factor Analysis of the Variance

If (a) point velocity measurements, "levels" are taken along x-axis, "factor X", and (b) point velocity measurements are taken along y-axis, "factor Y", then the xy plane consists of (ab) points, each point is specified by its xy-co-ordinates and has its specific gas velocity (point velocity).

The co-ordinates of these (ab) points will be as follows:

X: 1,1,.....,1,2,2,.....,2,3,3,.....3,.....a

Y: 1,2,.....b,1,2,.....b,1,2,.....b,.....b

And if several repackings, "replicates" were made, each consists of (ab) point velocity measurements, then it would be possible to analyse the data as a two-factor classification and test for significant differences among the (ab) point velocity means.

It is useful to make these remarks:

a = The number of point measurements, "levels", made along x-axis.

b = The number of point measurements, "levels", made along y-axis.

r = The number of bed repackings, "replicates".

ab = The number of point velocity measurements, "observations", made at each repacking.

rab = Total number of point velocity measurements, "observations" made at each experiment.

Note that the (ab) observations were chosen in such a way

that each level of x-axis is used once in conjunction with each level of y-axis.

In order to obtain an estimate of the experimental error in the experiment it is necessary to replicate, that is, to repeat the entire set of (ab) velocity measurements after repacking the bed, say, r times.

If (Y_{ijk}) is the gas velocity in the(Kth) replicate, taken at (ith) level of x-axis and (jth) level of y-axis, the model assumbed for the analysis of this kind of experiment is usually written as:

$$Y_{ijk} = \mu + \alpha + \beta_j + (\alpha\beta)_{ij} + \rho_k + \epsilon_{ijk} \quad \ldots\ldots \text{(A4.1)}$$

For $i = 1,2,3,\ldots,a$, $j = 1,2,3,\ldots\ldots,b$, $k = 1,2,3,\ldots\ldots,r$

μ = The grand mean "average velocity of all repackings".

α_i = The effect of the (ith) point velocity along the x-axis on the distribution of the gas.

β_j = The effect of the (jth) point velocity along the y-axis on the distribution of the gas

$(\alpha\beta)_{ij}$ = The interaction, or the joint effect, of (ith) level of x-axis and (jth) level of y-axis on the gas distribution.

ρ_k = The effect of the (kth) replicate on the gas distribution

ϵ_{ijk} = The values of independent random variables having normal distribution with zero means and the common variance σ^2.

A4.1.1 Mathematical Formulation

The following symbols are defined as:

$T_{ij.}$ = Sum of observations in the (ij)th position, "cell".

$T_{i..}$ = Sum of observations for the (ith) level of factor X.

$T_{.j.}$ = Sum of observations for the (jth) level of factor Y.

$T_{...}$ = Sum of all (a.b.r) observations.

$\bar{Y}_{ij.}$ = Mean of observations in the (ij)th cell.

$\bar{Y}_{i..}$ = Mean of observations for the (ith) level of factor X.

$\bar{Y}_{.j.}$ = Mean of observations for the (jth) level of factor Y.

$\bar{Y}_{...}$ = Mean of all observations (a.b.r).

The (abr) observations are arranged in Table A4.1.

The hypotheses to be tested are as follows:

(1) For a uniformly distributed gas emerging from the top of a packed bed:

$$H_o' : \alpha_1 = \alpha_2 = \alpha_3 = \ldots\ldots\ldots = \alpha_a = 0 \qquad \ldots\ldots \text{(A4.2a)}$$

$$H_o'' : \beta_1 = \beta_2 = \beta_3 = \ldots\ldots\ldots = \beta_b = 0 \qquad \ldots\ldots \text{(A4.2b)}$$

$$H_o''' : (\alpha\beta)_{11} = (\alpha\beta)_{12} = \ldots\ldots = (\alpha\beta)_{21} = (\alpha\beta)_{22} = \ldots\ldots = (\alpha\beta)_{ab} = 0 \qquad \ldots\ldots \text{(A4.2c)}$$

$$H_o'''' : \rho_1 = \rho_2 = \rho_3 = \ldots\ldots\ldots = \rho_r = 0 \qquad \ldots\ldots \text{(A4.2d)}$$

(2) For non-uniformly distributed gas emerging from the top of a packed bed:

At least one of the α_i's or β_j's or $(\alpha\beta)_{ij}$'s or ρ_k's is not equal to zero.

Each of these tests will be based on a comparison of independent estimates of the variance, σ^2, provided by splitting of the total sum of squares of the experimental data into five components by means of the following identity:

x \ y	1	2	3	.....	b	Total	Mean
1	Y_{111}	Y_{121}	Y_{131}	.....	Y_{1b1}	$T_{1..}$	$\bar{Y}_{1..}$
	Y_{112}	Y_{122}	Y_{132}	.....	Y_{1b2}		
	Y_{113}	Y_{123}	Y_{133}	.....	Y_{1b3}		
	.	.	.		.		
	.	.	.		.		
	.	.	.		.		
	.	.	.		.		
	Y_{11r}	Y_{12r}	Y_{13r}	.....	Y_{1br}		
2	Y_{211}	Y_{221}	Y_{231}	.....	Y_{2b1}	$T_{2..}$	$\bar{Y}_{2..}$
	Y_{212}	Y_{222}	Y_{232}	.....	Y_{2b2}		
	Y_{213}	Y_{223}	Y_{233}	.....	Y_{2b3}		
	.	.	.		.		
	.	.	.		.		
	.	.	.		.		
	.	.	.		.		
	Y_{21r}	Y_{22r}	Y_{23r}	.....	Y_{2br}		
.							
.							
.							
.							
a	Y_{a11}	Y_{a21}	Y_{a31}	.....	Y_{ab1}	$T_{a..}$	$\bar{Y}_{a..}$
	Y_{a12}	Y_{a22}	Y_{a32}	.....	Y_{ab2}		
	.	.	.		.		
	.	.	.		.		
	.	.	.		.		
	.	.	.		.		
	Y_{a1r}	Y_{a2r}	Y_{a3r}	.....	Y_{abr}		
Total	$T_{.1.}$	$T_{.2.}$	$T_{.3.}$	.....	$T_{.b.}$	$T_{...}$	
Mean	$\bar{Y}_{.1.}$	$\bar{Y}_{.2.}$	$\bar{Y}_{.3.}$	.....	$\bar{Y}_{.b.}$		$\bar{Y}_{...}$

$$\sum_{i=1}^{a}\sum_{j=1}^{b}\sum_{k=1}^{r}(Y_{ijk} - \bar{Y}_{...})^2 = rb\sum_{i=1}^{a}(\bar{Y}_{i..} - \bar{Y}_{...})^2$$

$$+ ra\sum_{j=1}^{b}(\bar{Y}_{.j.} - \bar{Y}_{...})^2$$

$$+ r\sum_{i=1}^{a}\sum_{j=1}^{b}(\bar{Y}_{ij.} - \bar{Y}_{i..} - \bar{Y}_{.j.} + \bar{Y}_{...})^2$$

$$+ ab\sum_{k=1}^{r}(\bar{Y}_{..k} - \bar{Y}_{...})^2$$

$$+ \sum_{i=1}^{a}\sum_{j=1}^{b}\sum_{k=1}^{r}(Y_{ijk} - \bar{Y}_{ij.} - \bar{Y}_{..k} + \bar{Y}_{...})^2$$

..... (A4.3)

The left hand term is referred to as "Total Sum of Squares", (SST), and the right hand terms are referred to as

Factor X Sum of Squares, SSX.

Factor Y Sum of Squares, SSY.

Interaction Sum of Squares, SS(XY).

Replicate Sum of Squares, SSR.

Error Sum of Squares, SSE.

Then equation A4.3 becomes

$$SST = SSX + SSY + SS(XY) + SSR + SSE \quad \text{..... (A4.4)}$$

where:

SST has (abr-1) degrees of freedom.

SSX has (a-1) degrees of freedom.

SSY has (b-1) degrees of freedom.

SS(XY) has (a-1)(b-1) degrees of freedom.

SSR has (r-1) degrees of freedom.

SSE has (ab-1)(r-1) degrees of freedom.

Dividing each of the sum of squares on the right hand side of eqn. A4.4 by their corresponding number of degrees of freedom results in five independent estimates of "Mean Squares" defined as

$$S_1 = \frac{SSX}{(a-1)} \qquad \ldots\ldots \text{(A4.5a)}$$

$$S_2 = \frac{SSY}{(b-1)} \qquad \ldots\ldots \text{(A4.5b)}$$

$$S_3 = \frac{SS(XY)}{(a-1)(b-1)} \qquad \ldots\ldots \text{(A4.5c)}$$

$$S_4 = \frac{SSR}{(r-1)} \qquad \ldots\ldots \text{(A4.5d)}$$

$$S = \frac{SSE}{(ab-1)(r-1)} \qquad \ldots\ldots \text{(A4.5e)}$$

Then five independent estimates of the variance, σ^2, can be obtained.

If the sums of squares are interpreted as "functions" of the independent random variable $y_{111}, y_{112}, \ldots\ldots, y_{abr}$ it can be verified that

$$E(S_1^2) = E\left[\frac{SSX}{(a-1)}\right] = \sigma^2 + \frac{rb\sum_{i=1}^{a}\alpha_i^2}{(a-1)} \qquad \ldots\ldots \text{(A4.6a)}$$

$$E(S_2^2) = E\left[\frac{SSY}{(b-1)}\right] = \sigma^2 + \frac{ra\sum_{j=1}^{b}\beta_j^2}{b-1} \qquad \ldots\ldots \text{(A4.6b)}$$

$$E(S_3^2) = E\left[\frac{SS(XY)}{(a-1)(b-1)}\right] = \sigma^2 + \frac{\sum_{i=1}^{a}\sum_{j=1}^{b}(\alpha\beta)_{ij}^2}{(a-1)(b-1)} \qquad \ldots\ldots \text{(A4.6c)}$$

$$E(S_4^2) = E\left[\frac{SSR}{(r-1)}\right] = \sigma^2 + \frac{ab\sum_{k=1}^{r}\rho_k^2}{(r-1)} \qquad \text{..... (A4.6d)}$$

$$E(S^2) = E\left[\frac{SSE}{(ab-1)(r-1)}\right] = \sigma^2 \qquad \text{..... (A4.6e)}$$

To test the hypothesis H_o', that is the effects of factor X are all equal to zero, the following ratio is computed:

$$f_1 = \frac{S_1^2}{S^2} \qquad \text{..... (A4.7a)}$$

which is the value of the random variable F_1 having the F-distribution with (a-1) and (ab-1)(r-1) degrees of freedom when H_o' is true. The above hypothesis, "null hypothesis", is rejected at the level of confidence (α) when;

$$f_1 > f_\alpha \quad [(a-1),(ab-1)(r-1)]$$

To test the hypothesis H_o'', that the effects of factor Y are all equal to zero, the ratio f_2 is computed as follows

$$f_2 = \frac{S_2^2}{S^2} \qquad \text{..... (A4.7b)}$$

which is the value of the random variable F_2 having the F-distribution with (b-1) and (ab-1)(r-1) degrees of freedom when H_o'' is true. This hypothesis is rejected at the (α) level of confidence when

$$f_2 > f_\alpha\ [(b-1),\ (ab-1)(r-1)]$$

Similarly, to test H_o''' and H_o''''.

The computations in an analysis of variance problem, for a two-factor experiment with (r) replications, "repackings", are usually summarized in Table A4.2.

The sums of squares are sually obtained by constructing a table of totals, as shown in Table A4.3, and using the following computational formulas:

$$SST = \sum_{i=1}^{b} \sum_{j=1}^{a} \sum_{k=1}^{r} Y_{ijk}^2 - \frac{T_{...}^2}{abr} \qquad \ldots\ldots \text{(A4.8a)}$$

$$SSX = \frac{\sum_{i=1}^{a} T_{1..}^2}{br} - \frac{T_{...}^2}{abr} \qquad \ldots\ldots \text{(A4.8b)}$$

$$SSY = \frac{\sum_{i=1}^{b} T_{.j.}^2}{ar} - \frac{T_{...}^2}{abr} \qquad \ldots\ldots \text{(A4.8c)}$$

$$SS(XY) = \frac{\sum_{i=1}^{a} \sum_{j=1}^{b} T_{ij.}^2}{r} - \frac{\sum_{i=1}^{a} T_{i..}^2}{br} - \frac{\sum_{j=1}^{b} T_{.j.}^2}{ar} + \frac{T_{...}^2}{abr}$$

$\ldots\ldots$ (A4.8d)

$$SSR = \frac{\sum_{k=1}^{r} T_{..k}^2}{ab} - \frac{T_{...}^2}{abr} \qquad \ldots\ldots \text{(A4.8e)}$$

$$SSE = SST - SSX - SSY - SS(XY) - SSR \qquad \ldots\ldots \text{(A4.8f)}$$

Table A4.2 Analysis of Variance for the Two-Factor Experiment with (r) Replications

Source of Variance	Sum of Squares	Degrees of Freedom	Mean Squares	Computed f
Replication	SSR	(r-1)	$S_4^2 = \frac{SSR}{r-1}$	$f_4 = \frac{S_4^2}{S^2}$
Main effects: x	SSx	(a-1)	$S_1^2 = \frac{SSx}{a-1}$	$f_1 = \frac{S_1^2}{S^2}$
y	SSy	(b-1)	$S_2^2 = \frac{SSy}{b-1}$	$f_2 = \frac{S_2^2}{S^2}$
Interaction xy	SS(xy)	(a-1)(b-1)	$S_3^2 = \frac{SS(xy)}{(a-1)(b-1)}$	$f_3 = \frac{S_3^2}{S^2}$
Error	SSE	(ab-1)(r-1)	$S^2 = \frac{SSE}{(ab-1)(r-1)}$	
	SST	abr-1		

Table A4.3 Sum of Squares for the Two-Factor Experiment with (r) Replications

x \ y	1	2	3	.....	6	
1	$T_{11\cdot}$	$T_{12\cdot}$	$T_{13\cdot}$	.....	$T_{1b\cdot}$	$T_{1\cdot\cdot}$
2	$T_{21\cdot}$	$T_{22\cdot}$	$T_{23\cdot}$	.....	$T_{2b\cdot}$	$T_{2\cdot\cdot}$
3	$T_{31\cdot}$	$T_{32\cdot}$	$T_{33\cdot}$	.....	$T_{3b\cdot}$	$T_{3\cdot\cdot}$
.	.	.	.			.
.	.	.	.			.
.	.	.	.			.
.	.	.	.			.
a	$T_{a1\cdot}$	$T_{a2\cdot}$	$T_{a3\cdot}$		$T_{ab\cdot}$	$T_{a\cdot\cdot}$
	$T_{\cdot 1\cdot}$	$T_{\cdot 2\cdot}$	$T_{\cdot 3\cdot}$		$T_{\cdot b\cdot}$	$T_{\cdot\cdot\cdot}$

A4.1.2 Application of the Two-factor Analysis of the Variance

Example (1): A 305 mm diameter bed packed with 25.4 mm pall rings to a height of 51 mm, with maldistributed feed flowing at a rate of 0.1 m^3/s. The bed was repacked three times and the following point velocities were recorded at positions $x_i y_j$, where i=1,2,.....,12 and j=1,2,.....,12

Note: The point velocities were recorded in (ft/min) for more convenience.

A computer statistical package, (UA10), is used to perform the solution.

Location		Replication Number			Total
x	y	1	2	3	
1	1	50	45	40	135
1	2	45	45	55	145
1	3	45	55	60	160
1	4	45	50	70	165
1	5	45	50	50	145
1	6	100	95	75	270
1	7	140	150	200	490
1	8	110	90	200	400
1	9	150	60	100	310
1	10	90	70	75	235
1	11	40	65	60	165
1	12	35	40	40	115
2	1	125	70	60	255
2	2	65	50	65	180
2	3	50	45	60	155
2	4	50	40	55	145
2	5	65	75	45	185
2	6	70	100	60	230
2	7	90	120	230	440
2	8	120	100	230	450
2	9	140	55	150	345
2	10	140	50	70	260
2	11	50	45	50	145
2	12	50	45	55	150
3	1	90	85	60	235
3	2	70	50	55	175
3	3	55	45	60	160
3	4	55	60	50	165
3	5	70	100	50	220
3	6	100	120	65	285
3	7	140	110	120	370
3	8	120	120	200	440
3	9	110	55	140	305

Location		Replication Number			Total
x	y	1	2	3	
3	10	80	35	75	190
3	11	60	40	70	170
3	12	45	50	70	165
4	1	120	125	120	365
4	2	75	55	75	205
4	3	50	50	100	200
4	4	50	70	75	195
4	5	70	135	85	290
4	6	100	110	90	300
4	7	150	100	125	375
4	8	120	100	140	360
4	9	90	75	190	355
4	10	75	75	140	290
4	11	65	60	100	225
4	12	85	70	140	295
5	1	140	220	170	530
5	2	120	75	120	315
5	3	65	70	130	265
5	4	40	75	115	230
5	5	70	175	160	405
5	6	85	160	160	405
5	7	130	90	160	380
5	8	160	75	220	455
5	9	110	140	200	450
5	10	55	120	160	335
5	11	65	100	160	325
5	12	150	85	160	395
6	1	125	270	160	555
6	2	130	230	150	510
6	3	75	100	75	250
6	4	50	50	200	300
6	5	60	140	240	440
6	6	105	190	220	515

Location		Replication Number			Total
x	y	1	2	3	
6	7	200	140	120	460
6	8	245	110	220	575
6	9	180	110	200	490
6	10	70	140	160	370
6	11	70	120	290	480
6	12	120	90	230	440
7	1	220	300	270	790
7	2	280	350	170	800
7	3	250	245	80	575
7	4	190	85	220	495
7	5	160	100	170	430
7	6	175	310	220	705
7	7	240	320	200	760
7	8	300	250	220	770
7	9	250	160	170	580
7	10	170	190	180	546
7	11	150	220	420	790
7	12	240	135	500	875
8	1	230	260	350	840
8	2	280	680	170	1130
8	3	450	480	50	980
8	4	500	300	140	940
8	5	350	270	200	820
8	6	280	350	150	780
8	7	420	400	150	970
8	8	450	240	165	855
8	9	420	200	350	970
8	10	400	250	320	970
8	11	320	420	430	1170
8	12	350	500	450	1300
9	1	60	345	480	885
9	2	110	480	80	670
9	3	420	250	80	750
9	4	500	200	130	830
9	5	520	210	350	1080
9	6	490	350	220	1060
9	7	710	180	230	1120
9	8	625	100	320	1045
9	9	420	240	340	1000
9	10	270	370	380	1020
9	11	450	450	300	1200
9	12	530	550	330	1410
10	1	130	245	500	875
10	2	210	500	220	930
10	3	630	200	400	1230
10	4	550	175	290	1015
10	5	400	200	335	935
10	6	580	250	250	1080
10	7	550	380	500	1430
10	8	800	180	620	1600
10	9	566	585	350	1495
10	10	370	450	450	1270
10	11	670	580	360	1610
10	12	850	760	330	1940
11	1	375	550	265	1190
11	2	200	320	260	780
11	3	450	150	570	1170
11	4	200	620	190	1010
11	5	295	400	130	825
11	6	800	500	720	2020
11	7	610	500	780	1890
11	8	165	700	700	1565
11	9	110	600	500	1210
11	10	130	400	600	1130
11	11	520	550	630	1700
11	12	630	850	870	2350

Location		Replication number			Total
x	y	1	2	3	
12	1	80	100	50	230
12	2	320	300	400	1020
12	3	560	400	650	1610
12	4	620	600	285	1505
12	5	760	270	310	1340
12	6	1510	1300	600	3410

Location		Replication number			Total
x	y	1	2	3	
12	7	1050	600	1050	2700
12	8	230	600	870	1700
12	9	90	550	260	900
12	10	170	400	260	830
12	11	600	450	230	1280
12	12	490	420	300	1210

$\therefore \sum_{i=1}^{12} \sum_{j=1}^{12} \sum_{k=1}^{3} Y_{ijk}^2 = 44489175$ (sum of squares of all observations)

$\sum_{i=1}^{12} \sum_{j=1}^{12} T_{ij\cdot}^2 = 119290875$ (sum of squares of the totals)

$T_{\cdot\cdot\cdot}^2 = (103775)^2 = 1.076925 \times 10^{10}$ (square of the sum of the totals)

$\sum_{k=1}^{r} T_{\cdot\cdot k}^2 = (36020)^2 + (33955)^2 + (33800)^2$ (sum of the squares of sums of observations at each replication)

The following table of totals is formed:

x \ y	1	2	3	4	5	6	7	8	9	10	11	12	TOTAL
1	135	145	160	165	145	270	490	400	310	235	165	115	2735
2	255	180	155	145	185	230	440	450	345	260	145	150	2940
3	235	175	160	165	220	285	370	440	305	190	170	165	2880
4	365	205	200	195	290	300	375	360	355	290	225	295	3455
5	530	315	265	230	405	405	380	455	450	335	325	395	4490
6	555	510	250	300	440	515	460	575	490	370	480	440	5385
7	790	800	575	495	430	705	760	770	580	540	790	875	8110
8	840	1130	980	940	820	780	970	855	970	970	1170	1300	11725
9	885	670	750	830	1080	1060	1120	1045	1000	1020	1200	1410	12070
10	875	930	1230	1015	935	1080	1430	1600	1495	1270	1610	1940	15410
11	1190	780	1170	1010	825	2020	1890	1565	1210	1130	1700	2350	16840
12	230	1020	1610	1505	1340	3410	2700	1700	900	830	1280	1210	17735
TOTAL	6885	6860	7505	6995	7115	11060	11385	10215	8410	7440	9260	10645	103775

$\therefore \sum_{i=1}^{12} T_{i..}^2$ = 1270030125 sum of squares of all observations in

(ith) level of factor X

$\sum_{j=1}^{12} T_{.j.}^2$ = 931774475 sum of squares of all observations in the

(jth) level of factor Y

Applying equations (8) to (13) where a = 12, b = 12, r = 3.

SST = 19560354	"Total sum of squares".
SS X = 10349794	"factor-X sum of squares".
SS Y = 953803	"factor-Y sum of squares".
SS(XY) = 3531207	"Interaction sum of squares".
SSR = 21335	"Relication sum of squares"
SSE = 4704215	"Error sum of squares"

The computed f-values are as follows:

Source of Variation	Degrees of freedom	sum of squares	Mean Squares	Computed f
Replication	3 - 1 = 2	21335	10667.5	0.6485
X	12 - 1 = 11	10349754	940890	57.203
Y	12 - 1 = 11	953803	86709	5.272
Interaction	(12-1)(12-1)=121	3531207	29183.5	1.7743
Error	286	4704215	16448.3	
Total	431			

Comparing the computed f values with the tabulated values of (F) at significance level of $\alpha = 0.05$ found in Table A4.4 under the appropriate degrees of freedom. The following results have been achieved

(1) For replication: $F_{0.05}\ (2,286) = 3$ (from Table 3A1 at $\nu_1 = 2$ degrees of freedom and $\nu_2 = 286$ degrees of freedom).

Compare the computed value of $f_1 = 0.6485$

$\therefore F_{0.05}\ (2,286) = 3 > 0.6485$

$\therefore$ Accept the hypothesis that replication or repacking has no significant effect on the whole picture of the gas distribution.

(2) For the effect of factor-X: $F_{0.05}\ (11,286) = 1.79$ (from Table 3A1) $1.79 < 57.203$

$\therefore$ reject the hypothesis that factor-X has no effect.

i.e. the gas is severly maldistributed along x-direction, which is the direction of the feed entering the column below the bed.

(3) Factor-Y effect: $F_{0.05}\ (11,286) = 1.79 < 5.272$

$\therefore$ Gas distribution is distributed for less extent along y-direction.

(4) Interaction effect: $F_{0.05}\ (121,286) = 1.22 < 1.7743$

$\therefore$ The combined effect of factor X and factor Y on the distribution is effective.

This means that the gas is severely maldistributed in the x-direction i.e. in the direction of feed below the packed bed. Also, it is maldistributed in the y-direction but to a smaller level. When the bed is repacked, the distribution as a whole remains unaffected despite some insignificant changes in the details of the distribution.

Table A4.4

VALUES OF $F_{.05}$*

n_2 = Degrees of freedom for denominator	n_1 = Degrees of freedom for numerator																		
	1	2	3	4	5	6	7	8	9	10	12	15	20	24	30	40	60	120	∞
1	161	200	216	225	230	234	237	239	241	242	244	246	248	249	250	251	252	253	254
2	18.50	19.00	19.20	19.20	19.30	19.30	19.40	19.40	19.40	19.40	19.40	19.40	19.40	19.50	19.50	19.50	19.50	19.50	19.50
3	10.10	9.55	9.28	9.12	9.01	8.94	8.89	8.85	8.81	8.79	8.74	8.70	8.66	8.64	8.62	8.59	8.57	8.55	8.53
4	7.71	6.94	6.59	6.39	6.26	6.16	6.09	6.04	6.00	5.96	5.91	5.86	5.80	5.77	5.75	5.72	5.69	5.66	5.63
5	6.61	5.79	5.41	5.19	5.05	4.95	4.88	4.82	4.77	4.74	4.68	4.62	4.56	4.53	4.50	4.46	4.43	4.40	4.37
6	5.99	5.14	4.76	4.53	4.39	4.28	4.21	4.15	4.10	4.06	4.00	3.94	3.87	3.84	3.81	3.77	3.74	3.70	3.67
7	5.59	4.74	4.35	4.12	3.97	3.87	3.79	3.73	3.68	3.64	3.57	3.51	3.44	3.41	3.38	3.34	3.30	3.27	3.23
8	5.32	4.46	4.07	3.84	3.69	3.58	3.50	3.44	3.39	3.35	3.28	3.22	3.15	3.12	3.08	3.04	3.01	2.97	2.93
9	5.12	4.26	3.86	3.63	3.48	3.37	3.29	3.23	3.18	3.14	3.07	3.01	2.94	2.90	2.86	2.83	2.79	2.75	2.71
10	4.96	4.10	3.71	3.48	3.33	3.22	3.14	3.07	3.02	2.98	2.91	2.85	2.77	2.74	2.70	2.66	2.62	2.58	2.54
11	4.84	3.98	3.59	3.36	3.20	3.09	3.01	2.95	2.90	2.85	2.79	2.72	2.65	2.61	2.57	2.53	2.49	2.45	2.40
12	4.75	3.89	3.49	3.26	3.11	3.00	2.91	2.85	2.80	2.75	2.69	2.62	2.54	2.51	2.47	2.43	2.38	2.34	2.30
13	4.67	3.81	3.41	3.18	3.03	2.92	2.83	2.77	2.71	2.67	2.60	2.53	2.46	2.42	2.38	2.34	2.30	2.25	2.21
14	4.60	3.74	3.34	3.11	2.96	2.85	2.76	2.70	2.65	2.60	2.53	2.46	2.39	2.35	2.31	2.27	2.22	2.18	2.13
15	4.54	3.68	3.29	3.06	2.90	2.79	2.71	2.64	2.59	2.54	2.48	2.40	2.33	2.29	2.25	2.20	2.16	2.11	2.07
16	4.49	3.63	3.24	3.01	2.85	2.74	2.66	2.59	2.54	2.49	2.42	2.35	2.28	2.24	2.19	2.15	2.11	2.06	2.01
17	4.45	3.59	3.20	2.96	2.81	2.70	2.61	2.55	2.49	2.45	2.38	2.31	2.23	2.19	2.15	2.10	2.06	2.01	1.96
18	4.41	3.55	3.16	2.93	2.77	2.66	2.58	2.51	2.46	2.41	2.34	2.27	2.19	2.15	2.11	2.06	2.02	1.97	1.92
19	4.38	3.52	3.13	2.90	2.74	2.63	2.54	2.48	2.42	2.38	2.31	2.23	2.16	2.11	2.07	2.03	1.98	1.93	1.88
20	4.35	3.49	3.10	2.87	2.71	2.60	2.51	2.45	2.39	2.35	2.28	2.20	2.12	2.08	2.04	1.99	1.95	1.90	1.84
21	4.32	3.47	3.07	2.84	2.68	2.57	2.49	2.42	2.37	2.32	2.25	2.18	2.10	2.05	2.01	1.96	1.92	1.87	1.81
22	4.30	3.44	3.05	2.82	2.66	2.55	2.46	2.40	2.34	2.30	2.23	2.15	2.07	2.03	1.98	1.94	1.89	1.84	1.78
23	4.28	3.42	3.03	2.80	2.64	2.53	2.44	2.37	2.32	2.27	2.20	2.13	2.05	2.01	1.96	1.91	1.86	1.81	1.76
24	4.26	3.40	3.01	2.78	2.62	2.51	2.42	2.36	2.30	2.25	2.18	2.11	2.03	1.98	1.94	1.89	1.84	1.79	1.73
25	4.24	3.39	2.99	2.76	2.60	2.49	2.40	2.34	2.28	2.24	2.16	2.09	2.01	1.96	1.92	1.87	1.82	1.77	1.71
30	4.17	3.32	2.92	2.69	2.53	2.42	2.33	2.27	2.21	2.16	2.09	2.01	1.93	1.89	1.84	1.79	1.74	1.68	1.62
40	4.08	3.23	2.84	2.61	2.45	2.34	2.25	2.18	2.12	2.08	2.00	1.92	1.84	1.79	1.74	1.69	1.64	1.58	1.51
60	4.00	3.15	2.76	2.53	2.37	2.25	2.17	2.10	2.04	1.99	1.92	1.84	1.75	1.70	1.65	1.59	1.53	1.47	1.39
120	3.92	3.07	2.68	2.45	2.29	2.18	2.09	2.02	1.96	1.91	1.83	1.75	1.66	1.61	1.55	1.50	1.43	1.35	1.25
∞	3.84	3.00	2.60	2.37	2.21	2.10	2.01	1.94	1.88	1.83	1.75	1.67	1.57	1.52	1.46	1.39	1.32	1.22	1.00

* This table is reproduced from M. Merrington and C. M. Thompson, "Tables of percentage points of the inverted beta (F) distribution," *Biometrika*, Vol. 33 (1943)

Example 2

The same bed described in Example 1, but with uniformly distributed feed below the bed. The bed was repacked three times and the following point velocities were recorded.

Location		Replication Number			Total
x	y	1	2	3	
1	1	355	85	55	495
1	2	205	210	165	580
1	3	260	445	110	815
1	4	155	440	225	820
1	5	140	200	200	540
1	6	295	150	390	835
1	7	110	310	315	735
1	8	120	235	415	770
1	9	310	215	330	855
1	10	340	65	240	645
1	11	420	175	200	795
1	12	420	215	280	915
2	1	275	300	180	755
2	2	220	185	275	680
2	3	95	260	260	615
2	4	105	280	190	575
2	5	185	195	285	665
2	6	580	550	550	1680
2	7	450	500	425	1375
2	8	455	175	420	1050
2	9	375	225	265	865
2	10	330	410	175	915
2	11	320	300	130	750
2	12	250	340	390	980
3	1	225	180	245	650
3	2	135	195	350	680
3	3	130	145	225	500
3	4	50	170	255	475
3	5	20	440	325	785
3	6	310	550	420	1280
3	7	455	360	510	1325
3	8	360	170	305	835
3	9	210	620	245	1075
3	10	110	400	240	750
3	11	115	370	290	775
3	12	170	115	390	675
4	1	410	190	285	885
4	2	320	190	230	740
4	3	325	200	280	805
4	4	195	160	335	690
4	5	190	350	290	830
4	6	500	430	235	1165
4	7	260	435	325	1020
4	8	350	375	170	895
4	9	340	470	210	1020
4	10	60	550	410	1020
4	11	445	480	415	1340
4	12	370	360	380	1110
5	1	345	295	230	870
5	2	380	350	100	830

Location		Replication Number			Total
x	y	1	2	3	
5	3	545	255	95	895
5	4	440	225	25	690
5	5	260	310	190	760
5	6	480	280	270	1030
5	7	375	480	395	1250
5	8	365	440	390	1195
5	9	340	395	480	1215
5	10	130	145	240	515
5	11	500	110	365	975
5	12	480	295	410	1185
6	1	390	155	70	615
6	2	225	230	270	725
6	3	405	165	160	730
6	4	420	175	260	855
6	5	220	400	190	810
6	6	95	265	85	445
6	7	260	350	160	770
6	8	460	440	320	1220
6	9	360	500	285	1145
6	10	450	385	330	1165
6	11	360	300	330	990
6	12	365	240	160	765
7	1	125	125	180	430
7	2	105	260	215	580
7	3	85	390	215	690
7	4	240	400	335	975
7	5	235	410	290	935
7	6	175	220	160	555
7	7	240	205	220	665
7	8	210	300	320	830
7	9	265	130	335	730
7	10	385	360	325	1070
7	11	320	380	270	970
7	12	215	315	270	800
8	1	155	280	300	735
8	2	105	310	265	680
8	3	120	235	360	715
8	4	155	110	275	540
8	5	265	140	250	655
8	6	170	135	80	385
8	7	180	260	170	610
8	8	115	360	315	790
8	9	110	145	300	645
8	10	560	415	285	1260
8	11	470	570	195	1235
8	12	500	270	395	1165
9	1	430	350	150	930
9	2	325	200	180	705
9	3	240	120	235	595
9	4	200	210	420	830

Location		Replication Number			Total
x	y	1	2	3	
9	5	440	220	265	925
9	6	270	150	100	520
9	7	155	320	215	690
9	8	115	370	305	790
9	9	190	285	500	975
9	10	165	115	440	720
9	11	435	250	190	875
9	12	330	400	350	1080
10	1	295	365	155	815
10	2	235	290	215	740
10	3	280	200	325	805
10	4	185	200	380	765
10	5	440	275	365	1080
10	6	580	280	360	1220
10	7	275	475	475	1225
10	8	235	400	445	1080
10	9	315	70	460	845
10	10	125	120	440	685
10	11	340	295	275	910
10	12	140	180	130	450
11	1	355	260	120	735
11	2	495	80	145	720
11	3	375	260	100	735
11	4	190	390	320	900
11	5	600	380	290	1270
11	6	390	315	510	1215
11	7	150	480	440	1070
11	8	280	370	440	1090
11	9	395	200	475	1070
11	10	295	250	495	1040
11	11	80	260	420	760
11	12	70	160	175	405
12	1	85	100	325	510
12	2	105	110	315	530
12	3	470	320	295	1085
12	4	215	370	235	820
12	5	250	305	290	845
12	6	295	265	400	960
12	7	375	195	270	840
12	8	360	340	115	815
12	9	325	335	105	765
12	10	395	330	115	840
12	11	115	220	310	645
12	12	190	230	350	770

$$\therefore \sum_{i=1}^{12} \sum_{j=1}^{12} \sum_{k=1}^{3} Y_{ijk}^2 = 40831200$$

$$\sum_{i=1}^{12} \sum_{j=1}^{12} T_{ij.}^2 = 111134950$$

$$T_{...}^2 = (122010)^2$$

$$\sum_{k=1}^{3} T_{..k}^2 = (40575)^2 + (40945)^2 + (40490)^2$$

The table of totals is formed as follows:

x \ y	1	2	3	4	5	6	7	8	9	10	11	12	TOTAL
1	495	580	815	820	540	835	735	770	855	645	795	915	8800
2	755	680	615	575	665	1620	1375	1050	865	915	750	980	10905
3	650	680	500	475	785	1280	1325	835	1075	750	775	675	9805
4	885	740	805	690	830	1165	1020	895	1020	1020	1340	1110	11520
5	870	830	895	690	760	1030	1250	1195	1215	515	975	1185	11410
6	615	725	730	855	810	445	770	1220	1145	1165	990	765	10235
7	430	580	690	975	935	555	665	830	730	1070	570	800	9230
8	735	680	715	540	655	385	610	750	645	1260	1235	1165	9415
9	930	705	595	830	925	520	690	790	975	720	875	1080	9635
10	815	740	805	765	1080	1220	1225	1080	845	685	910	450	10620
11	735	720	735	900	1270	1215	1070	1090	1070	1040	760	405	11010
12	510	530	1085	820	845	960	840	815	765	840	645	770	9425
TOTAL	8425	8190	8985	8935	10100	11290	11575	11360	11205	10625	11020	10300	122010

$$\therefore \sum_{i=1}^{12} T_{i..}^2 = 1249654250$$

$$\sum_{j=1}^{12} T_{.j.}^2 = 1257098550$$

Applying Equs. A4.8a - A4.8f, where a = 12, b = 12, r = 3

SST = 6371848

SSx = 253266

SSy = 260052

SS(xy) = 1872313

SSR = 813

SSE = 3985404

The computed f values are as follows:

Source of Variation	Degree of Freedom	Sum of Squares	Main Squares	Computed f
Replication	2	813	406.5	0.03
Factor -x	11	25366	23024	1.65
Factor -y	11	260052	23641	1.7
Interaction	121	1872313	15474	1.11
Error	286	3985405	13935	
Total	431	6371848		

Comparing computed f-values with tabulated F-values at significance level $\alpha = 0.05$ at appropriate degrees of freedom found in Table A4.4:

1) For replication: $F_{0.05}\ (2,286) = 3 > 0.03$

$\therefore$ Replication has no significant effect.

2) Factor X: $F_{0.05}\ (11,286) = 1.79 > 1.65$

$\therefore$ Gas distribution is not significantly effected along the x-direction.

3) Factor ^{Y}: $F_{0.05}\ (11,286) = 1.79 > 1.7$

$\therefore$ Gas distribution is not significantly changed along the y-direction.

4) Interaction: $F_{0.05}\ (121,286) = 1.22 > 1.11$

$\therefore$ The combined effect of x and y has no significant effect on gas distribution.

This means that there is no significant maldistribution in the gas emerging from the top of a packed bed whose feed is ideally distributed. Each time the bed is repacked, the distribution of gas emerging from the top of that bed is changed, but that change has no significant effect on the distribution as a whole.

A4.2 Three-Factor Analysis of the Variance

In this section, an experiment with three factors is considered. These three factors are the previously defined X and Y co-ordinates in the xy plane above the packed bed, and the diameter, D, of the packed bed. That is, the effects of x-axis, y-axis and the diameter scale on the distribution of the gas above geometrically similar beds of different size operated at similar Reynolds number, are tested.

These remarks should be made:

a = The number of point velocity measurements, "levels" taken along x-axis

b = The number of levels taken along y-axis

c = The number of beds, (of different diameters), the point velocities are measured.

r = The number of repackings made for each bed.

Assume that (r) observations are made for each of the (abc) treatments. That is, a similar number of repackings should be made for each bed.

The model for the three-factor experiment is given by:

$$Y_{ijkl} = \mu + \alpha_i + \beta_j + \gamma_k + (\alpha\beta)_{ij} + (\alpha\gamma)_{ik} + (\beta\gamma)_{jk} + (\alpha\beta\gamma)_{ijk} + \varepsilon_{ijkl} \quad \ldots\ldots (A4.9)$$

$i = 1,2,\ldots\ldots,a;\quad j = 1,2,\ldots\ldots,b;\quad k = 1,2,\ldots\ldots,c;\quad l = 1,2,\ldots\ldots,r.$

γ_i, β_j, γ_k = The effects of (ith) level, (jth) level and (kth) level of X, Y, and D respectively on the distribution of the gas above the geometrically similar beds of different size.

The general idea concerning this analysis is the same as that discussed for the two-factor analysis of the variance. The sum of squares is partitioned into eight terms, each representing a source of variation of the gas distribution above geometrically similar beds.

Proceeding directly to the computational procedure for obtaining the sums of squares in the three-factor analysis of the variance. The following notations should be made:

$T_{....}$ = Sum of all (abcr) observations.

$T_{i...}$ = Sum of the observations for the (ith) level of factor X.

$T_{.j..}$ = Sum of the observations for the (jth) level of factor Y.

$T_{..k.}$ = Sum of the observations for the (kth) level of factor D.

$T_{ij...}$ = Sum of the observations for the (ith) level of factor X and the (jth) level of factor Y.

$T_{i.k.}$ = Sum of the observations for the (ith) level of factor X and the (kth) level of factor D

$T_{.jk.}$ = Sum of the observation for the (jth) level of factor Y and the (kth) level of factor D

$T_{ijk.}$ = Sum of the observations for the (ijk) th treatment combination

The sums of squares are computed as follows:

$$SST = \sum_{i=1}^{a}\sum_{j=1}^{b}\sum_{k=1}^{c}\sum_{l=1}^{r} Y_{ijkl}^2 - \frac{T_{....}^2}{abcr} \quad \ldots\ldots \text{(A4.10a)}$$

$$SSX = \frac{\sum_{i=1}^{a} T_{i...}^2}{bcr} - \frac{T_{...}^2}{abcr} \quad \ldots\ldots \text{(A4.10b)}$$

$$SSY = \frac{\sum_{j=1}^{b} T_{.j..}^2}{acr} - \frac{T_{...}^2}{abcr} \quad \ldots\ldots \text{(A4.10c)}$$

$$SSD = \frac{\sum_{k=1}^{c} T_{..k.}^2}{abr} - \frac{T_{....}^2}{abcr} \quad \ldots\ldots \text{(A4.10d)}$$

$$SS(XY) = \frac{\sum_{i=1}^{a}\sum_{j=1}^{b} T_{ij..}^2}{cr} - \frac{\sum_{i=1}^{a} T_{i...}^2}{bcr} - \frac{\sum_{j=1}^{b} T_{.j..}^2}{acr} + \frac{T_{....}^2}{abcr}$$

..... (A4.10e)

$$SS(XD) = \frac{\sum_{i=1}^{a}\sum_{k=1}^{c} T_{i.k.}^2}{br} - \frac{\sum_{i=1}^{a} T_{i...}^2}{bcr} - \frac{\sum_{k=1}^{c} T_{..k.}^2}{abr} + \frac{T_{....}^2}{abcr}$$

..... (A4.10f)

$$SS(YD) = \frac{\sum_{j=1}^{b}\sum_{k=1}^{c} T_{.jk.}^2}{ar} - \frac{\sum_{j=1}^{b} T_{.j..}^2}{acr} - \frac{\sum_{k=1}^{c} T_{..k.}^2}{abr} + \frac{T_{....}^2}{abcr}$$

..... (A4.10g)

$$SS(XYD) = \frac{\sum_{i=1}^{a}\sum_{j=1}^{b}\sum_{k=1}^{c} T_{ijk.}^2}{r} - \frac{\sum_{i=1}^{a}\sum_{j=1}^{b} T_{ij..}^2}{cr} - \frac{\sum_{i=1}^{a}\sum_{k=1}^{c} T_{i.k.}^2}{br}$$

$$- \frac{\sum_{j=1}^{b}\sum_{k=1}^{c} T_{.jk.}^2}{ar} + \frac{\sum_{i=1}^{a} T_{i...}^2}{bcr} + \frac{\sum_{j=1}^{b} T_{.j..}^2}{acr}$$

$$+ \frac{\sum_{k=1}^{c} T_{..k.}^2}{abr} - \frac{T_{....}^2}{abcr}$$

..... (A4.10h)

$$SSE = SST - SSX - SSY - SSD - SS(XY) - SS(XD) - SS(YD) - SS(XYD)$$

..... (A4.10i)

Table A4.5 Analysis of the Variance for the Three-factor Experiment with (r) replicates

Source of Variance	Sum of squares	Degree of Freedom	Mean Squares	Computed-f
Main Effects:				
X	SSX	(a-1)	S_1^2	$f_1=S_1^2/S^2$
Y	SSY	(b-1)	S_2^2	$f_2=S_2^2/S^2$
D	SSD	(c-1)	S_3^2	$f_3=S_3^2/S^2$
Two-factor Interaction				
XY	SS(XY)	(a-1)(b-1)	S_4^2	$f_4=S_4^2/S^2$
XD	SS(XD)	(a-1)(c-1)	S_5^2	$f_5=S_5^2/S^2$
YD	SS(YD)	(b-1)(c-1)	S_6^2	$f_6=S_6^2/S^2$
Three-factor Interaction XYD	SS(XYD)	(a-1)(b-1)(c-1)	S_7^2	$f_7=S_7^2/S^2$
Error	SSE	abc(r-1)	S^2	
Total	SST	abcr-1		

The computations in an analysis of the variance problem, for a three-factor experiment with (r) replications, are summarized in Table A4.5.

Following the same method of the two-factor analysis of the variance, the significance of the effect of each term listed in Table A4.5 on the distribution of the gas is estimated. The solution was performed using a computer statistical package, (UA 27).

A4.2.1 Application of the Three-factor Analysis of the Variance

In this work the distribution of the air emerging from the top of two geometrically and dynamically similar packed beds of different size is analysed when the two beds were fed by

1 - Ideally distributed air.

2 - Maldistributed air.

In this analysis point Reynolds numbers were used instead of the point velocities, and

a = 12 (point measurements along x-axis).

b = 12 (point measurements along y-axis).

c = 2 (D_1 = 381 mm, D_2 = 610 mm).

r = 3 (each bed is repacked three times).

$\therefore$ ab = 144 (point measurements made above each bed at each repacking).

abr = 432 (point measurements made above each bed).

abcr = 864 (the total number of point measurements).

Re = 30,000 (for the two beds).

Example 1: Ideally distributed feed.

The dpecification of the two geometrically similar beds, (bed number 1 and bed number 2), are as follows:

	Bed number 1	Bed number 2
Diameter, D (mm)	381	610
Packed Height, P.H. (mm)	127	203
Pack Size, P.S. (mm)	16	25.4
D/P.H.	3	3
D/P.S.	24	24
Re	30,000	30,000

The test is performed by using a computer statistical package (UA 27) which computes f values. The results are listed in Table A4.6.

Example 2: Maldistributed feed.

The test was performed by the use of the statistical package (UA 27) on the same beds above but with maldistributed feed. The results are listed in Table A4.6.

Table A4.6. Computed f-values for two geometrically similar beds operated under Re = 30,000

Source of Variance	Computed f-values		Tabulated f-values
	Ideally distributed	Maldistributed	
X	1.613	11.753	1.71
Y	1.315	2.16	1.71
D	0.543	0.568	3.84
XY	1.416	1.325	1.22
XD	1.314	1.617	1.71
YD	1.482	1.47	1.71
XYD	0.74	0.953	1.22

The most important factors which effect the distribution of the gas are: Factor X, Factor Y and Factor D.

The comparison of the computed-f values of these factors with their corresponding tabulated f-values at $\alpha = 0.05$, (obtained from Table A4.4 at appropriate degrees of freedom), shows:

1) In the case of "Ideally" distributed feed the gas emerging from the top of the two beds is well distributed since the effects of X and Y factors are not significant. The diameter of the bed has no significant effect on the distribution of the gas emerging from the top of the two beds since the computed f-value of the factor D, (0.543) is smaller than the tabulated value, (3.84).

2) In the maldistributed feed case, the results show a severe maldistribution in the gas above the two beds specially along the x-axis.

Again the size of the bed, (Diameter), has no significant effect on the distribution of the gas above the two beds.

$\therefore$ For two geometrically similar beds of different size, the flow pattern of the gas is similar provided that they are operated at the same Re value.

APPENDIX A5

POINT VELOCITY MEASUREMENTS ABOVE PACKED BEDS SUPPLIED BY EXISTING DESIGNS OF GAS DISTRIBUTION DEVICES

Tables A5.1 to A5.4:	Radial feed inlet, no distributor, several P.Hs.
Tables A5.5 to A5.8:	Radial feed inlet, draw-off tray, several P.Hs.
Tables A5.9 to A5.10:	Tangential feed inlet, no distributor, P.H. = 12.30 cm
Tables A5.11 to A5.12:	Tangential feed inlet, draw-off tray, P.H. = 6,12 cm.
Table A5.13:	Tangential feed inlet, Internal cylinder P.H. = 6 cm.

Computer program to draw the response surfaces.

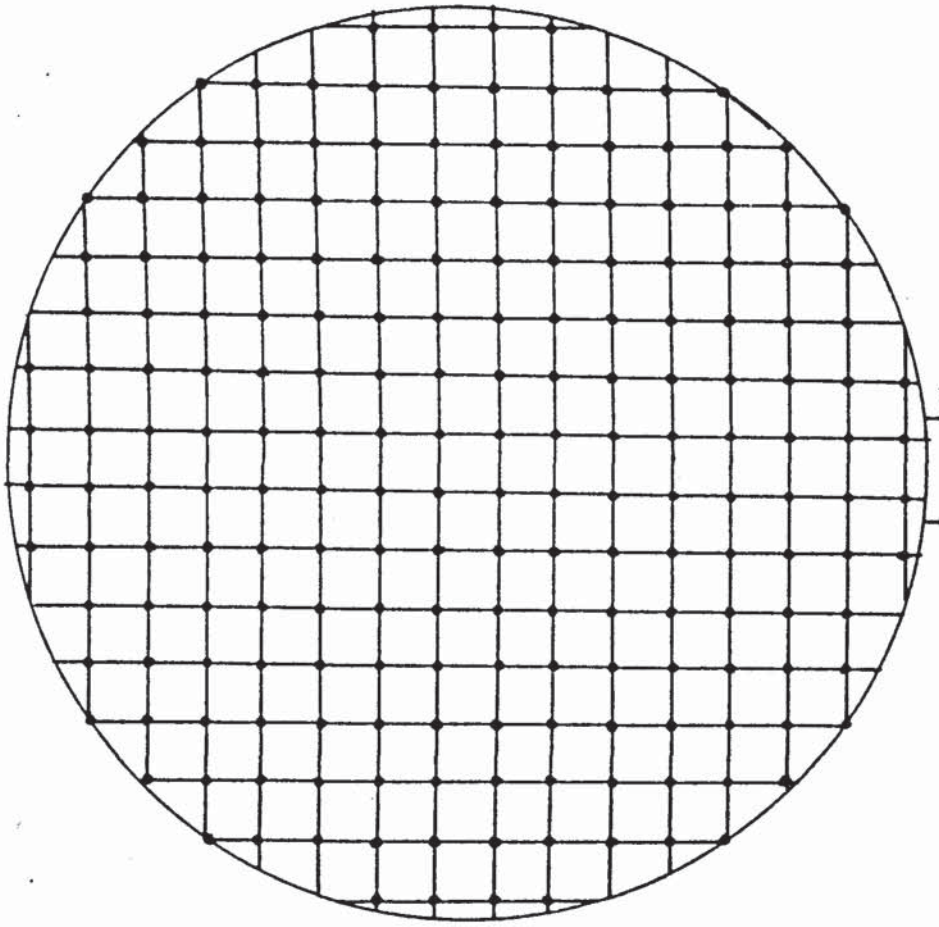

Key Figure A5.1

Positions of the 200 Point Velocity Measurements in Tables A5.1 5o A5.8

					45	45	40	50						
		100	75	45	50	45	45	45	45	25	20			
	350	75	50	50	50	50	50	45	35	35	30	30		
700	550	130	60	45	80	50	60	35	50	30	90	30	60	
900	600	85	50	60	80	50	35	35	45	80	25	100	50	
1050	450	100	34	50	45	50	40	30	35	40	40	35	30	
1000	1100	200	60	25	50	40	30	20	30	20	30	35	30	25	30
1500	1600	250	50	30	40	50	40	25	30	25	25	25	25	75	85
1550	1550	240	45	40	40	50	40	25	30	25	30	25	20	75	85
1000	1050	230	65	30	50	40	30	25	30	20	30	35	30	25	30
	1075	430	105	35	50	50	50	45	25	30	40	40	30	30	
	920	610	80	55	55	75	55	35	40	45	85	25	75	75	
	650	600	125	60	50	70	60	60	35	50	30	80	30	70	
		400	130	70	30	40	30	50	45	40	30	30	35		
			75	80	45	45	45	45	45	45	25	30			
						45	50	60	20						

Table A5.1: Point Velocity Measurements (ft/min); No Distributor, P.H. = 0.0 cm, Radial Inlet, P.S. = 16 mm

Re = 46000

ϕ = 836

					125	55	60	110					
		140	90	60	55	80	40	100	45	40	120		
	110	130	90	65	20	60	40	30	75	75	100	25	
135	140	55	45	10	10	50	45	55	40	100	75	110	65
260	75	140	10	10	10	40	35	75	60	85	80	85	95
125	145	80	30	10	15	35	50	75	70	45	15	80	100
320	400	135	20	50	10	10	45	35	50	10	35	45	50	80	85
360	550	170	50	25	10	10	40	55	90	90	40	40	10	70	100
420	260	200	80	10	10	10	20	50	70	70	70	70	60	80	110
300	270	140	40	10	10	10	45	40	50	50	85	40	80	50	100
	300	200	110	25	10	10	20	40	50	35	70	25	80	70	
	250	170	100	10	10	10	30	80	30	20	40	50	75	120	
	550	170	140	55	30	10	40	80	60	10	30	70	60	60	
		150	50	45	65	30	75	70	90	45	75	100	100		
			140	120	75	100	65	40	75	100	35	100			
						110	55	40	70						

Table A5.2 Point Velocity Measurements (ft/min); No Distributor, P.H. = 6 cm, Radial Inlet, P.S. = 16 mm

Re = 46000

ϕ = 210

					85	105	120	75						
		160	50	70	145	45	100	110	95	120	110			
	110	95	110	90	85	75	65	100	70	60	95	110		
160	200	70	80	70	50	65	125	75	90	95	90	90	135	
260	140	20	55	40	30	80	120	85	55	40	30	110	85	
200	210	35	100	85	65	75	110	40	80	90	105	85	100	
280	200	230	130	140	55	80	70	80	60	70	90	100	95	95	120
320	380	130	120	75	65	45	50	135	45	65	110	85	70	50	105
320	220	110	110	70	60	40	40	90	30	40	85	100	150	100	70
250	200	250	100	70	60	70	80	70	55	140	55	90	160	65	70
	330	160	100	80	55	85	80	130	75	90	100	120	65	135	
	260	180	35	50	80	40	45	45	90	120	30	65	100	35	
	270	160	130	90	130	100	70	75	85	70	80	110	110	120	
		200	110	105	75	45	75	30	60	100	85	120	60		
			100	20	75	60	95	150	50	120	140	55			
						120	105	55	75						

Table A5.3 Point Velocity Measurements (ft/min); No Distributor, P.H. = 12 cm, Radial Inlet P.S. = 16 mm

Re = 46000

ϕ = 69

					145	185	70	115						
		140	85	100	145	105	90	55	155	85	105			
	125	145	105	160	150	40	125	105	105	50	125	100		
120	160	145	110	110	160	75	85	100	130	175	140	70	95	
160	170	140	125	110	100	130	85	100	125	70	100	140	80	
220	190	185	75	135	110	90	205	105	125	110	80	140	115	
140	165	180	130	150	200	110	145	120	110	140	75	105	85	115	105
150	155	160	100	85	125	105	50	130	135	110	85	110	110	130	140
240	140	130	85	185	135	145	65	60	90	120	65	120	90	170	115
180	80	110	135	105	90	120	95	125	125	110	60	120	130	105	125
	110	65	210	145	70	130	150	85	130	55	140	145	120	90	
	150	100	100	125	115	135	85	140	175	130	85	95	140	120	
	80	165	165	75	140	125	115	165	135	105	85	150	135	230	
		170	105	115	150	80	130	25	105	65	115	165	10		
			175	200	20	90	20	160	180	110	65	110			
						65	70	140	150						

Table A5.4 Point Velocity Measurements (ft/min); No Distributor, P.H. = 30 cm, Radial Inlet, P.S. = 16 mm

Re = 46000

ϕ. = 21.4

					95	120	105	180						
		100	150	150	105	125	120	120	150	170	85			
	320	220	170	150	120	140	120	120	75	95	90	80		
550	360	200	150	120	125	120	100	75	60	75	95	120	90	
520	350	280	200	180	95	95	85	60	50	30	30	40	80	
370	300	270	165	170	160	100	105	70	30	30	50	40	80	
320	320	310	270	185	170	180	130	170	140	60	40	50	40	100	100
300	320	300	250	270	200	160	150	200	160	40	35	30	40	50	100
280	310	295	230	150	150	150	120	150	30	30	30	30	40	45	75
320	300	260	250	185	160	170	120	130	80	30	30	30	40	75	60
	360	320	200	145	170	100	120	120	30	30	30	30	40	100	
	350	250	250	170	130	80	100	60	30	30	40	30	40	150	
	400	350	280	200	100	100	60	120	50	40	80	100	150	100	
		450	390	180	150	120	100	150	100	100	100	155	50	
			260	180	150	160	155	200	110	100	90	80		
						75	100	130	100					

Table A5.5 Point Velocity Measurements (ft/min); Draw-off Tray P.H. = 0, Radial Inlet P.S. = 16 mm

Re = 46000

ϕ = 98

					185	195	90	105						
		130	200	110	135	145	110	30	305	125	150			
	80	90	135	175	165	200	100	75	185	165	165	150		
150	105	140	80	130	165	105	115	150	175	115	145	205	110	
145	310	190	85	120	75	115	145	220	130	170	150	140	75	
100	85	160	105	185	95	175	200	125	155	125	100	170	120	
140	50	130	130	75	95	130	180	50	180	160	155	145	140	100	70
155	60	130	160	80	180	70	90	170	165	140	180	170	155	285	90
195	145	205	260	155	45	215	255	110	130	55	70	175	85	70	200
225	75	170	130	100	85	145	190	150	140	90	225	75	110	170	170
	155	180	245	95	150	70	125	205	250	110	215	70	190	115	
	150	155	170	185	170	35	205	55	150	90	165	100	170	145	
	230	280	105	100	220	60	135	45	80	175	210	180	180	175	
		220	210	180	200	200	80	140	120	100	190	185	200		
			190	200	130	160	150	60	205	200	195	190			
						200	95	150	190						

Table A5.6 Point Velocity Measurements (ft/min); Draw-off Tray, P.H. = 6 cm, Radial Inlet P.S. = 16 mm

Re = 46000

ϕ = 27

				60	105	135	140							
		180	115	125	145	165	125	80	125	200	225			
	80	175	75	85	170	160	130	190	130	200	110	160		
140	115	30	105	75	130	190	120	110	180	75	100	210	40	
245	170	110	125	120	130	135	115	60	150	85	170	140	90	
180	85	165	105	140	160	250	140	70	140	120	170	50	230	
135	170	225	110	210	125	130	40	175	155	95	220	155	140	150	190
130	260	100	140	160	155	210	190	135	160	150	90	40	225	145	65
95	110	75	110	120	150	190	110	210	110	130	165	120	200	120	75
180	145	50	125	130	180	115	210	260	180	125	145	160	80	160	150
	205	50	100	160	90	130	135	155	200	130	170	170	150	150	
	135	80	195	105	220	115	130	135	155	155	120	205	150	125	
	145	155	175	160	110	170	165	140	170	135	95	200	185	140	
		200	160	190	85	200	220	135	120	210	120	240	135		
			130	230	175	220	280	110	170	160	210	190			
						290	110	150	155						

Table A5.7 Point Velocity Measurements (ft/min); Draw-off Tray, P.H. = 12 cm, Radial Inlet P.S. = 16 mm

Re = 46000

ϕ = 22.6

					110	150	155	85						
		145	100	150	125	135	215	130	60	165	110			
	110	125	65	155	155	165	145	145	120	150	140	135		
90	125	95	130	115	115	140	145	110	110	55	125	160	115	
140	140	125	145	155	125	135	110	135	140	115	130	110	115	
130	180	150	130	120	150	175	175	105	120	115	160	85	165	
160	95	175	180	135	155	70	130	150	85	165	30	70	110	160	170
125	110	110	125	140	160	65	130	145	105	130	140	130	140	175	145
130	105	180	130	125	115	230	100	170	145	145	180	150	185	160	135
165	150	240	180	65	210	150	100	65	130	145	160	45	160	105	135
	200	90	170	210	205	165	165	170	160	130	115	240	170	205	
	110	180	155	125	120	105	170	150	85	125	120	145	75	85	
	40	165	200	170	180	175	165	100	110	50	220	120	95	175	
		205	135	80	120	155	55	130	125	150	130	190	140		
			65	115	175	200	240	100	200	130	55	85			
						35	220	65	25						

Table A5.8 Point Velocity Measurements (ft/min); Draw-off Tray, P.H. = 30 cm, Radial Inlet P.S. = 16 mm

Re = 46000

ϕ = 19

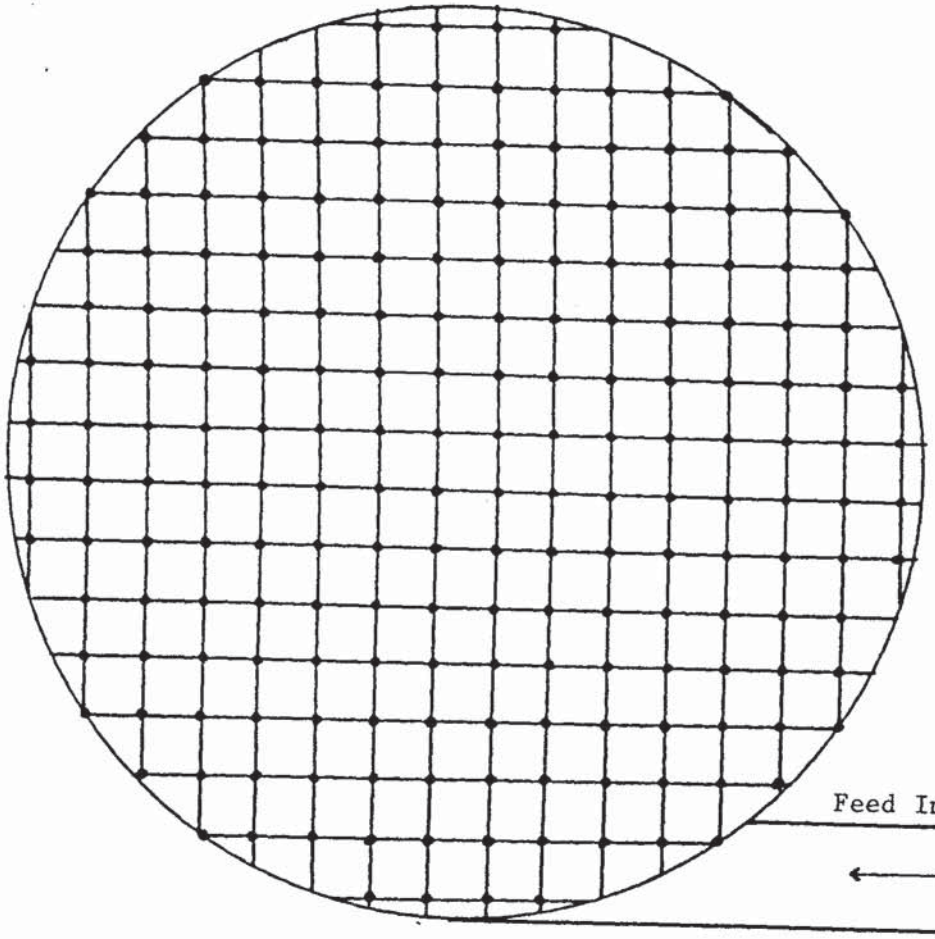

Key Figure A5.2

Positions of the 200 point velocity measurements in tables A5.9 to A5.13

					220	190	115	90						
			210	295	130	210	55	50	75	155	190	175		
		235	250	200	170	145	85	65	110	65	130	125	200	
	300	225	280	75	160	35	95	80	40	45	110	135	310	190
	305	230	110	100	105	40	25	50	50	55	75	85	160	220
	375	200	125	105	40	55	-5	-75	35	35	30	110	110	200
370	400	240	140	40	50	-20	-20	-60	25	20	105	65	120	175	215
585	255	285	160	70	-55	-40	-60	-40	-65	40	10	100	35	175	340
320	300	280	145	80	20	-40	-25	-55	100	80	70	120	140	205	230
270	305	320	50	40	35	-50	-75	-55	-80	50	90	160	190	220	270
	350	235	110	70	80	95	70	-60	70	75	80	105	75	270	
45	450	270	255	155	65	75	70	80	130	130	180	140	130	180	
	450	630	275	130	25	130	80	150	230	200	190	250	225	220	
		740	285	360	210	45	70	160	180	180	230	245	160		
			400	240	240	140	180	235	320	305	130	30			
						180	180	175	205						

Table A5.9 Point Velocity Measurements (ft/min); No Distributor, P.H. = 12 cm. Tangential Inlet, P.S. = 16 mm

Re = 46000

ϕ = 148.5

					280	155	165	80						
		180	185	120	165	65	125	100	135	75	130			
	140	70	160	115	135	125	105	115	85	140	155	75		
140	170	175	115	140	100	150	100	105	135	155	130	105	70	
210	240	155	170	145	100	140	100	120	160	110	105	40	80	
270	185	155	30	105	120	115	200	90	120	105	70	150	170	
190	195	140	175	115	230	75	65	20	105	150	105	135	105	155	95
275	200	160	165	260	125	110	135	135	125	80	125	135	30	120	185
255	170	140	100	200	105	140	110	45	220	50	90	155	125	140	130
260	150	155	75	75	65	195	145	140	135	115	80	110	120	215	140
180	180	200	155	130	100	140	180	40	150	125	230	125	115		
220	90	155	255	140	205	125	170	220	190	130	135	290	155		
180	180	250	135	170	140	150	225	160	145	115	170	155	175		
245	95	110	220	150	140	20	170	140	230	130	185				
	160	220	155	160	125	180	90	155	110	180					
				140	90	210	130							

Table A5.10 Point Velocity Measurements (ft/min); No Distributor, P.H. = 30 cm, Tangential Inlet, P.S. = 16 mm

Re = 46000

ϕ = 26

					20	140	170	170						
		220	145	95	90	110	15	45	180	150	230			
	120	135	140	90	95	105	155	170	185	250	225	90		
80	135	130	105	140	125	150	80	165	170	100	65	270	180	
130	185	180	160	130	90	100	95	205	100	135	145	90	150	
230	180	115	80	140	85	125	45	125	100	135	145	90	150	
140	275	180	170	155	80	90	100	70	75	125	135	150	85	185	260
250	265	235	160	165	150	145	65	75	100	95	100	15	165	160	135
200	240	95	155	160	110	125	125	100	145	90	65	125	150	260	215
480	200	135	175	95	70	165	105	90	55	20	110	130	160	150	110
	200	260	90	125	100	160	145	80	70	110	135	35	30	175	
	165	115	165	130	135	140	95	155	90	125	85	65	105	100	
	215	155	155	130	100	190	70	115	105	170	180	160	210	100	
		125	130	190	170	155	175	175	160	210	160	150	120		
			100	300	305	135	240	185	100	80	120	160			
						180	155	180	300						

Table A5.11 Point Velocity Measurements (ft/min); Draw-off Tray, P.H. = 6 cm, Tangential Inlet P.S. = 16 mm

Re = 4600

ϕ = 60

					110	110	115	115						
		110	145	110	105	100	150	170	135	160	125			
	145	160	155	155	120	130	80	120	215	110	195	235		
130	45	155	145	105	135	165	200	30	55	215	180	200	130	
140	150	155	180	175	155	140	45	130	145	150	95	220	240	
150	210	70	50	100	140	120	95	130	125	110	135	220	260	
255	140	120	185	30	140	85	115	105	85	85	125	200	135	70	205
495	220	115	230	165	20	135	40	105	50	95	145	135	70	180	150
285	175	230	250	95	15	145	135	145	135	90	175	200	165	200	175
100	120	150	75	45	155	170	65	105	170	120	85	130	135	140	100
	160	115	95	25	65	90	120	105	80	125	80	55	105	75	
	105	145	190	120	100	95	45	120	150	130	170	170	125	115	
	150	75	100	225	95	85	30	160	160	50	200	100	70	110	
		155	115	120	180	160	140	130	120	120	180	80	90		
			15	160	200	140	135	185	85	90	110	25			
						135	210	220	180						

Table A5.12 Point Velocity Measurements (ft/min.); Draw-offTray, P.H. =12 cm, Tangential Inlet, P.S. = 16 mm

Re = 46000

ϕ = 38

					520	360	180	200					
		245	240	500	440	175	155	210	175	220	30		
	140	240	285	300	300	260	125	95	120	285	310	500	
250	380	245	140	180	80	-35	-35	-25	80	100	300	350	350
320	275	260	230	120	-50	-80	-40	-30	-10	95	120	100	250
440	260	180	120	-25	-80	-125	-70	-80	-60	15	100	210	220
200	180	130	130	10	-50	-130	-180	-140	-130	-100	15	100	90	400	300
300	230	215	50	10	-75	-140	-160	-140	-120	-100	10	75	160	300	500
305	275	200	75	15	-105	-160	-165	-165	-125	-100	10	30	250	240	240
400	360	200	10	-50	-85	-150	-185	-160	-160	-75	25	90	200	500	300
405	300	100	40	-50	-130	-125	-90	-70	-80	10	120	100	270		
500	250	160	55	-10	-100	-60	-100	-25	80	120	200	300	350		
300	390	250	200	150	-15	-40	-35	15	50	210	410	200	320		
	250	200	280	400	200	160	180	120	460	180	250	300			
		200	340	300	215	90	100	110	240	160	270				
					480	360	300	300					

Table A5.13 Point Velocity Measurements (ft/min); Internal Cylinder, P.H. = 6 cm, Tangential Inlet P.S. = 16 mm

Re = 46000

ϕ = 337.6

A COMPUTER PROGRAM TO DRAW THE RESPONSE SURFACES

```
 INTEGER I,J,NP
 DIMENSION ZARR(48,48),XX(144),YY(144),ZZ(144)
 DIMENSION WW(5184),WXL(4),WYL(4),WXH(4),WYH(4)
 DATA M/48/,N/48/,NW/5184/,XL/1.0/,YL/1.0/,XH/12.0/,YH/12.0/,
+      IFR/1/,HTRAT/0.5/,XIU/0.0/,YIU/0.0/,ZIU/0.0/,NP/144/
 DATA WXL(1),WXL(2),WXL(3),WXL(4)/0.0,120.0,0.0,120.0/
 DATA WXH(1),WXH(2),WXH(3),WXH(4)/120.0,240.0,120.0,240.0/
 DATA WYL(1),WYL(2),WYL(3),WYL(4)/120.0,120.0,0.0,0.0/
 DATA WYH(1),WYH(2),WYH(3),WYH(4)/240.0,240.0,120.0,120.0/
 DATA (XX(I),I=1,144)/1,1,1,1,1,1,1,1,1,1,1,1,2,2,2,2,2,2,2,2,2,2,
+2,
+2,3,3,3,3,3,3,3,3,3,3,3,3,4,4,4,4,4,4,4,4,4,4,4,4,5,5,5,5,5,5,5,5,
+5,5,5,5,6,6,6,6,6,6,6,6,6,6,6,6,7,7,7,7,7,7,7,7,7,7,7,7,8,8,8,8,8,
+8,8,8,8,8,8,8,9,9,9,9,9,9,9,9,9,9,9,9,10,10,10,10,10,10,10,10,10,
+10,10,10,11,11,11,11,11,11,11,11,11,11,11,11,12,12,12,12,12,12,12,
+12,12,12,12,12/
 DATA (YY(I),I=1,144)/12,11,10,9,8,7,6,5,4,3,2,1,12,11,10,9,8,7,6,
+5,
+4,3,2,1,12,11,10,9,8,7,6,5,4,3,2,1,12,11,10,9,8,7,6,5,4,3,2,1,12,
+11,10,9,8,7,6,5,4,3,2,1,12,11,10,9,8,7,6,5,4,3,2,1,12,11,10,9,8,7,
+6,5,4,3,2,1,12,11,10,9,8,7,6,5,4,3,2,1,12,11,10,9,8,7,6,5,4,3,2,1,
+12,11,10,9,8,7,6,5,4,3,2,1,12,11,10,9,8,7,6,5,4,3,2,1,12,11,10,9,
+8,7,6,5,4,3,2,1/
 DATA (ZZ(I),I=1,144)/123,112,102,75,87,75,132,127,102,107,120,87,
+115,123,127,152,132,122,153,132,132,133,127,123,
+165,142,105,107,112,138,145,160,113,127,145,128,
+112,128,160,132,132,138,135,160,132,82,133,133,
+88,102,125,152,130,97,77,133,158,152,122,108,
+130,102,107,132,137,127,135,107,113,157,113,103,
+145,122,142,120,137,145,148,145,145,130,112,115,
+142,107,113,92,145,127,147,145,115,123,132,140,
+160,120,157,127,137,137,152,165,113,125,178,148,
+135,172,207,165,197,138,142,160,125,183,163,153,
+142,162,145,133,160,168,143,113,202,205,230,105,
+167,148,235,240,212,227,192,118,158,243,187,168/
 CALL OPEN
 CALL RANGRD(NP,XX,YY,ZZ,M,XL,XH,N,YL,YH,ZARR,NW,WW)
 CALL ISOFRA(IFR)
 CALL HEIRAT(HTRAT)
 CALL ISOSCA(XIU,YIU,ZIU)
 DO 5 J=1,4
 CALL WINDO2(WXL(J),WXH(J),WYL(J),WYH(J))
 CALL ISOPRJ(M,XL,XH,N,YL,YH,ZARR,J-1,NW,WW)
 CONTINUE
 CALL DEVEND
 STOP
 END
```

APPENDIX A6

POINT VELOCITY MEASUREMENTS ABOVE PACKED BEDS SUPPLIED BY MODIFIED GAS DISTRIBUTORS

Tables A6.1 and A6.2:	Modification A, P.H. = 6.12 cm
Tables A6.3 and A6.4:	Modification B with six baffles P.H. = 6.12 cm
Tables A6.5 and A6.6:	Modification B with 24 baffles P.H.= 6.12 cm
Tables A6.7 and A6.8:	Modification C, P.H. = 6.12 cm
Tables A6.9 and A6.10:	Modification C + draw-off tray, P.H. = 6.12 cm.

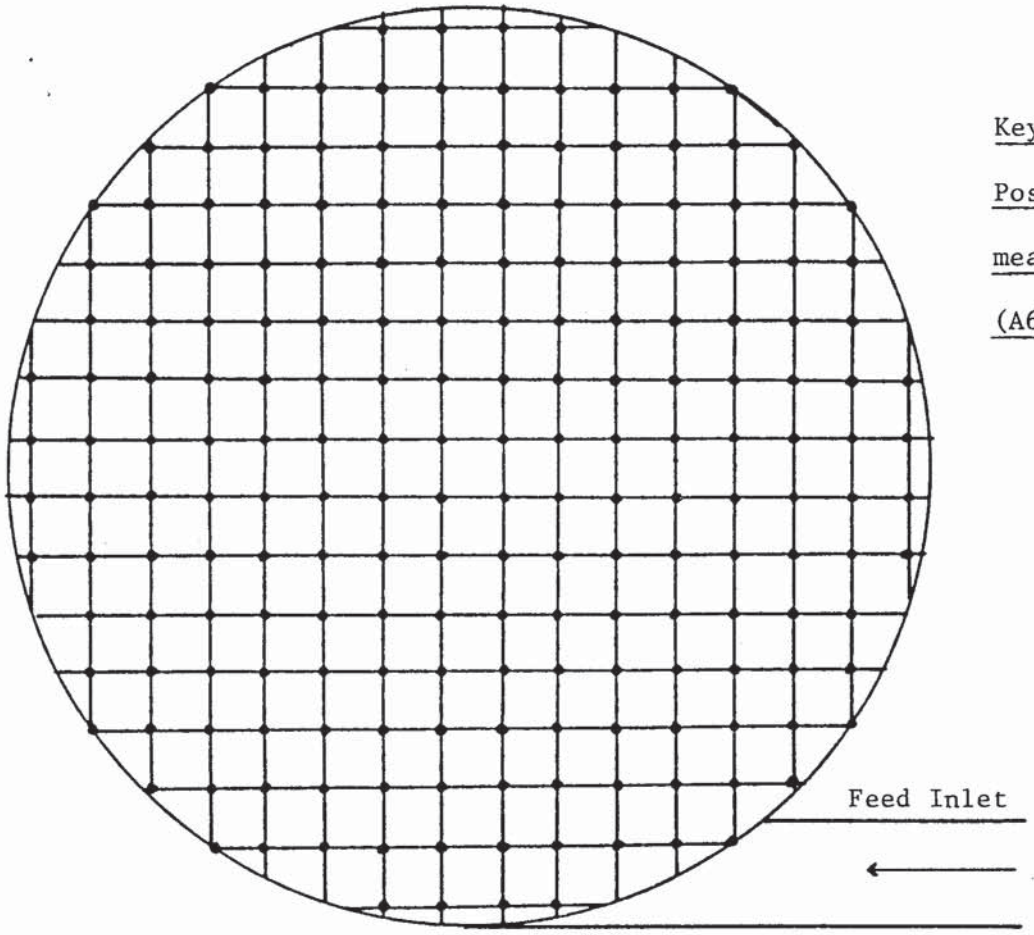

Key Figure A6.1

Positions of the 200 point velocity measurements for tables (A6.1) to (A6.10)

					195	185	165	165						
		70	150	240	160	135	120	180	105	30	235			
	85	225	155	200	120	225	95	145	135	165	175	315		
160	220	165	165	160	100	90	125	125	70	85	220	225	125	
210	125	220	210	155	125	110	80	40	155	165	125	80	210	
260	160	190	165	100	115	90	105	55	75	35	135	120	135	
120	150	145	210	165	185	60	120	70	120	125	50	80	70	180	205
170	160	170	45	210	70	140	55	125	75	90	115	125	80	130	270
250	170	150	145	90	120	55	95	35	75	50	70	150	200	120	105
125	105	170	120	25	5	65	65	120	120	140	140	35	130	55	150
210	110	140	165	40	40	40	90	50	50	100	105	165	45		
280	145	115	145	120	80	110	35	95	90	150	130	200	270		
250	25	130	240	164	100	45	50	160	245	230	165	270	125		
220	165	265	145	45	40	200	60	260	65	210	200				
	130	205	200	80	200	110	190	185	155	80					
				230	200	220	110							

Table A6.1 Point Velocity Measurements (ft/min); Modification A, P.H. = 6 cm. P.S = 16 mm

Re = 60000

ϕ = 42.7

					180	205	165	215						
		225	210	185	125	200	155	135	165	110	60			
	85	250	125	115	105	110	80	55	120	235	185	175		
100	260	160	160	180	100	160	110	60	75	150	145	165	175	
160	75	190	70	205	10	100	130	130	130	95	115	170	200	
200	140	165	170	200	180	135	150	80	150	105	165	120	60	
20	240	125	150	130	130	110	30	80	140	115	115	110	135	165
195	165	180	105	10	130	90	90	110	150	30	95	200	160	110
140	130	120	135	15	30	135	160	130	110	105	165	110	165	85
160	45	125	120	75	90	105	85	130	50	130	120	80	140	75	245
130	105	155	175	145	140	110	85	130	140	125	110	120	165	
20	145	150	125	140	140	185	245	80	140	45	230	130	155	
245	110	105	180	145	105	160	160	45	150	125	190	120	130	
160	260	170	210	120	105	150	130	150	135	200	140			
75	35	70	95	150	180	195	20	60	240					
			140	180	160	300								

Table A6.2 Point Velocity Measurements (ft/min); Modification A, P.H. = 12 cm, P.S. = 16 mm

Re = 60000

ϕ = 31.3

					106	45	85	140						
		45	180	300	165	140	170	145	145	135	60			
	70	60	230	180	165	230	45	200	145	175	200	165		
105	160	225	135	135	20	180	130	145	185	70	60	160	170	
85	150	220	135	190	150	145	80	120	215	190	245	85	210	
135	155	75	45	210	70	100	150	100	130	10	120	130	170	
120	140	150	220	15	160	125	165	110	145	225	55	120	35	155	220
35	60	140	120	125	60	125	130	160	165	125	155	160	115	140	150
215	170	150	130	110	180	70	50	40	110	110	90	160	205	125	140
170	175	80	30	75	130	140	120	75	110	20	75	190	105	90	165
75	115	260	120	80	85	80	120	70	70	135	150	135	80		
125	160	60	35	165	180	125	75	110	160	115	90	190	145		
140	170	60	125	145	130	100	115	120	130	90	125	160	145		
	335	200	160	160	210	50	180	100	210	100	160	160			
		140	135	170	135	210	100	160	150	110	155				
					170	135	80	120						

Table A6.3 Point Velocity Measurements (ft/min); Modification B with six baffles, P.H. = 6 cm, P.S. = 16 mm

Re = 60000

ϕ = 33.5

					155	120	180	180						
		165	210	160	135	85	145	60	170	175	145			
	125	110	50	170	225	225	160	110	170	160	125	170		
115	80	135	145	105	155	70	170	120	135	60	145	145	180	
165	205	140	145	115	180	180	140	105	145	125	200	130	100	
180	160	225	130	145	180	105	125	130	245	155	110	200	135	
160	165	80	265	145	160	160	265	120	55	180	155	80	130	200	195
145	135	180	165	80	120	140	150	140	130	60	105	135	125	40	125
165	180	15	140	140	85	50	85	160	60	120	180	150	40	155	85
210	230	175	85	45	115	155	110	140	130	30	165	100	230	190	110
	105	90	55	110	200	175	145	95	165	35	230	110	120	170	
	80	105	145	90	115	220	125	110	150	170	130	70	190	180	
	115	135	190	140	135	80	170	65	180	125	30	175	160	200	
		230	140	220	140	180	125	65	30	180	10	155	170		
			140	220	200	80	120	160	100	140	170	80			
						145	10	130	180						

Table A6.4 Point Velocity Measurements (ft/min); Modification B with six Baffles, P.H. = 12 cm, P.S. = 16mm

Re = 60000

ϕ = 26

					150	100	55	130						
		100	130	100	255	205	140	105	45	130	220			
	180	215	165	185	245	130	135	140	200	260	250	180		
170	160	200	165	220	235	130	125	180	85	140	240	170	125	
70	135	130	175	115	145	110	65	90	95	130	140	170	140	
65	170	210	130	100	140	110	100	140	140	160	140	125	170	
200	230	200	215	160	125	110	65	50	130	65	125	100	195	180	150
205	205	240	135	90	170	95	110	45	70	90	70	160	100	150	175
180	105	185	155	190	70	100	85	115	100	50	135	45	90	120	155
60	175	105	135	150	100	80	30	45	50	80	80	130	200	120	120
	200	160	85	175	140	40	80	95	55	110	160	155	130	135	
	125	200	160	210	190	85	115	105	120	100	110	60	150	165	
	10	130	115	105	60	145	125	70	185	115	180	150	215	40	
		175	80	80	180	135	145	200	115	200	145	175	120		
			130	110	230	190	90	50	75	240	125	240			
						140	60	125	145						

Table A6.5 Point Velocity Measurements (ft/min); Modification B with 24 Baffles, P.H. = 6cm, P.S. = 16 mm

Re = 60000

ϕ = 30

					130	140	165	165						
		170	130	135	120	105	170	90	60	130	125			
	140	175	95	140	95	215	145	150	175	200	95	145		
75	110	75	150	125	65	85	160	90	165	145	210	130	185	
130	200	55	120	155	105	130	95	40	105	120	170	170	225	
165	240	215	155	135	120	45	55	90	150	130	75	135	180	
160	95	120	195	160	155	130	105	70	125	120	130	140	95	120	145
195	70	115	140	105	55	205	125	105	80	120	130	250	75	125	80
110	215	20	110	125	100	125	70	130	30	100	140	105	90	130	35
145	220	130	165	90	135	120	105	90	165	105	125	165	110	145	90
	230	150	140	170	150	130	150	140	105	110	225	70	110	190	
	160	90	120	210	100	110	125	35	170	135	160	105	110	160	
	140	125	30	90	125	155	90	45	130	70	60	140	85	120	
		105	180	140	145	150	110	180	100	90	130	240	190		
			205	200	190	80	135	90	115	160	180	80			
						220	125	145	190						

Table A6.6 Point Velocity Measurements (ft/min); Modification B with 24 Baffles, P.H. = 12 cm, P.S. = 16 mm

Re = 60000

ϕ = 24.8

					155	110	125	200						
		180	270	145	160	130	135	140	155	130	110			
	165	140	105	185	125	210	115	90	125	140	190	145		
115	230	150	110	140	110	170	90	150	25	130	80	110	100	
205	145	110	155	45	145	125	100	95	65	60	90	175	135	
100	80	55	60	130	110	155	105	130	70	140	120	95	210	
140	100	175	135	115	140	125	145	240	165	130	80	160	80	120	260
130	145	140	95	125	90	105	140	110	160	100	125	160	200	130	150
120	100	125	120	155	150	170	90	220	195	75	130	150	140	135	185
115	210	135	90	125	15	110	200	130	105	170	160	170	120	135	300
250	45	95	200	60	190	15	170	70	100	130	155	75	180		
145	180	160	160	160	140	150	40	105	75	130	160	125	150		
155	165	75	200	125	170	85	85	130	155	190	160	150	190		
	150	175	150	225	135	105	115	165	160	155	110	30			
		140	140	125	255	145	105	105	150	210	160			
					65	105	120	145						

Table A6.7 Point Velocity Measurements (ft/min); Modification C, P.H. = 6 cm, P.S. = 16 mm

Re = 60000

ϕ = 23.3

					190	200	85	160						
		170	175	215	170	190	150	55	165	75	135			
	140	50	175	175	120	175	105	125	145	160	160	130		
110	150	175	130	170	50	160	100	60	130	105	155	160	125	
160	185	130	220	115	130	85	80	100	95	140	170	140	160	
135	55	140	190	85	50	105	145	115	135	130	165	100	70	
200	145	75	120	115	125	120	130	50	105	155	145	115	175	160	85
155	200	225	140	110	135	105	250	70	110	125	85	125	230	140	150
80	220	105	85	210	145	120	125	175	105	145	145	155	175	100	125
130	75	140	55	95	140	105	135	190	145	155	145	90	120	80	145
	195	220	145	120	190	75	190	105	165	115	180	210	100	130	
	125	165	175	100	110	5	115	165	190	105	240	160	150	100	
	210	130	95	120	120	50	90	105	75	45	110	190	110	125	
		45	180	155	130	130	60	130	120	180	115	175	100		
			175	160	220	80	165	160	165	125	200	140			
						160	90	130	180						

Table A6.8 Point Velocity Measurements (ft/min); Modification C, P.H. = 12 cm, P.S. = 16 mm

Re = 60000

ϕ = 21.1

					145	80	25	85						
		240	65	200	60	150	160	90	90	225	240			
	180	165	65	135	130	70	50	105	85	130	200	120		
30	140	170	160	120	110	140	100	155	110	135	120	175	135	
120	150	45	145	145	150	115	145	10	140	130	125	125	160	
135	125	50	100	125	150	100	135	130	175	190	115	110	165	
75	215	165	100	160	125	120	140	90	120	85	70	75	120	120	155
155	170	210	180	165	155	95	120	110	195	160	145	125	140	155	95
135	280	75	145	145	205	70	150	150	200	140	85	175	70	150	125
220	100	115	160	150	185	140	120	140	125	130	110	40	160	125	95
	210	120	220	150	160	190	155	110	145	45	135	145	75	165	
	160	105	130	70	110	155	150	175	100	60	110	120	85	160	
	145	80	90	115	145	125	145	125	145	100	120	200	125	240	
		240	100	125	150	165	190	260	160	160	30	100	105	
			140	90	80	150	110	170	70	145	100	180		
						200	125	140	135					

Table A6.9 Point Velocity Measurements (ft/min); Modification C + Draw-off Tray, P.H. = 6 cm, P.S. = 16 mm

Re = 60000

ϕ = 22.8

					145	145	180	165					
		180	90	165	130	145	170	190	135	130	135		
	175	190	140	150	105	100	145	155	170	110	115	65	
155	160	165	150	125	140	205	105	175	180	175	210	180	125
165	45	145	15	75	105	140	190	125	195	125	20	140	190
110	135	180	105	10	105	60	290	115	100	180	130	160	70
30	100	115	120	165	110	145	110	25	90	115	100	180	150	100	195
140	180	155	110	140	170	140	80	110	215	85	115	130	160	115	125
130	170	155	125	100	195	185	90	135	130	110	170	110	35	80	115
120	155	240	140	140	160	125	215	165	100	130	155	100	240	160	170
	200	135	180	190	180	200	65	60	70	165	120	140	130	130	
	85	140	135	135	120	105	145	215	180	155	210	145	100	110	
	280	100	145	165	95	135	235	165	90	125	115	80	145	180	
		200	145	240	175	15	110	160	25	165	225	145	145		
			95	195	60	60	130	165	260	100	145	90			
						245	105	180	225						

Table A6.10 Point Velocity Measurements (ft/min); Modification C + Draw-off Tray, P.H. = 12 cm, P.S. = 16 mm

Re = 60000

ϕ = 21

BIBLIOGRAPHY

1. Mullin, J.W. Industrial Chemist, 33 408, (1957)
2. Huber, M. and Hiltbrunner, R. Chemical Eng. Sci., 21 819 (1966)
3. Thormann, K. Distillation and Rectification, Chapter 5 86 (1928)
4. Scott, A.M. Trans. Ind. Chem. Eng. 13 211 (1935)
5. Tour, R.S. and Lerman, F. Trans. Am. Inst. Chem. Eng. 35 709 (1938)
6. Tour R.S. and Lerman, F. Trans. Am. Inst. Chem. Eng. 40 79 (1943)
7. Cihla, Z and Schmidt, O. Coll. Szech. Chem. Comm. 22 896 (1957)
8. Porter, K.E. and Jones, M.C. Trans. Inst. Chem. Engrs. 41 240 (1963)
9. Dutkai, E. and Rukenstein, E. Chem. Eng. Sci. 23 1365 (1968)
10. Onda, K., Takeuch, H., Meada, Y and Takeuchi, N. Chem. Eng. Sci. 28 1677 (1973)
11. Le Goff, P. and Lespinass, B. Revue I.F.P. 17 21 (1962)
12. Porter, K.E. Trans. Instn. Chem. Engrs. 46 T69 (1968)
13. Porter K.E., Barnett, V.D. and Templeman, J.J. Trans. Insth. Chem. Engrs. 46 T74 (1968)
14. Charpentier, J.C., Prost, C., Van Swaag W. and Le Goff, P. Chem. et. Ind-Gen. Chim. 99 803 (1968)
15. Charpentier, J.C., Prost, C., and Le Goff, P. Chem. et. Ind-Gen. Chim. 100 653 (1968)
16. Bemer, G.G. and Zuiderweg, F.J. Chem. Eng. Sci. 33 1637 (1978)
17. Zaytoun, A. MSc. Thesis University of Aston in Birmingham (1981)

18. Sounder and Ford. Iron and Steel Inst. 141 314 (1940)

19. Schwartz, C.Z. and Smith J.H. Ind. Chem. Eng. 35 1209 (1953)

20. Calderbank, P.H. and Porgorski. Trans. Inst. Chem. Engrs. 30 195 (1957)

21. Roblee, L.H.S., Baird R.M. and Tierney, J.W. AIChEJ 4 359 (1958)

22. Johnston and Thring, M.W. Pilot Plant Models and Scale-up Methods. McGraw-Hill (1957)

23. Moor, F.K. Theory of Laminar Flow. IV 169 (1964)

24. Kay, J.M. and Nederman, R.M. An Introduction to Fluid Mechanics and Heat Transfers. Cambridge University Press, 3rd edition, 264 (1972)

25. Porter, K.E. Gas Maldistribution in Shallow Large Diameter Packed Beds. Helsinki Notes (1982)

26. Robert, H. Perry and Cecil H. Chilton. Chemical Engineers' Handbook. McGraw-Hill. 1973.

27. KENT The DALL TUBE. KENT Publications